UNIVERSIDADE ESTADUAL DE CAMPINAS
INSTITUTO DE BIOLOGIA

CAROLINE BRANDÃO TELES

EMPREGANDO A PROTEÔMICA PARA COMPREENDER OS MECANISMOS DE AÇÃO DOS ANTIPSICÓTICOS EM OLIGODENDRÓCITOS HUMANOS

EMPLOYING PROTEOMICS TO UNDERSTAND THE MECHANISMS OF ACTION OF ANTIPSYCHOTICS IN HUMAN OLIGODENDROCYTES

CAMPINAS
2018

CAROLINE BRANDÃO TELES

EMPREGANDO A PROTEÔMICA PARA COMPREENDER OS MECANISMOS DE AÇÃO DOS ANTIPSICÓTICOS EM OLIGODENDRÓCITOS HUMANOS

EMPLOYING PROTEOMICS TO UNDERSTAND THE MECHANISMS OF ACTION OF ANTIPSYCHOTICS IN HUMAN OLIGODENDROCYTES

Dissertação apresentada ao Instituto de Biologia da Universidade Estadual de Campinas como parte dos requisitos exigidos para a obtenção do título de Mestra em Biologia Funcional e Molecular, na área de Bioquímica

Dissertation presented to the Biology Institute of the University of Campinas as part of the requisites required to obtain of Master's degree in Functional and Molecular Biology in the area of Biochemistry

ESTE ARQUIVO DIGITAL CORRESPONDE À VERSÃO FINAL DA DISSERTAÇÃO DEFENDIDA PELA ALUNA CAROLINE BRANDÃO TELES, E ORIENTADA PELO PROF. DR. DANIEL MARTINS DE SOUZA E CO-ORIENTADA PELA PROF. DRª JULIANA SILVA CASSOLI

Orientador: PROF. DR. DANIEL MARTINS DE SOUZA
Coorientador: DRª. JULIANA SILVA CASSOLI

CAMPINAS
2018

Agência(s) de fomento e nº(s) de processo(s): FAPESP, 2015/23049-0

Ficha catalográfica
Universidade Estadual de Campinas
Biblioteca do Instituto de Biologia
Mara Janaina de Oliveira - CRB 8/6972

Brandão-Teles, Caroline, 1990-
B733e Empregando a proteômica para compreender os mecanismos de ação dos antipsicóticos em oligodendrócitos humanos / Caroline Brandão Teles. – Campinas, SP : [s.n.], 2018.

Orientador: Daniel Martins de Souza.
Coorientador: Juliana Silva Cassoli.
Dissertação (mestrado) – Universidade Estadual de Campinas, Instituto de Biologia.

1. Esquizofrenia. 2. Clorpromazina. 3. Haloperidol. 4. Fumarato de quetiapina. 5. Risperidona. 6. Proteoma. 7. Oligodendroglia. I. Martins-de-Souza, Daniel, 1979-. II. Cassoli, Juliana Silva. III. Universidade Estadual de Campinas. Instituto de Biologia. IV. Título.

Informações para Biblioteca Digital

Título em outro idioma: Employing proteomics to understand the mechanisms of action of antipsychotics in human oligodendrocytes
Palavras-chave em inglês:
Schizophrenia
Chlorpromazine
Haloperidol
Quetiapine fumarate
Risperidone
Proteome
Oligodendroglia
Área de concentração: Bioquímica
Titulação: Mestra em Biologia Funcional e Molecular
Banca examinadora:
Daniel Martins de Souza [Orientador]
Lucilene Delazari dos Santos
André Schwambach Vieira
Data de defesa: 21-02-2018
Programa de Pós-Graduação: Biologia Funcional e Molecular

Campinas, 21 de Fevereiro de 2018.

COMISSÃO EXAMINADORA

Prof. Dr. Daniel Martins de Souza

Prof. Dra. Lucilene Delazari dos Santos

Prof. Dr. André Schwambach Vieira

Os membros da Comissão Examinadora acima assinaram a Ata de Defesa, que se encontra no processo de vida acadêmica do aluno

DEDICATÓRIA

Dedico essa dissertação aos meus pais, que foram o meu maior apoio nos momentos de angústia. Mãe, seu cuidado, força e dedicação em olhar por mim, foram os que deram,nos momentos mais difíceis, a esperança para continuar seguindo em frente. Pai, sua presença significou segurança e certeza de qve não estou sozinha nessa caminhada.

AGRADECIMENTOS

À Fundação de Amparo à Pesquisa do Estado de São Paulo – FAPESP pelo apoio financeiro (Processo 2015/23049-0), concedida como ítem orçamentário do projeto Jovem Pesquisador (2013/08711-3).

Se você está lendo essa página, é porque aquele ditado "no final tudo dá certo" de fato é verdadeiro, porque eu cheguei até aqui. Do processo seletivo, aprovação e conclusão do mestrado foram longos (e curtos) dois anos que acrescentaram além de um título de mestre, algumas rugas e cabelos brancos. Mas quem disse que seria fácil? E eu nem gostaria que tivesse sido! Se o fosse, a vida não teria me dado tantas pessoas maravilhosas, que de alguma forma, no seu jeito, me apoiaram e me fizeram seguir em frente. E são a esses que quero agradecer, do fundo e local mais sincero do meu coração.

Primeiramente agradeço a Deus, que sempre olhou por mim, independente das vírgulas e reticências encontradas pelo caminho.

Aos meus amados pais, Vilma e Wilson, pelo seu tempo, amor e dedicação em sempre cuidar de mim. Por não desistirem, por acreditarem que eu era capaz de chegar até aqui. A minha mãe, que tem uma força sobrenatural, guerreira, aquela que ajudou em me tornar a mulher que sou hoje. A minha família, que estão comigo desde o início, constituindo a base mais firme que alguém pode querer. Obrigada as tias e tios, por serem minhas segundas, terceiras e quartas mães e pais! A minha vozinha que ainda está aqui, sempre me amando e apoiando e aquela vózinha que já se foi, anjo de olhos azuis que tem grande participação na minha caminhada até aqui. Sem ela, não sei aonde estaria hoje.

Ao meu orientador prof. Dr. Daniel Martins de Souza, que um dia me deu a oportunidade de fazer parte da família LNP. Proporcionando inúmeras oportunidades, ensinando e investindo na minha formação como futura educadora e pesquisadora.

A minha co-orientadora JuCa, por não só ter me orientado, mas por ter se tornado uma amiga. Você me apresentou a esse mundo da espectrometria de massas, com paciência e dedicação. Obrigado por cada hora do seu tempo dedicado a mim, não só me ajudando a construir conhecimento, mas compartilhando da vida.

A família LNP, onde passei a maior parte dos meus dias nesses últimos dois anos. Sem vocês, eu com toda certeza não chegaria até aqui. Em especial a Giu, cúmplice e parceira desde a graduação, que vem compartilhando comigo risos e lágrimas. Obrigada por cada respirada nos banquinhos do IB, recompondo nossas forças para continuar seguindo em frente.

Ao Clube das Bonitas, por estarem nessa caminhada comigo há uns bons anos, partilhando das angústias, crises, sonhos e alegrias. São vocês que fazem com que a vida seja mais leve nas horas difíceis!

Aos meus amigos de tatame, que nos dias nublados e escuros estavam lá, não só para trocar socos e chutes, mas para me ajudarem a prosseguir. O Muay Thai trouxe novos maravilhosos amigos, 7kg a menos e o amor da minha vida. Amor, estamos apenas começando. Obrigada por me dar o melhor colo e por me ouvir quando mais precisei.

Com vocês amados, divido a alegria desse momento.

"Cada um que passa em nossa vida, passa sozinho, pois cada pessoa é única e nenhuma substitui outra. Cada um que passa em nossa vida, passa sozinho, mas não vai só nem nos deixa sós. Leva um pouco de nós mesmos, deixa um pouco de si mesmo. Há os que levam muito, mas não há os que não levam nada. Essa é a maior responsabilidade de nossa vida, e a prova de que duas almas não se encontram ao acaso."

~ O pequeno príncipe

RESUMO

A esquizofrenia é um transtorno mental crônico que atinge em média 0,7% da população mundial, sendo seu desenvolvimento relacionado a soma de fatores genéticos e ambientais. Distúrbios cognitivos como atenção, memória e funções executivas são frequentemente observados em pacientes com a doença. Os antipsicóticos consistem na principal forma de tratamento, sendo amplamente utilizados na clínica. No presente projeto foram analisados o proteoma de uma linhagem celular de oligodendrócitos humanos (células MO3.13) tratados com quatro antipsicóticos, sendo dois de primeira-geração (clorpromazina e haloperidol) e dois de segunda-geração (quetiapina e risperidona). Primeiramente, foi estabelecido um protocolo para cultivo das células, publicado como um capítulo de livro. Por conseguinte, a análise dos tratamentos foi realizada através de nano-cromatografia líquida seguida de espectrometria de massas em tandem (nano LC-MS/MS). Posteriormente, as proteínas encontradas com p-value < 0,05 foram submetidas a análise no programa Ingenuity Pathway Analysis (IPA) para obtenção das vias metabólicas relacionadas a cada tratamento. Foram encontradas vias de sinalização em comum e específicas para cada antipsicótico. Os dados gerados nesta dissertação de mestrado auxiliarão na compreensão das vias bioquímicas envolvidas no mecanismo de ação desses medicamentos, que podem orientar o desenvolvimento de novos tratamentos.

ABSTRACT

Schizophrenia is a chronic mental disorder that affects on average 0.7% of the world population, and its development is related to genetic and environmental factors. Cognitive disorders such as attention, memory and executive functions are often observed in patients with the disease. Antipsychotics consist of the main form of treatment and are widely used in the clinic. In the present project the proteome of a human oligodendrocyte cell line (MO3.13 cells) treated with four antipsychotics, two of the first generation (chlorpromazine and haloperidol) and two of the second generation (quetiapine and risperidone) were analyzed. The analysis of the treatments was performed by liquid nano-chromatography followed by tandem mass spectrometry (nano LC-MS / MS). Subsequently, the proteins found with p-value <0.05 were submitted to analysis in the Ingenuity Pathway Analysis (IPA) program to obtain the metabolic pathways related to each treatment. Canonical pathways were found in common and specific for each antipsychotic. The data generated in this dissertation helped to understand the biochemical pathways involved in the mechanism of action of these drugs, which may guide the development of new treatments.

ÍNDICE DE FIGURAS

ÍNDICE DE TABELAS

SUMÁRIO

6. INTRODUÇÃO

6.1 A esquizofrenia

A esquizofrenia é uma doença psiquiátrica crônica, grave e incapacitante caracterizada por funções mentais anormais e distúrbios de comportamento (OWEN; SAWA; MORTENSEN, 2016; “WHO | Schizophrenia”, 2016). Os sintomas são divididos em três classes: produtivos, negativos e cognitivos. Os sintomas produtivos incluem delírios (falsas crenças), alucinações (falsas percepções) e desorganização do pensamento. Os sintomas negativos referem-se a perda de motivação e da vivacidade emocional. Distúrbios cognitivos como atenção, memória e funções executivas são frequentemente observados em pacientes com a doença (OWEN; SAWA; MORTENSEN, 2016; “WHO | Schizophrenia”, 2016). A esquizofrenia tende a se desenvolver por volta dos 16 a 30 anos de idade e persiste durante toda a vida do paciente, consistindo em um dos mais importantes problemas de saúde pública do mundo afetando mais de 21 milhões de pessoas (OWEN; SAWA; MORTENSEN, 2016; “WHO | Schizophrenia”, 2016). Atualmente, o diagnóstico da esquizofrenia é baseado em entrevistas realizadas entre médico e paciente, envolvendo a comunicação dos sintomas subjetivos e relato da história do paciente. A categorização deste é realizada utilizando-se o Manual Diagnóstico e Estatístico de Transtornos Mentais (DSM-5) ou através da Classificação Estatística Internacional de Doenças e Problemas Relacionados à Saúde (“WHO | Schizophrenia”, 2016). O tratamento da esquizofrenia deve abordar a multifatorialidade da doença por meio da integração de drogas e tratamentos psicossociais para lidar com uma pessoa cronicamente desabilitada (SPOHN, 1985).

6.2 As causas da esquizofrenia

Inúmeros estudos genéticos e epidemiológicos demonstraram durante os últimos anos que fatores genéticos possuem uma grande contribuição, porém não exclusiva, com as causas da esquizofrenia (OWEN; SAWA; MORTENSEN, 2016). Estudos genéticos utilizando gêmeos, adoção e históricos familiares demonstraram que o risco para desenvolvimento da doença é elevado nos indivíduos que possuem uma relação biológica com a desordem, quanto mais próximo o nível da relação genética, maior a probabilidade do desenvolvimento do transtorno (SULLIVAN; DALY; O’DONOVAN, 2012; VAN OS; KAPUR, 2009).

Um dos desafios ao se estudar a esquizofrenia é a compreensão de como um distúrbio neurológico mediado geneticamente se expressa clinicamente em um período específico da vida. Além da influência genética, fatores ambientais, tais como infecções por vírus durante o período pré-natal, complicações obstétricas que impliquem em hipóxia, estresse durante o neurodesenvolvimento e estresse crônico podem contribuir para o desenvolvimento da doença (SCHMITT et al., 2014).

6.2.1 A hipótese do neurodesenvolvimento

Desde a publicação dos artigos de Weinberger (WEINBERGER, 1987) e Murray (MURRAY, 1987) há trinta anos atrás, a hipótese do neurodesenvolvimento tem sido uma das principais teorias para a explicação do surgimento da esquizofrenia (OWEN; O'DONOVAN, 2017). Essa hipótese baseia-se na proposta de que o surgimento do transtorno no final da adolescência/início da idade adulta possa ser explicado por disfunções precoces no cérebro em desenvolvimento, devido a fatores genéticos e ambientais e processos do desenvolvimento normais. Dessa forma, a medida que ocorre o desenvolvimento cerebral e este assume novas funções e mais complexas (como mielinização, poda sináptica somado aos efeitos hormonais da puberdade no sistema nervoso central [SNC]), o impacto da alteração ocorrida durante o neurodesenvolvimento inicial torna-se aparente (LEWIS; LIEBERMAN, 2000; OWEN; O'DONOVAN, 2017). Por exemplo, já se foi observado alterações no hipocampo e córtex pré-frontal durante o neurodesenvolvimento de pacientes com esquizofrenia (WEINBERGER, 1987). Ademais, alterações no neurodesenvolvimento também vem sendo relacionado a problemas durante a gravidez como a desnutrição materna antes e durante a gravidez. Análise oriunda de dados obtidos durante dois grandes períodos de fome, sendo uma a Ducth Hunger winter de 1944 a 1945 e a outra na China durante 1959 a 1961 demonstrou um aumento de cerca de 2 vezes na taxa de esquizofrenia nos filhos de mães nascidas durante este período (MCGRATH; BROWN; ST CLAIR, 2011; XU et al., 2009). Todos esses fatores levaram a busca de quais sistemas neuroquímicos estão envolvidos e podem mediar as alterações progressivas observadas durante as fases iniciais da esquizofrenia.

6.3 Fisiopatologia da esquizofrenia

Inúmeros estudos de imagem e neuropatológicos cerebrais tentaram relacionar as alterações observadas na esquizofrenia e funções alteradas do cérebro (JARSKOG; MIYAMOTO; LIEBERMAN, 2007; LINDEN, 2012). Estudos indicam que a fisiopatologia do transtorno envolvem uma conectividade sináptica interrompida que afeta tanto os circuitos

excitatórios quanto inibitórios (JARSKOG; MIYAMOTO; LIEBERMAN, 2007). Dessa forma, grande número de evidências sugere que alterações em vários sistemas de neurotransmissores estão envolvidos na sintomatologia do transtorno. Dentre estes, os sistemas de dopamina (DA) e glutamato (GLU) receberam maior foco, embora outros sistemas também sejam implicados como GABAérgicos, serotonérgicos e opióides (LARUELLE; KEGELES; ABI-DARGHAM, 2003).

6.3.1 Hipótese dopaminérgica

A hipótese dopaminérgica postula que a esquizofrenia está associada a hiperatividade subcortical dos receptores D_2 de dopamina, validada através de tomografia por emissão computadorizada de um único fóton (SPECT) (ABI-DARGHAM et al., 2000) . A primeira formulação da hipótese foi feita em 1963 por Carlsson e Lindqvist que propuseram que a hiperatividade da transmissão de DA era responsável pelos sintomas produtivos (alucinações e delírios) observados na esquizofrenia (CARLSSON; LINDQVIST, 1963). A hipótese foi baseada na correlação entre o uso dos antipsicóticos em doses clínicas e seu potencial em bloquear os receptores D_2 de DA (para revisão ver (ABI-DARGHAM; MOORE, 2003). As primeiras evidências de estudos *post mortem* de cérebros de pacientes com esquizofrenia sugeriram que as alterações neuropatológicas observadas no transtorno incluíam tanto o aumento dos níveis de dopamina estriatal quanto o aumento da densidade do receptor D_2 (MACKAY et al., 1982). Ademais, estudos recentes trouxeram maior entendimento em relação às alterações dopaminérgicas observadas. Por exemplo, foi observado aumento nos níveis da enzima limitante envolvida na síntese de dopamina na substância negra de pacientes com esquizofrenia quando comparados com controle não acometidos pelo transtorno (HOWES et al., 2013). Em adição, um estudo utilizando 176 amostras de tecido *post mortem* do córtex pré-frontal dorsolateral de pacientes com esquizofrenia mostrou que a expressão do receptor D_2 pré-sináptico foi aumentada, enquanto que a expressão de variantes predominantemente pós-sinápticas foi diminuída quando comparado com os controles (KAALUND et al., 2014). Todavia, existem evidências de que a patofisiologia dos sintomas de uma boa parte dos pacientes com esquizofrenia envolve mais do que um excesso de dopamina. Por exemplo, um estudo demonstrou que a capacidade de síntese de dopamina foi aumentada em indivíduos que responderam ao tratamento com antipsicóticos (que agem bloqueando o receptor D_2) mas não em pacientes resistentes ao tratamento (DEMJAHA et al., 2012). Dessa forma, sugere-se que os pacientes que não respondem ao tratamento

provavelmente não exibem aumento da capacidade de síntese de dopamina comumente observada na desordem, refletindo uma fisiopatologia diferente.

6.3.2 Hipótese serotoninérgica

A hipótese serotoninérgica surgiu devido a propriedade da dietilamida do ácido lisérgico (LSD) em ser um agonista do receptor 5-HT (receptor de serotonina), produzindo sintomas alucinógenos e psicose aguda quanto utilizado. A hipótese serotoninérgica para a esquizofrenia ganhou suporte com a descoberta de anormalidades no receptor 5-HT2 em tecidos cerebrais *post mortem* de pacientes com esquizofrenia (MITA et al., 1986). Rasmussen e colaboradores avaliaram 30 pacientes com esquizofrenia não tratados comparados com controle saudáveis com a finalidade de avaliar o potencial de ligação da serotonina (2A) no cérebro in vivo. Eles observaram que os pacientes com esquizofrenia apresentaram associação significativamente mais baixa de serotonina (2A) no córtex frontal do que os indivíduos controle, sugerindo que esses receptores corticais estão envolvidos na fisiopatologia da esquizofrenia (PINBORG; BAARE, 2010). Ademais, a descoberta dos antipsicóticos de segunda geração que constituem antagonistas do receptor 5-HT_{2A} sugerem um papel da serotonina nos efeitos antipsicóticos dessas drogas. Esse fato é apoiado pela interação entre DA e 5-HT que ocorre em diferentes níveis anatômicos e mediado por diferentes subtipos de receptores 5-HT que afetam de diferentes maneiras a transmissão de DA. Esta interação tem sido sugerida para explicar os efeitos benéficos dos medicamentos antipsicóticos atípicos na esquizofrenia, especificamente a redução dos sintomas extrapiramidais (EPS) e a melhora nos sintomas negativos, atribuídos ao antagonismo de 5-HT_{2A} (LIEBERMAN et al., 1998).

6.3.3 Hipótese glutamatérgica

O glutamato consiste no aminoácido mais abundante do cérebro e possui um papel fundamental como um importante neurotransmissor excitatório. Evidências crescentes indicam que anormalidades na neurotransmissão glutamatérgica podem ser a base de alguns dos fenômenos psicopatológicos fundamentais observados na esquizofrenia, posto que foi encontrado uma diminuição dos níveis de glutamato no líquido cefalorraquidiano em pacientes acometidos pelo transtorno (KIM et al., 1980). A hipótese glutamatérgica da esquizofrenia foi fundamentada no uso crônico e abusivo da fenilciclidina (PCP), um antagonista do receptor ionotrópico N-metil-D-aspartato do glutamato (NMDAr). A exposição ao PCP como droga recreativa provocava nos usuários sintomas positivos,

negativos e cognitivos semelhantes aos observados na patologia (JAVITT; ZUKIN, 1991). Ademais, a administração aguda de cetamina (antagonista de NMDA) em doses sub-anestésicas em voluntários saudáveis induziu a efeitos psicopatológicos semelhantes ao encontrado em pacientes com esquizofrenia (ADLER et al., 1999). Desta maneira, o uso de antagonistas do NMDAr não somente agrava os sintomas da esquizofrenia como também induzem sintomas similares à doença, dando suporte a hipótese de que a hipofunção do NMDAr talvez tenha um papel crítico na patofisiologia da esquizofrenia. Estudos demonstraram que animais submetidos a indução de esquizofrenia por um antagonista de NMDA resultou em alteração da expressão de genes relacionados a processos de mielinização, que estão associados aos oligodendrócitos (KAISER et al., 2004).

6.4 Os oligodendrócitos e a esquizofrenia

Os oligodendrócitos são as células responsáveis pela mielinização do SNC. Estas expressam os genes que codificam as proteínas estruturais de mielina de forma específica e regulada dentro da célula. Aproximadamente metade do cérebro humano compreende traços axonais mielinizados que conectam o córtex com estruturas subcorticais e interligam áreas corticais entre si. Dessa forma, lesões que afetem a substância branca do SNC, como as doenças desmielinizantes, causam déficits motores e sensoriais, bem como disfunções cognitivas, como observadas nas condições psiquiátricas (NAVE; EHRENREICH, 2014).

Estudos em tecido *post mortem*, incluindo os de nosso grupo, direcionam para alterações nos oligodendrócitos na esquizofrenia. No córtex pré-frontral de pacientes com esquizofrenia foi observado menor densidade de oligodendrócitos, juntamente com níveis maiores de apoptose e necrose dessas células, acompanhados de redução nos níveis de mielina, fornecendo evidências de que a disfunção dos oligodendrócitos pode ser essencial na fisiopatologia da esquizofrenia (FLYNN et al., 2003; “Oligodendroglial density in the prefrontal cortex in schizophrenia and mood disorders: a study from the Stanley Neuropathology Consortium”, 2004; STARK et al., 2004; URANOVA et al., 2001). A análise do proteoma do tálamo mediodorsal do cérebro de pacientes com esquizofrenia resultou em proteínas diferencialmente expressas relacionadas ao metabolismo de oligodendrócitos (MARTINS-DE-SOUZA et al., 2010). Além disso, já foi relatado alterações nos níveis de expressão de genes relacionados a mielinização no córtex pré-frontal de indivíduos acometidos pelo transtorno (HAKAK et al., 2001). Ademais, as variantes genéticas relacionadas aos oligodendrócitos tem sido implicadas a integridade da substância branca,

desempenhando um papel importante na disfunção cognitiva observada na esquizofrenia (PRATA et al., 2013; VOINESKOS et al., 2013).

Estudos utilizando modelos animais tambétt m vem fornecendo evidências quanto a alterações relacionadas a mielina na esquizofrenia. Animais tratados com antagonistas do NMDAr são utilizados como modelos para o transtorno (NEILL et al., 2010; PAULSON et al., 2003). Já foi demonstrado que animais tratados com MK-801, um antagonista do NMDAr, apresentaram redução nos níveis da proteína básica de mielina (MBP), diminuição do volume total de substância branca e do corpo caloso quando comparados com animais não tratados (XIU et al., 2014). Ademais, os modelos *in vitro* utilizando agonistas e antagonistas de neurotransmissores podem complementar os estudos in vivo e em tecidos, fornecendo novos conhecimentos sobre a fisiopatologia da esquizofrenia. Por exemplo, linhagens celulares de astrócitos, neurônios e oligodendrócitos foram tratadas com MK-801 e mensurado os níveis de seis enzimas glicolíticas. Foi observado que o MK-801 afeta a glicólise nos oligodendrócitos em maior extensão do que as células neuronais e pode ser modulado pelo tratamento antipsicótico (GUEST et al., 2015). Além disto, um estudo proteômico do nosso grupo tratou oligodendrócitos com MK-801 e observou que o tratamento levou alteração de proteínas envolvidas principalmente no metabolismo energético. Ainda, a adição da clozapina às culturas de oligodendrócitos tratados com MK-801, resultou na expressão diferencial de proteínas, nas quais muitas delas apresentaram alterações opostas aos efeitos do antagonista de NMDAr. Portanto, alterações destas proteínas e as vias de metabolismo energético associadas em oligodendrócitos podem ser exploradas como potenciais biomarcadores da eficácia antipsicótica (CASSOLI et al., 2016).

6.5 O emprego dos antipsicóticos

Os tratamentos atuais foram disponibilizados no final de 1990 e reduziram o sofrimento dos pacientes consideravelmente. Porém, cerca de 2/3 das pessoas que desenvolvem a doença necessitam de assistência pública a partir de sistemas de segurança social governamentais dentro de poucos anos após o início. A maioria das pessoas que desenvolvem esquizofrenia são incapazes de retornar ao trabalho ou à escola e ter interações sociais relativamente mínimas (“WHO | Schizophrenia”, 2016). O tratamento medicamentoso da esquizofrenia tem como objetivo reduzir a frequência e a gravidade da exacerbação psicótica, melhorar os sintomas gerais e proporcionar uma qualidade de vida para o paciente. Os antipsicóticos são divididos em duas categorias: os medicamentos típicos (primeira

geração), e os atípicos (segunda geração). Uma propriedade farmacológica comum entre essas duas categorias de antipsicóticos é que ambos bloqueiam o receptor de dopamina D_2.

6.5.1 Antipsicóticos de primeira geração (típicos)

Os antipsicóticos de primeira geração ou típicos surgiram na década de 1950, com a introdução da clorpromazina, em que, pela primeira vez, estava disponível um medicamento oral que aliviava os sintomas positivos da esquizofrenia, como delírios, alucinações e desorganização do pensamento, entre 70 % dos pacientes (MEYER; SIMPSON, 1997). Os antipsicóticos típicos atuam bloqueando o receptor dopamina D_2, e são efetivos em reduzir os sintomas produtivos, como alucinações, por exemplo. No entanto, são minimamente eficazes para os sintomas negativos e cognitivos, que contribuem para a maior parte da deficiência associada com a esquizofrenia (LEUCHT et al., 2009; MAILMAN; MURTHY, 2010). Em média, de 25 a 60% dos pacientes são resistentes ou parcialmente responsivos ao tratamento com os antipsicóticos típicos. Ademais, também são responsáveis por uma variedade de efeitos adversos tanto no tratamento agudo quanto a exposição a longo prazo, como sedação, efeitos autonômicos e cardiovasculares, muitas vezes devidos às ações em outros receptores (MAILMAN; MURTHY, 2010). Essas drogas ainda induzem a uma variedade de efeitos neurológicos agudos, como efeitos colaterais extrapiramidais e efeitos devido a exposição a longo prazo como discinesia tardia (LEUCHT et al., 2009; MAILMAN; MURTHY, 2010).

6.5.2 Antipsicóticos de segunda geração (atípicos)

Os antipsicóticos de segunda geração, ou atípicos, surgiram alguns anos após os típicos e podem ser classificados como antagonistas $5HT_{2A}$ / D_2 (MAILMAN; MURTHY, 2010). São mais eficazes quanto a diminuição dos sintomas negativos, porém apresentam alguns efeitos colaterais como aumento de peso e sedação (KANTOFF et al., 2010; MAILMAN; MURTHY, 2010).

Estudos recentes demonstraram que a adição de clozapina em astrócitos tratados com MK-801 reverteu a expressão diferencial de proteínas encontradas nos astrócitos tratados com MK-801 na ausência do antipsicótico, sugerindo que a ação desta droga vai além de suas ações sobre os receptores de serotonina e dopamina (MARTINS-DE-SOUZA; LEBAR; TURCK, 2011). Visto que a esquizofrenia constitui uma doença multifatorial com um início pérfido, o estudo da mesma requer métodos que permitam investigar e elucidar os mecanismos moleculares envolvidos em sua patologia (GUEST et al., 2015). Dessa forma, a proteômica pode ser uma destas ferramentas.

6.6 Proteômica

Um proteoma compreende todo o conjunto de proteínas em um sistema biológico (célula, tecido ou organismo) em um determinado estado e momento (WILKINS et al., 1996). As técnicas de proteômica podem complementar os estudos genéticos e vem sendo utilizadas na identificação de biomarcadores em esquizofrenia, propiciando perspectivas sobre a fisiopatologia da doença. Ademais, constitui uma técnica de alto rendimento que detecta expressões baixas de proteínas, fornecendo um perfil preciso e funcional do estado fisiológico atual, reflexo da complexa interação do gene com o ambiente. A importância dessas interações tem aumentado na pesquisa da esquizofrenia e outras doenças neurológicas (NASCIMENTO; MARTINS-DE-SOUZA, 2015).

Nas primeiras décadas do surgimento da proteômica, o principal método quantitativo utilizado era baseado em gel, como a eletroforese em gel bi-dimensional (2DE) e a eletroforese em gel bi-dimensional fluorescente (2D-DIGE) (OLIVEIRA; COORSSEN; MARTINS-DE-SOUZA, 2014) . Apesar de muito utilizado, as técnicas baseadas em gel foram sendo substituídas após a introdução do conceito de proteômica em larga escala, que faz uso da cromatografia líquida acoplada a um espectrômetro de massas (LC/MS)(LINK et al., 1999). A proteômica com base na espectrometria de massas foi a responsável por oferecer informações sobre a abundância de proteínas, perfis de expressão de acordo com o tipo celular, modificações pós-traducionais e interações proteínas-proteínas, aumentando a possibilidade de se estudar as modificações a nível protéico (JENSEN, 2006).

6.6.1 Espectrometria de massas

A espectrometria de massas consiste em uma técnica de análise qualitativa e quantitativa, que se baseia na medida da razão massa/carga (*m/z*) dos íons das moléculas para sua identificação. Inúmeras técnicas de ionização são utilizadas em espectrometria de massas. Os fatores mais importantes a serem considerados referem-se a energia interna transferida para o íon durante o processo de ionização e as propriedades físico-químicas do analito que podem ser ionizados. Algumas técnicas são altamente energéticas e causam fragmentação extensiva, enquanto que outras são mais suaves e produzem apenas íons das espécies moleculares. As principais técnicas de ionização utilizadas em proteômica são a ionização dessorção a laser auxiliada por matriz (Matrix Assisted Laser Desorption Ionization, MALDI) e a ionização por eletrospray (ESI).

6.6.1.1 Técnicas de ionização

Na ionização por MALDI os analitos são incorporados em matrizes orgânicas em fase sólida ou viscosa. Um laser pulsado reflete na amostra para facilitar as reações de ionização/dessorção. Durante a excitação do laser, a matriz retoma e redistribui a energia emitida para a dessorção e ionização dos analitos (ver revisão 44). Já a ionização por ESI utiliza energia elétrica para auxiliar a transferência dos íons da solução para a fase gasosa, que envolve três etapas: nebulização de uma solução de amostra em gotículas carregadas eletricamente; liberação de íons das gotículas e transporte dos íons gerados da região da fonte de ionização para o espectrômetro de massa, para descrição em detalhes dos mecanismos de ESI ver revisão (BRUINS, 1998). Uma vez que os íons gasosos foram produzidos, é necessário que estes sejam separados de acordo com suas massas. A propriedade física dos íons que é medida por um analisador de massa é sua relação *m/z*, e não sua massa isolada. Dessa forma, um espectrômetro de massas, além da fonte de ionização, contém também um analisador de massas (onde a relação *m/z* é medida) e um detector, que é responsável por detectar e amplificar a informação do analisador.

6.6.1.2 Analisadores

Existem vários tipos de analisadores, cada um possuindo vantagens e desvantagens. De maneira geral, todos os analisadores de massa utilizam energia elétrica estática ou dinâmica e campos magnéticos isolados ou combinados. As diferenças entre os tipos residem basicamente na maneira como esses campos são utilizados para alcançar a separação. Dois exemplos de analisadores largamente utilizados em proteômica são o analisador por tempo de voo (time of flight, TOF) e o quadrupolo. O TOF analisa os espectros de massa através do tempo de vôo dos íons por um tubo, que dependendo das relações *m/z* evidenciam diferentes tempos de voo. Já o analisador de quadrupolo utiliza da trajetória em campos elétricos oscilantes para separar os íons de acordo com suas *m/z* (HOFFMANN, EDMOND DE; STROOBANT, [s.d.]). Finalmente, quando o detector de MS registra o momento de chegada dos feixes de íons, estes serão convertidos em sinais elétricos que geram espectros de massas.

As técnicas baseadas em espectrometria de massas são capazes de quantificar milhares de proteínas em grandes números de amostras, gerando grandes conjuntos de dados que podem ser extraídos por ferramentas computacionais específicas, como MASCOT®, PLGS®, MaxQuant e Progenesis®.

6.6.1.3 Synapt G2-Si

O espectrômetro de massas (MS) utilizado para as análises realizadas nesta dissertação de mestrado foi o Synapt G2-Si HDMS (Waters Corp., Milford, EUA), que consiste em um MS com uma fonte de ionização do tipo ESI e analisador do tipo Q-TOF, ou seja, possui dois analisadores hibridizados: um quadrupolo (Q) seguido de um analisador do tipo TOF. Ademais, o Synapt G2-Si também está equipado com uma cela de mobilidade iônica de alta eficiência (IMS). Com este aparelho é possível realizar tanto a análise dependente de dados (data-dependent analysis, DDA) quanto a análise independente de dados (data-independent analysis, DIA do tipo MS^E). A DDA consiste em um processo de seleção e fragmentação de peptídeos que acontece de forma seriada. O ciclo inicia-se através da aquisição de um espectro MS seguido da seleção de íons precursores para a fragmentação MS/MS. Os íons precursores selecionados são isolados em série para aquisição MS/MS por um período definido. Este ciclo de aquisições de MS e MS/MS continua ao longo do tempo de execução. Os dados então gerados *m/z* e tempo de retenção (RT) para os íons de precursores e fragmentos são então extraídos e processadas para identificação de peptídeos e proteínas. Já para a análise MS^E, o quadrupolo é utilizado como um guia para transferir os íons para a célula de colisão. Nesta, a energia de colisão é alternada de baixa a alta energia ao longo do tempo de execução. Os íons precursores são medidos nas varreduras de baixa energia, enquanto que os fragmentos são medidos nas varreduras de alta energia (LEVIN; HRADETZKY; BAHN, 2011). Desta forma, não há seleção de ions precursores, já que todos serão fragmentados.

Como mencionado anteriormente, o Synapt G2-Si possui uma cela IMS, que confere mais uma dimensão para separação dos íons. Dessa forma, para cada valor de *m/z* há um espectro de *drift time*, ou seja, a velocidade com que um íon se desloca em uma câmara contendo um gás inerte, influenciado por um campo elétrico. A cela IMS é dividida em três partes: a TRAP, onde os íons são acumulados e lançados em períodos regulares para a câmara de mobilidade, na qual ocorre a separação em função da mobilidade; e a TRANSFER, que conduz os íons para o analisador TOF. A junção das técnicas de IMS e MS^E confere o modo de *High Definition Mass Spectrometry* (HDMSe). Todavia, os dados obtidos neste estudo foram realizados em UDMSe. Nesta abordagem, é utilizado os perfis de energia de colisão e *drift time* específicos para melhorar a eficiência da fragmentação dos precursores em relação às técnicas independentes de dados de MS^E e HDMSe (DISTLER et al., 2013).

7. OBJETIVOS

A presente dissertação teve como objetivo avaliar os efeitos moleculares dos antipsicóticos de primeira e segunda geração (típicos e atípicos, respectivamente) sob o proteoma de uma linhagem celular de oligodendrócitos humanos (MO3.13). Os objetivos específicos foram cultivar a linhagem celular e tratar tais células com clorpromazina, haloperidol, quetiapina e risperidona.

8. CAPÍTULO 1

MK-801-treated oligodendrocytes as a cellular tool to study schizophrenia

Caroline Brandão-Teles[1], Daniel Martins-de-Souza[1,2] Juliana S. Cassoli[1],*

1Department of Biochemistry and Tissue Biology, Institute of Biology, University of Campinas (UNICAMP)
2 UNICAMP´s Neurobiology Center, Campinas, SP, Brazil.
* jscassoli@gmail.com

P.C. Guest (ed.), Proteomic Methods in Neuropsychiatric Research, Advances in Experimental Medicine and Biology, DOI 10.1007/978-3-319-52479-5_25

Abstract

Glutamate is the most important excitatory neurotransmitter in the brain. N-methyl-D-aspartate (NMDA) is one of the glutamate receptors, which is found both in neurons as glial cells. Oligodendrocytes express NMDA receptors and these cells have been largely implicated in schizophrenia. The interest in understanding the roles of oligodendrocytes in human diseases led to the development of oligodendroglial models for testing hypotheses under a controlled environment. MO3.13 is a cell line which is likely to represent immature oligodendrocytes. These cells may be used as a model to study glutamatergic dysfunction, if pharmacological agents as PCP and MK-801, are employed. As NMDA receptor antagonists, these agents have been used to mimic the molecular features of schizophrenia in vitro. Here, we describe a comprehensive protocol to culture MO3.13 and MK-801 treatment to induce a glutamatergic dysfunction. These cells may ben further analyzed by proteomic approaches, which we also describe here to identify the differential expression of proteins in order to reveal more about the pathophysiology of schizophrenia.

1 Introduction

The brain is the main organ of the central nervous system (CNS) and it is composed by a heterogeneous group of cells. These are classically divided into two large categories: neurons and glia. Glial cells are represented by astrocytes, oligodendrocytes and microglia. For over a century, neurons have been perceived as lords of the brain function and glia used to

be seen as simple tissue glue. Recent basic and translational studies have clearly indicated the important role of glia in brain function. Glial cells are responsible for many functions, such as power support, neuronal control, maintenance and plasticity of synaptic contacts1. Many studies have shown that neurons and glial cells communicate bidirectionally in both structural and functional levels. Remarkably, glutamate, the most abundant amino acid in the brain, has been involved in a variety of responses in astrocytes and oligodendrocytes. Thus, glial cells may act as partners of neurons in the formation of information processing mediated by glutamate1,2,3.

Glutamatergic transmission occurs throughout the CNS and is responsible for numerous essential brain functions such as cognition, learning and memory. The inhibition of glutamatergic transmission leads the brain to coma, disabling the entire nervous system. Each glutamatergic synaptic event is initiated by an action potential that leads to Ca2+ influx in the presynaptic terminal, resulting in the release of the neurotransmitter into the synaptic cleft. After being released, glutamate readily crosses the synaptic cleft and activates specific receptors resident in the postsynaptic membrane3.

The interaction of glutamate to glia cells is basically mediated by four molecular mechanisms: G-protein coupled metabotropic receptors and three families of ionotropic glutamate receptors: AMPA (α-amino-3-hydroxy-5-methyl-4-isoxazolepropionic acid), kainate and NMDA (N-methyl-D-aspartate)1,4,5. Although the existence of this variety of receptors, since the emergence of phencyclidine (PCP), around 1950, NMDA receptor antagonists have played an important role in the pathophysiology of neuropsychiatric disorders6.

The NMDA receptor is a glutamate-activated cation channel, encoded by seven genes, which has four sites of pharmacological relevance: the glutamate recognition site; the glycine modulating site; the binding site for phencyclidine (PCP) and its analogue; and a cation-binding site within the channel, where magnesium acts3,7. In Alzheimer's disease, impaired memory and learning has been linked to the NMDA receptor8. It has also been shown that the use of NMDA antagonists in patients with chronic pain reduced the need of opioid use and in epilepsy patients also exhibit anticonvulsant properties and are used for the treatment of the disease9. Studies using PCP generated the glutamatergic hypothesis of schizophrenia involving remarkable similarities regarding symptomatic manifestations of PCP-induced psychosis and observed in schizophrenic patients2,7.

Schizophrenia is a disease of multiple etiologies, expressed through positive, negative symptoms and cognitive deficits. These normally emerge during young adulthood (16-30 years of age), persisting throughout the life of the patient10.

Added to PCP, other pharmacological agents have been used to study the pathophysiology of schizophrenia through the modulation of neurotransmitter systems. One of them is dizocilpine (also known as MK-801), the most powerful antagonist of the NMDA receptor11. Studies have revealed that neurons, astrocytes and oligodendrocytes are affected by MK-801 treatment, but differentially. The treatment showed that glycolysis is more affected in oligodendrocytes than in the other cell types12. Recent studies showed that many proteins associated with energy metabolism were upregulated in MK 801-treated oligodendrocyte cell line (MO3.13)13.

The interest in understanding the roles of oligodendrocytes in human diseases led to creation of oligodendroglial models for testing hypotheses under a controlled environment. The MO3.13 cell line come from the fusion of a 6-thioguanine-resistant mutant of the human rhabdomyosarcoma RD with adult human oligodendrocytes cultured from surgical specimen14,15. This cell line showed markers of immature oligodendrocytes, such as CNPase and GalC15. Thus, the overall protein expression. Of MO3.13 could help in undertanding the mechanisms of action of pharmacological agentes in the comprehension of the pathophysiology of psychiatric disorders such as schizophrenia. Proteins are molecules that play many critical tasks in the body. They do most of the work in cells and are required for the function, structure and regulation of the body's tissues and organs. Through the study of proteins, it is possible to understand the cellular functions and their responses to external and internal disturbances16. Through proteomics, it is possible to investigate in a quantitative manner the general expression of proteins as well as their post-translational modifications, thus providing an accurate functional profile of the current physiological state17. The use of mass spectrometry (MS) to identify and characterize biological molecules is a fundamental technology in biochemical analysis of proteins and proteomics18.

Here, a protocol of MO3.13 cell culture, treatment with MK-801 and proteomic analyses is presented. This strategy may provide new insights about glutamatergic dysfunction and the pathophysiology of schizophrenia.

---

2 Materials

All the solutions and buffers should be prepared with Milli-Q water (UHQ), analytical grade reagents, and highest purity chemicals. Organic solutions should be prepared fresh.

2.1. MO3.13 Cell Culture

1. Human Oligodendroglia Cell Line MO3.13 (Cedarlane, cat. no. CLU301)
2. Culture medium: DMEM, high glucose (Life/Thermo, cat. no. 11960-044) supplemented with 10% fetal bovine serum (FBS) (South America origin, Life/Thermo, cat. no. 12657029) and 1% penicillin-streptomycin (5,000 U/mL) (Life/Thermo, cat. no. 15070063)
3. Flask Nunclon Delta-treated Vent/Close 75 (Nunc, cat. no. 156472)
4. Microtube 1.5mL Maxymum recovery (Axygen, cat. no. MCT-150-L-C)
5. Pipette tips, 100–1,000 µL (Axygen, cat. no. T-1000-B)
6. Pipette tips, 20–200 µL (Axygen, cat. no.T-200-Y)
7. Pipette tips, 1–10 µL (Axygen, cat. no. T-300)
8. Serological pipet 25 mL (Corning, cat. no. 4489)
9. Conical centrifuge tube 15 mL (Nunc/Thermo cat. no. 339650)
10. Transfer Pipette Sterile (Corning, cat. no. 184330)

2.2. Collecting the cells

1. Phosphate buffered saline (Sigma, cat. no. P5493)
2. Cell Scraper (Sarsted, cat. no. 831830)

2.3. Cell treatment

1. MK-801 hydrogen maleate (Sigma, cat. no. M107)

2.4. Lysis, Reduction, Alkylation, and Digestion

1. Ultrasonic Homogenizer (Cole Parmer Instrument Co.)
2. Vortex Genie 2 (Scientific Industries)
3. Lysis and reduction: 6 M urea (PlusOne Urea GE, cat. no. 17-1319-01), 2 M thiourea (PlusOne Thiourea GE, cat. no. RPN6301), 10 mM dithiot-reitol (PlusOne DTT GE, cat. no. 17-1318-02), 0.1 mM sodium pervanadate (Sodium Orthovanadate Sigma, cat. no. S6508 and Hydrogen peroxide solution Sigma, cat. no. 349887), protease and phosphatase inhibitors (cOmplete ULTRA (Roche, cat. no. 05 892 970 001).
4. Alkylation: 20 mM Iodoacetamide (GE cat. no. RPN6302) in 20mM Triethylammonium bicarbonate buffer (TEAB) (Sigma, cat. no. T7408)
5. Digestion: 2% trypsin (Sequencing Grade Modified Trypsin, Promega, cat. no. V5111).
6. Stop digestion: 100% Formic acid (FA) (Sigma, cat. no. 94318)

2.5. Desalting and Concentration of Peptides

1. Oasis® HLB Short Cartridge (Waters, cat. no. 186000132)
2. Qubit® Assay Tubes (Life/Thermo cat. no. Q32856)
3. Qubit® Protein Assay Kit (Life/Thermo, cat. no. Q33212)
4. Concentrator plus (Eppendorf)
5. Activation solution 1: 100% Methanol (HPLC grade, Sigma, cat. no. 34966)
6. Activation solution 2: 100% Acetonitrile (ACN) (LC-MS grade Sigma, cat. no. 14261)
7. RP loading solution: 0.1 % trifluoroacetic acid (TFA) (Sigma, cat. no. 302031)
8. RP elution solution: 70% ACN, 01% TFA

2.6. NanoLC-MS/MS analyses

1. Solvent A: 0,1% FA in water
2. Solvent B: 0,1% FA in ACN
3. Lock Spray solution: 100 fmol/µL [Glu1]-Fibrinopeptide B Standard (Waters, cat. no. 700004729) in methanol/water/FA (50:50:0.1 %)
4. Ammonium hydroxide (Sigma, cat. no. 320145)
5. ACQUITY UPLC M-Class system with 2D Technology: binary solvent manager (Waters, cat. no. 186016002); auxiliary solvent manager (Waters, cat. no. 186016021); sample manager (Waters, cat. no. 186016007)
6. Analytical columns: 1st Dim: M-Class Peptide BEH C18 Trap Column, 130Å, 5 µm, 300 µm x 50 mm (Waters, cat. no. 186007471); 2nd Dim: M-Class Symmetry C18 Trap Column, 100Å, 5 µm, 180 µm x 20 mm, 2D, V/M (Waters, cat. no. 186007497) and M-Class HSS T3 Column, 1.8 µm, 75 µm x 150 mm (Waters, cat. no. 186007473)
7. Autosampler vials: total recovery glass vials (Waters, cat. no. 600000750cv)
8. Instrument control software for UPLC: MassLynx (version 4.1; Waters)
9. SYNAPT G2-Si high definition mass spectrometer (Waters)
10. NanoLockSpray dual electrospray ion source (Waters)
11. Pre-Cut Picotip Emitter (Waters, cat. no. 186003916)
12. MS instrument control software: MassLynx (version 4.1; Waters)

2.7. Data processing

Software for raw data processing, database searching and label-free quantification: Progenesis QI for Proteomics version 3.0 (Nonlinear Dynamics, Waters)

---

3 Methods

3.1 Cell Culture

Remind to make sure that all materials are ready for use, e.g., the medium to be at the right temperature, 37ºC.

1. Take off the cryogenic vial from liquid nitrogen and unfreeze quickly in a 37°C water bath (Note 1).
2. Promptly, transfer the content to a centrifuge tube containing 10 mL of DMEM and centrifuge for 5 min at 1200 rpm (Note 2).
3. Discard the supernatant and distribute the cell pellet in T75 cell culture flask with 25 mL of culture medium (Note 3).
4. Grow MO3.13 cells at 37oC in 5% CO2 atmosphere. Change culture medium each 2-3 days, depending on rate of growth (Note 4).
5. Remove cells from flask using 0.25% trypsin-EDTA solution (~5 ml for T75 flask, 3 min at 37°C) and transfer to a centrifuge tube containing 10 mL of DMEM.
6. Centrifuge for 5 min at 1200 rpm and discard the supernatant. Divide into parts cell pellet into 4-5 new T75 flasks to continue cell culture growth or freeze the cells (See 3.2).

3.2 Freezing:

It is recommended to freeze a few aliquots of the cells promptly after the initial growth/split to prevent losing the cell line.

1. Prepare the number of cryogenic vials according to the amount of cells to be frozen. The freezing medium recommended is as follows: 60% DMEM, 30% FBS supplemented with 10% DMSO.
2. Take the flask containing the cells and discard the medium.
3. Remove the cells from flask using 0.25% trypsin-EDTA solution (~5 ml for T75 flask, 3 min at 37°C) and transfer to a centrifuge tube containing 10 mL of DMEM.
4. Centrifuge for 5 min at 1200 rpm and discard the supernatant.
5. Resuspend the cells with the target concentration of 105/ml of freezing medium.
6. The cryogenic vials are frozen firstly, in a -20ºC freezer for 2-3 hours, then in a -80ºC freezer. The next day the vials are transferred to a liquid nitrogen tank. It is recommended to test the cells for regrowth after freezing to be sure that the freezing procedure was performed correctly.

3.3 Acute 8h treatment with MK-801

It is recommended grow MO3.13 cells until 90 % confluence in T25 cell culture flask to initiate the treatment. It is very suggested to treat in triplicate. Be sure that everything is clean.

1. Dilute MK-801 in HCL solution.
2. Dilute the MK-801 solution with 15mL DMEM in a final concentration of 50 µM.
3. Discard the medium and transfer 5mL medium with MK-801 50 µM in each T25 cell culture flask.

4. After 8 hours, collect the cells (See 3.4).

3.4 Collecting the cells

1. Discard culture medium. Add 600µL PBS 1x in the flask and harvest cells by scraping them off the flask.
2. Wash the cells with 600µL PBS 1x containing protease and phosphatase inhibitors (optional).
3. Collect cells into 15 mL falcon tube and pellet them by 5 min centrifugation (1200 RPM).
4. Remove supernatant and snap-froze the cell pellet containing lysis buffer in liquid nitrogen until further sample preparation.

Topics 3.5 and 3.6 are optimized versions of Melo-Braga et al. (2015).

3.5 Lysis, Reduction, Alkylation, and Digestion

1. Lysing the cells add 100 µL of a solution composed for 6 M urea, 2 M thiourea, 10 mM DTT, protease and phosphatase inhibitors, 0.1 mM sodium pervanadate (lysis buffer) to the MO3.13 pellet (Note 5).
2. Stir well after adding lysis buffer and incubate for 2 h at 37oC (Note 6).
3. After incubation, dilute the sample ten times with 20 mM TEAB, pH 7.5 and sonicate on ice (Note 7).
4. Add 100 µL of 200 mM iodoacetamide in 20 mM triethylammonium bicarbonate to achieve final concentration of 20 mM iodoacetamide and incubate the sample for 20 min in the dark at RT.
5. After incubation, digest the sample using 5.5 µL of trypsin (enzyme to substrate ratio 1:50 – 2 % trypsin; one or two µg of enzyme) overnight (12–16 h) at 37oC.
6. To stop the reaction, add 100 % Formic Acid to a final concentration of 5% (add 56 µL FA) and leave for 5 min at RT.
7. Centrifuge for 45 min at 14,000g 4º C in order to remove pellet lipids and other vestiges.
8. Removal the supernatant to another microtube (Note 8).

3.6 Desalting and Concentration of Peptides

1. Use 0.1 % TFA to dilute the peptide sample achieving 1 mL of final volume and adjusting the pH to 2.0.
2. Wash the cartridge with 1 mL of 100 % methanol (activation solution 1) followed by 1 mL of 100 % ACN (activation solution 2) (Note 9).
3. Balance the cartridge twice using 2 mL of 0.1 % TFA.
4. Load the sample onto the cartridge slowly and collect the flow through (FT).
5. Apply again the FT slowly in the same cartridge.
6. Wash the cartridge twice with 1 mL of 0.1% TFA.

7. Elute the peptides in a new microtube with 1 mL of solution composed by 70 % ACN/0.1 % TFA.
8. Dry the sample in a concentrator or lyophilizer.
9. Reconstitute the sample in 20 mM ammonium formate pH 10.

3.7 NanoLC-MS/MS analyses

Before starting a gradient for peptide separation, make sure that your LC system is set up properly and that you use freshly prepared and degassed solvents. Set and keep the temperature of the sample manager at a constant temperature of 6 oC while samples are stored therein.

1. Create your LC-MS/MS method. Load samples of 500 ng into a M-Class HSS T3 column. Set peptide elutions using an acetonitrile gradient from 7% to 40% (v/v) for 90 min at a flow rate of 0.4 µL/min directly into a Synapt G2-Si HDMS.
2. Use [Glu1]-fibrinopeptide B at a concentration of 100 fmol/µl as a lock mass compound. Use the auxiliary pump of the LC system to deliver GFP to the reference sprayer of the NanoLockSpray source at 0.5 µL/min.
3. Turn MS acquisition on by the LC-software aligning the gradient of reversed phase chromatography with the beginning of MS acquisition. Perform MS analysis in DIA mode using ion mobility separation and CID fragmentation. Ramp your transfer cell collision energy from 25 to 55 eV in the elevated energy scan.
4. Perform triplicate LC-MS analysis of each sample.

3.8 Data processing

1. Perform initial signal processing of continuum LC-IMS-MSE data using Progenesis QI for Proteomics. Create a new project for your experiment.
2. Add the acquired raw data files to the project.
3. Provide lock mass m/z as 785.8426 to perform the calibration
4. Set up processing parameters: MSe experiment, 150 counts for the low energy threshold, 50.0 counts for the elevated energy threshold and 750 counts for the intensity threshold. Import the data.
5. Start automatic processing selecting for automatic alignment of the runs (assess all runs in the experiment for suitability).
6. Proceed with automatic peak picking using 8 as maximum ion charge and adjust the sensitivity method of the automatic peak picking algorithm for 4.
7. Define your experiment design (optional).
8. Set the parameters for automatic peptide identification: choose your target-decoy database for peptide and protein identification; trypsin should be selected as digestion enzyme and one missed cleavage can be allowed. Set carbamidomethyl C and oxidation M as fixed and variable modifications, respectively.
9. Choose relative quantitation using Hi-N and 3 peptides to measure per protein.
10. Use protein grouping.

4. Notes

1. During unfreezing, it is indicated move the cryovial circularly inside the bath.
2. For centrifuge cells, it is better to use mobile centrifuge rotor angle.
3. Depending on the number of cells, it is possible to divide the pellet in more than one T75 cell culture flask.
4. Cultures should be split at ~90% confluency.
5. Lysis buffer volume depends on the pellet size; here we used 107 cells.
6. Mix by vortexing and pipette cell pellet up and down. Cell lysate is going to form a viscous solution due to the presence of DNA.
7. Probes/tips must be submerged properly. If the tip is not submerged enough the sample will foam or bubble. If the tip is too deep it will not circulate the sample effectively. Both conditions will end up with poor results. Foaming can also be caused when the amplitude setting is too high. The tip must not touch the sides of the tube to avoid releasing plastic on the sample.
8. It is better use microtubes with low protein retention, i.e. LoBind from Eppendorf or Maximmun Recovery from Axygen.
9. The option of cartridges depends on the quantity of material. For peptide samples with quantity higher or equal to 500 μg, the Oasis HLB cartridges are often a choice.

5 References

1. Verkhratsky, A., Kirchhoff, F., Planck, M. & Medicine, E. Glutamate-mediated neuronal – glial transmission. 651–660 (2007). doi:10.1111/j.1469-7580.2007.00734.x
2. Hashimoto, K., Malchow, B., Falkai, P. & Schmitt, A. Glutamate modulators as potential therapeutic drugs in schizophrenia and affective disorders. Eur. Arch. Psychiatry Clin. Neurosci. 263, 367–377 (2013).
3. Verkhratsky, A. & Kirchhoff, F. NMDA Receptors in Glia. 13, (2016).
4. Mayer, M. L. & Armstrong, N. Structure and function of glutamate receptor Ion channels. (2004). doi:10.1146/annurev.physiol.66.050802.084104
5. Meador-woodruff, J. H. & Healy, D. J. Glutamate receptor expression in schizophrenic brain 1. 288–294 (2000).
6. Krystal, J. H. et al. REVIEW NMDA Agonists and Antagonists as Probes of Glutamatergic Dysfunction and Pharmacotherapies in Neuropsychiatric Disorders. 125–143 (1999).
7. Coyle, J. T. The Glutamatergic Dysfunction Hypothesis for Schizophrenia. (1996).
8. Arbor, A. Excitatory Amino Acids and Alzheimer ' s Disease. 10, 593–602 (1989).
9. Michael, A. The NMDA Receptor, NMDA Antagonists and Epilepsy Therapy. 44, 279–292 (1992).
10. Lewis, D. a & Lieberman, J. a. Catching up on schizophrenia: natural history and neurobiology. Neuron 28, 325–334 (2000).

11. Lodge, D. & Mercier, M. S. Ketamine and phencyclidine: The good, the bad and the unexpected. Br. J. Pharmacol. 172, 4254–4276 (2015).
12. Guest, P. C. et al. MK-801 treatment affects glycolysis in oligodendrocytes more than in astrocytes and neuronal cells: insights for schizophrenia. Front. Cell. Neurosci. 9, 1–10 (2015).
13. Cassoli, J. S. et al. Effect of MK-801 and clozapine on the proteome of cultured human oligodendrocytes. Front. Cell. Neurosci. (2016). doi:10.3389/fncel.2016.00052
14. Mclaurin, J., Trudel, G. C., Shaw, I. T., Antel, J. P. & Cashman, N. R. A Human Glial Hybrid Cell Line Differentially Expressing Genes Su bserving Oligodendrocyte and Astrocyte Phenotype. 283–293 (1993).
15. Buntinx, M. et al. Characterization of three human oligodendroglial cell lines as a model to study oligodendrocyte injury: Morphology and oligodendrocyte-specific gene expression. J. Neurocytol. 32, 25–38 (2003).
16. Riper, S. K. Van, Jong, E. P. De, Carlis, J. V & Griffin, T. J. Mass Spectrometry-Based Proteomics: Basic Principles and Emerging Technologies and Directions. (2013). doi:10.1007/978-94-007-5896-4
17. Nascimento, J. M. & Martins-de-Souza, D. The proteome of schizophrenia. npj Schizophr. 1, 14003 (2015).
18. Gundry, R. L. et al. Preparation of Proteins and Peptides for Mass Spectrometry Analysis in a Bottom-Up Proteomics Workflow. 1–23 (2009). doi:10.1002/0471142727.mb1025s88
19. Distler, U., Kuharev, J., Navarro, P. & Tenzer, S. Label-free quantification in ion mobility-enhanced data-independent acquisition proteomics. Nat. Protocols 11, 795-812, doi:10.1038/nprot.2016.042
20. Melo-Braga, Marcella Nunes, et al. "Comprehensive protocol to simultaneously study protein phosphorylation, acetylation, and N-linked sialylated glycosylation." Proteomic Profiling: Methods and Protocols (2015): 275-292.

9. CAPÍTULO 2

Biochemical pathways triggered by antipsychotics in human oligodendrocytes: potential of discovering new treatment targets

Caroline Brandão-Teles[1]; Valéria de Almeida[1];
*Juliana S. Cassoli[1]; Daniel Martins-de-Souza[1,2,3, *]*

1- LaboratoryofNeuroproteomics, Institute of Biology, Department of Biochemistry and Tissue Biology, Universityof Campinas (UNICAMP), Campinas, SP, Brazil.

2- UNICAMP's Neurobiology Center, Campinas, SP, Brazil

3- Instituto Nacional de Biomarcadores em Neuropsiquiatria (INBION) Conselho Nacional de Desenvolvimento Científico e Tecnológico, São Paulo, Brazil

* Correspondence:
Prof. Daniel Martins-de-Souza, PhD
Department of Biochemistry and Tissue Biology
Universityof Campinas (UNICAMP)
Rua Monteiro Lobato 255
13083-862, Campinas/Sao Paulo/Brazil
Telephone: +55 (19) 35216129
E-mail: dmsouza@unicamp.br

Abstract

Schizophrenia is a psychiatric disorder that affects more than 21 million people worldwide. It is an incurable disorder and the primary means of managing symptoms is through administration of pharmacological treatments, which consist heavily of antipsychotics. First-generation antipsychotics have the properties of D_2 receptor antagonists. Second-generation antipsychotic are antagonists of both D_2 and $5HT_2$ receptors. Recently, there has been increasing interest in the effects of antipsychotics beyond their neuronal targets and oligodendrocytes are one of the main candidates. Thus, our aim was to evaluate the molecular effects of typical and atypical drugs across the proteome of the human oligodendrocyte cell line, MO3.13. For this, we performed a mass spectrometry-based, bottom-up shotgun proteomic analysis to identify differences triggered by typical (chlorpromazine and haloperidol) and atypical (quetiapine and risperidone) antipsychotics. Proteins which showed changes in their expression levels were analyzed *in silico* using Ingenuity® Pathway Analysis, which implicated dysregulation of canonical pathways for each treatment. Our results shed light on the biochemical pathways involved in the mechanisms of action of these drugs, which may guide the identification of novel biomarkers and the development of new and improved treatments.

Keywords: Schizophrenia, mechanism of action, proteomics, biomarkers, chlorpromazine, haloperidol, quetiapine, risperidone

Introduction

Schizophrenia is a chronic and debilitating psychiatric disorder characterized by positive (e.g., hallucinations and delusions), negative (e.g., anhedonia, alogia, apathy and poor self-care) and cognitive (e.g., deficits in executive function, working memory and recognition memory) symptoms. The risk for schizophrenia is 0.7% in the broad population but increases with the degree of genetic relationship (HAYASHI-TAKAGI, 2016). Treatment is based on administration of antipsychotics to reduce the recurrence and severity of psychosis and improve general symptoms, thereby providing some degree of improvement in quality of life for patients. Antipsychotics can be divided into two categories known as typical (first-generation) and atypical (second-generation) drugs. A common pharmacological property present in both is blockage of the dopamine D_2 receptor (KANTOFF et al., 2010; LEUCHT et al., 2009; SHEN, 1999).

First-generation antipsychotics such as chlorpromazine and haloperidol are effective in reducing positive symptoms but they can cause severe side effects such as extrapyramidal symptoms and tardive dyskinesia. Additionally, they are not as effective against the negative and cognitive symptoms, which contribute to most of the deficiency associated with schizophrenia (LIEBERMAN et al., 2005). Second-generation antipsychotics like quetiapine and risperidone are also effective against positive symptoms but are more effective in reducing negative symptoms compared to first-generation drugs. However, severe side effects such as weight gain, metabolic syndrome and sedation may occur.

The pathophysiology of schizophrenia has been associated with disturbances in several neurotransmitter systems. One of the most well established theories is the dopamine hypothesis, which agrees with current antipsychotics targeting dopaminergic systems. This and other hypotheses have normally implicated neurons, although other molecular mechanisms involving different cell types in the brain may be associated with the pathophysiology of schizophrenia (COYLE, 1996; JU; CUI, 2015). Oligodendrocytes are the cells responsible for myelination in the central nervous system (CNS) through expression of genes that encode myelin structural proteins in a specific and regulated manner, and myelination of axon fibers by oligodendrocytes is essential for the rapid conduction of action potentials (BUNTINX et al., 2003).

Scientific evidence suggests that one of the reasons for neuronal disconnection is a due to disruptions in myelination. This could be due to poor functioning of oligodendrocytes. Such a disruption may lead to dysfunctions of perception, behavior and cognition as seen in

schizophrenia (BUNTINX et al., 2003). It is important to mention that myelination continues throughout development of the young adult brain, coinciding with the average age of onset of the pathology. We have demonstrated recently an increase in the levels of many proteins in cultured oligodendrocytes treated with MK-801, an antagonist of the NMDA receptor, suggesting that these cells may be targets for antipsychotics (CASSOLI et al., 2016).

Here we performed a quantitative proteomic analysis to investigate changes in protein expression triggered by antipsychotics in a cell line of human oligodendrocytes (MO3.13). The effects of two first-generation (chlorpromazine and haloperidol) and two second-generation (quetiapine and risperidone) antipsychotics were investigated. Our aim was to better understand the biochemical pathways involved in the mechanisms of action of these drugs in attempts to find new biomarkers and targets which may increase our understanding of the disease and therapeutic response and assist in the development of more specific and improved treatments for patients with schizophrenia.

Experimental Procedures

Cell culture, treatments and proteome extraction

Human hybrid MO3.13 cells are classified as an immature oligodendrocyte cell line (BUNTINX et al., 2003). MO3.13 cells were grown in DMEM medium supplemented with 0.5% penicillin/streptomycin (Sigma-Aldrich, St. Louis, MO, USA) and 10% heat-inactivated fetal bovine serum (Life Technologies, Darmstadt, Germany) at 37◦C in a humidified atmosphere containing 5% CO_2 as described previously (BRANDÃO-TELES et al., 2017). The cells were treated with each antipsychotic once and collected after 8h as follows with respect to dosage and drug: Group 1 – 10 µM chlorpromazine; Group 2 – 50 µM haloperidol; Group 3 – 50 µM quetiapine; Group 4 – 50 µM risperidone; Group 5 – chlorpromazine and haloperidol vehicle solution (0.01 M HCl); Group 6 - quetiapine and risperidone vehicle solution (DMSO). The antipsychotic doses were chosen as described previously (MARTINS-DE-SOUZA; LEBAR; TURCK, 2011). It should be noted that the levels of glycine (0.4 mM) and glutamate (20 uM) contained in DMEM and FBS respectively are adequately high to activate NMDA receptors (BLANKE; VANDONGEN, 2009; CUMMINGS; POPESCU, 2015). MO3.13 cells were centrifuged at 1,200g for 5 min and the pellets homogenized in a lysis buffer consisting of 6M urea, 2M thiourea, 10mM DTT, with protease and phosphatase inhibitors, 0.1 mM sodium pervanadate (lysis buffer). Protein lysates were centrifuged at 14,000g for 45 min at 4ºC in order to remove pelleted lipids and other vestiges. The

supernatants were collected, desalted and concentrated as described in Brandão-Teles et al, 2017. Protein concentrations were determined by Qubit® Protein Assay Kit.

NanoLC-ESI MS/MS, data processing and database searching

Proteomic analyses were performed in a bidimensional microUPLC tandem nanoESI-UDMSE platform by multiplexed data-independent acquisitions experiments, using a 2D-RP/RP Acquity UPLC M-Class System (Waters Corporation, Milford, MA) coupled to a Synapt G2-Si mass spectrometer (Waters Corporation, Milford, MA). First, the samples were fractionated using a one-dimension reversed-phase approach and the constituent proteins (0.5µg) were loaded into a M-Class HSS T3 column (100 Å, 1.8 µm, 75 µm × 150 mm, Waters Corporation, Milford, MA). The fractionation was achieved using an applied acetonitrile gradient from 7% to 40% (v/v) over 95 min at a flow rate of 0.4 µL/min. MS and MS/MS data were acquired in positive resolution mode in the Synapt G2-Si mass spectrometer with a resolving power around 25,000 FWHM using the ion mobility separation of precursor ions method (Geromanos et al., 2012) over a range of 50-2000 m/z. Precursor ion information was collected in low-energy MS mode by applying a constant collision energy of 4 eV in the range of 50-2000 m/z. Fragment ion information was obtained in the elevated energy scan using drift-time specific collision energies as detailed previously (CASSOLI et al., 2017). The spectral acquisition time in each mode was 0.6 s with a 0.05 s-interscan delay, resulting in an overall cycle time of 1.3s for the acquisition of one cycle of low and high energy data. The lock mass channel was sampled every 30s. The mass spectrometer was calibrated using a human [Glu1]-Fibrinopeptide B (785.8426 m/z) solution delivered through the reference sprayer of the NanoLock Spray source.

Data processing and database searches

Proteins were identified using dedicated algorithms and searching against the Uniprot Human Proteomic Database, version 2016/09, with the default parameters for ion accounting (CASSOLI; MARTINS-DE-SOUZA, 2017; LI et al., 2009). The databases used were reversed “on the fly” during the search queries and appended to the original database to assess the false-positive identification rate. For correct spectral processing and database searching conditions, we used the Progenesis QI for Proteomics software package with Apex3D, Peptide 3D, and Ion Accounting informatics (Waters Corporation). This software starts with loading of the LC-MS data, followed by alignment and peak detection, which creates a list of

interesting peptide ions that are explored within Peptide Ion Stats by multivariate statistical methods. The following parameters were considered in identification of peptides/proteins: 1) digestion by trypsin with one or more missed cleavages; 2) variable modification by oxidation (M) and fixed modification by carbamidomethyl (C); and 3) a false discovery rate (FDR) less than 4%. Identifications that did not satisfy these criteria were rejected.

In addition, all proteins had to fit the following criteria in all analyzed datasets to be considered for quantification: (1) identification by at least 1 non-redundant peptide with at least 4 ion counts; and (2) an ANOVA of less than 0.05.

Analysis in silico

For interpreting the functional significance of differentially expressed proteins, their UniProt accession IDs were uploaded into the Ingenuity Pathways Knowledgebase (IPKB) through the algorithm Ingenuity Pathway Analysis (IPA, Ingenuity Systems, Qiagen, Redwood, CA, USA; www.ingenuity.com) to determine potential interactions between these proteins, between these proteins and other proteins, to canonical pathways and to disease lists contained in the IPKB.

Results

All antipsychotics affected the expression levels of some proteins (**Figure 1**) and consequently triggered changes in several biological processes, according to the *in silico* IPA profiling. Some of these differences were common among treatments and others were specific to each antipsychotic analyzed.

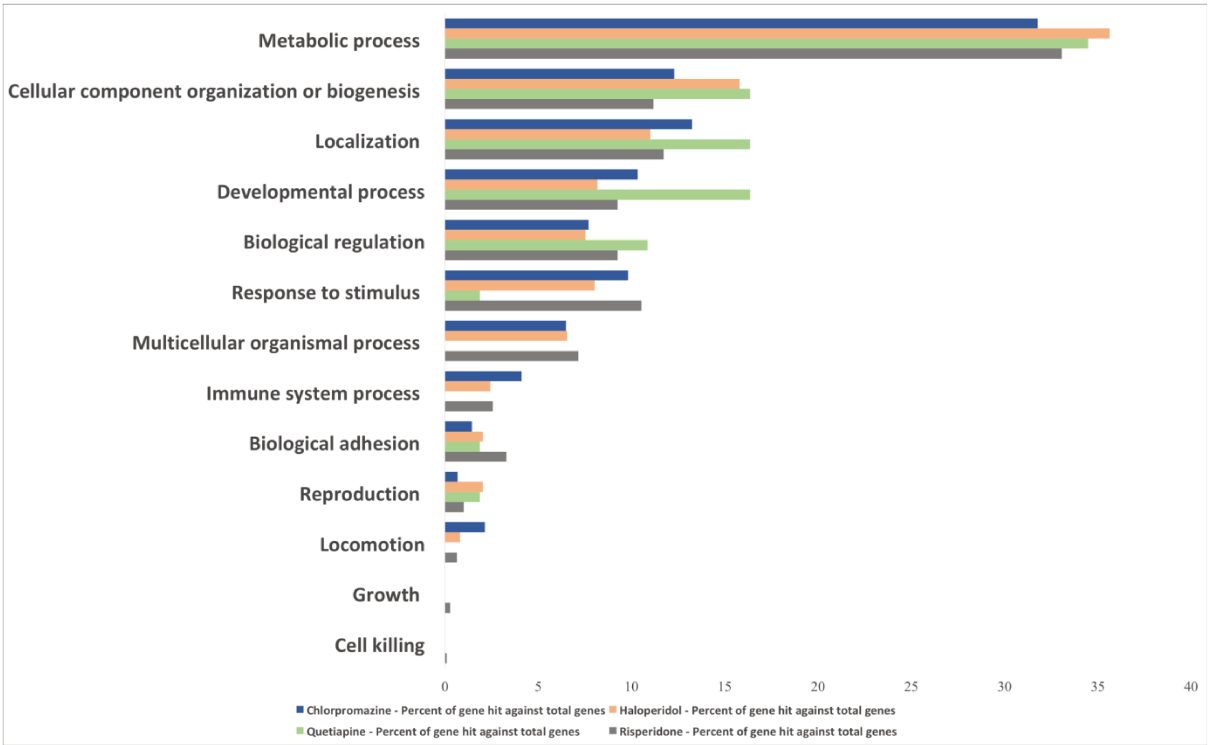

Figure 1: GO biological processes affected by antipsychotic treatment in MO3.13 cell cultures.

Chlorpromazine treatment induced changes in the abundance of 609 proteins and haloperidol induced alterations in 942 proteins, compared to the levels of these proteins in un-treated control cells (**Tables 1** and **2**, respectively). Proteins with different abundances affected 80 and 74 canonical pathways in cells treated with chlorpromazine and haloperidol, respectively (**Table 3**). For atypical antipsychotics, the quetiapine treatment affected expression of 99 proteins, while risperidone induced changes in 1041 proteins (**Tables 4** and **5,** respectively). These proteome changes showed associations with 10 and 123 canonical pathways, respectively (**Table 6**).

Figure 1 shows the biological pathways which were affected both uniquely and in common by the tested antipsychotics. All antipsychotic medications caused changes in metabolic processes. The quetiapine treatment affected fewer biological processes than the other antipsychotics, reflected by the lowest number of proteins at expressed at different levels in the MO3.13 cells. On the other hand, processes such as “localization” and “developmental process” were affected more by the quetiapine treatment. Risperidone treatment triggered marked differences in “biological adhesion”, compared to the other antipsychotics and, at a lower scale, it induced changes in “growth” and “cell killing”

pathways, which were not affected by any of the other treatments. Chlorpromazine induced more differences in “Immune system process” compared to other treatments.

Proteins identified with different abundances were analyzed at IPA according to their canonical pathways. We only considered pathways represented by at least 10 proteins. For typical antipsychotics, haloperidol modulated almost twice the number of canonical pathways (40) compared to the chlorpromazine treatment (22) (**Table 3**). In addition, 59% of the pathways were altered by both drugs, suggestive of similarities in their mechanisms of action. On the other hand, only 32.5% of the pathways affected by haloperidol overlapped with those altered by chlorpromazine, suggesting that haloperidol may induce its effects by acting through more specific pathways.

For atypical antipsychotics, no overlaps in the canonical pathways affected were observed, most likely because quetiapine only enriched 10 canonical pathways and no more than 2 associated proteins were identified. Oppositely, the risperidone treatment led to an enrichment of the largest number (77) of canonical pathways. Compared to typical antipsychotics, 55% and 58% of the pathways enriched by chlorpromazine and haloperidol, respectively, overlapped with those triggered by risperidone. Although presenting specific pathway differences (66%), this does not rule out the possibility that risperidone may eventually use routes similar to typical antipsychotics while modulating the MO3.13 cell response. Depending on the dosage, risperidone may be considered clinically as a typical antipsychotic and this could be due to the high specificity of the effects induced by the risperidone treatment.

Discussion

Most of what we know about antipsychotic mechanisms of action was discovered originally through effects on receptors in neuronal studies. However, fewer studies have been carried out investigating the effects of these drugs on glial cells. Considering the growing interest in the role of oligodendrocytes in neurotransmission, it makes sense to characterize the modulatory effects of antipsychotics on the biological processes of these cells. Thus, we investigated the acute response of healthy oligodendrocytes to both first- and second-generation antipsychotics through identification of proteins that were changed subsequently in their abundance.

Common effects

AKT

Protein kinase B (AKT) is present in mammalians cells in three different isoforms: AKT1, AKT2 and AKT3. AKT participates in numerous cellular functions such as survival, proliferation, migration, cell death and growth. In the nervous system, AKT is one of the proteins involved in modulation of synaptic plasticity, which can affect processes such as long-term potentiation, working memory and fear conditioning. This protein is also important in the pre-synaptic trafficking of dopamine and norepinephrine transporters (EMAMIAN, 2012; STEPHEN; JONATHAN, 2010).

AKT1 has been shown to be associated with schizophrenia (BALU; COYLE, 2011; STEPHEN; JONATHAN, 2010), with decreased levels found in lymphocytes and frontal cortex (EMAMIAN et al., 2004), while no changes have been observed in the levels of AKT2 and AKT3 (EMAMIAN et al., 2004). Decreased AKT1 was also reported in the prefrontal cortex of schizophrenia patients but not in bipolar disorder patients (THISELTON et al., 2008). Considering that chlorpromazine increased AKT1 levels in this study, this protein could be an important biomarker for the pharmacological effects of this drug. Dopamine D2 receptors (D2R) are modulated by AKT (BEAULIEU et al., 2007) and activation of D2R by dopamine results in formation of a signaling complex containing β-arrestin 2, PP2A and AKT. PP2A inactivates AKT via dephosphorylation, leading to an increase of GSK3 activity. Thus, D2 antagonists, such as chlorpromazine and antipsychotics in general, may prevent AKT inactivation by non-recruitment of β-arrestin 2 and consequently by non-formation of the protein complex (EMAMIAN, 2012; ZHENG et al., 2012). Although the treatments with haloperidol and risperidone did not alter levels of AKT1, they affected proteins associated with AKT1-linked pathways, such as EIF2 signaling, PI3K/AKT signaling, Wnt/β-catenin signaling, as well as regulation of eIF4 and p70S6K and mTOR signaling (Figure 2). These pathways are important in cellular growth, proliferation and development (EMAMIAN, 2012). In this regard, our data point to a possible role of dopamine receptor antagonists in increasing AKT1 levels in healthy oligodendrocytes.

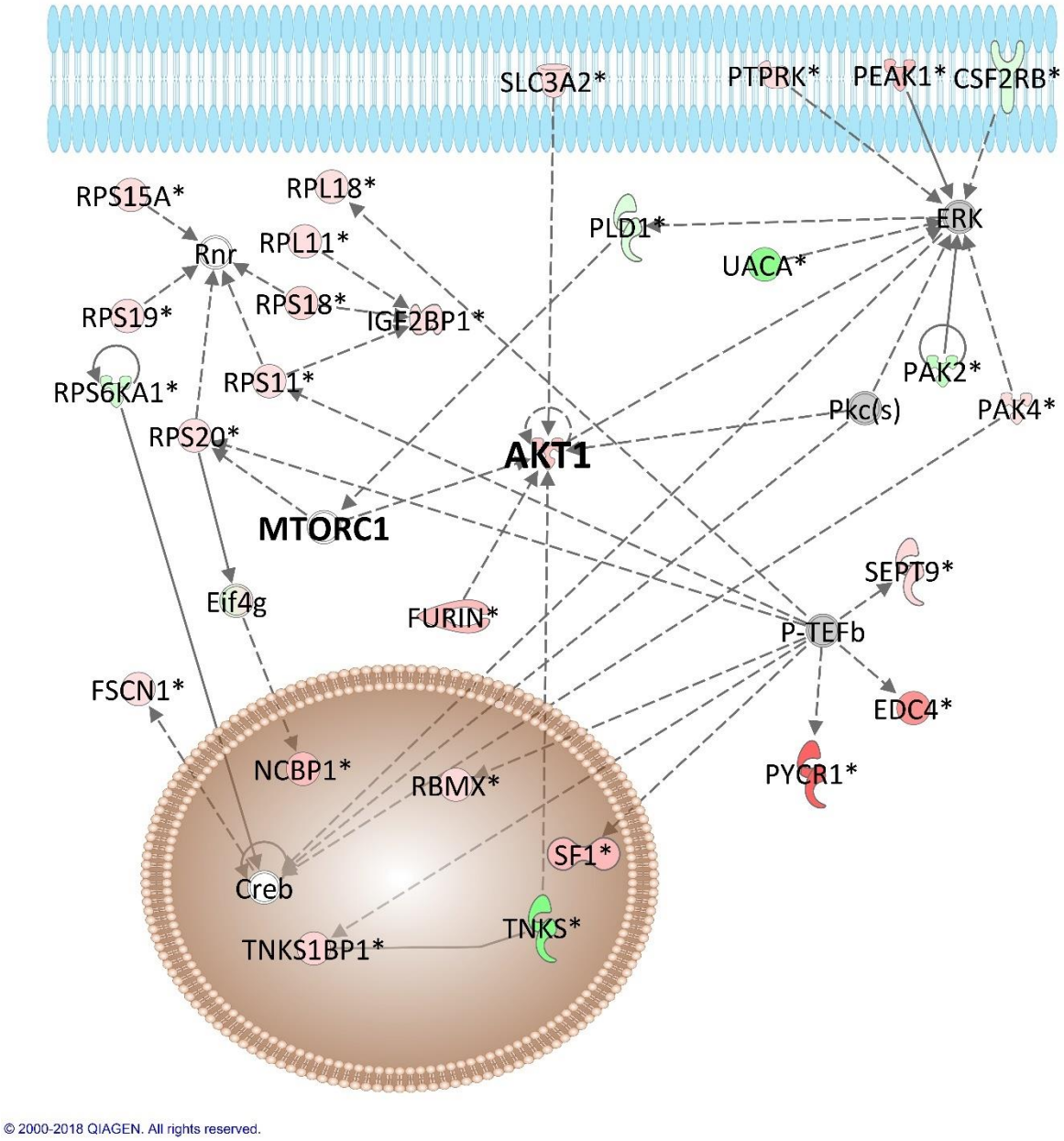

Figure 2: Network interactions, and their interactors, of differentially expressed proteins of chlorpromazine-treated oligodendrocytes. The network was generated from differentially expressed proteins by IPA. Colored interactors represent proteins previous found in the proteome. Full and dashed lines depict direct and indirect connections respectively.

EIF2

Another effect of antipsychotics is related to the translation initiation factors, an important group of proteins required for protein synthesis on ribosomes. EIF2 (eukaryotic initiation factor-2) mediates the binding of Met-tRNA to the ribosome in a GTP-dependent manner (CARTER, 2007). While chlorpromazine increased the expression of proteins

associated with EIF2 signaling, haloperidol treatment led to decreased levels, and both increased and decreased levels were observed following risperidone treatment. This suggests that these drugs may have differential effects on protein synthesis.

mTOR

The mammalian target of rapamycin (mTOR) signaling pathway plays an important role in regulation of protein synthesis, mainly in neurodevelopment and synaptic plasticity (YOON et al., 2008). One study observed that acute treatment with the NMDA receptor antagonist MK-801 resulted in increased phosphorylation of proteins in the mTOR-p70S6K pathway in rat frontal cortex (YOON et al., 2008). Another investigation showed that haloperidol treatment appears to activate the AKT-mTORC1 pathway leading to changes in protein synthesis (BOWLING et al., 2014). In contrast, we observed that the treatments with chlorpromazine, haloperidol and risperidone may lead to decreased activation of the mTOR pathway. These differential effects could be due to variations in brain regions and cell types as we have specifically investigated an oligodendrocyte cell line in this study. This possibility is supported by the finding that components of the mTOR pathway were found to be decreased in post mortem brain tissue from patients with schizophrenia (ENGLISH et al., 2015).

Ubiquitination pathway

We also observed that the treatment with chlorpromazine and haloperidol resulted in alterations in the levels of proteins associated with the ubiquitination pathway. The treatment with chlorpromazine increased levels of BIRC6 (a protein that is part of the E2 complex), heat shock family proteins (HSP90AB1, HSP90B1, HSPA8, and HSPA1L), proteins belonging to the proteasome (PSMA6, PSMB6, PSMD4, and PSMD7) and ubiquitin specific peptidases (USP25, USP28, USP48, USP53). The main role of ubiquitination pathway is protein degradation through the conjugation of various portions of ubiquitin to the target protein followed by degradation of the protein bound to the polyubiquitin chain by the 26S proteasome complex (RYAN et al., 2006). Studies have shown decreased expression of genes related to this pathway in the dentate granule neurons and prefrontal cortex of schizophrenia patients (ALTAR et al., 2005; MIDDLETON et al., 2002). Another study which carried out a blood-based microarray analysis found changes in the ubiquitin proteasome pathway of schizophrenia patients (BOUSMAN et al., 2010). We suggest that chlorpromazine may restore the levels of the proteins involved in the ubiquitin pathway in schizophrenia, possibly

aiding cellular processes regulated by this pathway such as signal transduction, synaptic plasticity, intracellular trafficking, endocytosis, DNA repair and neural activity.

Energy metabolism

Multiple studies have now demonstrated a dysregulation in energy metabolism in schizophrenia. Proteomics analysis of *post mortem* brains of patients with schizophrenia showed alterations in the levels of energy metabolism-associated proteins, such as aldolase C (ALDOC), enolase 2 (ENO2) and glyceraldehyde-3-phosphate dehydrogenase (GAPDH) (Saia et al., 2015). Another investigation using samples of *post mortem* hippocampus of patients with schizophrenia found that glycolysis- and gluconeogenesis-associated proteins were altered, as seen by decreased levels of ALDOC and increased ENO1 (SCHUBERT; FÖCKING; COTTER, 2015). Changes in energy metabolism have also been implicated in the effects of antipsychotics in oligodendrocytes. One study showed that haloperidol increased the amount of glucose and decreased the lactate levels present in the extracellular medium of cultured oligodendrocytes, suggesting that haloperidol affected glucose uptake in these cells (STEINER et al., 2014). In the present study, most proteins related to glycolysis and gluconeogenesis were decreased by haloperidol, whereas the haloperidol and chlorpromazine treatments increased the levels of glycolysis-related proteins and none of the atypical antipsychotics used in this study altered the levels of proteins belonging this pathway.

CYP450 family

The finding that the haloperidol treatment resulted in increased levels of cytochrome P450 3A43 (CYP3A43) in oligodendrocytes is interesting as CYP450 family of proteins are responsible for metabolism of practically all antipsychotics and other drugs in liver tissue (BRANDL et al., 2015). This essentially serves as a mechanism to regulate the levels of active drug hitting the target cells. It is already well known that CYP genes are involved in liver metabolism and, therefore, the therapeutic efficacy of psychotropic drugs used in the treatment of schizophrenia, depression and bipolar disorder (ALTAR et al., 2013). For example, it has been shown that haloperidol can inhibit the CYP2D6 enzyme, potentially leading to abnormally high concentrations of this drug in plasma (LLERENA et al., 2004). Another study proposed that an explanation for the variability in pharmacokinetics among subjects using haloperidol may be the partitioning of the CYP3A isoenzymes, CYP3A4 and CYP3A5 (KALGUTKAR et al., 2003). Therefore, our finding of increased levels of CYP3A43 in oligodendrocytes suggests that this enzyme may deliver enhanced metabolism

and increased turnover of active haloperidol directly in these cells. These findings are consistent with a recent study that found expression of multiple CYP450 enzymes at high levels in neurons and astrocytes, and at lower levels in oligodendrocytes, confirming the cell-specific localization of CYPs in the brain (VICHI et al., 2015). Thus, brain cell cultures could potentially be used as models for assessing toxicity and detoxification of new drugs targeting the brain. In line with this, we also found that the treatment with risperidone led to decreased levels of another two proteins belonging to the CYP family, CYP2U1 and CYP3A5. It is likely therefore that the decrease in CYP3A5 induced by risperidone could result in decreased metabolism of the drug in oligodendrocytes, potentially leading to toxic levels of this drug.

Spliceosome

Another group of proteins modulated by chlorpromazine, haloperidol and risperidone in oligodendrocytes was associated with spliceosome complex. The spliceosome machinery is composed of five different RNP subunits and numerous protein cofactors that together will participate in the splicing process, i.e., removal of the introns in the pre-mRNA (MATERA; WANG, 2014). Among the proteins identified, treatment with chlorpromazine altered the levels of a few proteins, such as increased levels of splicing factor 3a subunit 1 (SF3A1) and decreased levels of nuclear heterogeneous ribonucleoprotein M (hnRNPM). The haloperidol treatment also increased the levels of spliceosome proteins, such as U2SURP and the risperidone treatment increased the levels of hnRNPK and decreased hnRNPA3, hnRNPC, small nuclear ribonucleoprotein U1 subunit 70 (snRNP70), snRNPA1 and snRNPE. Recently, we found changes in 8 proteins belonging to the hnRNP family in oligodendrocytes treated with clozapine (CASSOLI et al., 2016). We also found altered levels of hnRNPC, hnRNPK and hnRNPU in *post mortem* samples of the anterior temporal lobe (ATL) from patients with schizophrenia (SAIA-CEREDA; SANTANA, 2017). Additionally, we found changes in hnRNPC levels in the temporo-posterior gyrus of patients with schizophrenia (MARTINS-DE-SOUZA et al., 2009). Finally, Iwata et al reported that overexpression of the hnRNP C2 variant leads to a decrease in MBP expression (IWATA et al., 2011).

14-3-3 family

Another set of proteins found at altered levels following all treatments, except in chlorpromazine, was proteins from the 14-3-3 family. There are seven known mammalian 14-3-3 isoforms, and 14-3-3 proteins are abundant in the brain, accounting for approximately 1% of the total soluble proteins (FU; SUBRAMANIAN; MASTERS, 2000). 14-3-3 proteins play

fundamental roles in many processes, including the cell cycle, apoptosis, synaptic plasticity and neuronal differentiation and migration (FU; SUBRAMANIAN; MASTERS, 2000). In this study, the haloperidol treatment led to decreased levels of 14-3-3 epsilon (YWHAE), beta/alpha (YWHAB) and gamma (YWHAG) and the quetiapine and risperidone treatments induced increased levels of 14-3-3 beta/alpha (YWHAB). Several studies found changes in proteins of the 14-3-3 family in brain tissues from schizophrenia patients (MIDDLETON et al., 2005; QING et al., 2016; SCHUBERT; FÖCKING; COTTER, 2015). Our group found disruption of 14-3-3 signaling in the corpus callosum of patients with schizophrenia (SAIA et al., 2015). We also observed that clozapine treatment resulted in increased levels of 14-3-3 protein eta (YWHAH) (CASSOLI et al., 2016), consistent with the effects of the atypical antipsychotics used in this study.

Drug-specific differences triggered by antipsychotics in the oligodendrocytes proteome

Chlorpromazine

Neuregulins are member proteins of the epidermal growth factor (EGF) family and are ligands for tyrosine kinases receptors (ErbB family), which play a key role in the development, maintenance, and repair of the nervous system. Recent genetic studies have demonstrated a possible role of neuregulin 1 and its receptor erbB in the pathophysiology of schizophrenia (AVRAMOPOULOS, 2017; HAHN et al., 2006; HASHIMOTO et al., 2004). Moreover, neuregulins play role in some process implicated in schizophrenia, such as neuronal migration, neurotransmitter function such as NMDA, GABA, α-7, as well as dopamine and oligodendrocyte biology (LAW et al., 2006). Although one study using mRNA expression profiling found no changes in neuregulins (type I, type II, and type III) in the dorsolateral prefrontal cortex of patients with schizophrenia (HASHIMOTO et al., 2004), another study analyzed mRNA abundance of Neuregulin I (types I-IV) in the hippocampus of patients with schizophrenia and found a variation in the expression of these isoforms (LAW et al., 2006). Although neuregulin expression was not affected by chlorpromazine, according to the IPA analysis, some neuroregulin-associated proteins, such as AKT1, DLG4, HSP90AB1, HSP90B1, PLCG1, SOS2, and ITGA5, were altered. Additionally, proteins belonging to ErbB signaling were also found to be changed, such as increased AKT1, CDC42, PAK4, PLCG1 and SOS2 and decreased levels of MAPK10 and PAK2.

Interestingly, neuregulin is associated with the hypofunction of the NMDA receptor through ErbB in schizophrenia (LAW et al., 2006). One study evaluated the regulation of

NMDA receptor currents mediated by neuregulin signaling pathways and found that neuregulin significantly decreased these in prefrontal neurons and slices (WANG et al., 2003). These data suggest that increased neuregulin levels could cause reduced NMDA receptor mediated signaling, consistent with one of the main hypotheses of the pathophysiology of schizophrenia (hypofuction of NMDA receptors) (WANG et al., 2003). Interestingly, our data showed that chlorpromazine reduced levels of the NMDA2A receptor subunit. From this it can be speculated that the chlorpromazine-induced increase in the neuregulin pathway may contribute to the accentuation of NMDA receptor hypofunction in patients with schizophrenia treated with this antipsychotic.

Haloperidol

A regular side effect of haloperidol treatment and its limitation in the clinic is the extrapyramidal symptoms and tardive dyskinesia. However, the exact pathophysiology of how this drug induces these side effects has not yet been clearly elucidated (PERERA et al., 2011). Oxidative stress constitutes a potential pathogenic mechanism that may contribute to extrapyramidal symptoms, especially to tardive dyskinesia (J.Q. et al., 2014; PERERA et al., 2011; SAMAD; HALEEM, 2017). Recent studies have shown that the repeated administration of haloperidol is able to induce tardive dyskinesia in rats (SAMAD; HALEEM, 2017). Another study using plasma and the enzyme manganese superoxide dismutase (MnSOD) as a biomarker of patients with schizophrenia analyzed the relationship of oxidative stress and tardive dyskinesia. The findings suggested that tardive dyskinesia is more severe in patients suffering from oxidative stress compared with patients who do not have tardive dyskinesia (J.Q. et al., 2014). Furthermore, haloperidol was able to induce oxidative stress, potentially by decreasing the levels of mnSOD and glutathione peroxidase (GPx) in rats (PERERA et al., 2011). Here, we showed that levels of GPx and SOD were decreased in oligodendrocytes treated with haloperidol, consistent with published findings.

As previously mentioned, the oligodendrocytes used in this study consisted of OPCs. It is known that oxidative stress levels in OPCs are naturally high and glutathione levels are considerably lower when compared to astrocytes for example (THORBURNE; JUURLINK, 1996). This is mainly due to the fact that these cells are responsible for the synthesis of myelin that requires a high metabolic level. Furthermore, oxidative stress impairs myelination-related enzymes (JANA; PAHAN, 2013).

Abnormalities in the myelination process have been well documented in schizophrenia, along with a relatively high number of reactive oxygen species (ROS) (MAAS;

VALLÈS; MARTENS, 2017). The redox-induced prefrontal OPC-dysfunction hypothesis suggests that the etiology of cognitive symptoms in schizophrenia is due to action of ROS in innumerable signaling pathways, mainly by inactivation of the mTOR-P70S6K pathway, negatively influencing the proliferation and differentiation of these cells. Dysfunctions in OPCs are observed mainly in the critical period of myelination, which occurs in late adolescence and the associated decrease in myelination in patients with schizophrenia could induce the cognitive symptoms observed in the disease state (MAAS; VALLÈS; MARTENS, 2017). Thus, haloperidol may exacerbate oxidative stress in oligodendrocytes, which may worsen cognitive dysfunction in schizophrenia. Additionally, the condition may be worse when given to patients who are in the critical period of myelination, which coincide with the beginning of the disorder. However, a next step would be to further evaluate the results obtained here, especially during the maturation of these cells.

We found upregulation of the protein Arachidonate 12-lipoxygenase 12S-type (ALOX12), that oxygenates the C-12 of arachidonic acid, producing 12-HPETE (12-hydroperoxyeicosatetraenoic acid), which inhibits protein kinase II. Protein kinase II is responsible for phosphorylation of the rate-limiting enzyme of catecholamine biosynthesis (tyrosine hydroxylase). In this way, levels of 12-HPETE may influence dopamine synthesis (BAE et al., 2012; FUJISAWA; OKUNO, 1989; PIOMELLI; GREENGARD, 1990). A study showed that ALOX 12 could be involved with negative symptoms in schizophrenia (BAE et al., 2012). Consistent with this idea, haloperidol increased the expression of ALOX12 and consequently more 12-HPETE will be available which, in turn, may lead to decreased dopamine levels. Moreover, the activity of ALOX12 can be modulated by glutathione, the main antioxidant in cells. A study using premyelinating oligodendrocytes showed that ALOX12 may be involved in cell death induced by ROS and glutathione depletion (WANG et al., 2004). It has also been found that by blocking the activity of this enzyme using vitamin K, for example, it is possible to prevent arachidonic acid-induced oxidative injury, once the metabolism of amino acids via ALOX12 generates free radicals (LI; WANG; ROSENBERG, 2009). In addition, haloperidol most likely increases oxidative stress in cells, not only by lowering enzyme levels that prevent oxidative stress, but also by increasing ROS production via higher ALOX12 levels.

Quetiapine

Quetiapine has higher affinity for serotonin 5HT2 receptors than D2 dopamine receptors (LEUCHT et al., 1999). In our study, only the glutamic-oxaloacetic transaminase

(GOT) was found to be increased by quetiapine. IPA-analysis showed that in four of the top five canonical pathways, GOT was present in the processes of glutamate degradation, aspartate biosynthesis, L-cysteine degradation, and aspartate degradation II. Numerous transaminases have been implicated in several diseases and GOT has high clinical importance as a potential biomarker (WROBLEWSKI, 1958). Studies have shown that GOT levels are different across tissues, with higher levels in the CNS. Therefore, GOT may have an important role in neurological diseases, such as epilepsy and cerebral tumors (MELLICK; BASSETT, 1956).

Another protein found to be increased following quetiapine treatment belonged to the Notch family (NOTCH2). Notch proteins play an important role in many developmental processes through controlling cell fate decisions (WANG et al., 1998). In animal models, the differentiation of oligodendrocytes can be inhibited by the activation of the Notch pathway (WANG et al., 1998). In schizophrenia, genetic abnormalities in Notch signaling have been reported that may contribute to disease vulnerability during neural development (MAYNARD et al., 2001). Genetic alterations were found in NOTCH2 and these were related to increased waist circumference in patients with schizophrenia (HUKIC et al., 2017). It is already well known that one of the main side effects associated with second generation antipsychotics is the associated weight gain (LEUCHT et al., 2009). Thus, the finding of altered NOTCH2 levels after the quetiapine treatment may be one of the molecular mechanisms associated with this metabolic alteration.

It is known that the metabolism of carbohydrates and lipids are regulated by peroxisome proliferator-activated receptor-γ (PPAR-γ) (AGONISTS, 2003; LIU et al., 2014), and this protein plays role in maintaining normal adipocyte viability as well as insulin sensitivity in both liver and adipose tissue (HE et al., 2003). In our study, we found PPAR-γ levels decreased following the quetiapine treatment. Since increased levels of PPAR-γ have been seen as an important anti-inflammatory factor in both neurological and cardiac diseases (AGONISTS, 2003; GARCIA-BUENO; PEREZ-NIEVAS; LEZA, 2010), the observed decrease here may be indicative of increased cardiovascular risk in patients. It has been suggested that PPAR-γ has a role in psychosis profiles in schizophrenia patients with antipsychotic-increased glucose levels (LIU et al., 2014). In this regard, we suggest that changes in PPAR-γ by quetiapine may be associated with metabolic disturbances in the treatment of patients. In addition, given the anti-inflammatory role of PPAR-γ, agonists of this receptor have been used as a possible neuroprotective agent in several studies of animal models of oral dyskinesia (AGONISTS, 2003; GROVER et al., 2013).

Risperidone

Compared with all other antipsychotics analyzed, risperidone affected a greater number of pathways enriched by IPA. The top five biological pathways of the significantly expressed proteins were epithelial adherens junction signaling, germ cell-sertoli cell junction signaling, EIF2 Signaling, sertoli cell-sertoli cell junction signaling and remodeling of epithelial adherens junctions. There is still little in the literature on the relation of these pathways to schizophrenia. However, these results may be relevant to a more specific mechanism of action of risperidone, although it is not clear whether these are side effect or efficacy-related.

Atypical antipsychotics such as risperidone, seem to be most effective in improving cognitive symptoms of schizophrenia compared to the typical antipsychotics. The integrity of the PFC is closely related to working memory operation, which provides temporary storage and manipulation of the information necessary for complex cognitive tasks such as reading, learning, thinking, language comprehension and reasoning. One of the known mechanisms by which cognition, especially memory, occurs is related to the cAMP-element binding protein transcription factor (CREB). It is well known that CREB is related to neuroplasticity and plays an important role in the formation of long-term memory (SAURA; VALERO, 2011) and down-regulation of CREB has been observed in the pathophysiology of cognitive disorders. In addition, increasing the levels of CREB is being considered as a possible therapeutic target for Alzheimer's disease (PUGAZHENTHI et al., 2011). In the current study, treatment with risperidone decreased proteins linked to CREB function (as shown by IPA) although we did not find any changes in levels of the CREB protein. It has already been shown that in oligodendrocyte progenitors, CREB signaling plays a role in linking proliferation and survival pathways (SAINI et al., 2004). Thus, the inactivation of this signaling pathway by risperidone may affect these functions in oligodendrocytes.

Another pathway that seems to be inhibited by IPA analysis is Ciliary Neurotrophic factor (CNTF) signaling. CNTF is part of the four alpha-helical cytokine family that has been proposed to promote oligodendrocytes differentiation, maturation and survival (ALBRECHT et al., 2007) and a role of CNTF has been shown in demyelinating diseases, such as multiple sclerosis (LINKER et al., 2002). A study using animal models of CNTF-deficiency found decreased numbers of OPCs through increased apoptosis (LINKER et al., 2002). In agreement, the increase of endogenous levels of CNTF can raise proliferation of OPCs, which is fundamental for remyelination and repair. However, it has also reported that risperidone

treatment increased the frontal lobe intracortical myelin volume (BARTZOKIS et al., 2012). Nonetheless, we proposed that treatment with risperidone by inhibiting CNTF signaling may act in a detrimental way in the maturation of oligodendrocytes, inducing death of these cells and consequent impairment of myelination.

Risperidone treatment also increased levels of synaptotagmin V (SYT5), a member of the synaptotagmin family, which acts as a calcium sensor (INOUE et al., 2007). We also found that many proteins belonging to the calcium signaling were altered and IPA results suggested that risperidone may inhibit calcium signaling. Numerous studies have reported the participation of proteins belonging to synaptotagmin family in the development of schizophrenia, such as SXI and SVI (INOUE et al., 2007; SCHMITT et al., 2012). In another study, SYT5 was found to be decreased in the prefrontal cortex of patients with schizophrenia (MIRNICS et al., 2000). The treatment with clozapine, a second-generation antipsychotic, also affected SYT5 levels in the rat cortex (KONTKANEN; TO, 2002), but only risperidone affected the levels of this protein in this study.

As mentioned above, studies suggest the role of hypofunction of NMDA receptors in the pathophysiology of schizophrenia. In this regard, the importance of NMDA receptor co-agonists in the pathophysiology of schizophrenia has been considered. For example, serine and glycine levels were found to be altered in cerebrospinal fluid and brains of schizophrenia patients (HASHIMOTO et al., 2003, 2005; KIM et al., 2017; WAZIRI et al., 1990). In this way, the enzymatic activities associated with glycine and serine metabolism may influence the levels of these amino acids. In this study, D-3-phosphoglycerate dehydrogenase (PHGDH) levels were increased by the risperidone treatment. PHGDH is an enzyme which catalyzes the first and rate-limiting step that converts 3-phosphoglycerate into 3-phosphohydroxypyruvate, one of the metabolic pathways that synthesize L-serine (OHNUMA et al., 2009). In addition, recent studies analyzing mRNA expression levels of several enzymes that play a role in L-serine synthesis (including PHGDH) have found that the synthesis of this amino acid is altered in patients with schizophrenia (OZEKI et al., 2016). Thus, treatment with risperidone may help increase L-serine levels and improve the cognitive and negative symptoms of schizophrenia, since it has been seen that the effects of co-agonists act mainly on these two classes of symptoms (HASHIMOTO et al., 2005).

We also found that the risperidone treatment led to decreased levels of both glutamate ionotropic receptor NMDA type subunit 2A (NR2A) and glutamate ionotropic receptor AMPA type subunit 1 (GluA1) (MAGRI et al., 2006; MEAD; STEPHENS, 2003). The decreased levels of NMDA in medial and lateral caudate-putamen was seen in long-term

treatment of rats with risperidone, olanzapine and quetiapine, and treatment with risperidone led to decreased NMDA binding in caudate-putamen of juvenile and adult animals at some dosages (CHOI Y-K, GARDNER MP, 2009; TARAZI et al., 2003). In contrast, it has been shown that treatment with risperidone and other antipsychotics leads to increased AMPA receptor levels in some brain regions (CHOI Y-K, GARDNER MP, 2009; TARAZI et al., 2003).

It is well known that patients with schizophrenia have a reduced life expectancy because they present many problems such as cardiovascular disorders, metabolic syndrome, insulin resistance, type II diabetes and hormonal imbalances, which are often caused by the use of antipsychotics (TANDON; HALBREICH, 2003). Treatment with risperidone has led to increased levels of growth hormone and prolactin and altered the levels of innumerable proteins related to insulin receptor signaling, such as SYNJ2, PIK3CA, MAP2K2, PIK3C2A, INPP5J, FGFR4, SOS1, GSK3A, PIK3R2, PIK3R4, INPP5D and IGF1R (TANDON; HALBREICH, 2003). In another study, a comparison between clozapine and risperidone did not find significant differences in relation to the levels of growth hormone (BREIER et al., 1999). However, the latter study also found that clozapine produces lower effects on plasma prolactin than risperidone. Hyperprolactinemia has been observed frequently in the use of typical antipsychotics and risperidone (KINON et al., 2003). The results obtained in the current study of oligodendrocyte cells are in agreement with the data observed in the literature and strengthen this relationship of the use of risperidone with hyperprolactinemia. In addition, risperidone may include growth hormone as a component of its mechanism of action as increased levels of this hormone may be related to the weight gain observed in patients taking atypical drugs (FLINT et al., 2003). Metabolite abnormalities have been found in response to treatment with many atypical antipsychotics, such as clozapine and olanzapine (MELKERSSON; DAHL, 2003). Although we cannot conclude that risperidone causes insulin resistance from the current data, risperidone did alter the expression of proteins involved in insulin signaling pathways, consistent with this possibility.

Conclusion

Considering the results discussed above, this study has led to identification of some pathways and proteins that can be modulated by antipsychotics in oligodendrocytes. It was possible to observe that risperidone had more pathways in common with chlorpromazine and haloperidol than with quetiapine. It is known that different doses of this drug can lead to different

responses in patients, with the capability of behaving as a typical antipsychotic rather than an atypical one. Thus, we suggest that the dose used in the present study resulted in a closer response to typical antipsychotics. In addition, chlorpromazine appears to act by increasing protein levels, whereas haloperidol has the opposite effect. Although both are first-generation antipsychotics, they appear to have different mechanisms of action in oligodendrocytes. Finally, quetiapine altered fewer proteins compared to the other three drugs. Although *in vitro* studies have numerous limitations and may be distant from the *in vivo* scenario, our results provide detailed information on proteins and pathways modulated by the four antipsychotics studied here and show the importance of studying cell types other than neurons to fully comprehend the molecular changes involved in both the disease and treatment response.

Reference

Agonists, P. R. (2003). Therapeutic Potential of Peroxisome Proliferator-Activated Receptor Agonists for Neurological Disease. 5, 1–3.

Albrecht, P. J., Enterline, J. C., Cromer, J., and Levison, S. W. (2007). CNTF-activated astrocytes release a soluble trophic activity for oligodendrocyte progenitors. *Neurochem. Res.* 32, 263–271. doi:10.1007/s11064-006-9151-6.

Altar, C. A., Hornberger, J., Shewade, A., Cruz, V., Garrison, J., and Mrazek, D. (2013). Clinical validity of cytochrome P450 metabolism and serotonin gene variants in psychiatric pharmacotherapy. *Int. Rev. Psychiatry* 25, 509–533. doi:10.3109/09540261.2013.825579.

Altar, C. A., Jurata, L. W., Charles, V., Lemire, A., Liu, P., Bukhman, Y., et al. (2005). Deficient hippocampal neuron expression of proteasome, ubiquitin, and mitochondrial genes in multiple schizophrenia cohorts. *Biol. Psychiatry* 58, 85–96. doi:10.1016/j.biopsych.2005.03.031.

Avramopoulos, D. (2017). Neuregulin 3 and its roles in schizophrenia risk and presentation. *Am. J. Med. Genet. Part B Neuropsychiatr. Genet.*, 1–10. doi:10.1002/ajmg.b.32552.

Bae, J. W., Kim, H. J., Ban, J. Y., Park, H. J., Kim, S. K., Kang, S. W., et al. (2012). Association between polymorphisms of TAL1 gene and schizophrenia in a Korean population. *Psychiatr. Genet.* 22, 50. doi:10.1097/YPG.0b013e328345464b.

Balu, D. T., and Coyle, J. T. (2011). Neuroplasticity signaling pathways linked to the pathophysiology of schizophrenia. *Neurosci. Biobehav. Rev.* 35, 848–870. doi:10.1016/j.neubiorev.2010.10.005.

Bartzokis, G., Lu, P. H., Raven, E. P., Amar, C. P., Detore, N. R., Couvrette, A. J., et al. (2012). Impact on intracortical myelination trajectory of long acting injection versus oral risperidone in first-episode schizophrenia. *Schizophr. Res.* 140, 122–128. doi:10.1016/j.schres.2012.06.036.

Beaulieu, J.-M., Tirotta, E., Sotnikova, T. D., Masri, B., Salahpour, A., Gainetdinov, R. R., et al. (2007). Regulation of Akt Signaling by D2 and D3 Dopamine Receptors In Vivo. *J. Neurosci.* 27, 881–885. doi:10.1523/JNEUROSCI.5074-06.2007.

Blanke, M. L., and VanDongen, A. M. J. (2009). *Activation Mechanisms of the NMDA Receptor*. CRC Press/Taylor & Francis Available at: http://www.ncbi.nlm.nih.gov/pubmed/21204408 [Accessed January 10, 2018].

Bousman, C. A., Chana, G., Glatt, S. J., Chandler, S. D., May, T., Lohr, J., et al. (2010). Positive symptoms of psychosis correlate with expression of ubiquitin proteasome genes in peripheral blood. *Am. J. Med. Genet. Part B Neuropsychiatr. Genet.* 153, 1336–1341. doi:10.1002/ajmg.b.31106.

Bowling, H., Zhang, G., Bhattacharya, A., Pérez-Cuesta, L. M., Deinhardt, K., Hoeffer, C. A., et al. (2014). Antipsychotics activate mTORC1-dependent translation to enhance neuronal morphological complexity. *Sci. Signal.* 7, ra4. doi:10.1126/scisignal.2004331.

Brandão-Teles, C., Martins-de-Souza, D., Guest, P. C., and Cassoli, J. S. (2017). "MK-801-Treated Oligodendrocytes as a Cellular Model to Study Schizophrenia," in (Springer, Cham), 269–277. doi:10.1007/978-3-319-52479-5_25.

Brandl, E. J., Chowdhury, N. I., Tiwari, A. K., Lett, T. A. P., Meltzer, H. Y., Kennedy, J. L., et al. (2015). Genetic variation in CYP3A43 is associated with response to antipsychotic medication. *J. Neural Transm.* 122, 29–34. doi:10.1007/s00702-014-1298-8.

Breier, A. F., Malhotra, A. K., Su, T. P., Pinals, D. A., Elman, I., Adler, C. M., et al. (1999). Clozapine and risperidone in chronic schizophrenia: Effects on symptoms, Parkinsonian side effects, and neuroendocrine response. *Am. J. Psychiatry* 156, 294–298. doi:10.1176/ajp.156.2.294.

Buntinx, M., Vanderlocht, J., Hellings, N., Vandenabeele, F., Lambrichts, I., Raus, J., et al. (2003). Characterization of three human oligodendroglial cell lines as a model to study oligodendrocyte injury: Morphology and oligodendrocyte-specific gene expression. *J. Neurocytol.* 32, 25–38. doi:10.1023/A:1027324230923.

Carter, C. J. (2007). EIF2B and oligodendrocyte survival: Where nature and nurture meet in bipolar disorder and schizophrenia? *Schizophr. Bull.* 33, 1343–1353. doi:10.1093/schbul/sbm007.

Cassoli, J. S., Brandão-Teles, C., Santana, A. G., Souza, G. H. M. F., and Martins-de-Souza, D. (2017). Ion Mobility-Enhanced Data-Independent Acquisitions Enable a Deep Proteomic Landscape of Oligodendrocytes. *Proteomics* 17, 1700209. doi:10.1002/pmic.201700209.

Cassoli, J. S., Iwata, K., Steiner, J., Guest, P. C., Turck, C. W., Nascimento, J. M., et al. (2016). Effect of MK-801 and Clozapine on the Proteome of Cultured Human Oligodendrocytes. 10, 1–14. doi:10.3389/fncel.2016.00052.

Cassoli, J. S., and Martins-de-Souza, D. (2017). "Comprehensive Shotgun Proteomic Analyses of Oligodendrocytes Using Ion Mobility and Data-Independent Acquisition," in (Humana Press, New York, NY), 65–74. doi:10.1007/978-1-4939-7119-0_5.

Choi Y-K, Gardner MP, T. F. (2009). Effects of risperidone on glutamate receptor subtypes in developing rat brain. *Eur. Neuropsychopharmacol.* 19, 77–84. doi:10.1016/j.euroneuro.2008.08.010.Effects.

Coyle, J. T. (1996). The Glutamatergic Dysfunction Hypothesis for Schizophrenia.

Cummings, K. A., and Popescu, G. K. (2015). Glycine-dependent activation of NMDA receptors. *J. Gen. Physiol.* 145, 513–527. doi:10.1085/jgp.201411302.

Emamian, E. S. (2012). AKT/GSK3 signaling pathway and schizophrenia. *Front. Mol. Neurosci.* 5, 1–12. doi:10.3389/fnmol.2012.00033.

Emamian, E. S., Hall, D., Birnbaum, M. J., Karayiorgou, M., and Gogos, J. A. (2004). Convergent evidence for impaired AKT1-GSK3β signaling in schizophrenia. *Nat. Genet.* 36, 131–137. doi:10.1038/ng1296.

English, J. A., Fan, Y., Föcking, M., Lopez, L. M., Hryniewiecka, M., Wynne, K., et al. (2015). Reduced protein synthesis in schizophrenia patient-derived olfactory cells. *Transl. Psychiatry* 5, e663. doi:10.1038/tp.2015.119.

Flint, D. J., Binart, N., Kopchick, J., and Kelly, P. (2003). Effects of growth hormone and prolactin on adipose tissue development and function. *Pituitary* 6, 97–102. doi:10.1023/B:PITU.0000004800.57449.67.

Fu, H., Subramanian, R. R., and Masters, S. C. (2000). 14-3-3 P ROTEINS : Structure , Function , and Regulation.

Fujisawa, H., and Okuno, S. (1989). Regulation of the activity of tyrosine hydroxylase in the central nervous system. *Adv. Enzyme Regul.* 28, 93–110.

Garcia-Bueno, B., Perez-Nievas, B. G., and Leza, J. C. (2010). Is there a role for the nuclear receptor PPARgamma in neuropsychiatric diseases? *Int. J. Neuropsychopharmacol.* 13, 1411–1429. doi:10.1017/S1461145710000970.

Grover, S., Kumar, P., Singh, K., Vikram, V., and Budhiraja, R. D. (2013). Possible beneficial effect of peroxisome proliferator-activated receptor (PPAR) - α and γ agonist against a rat model of oral dyskinesia. *Pharmacol. Biochem. Behav.* 111, 17–23. doi:10.1016/j.pbb.2013.08.001.

Hahn, C.-G., Wang, H.-Y., Cho, D.-S., Talbot, K., Gur, R. E., Berrettini, W. H., et al. (2006). Altered neuregulin 1–erbB4 signaling contributes to NMDA> receptor hypofunction in schizophrenia. *Nat. Med.* 12, 824–828. doi:10.1038/nm1418.

Hashimoto, K., Engberg, G., Shimizu, E., Nordin, C., Lindström, L. H., and Iyo, M. (2005). Reduced D-serine to total serine ratio in the cerebrospinal fluid of drug naive schizophrenic patients. *Prog. Neuro-Psychopharmacology Biol. Psychiatry* 29, 767–769. doi:10.1016/j.pnpbp.2005.04.023.

Hashimoto, K., Fukushima, T., Shimizu, E., Komatsu, N., Watanabe, H., Shinoda, N., et al. (2003). Decreased Serum Levels of D-Serine in Patients With Schizophrenia. *Arch. Gen. Psychiatry* 60, 572. doi:10.1001/archpsyc.60.6.572.

Hashimoto, R., Straub, R. E., Weickert, C. S., Hyde, T. M., Kleinman, J. E., and Weinberger, D. R. (2004). Expression analysis of neuregulin-1 in the dorsolateral prefrontal cortex in schizophrenia. *Mol. Psychiatry* 9, 299–307. doi:10.1038/sj.mp.4001434.

Hayashi-Takagi, A. (2016). Synapse pathology and translational applications for schizophrenia. *Neurosci. Res.* 114, 3–8. doi:10.1016/j.neures.2016.09.001.

He, W., Barak, Y., Hevener, A., Olson, P., Liao, D., Le, J., et al. (2003). Adipose-specific peroxisome proliferator-activated receptor knockout causes insulin resistance in fat and liver but not in muscle. *Proc. Natl. Acad. Sci.* 100, 15712–15717. doi:10.1073/pnas.2536828100.

Hukic, D. S., Ösby, U., Olsson, E., Hilding, A., Östenson, C.-G., Gu, H. F., et al. (2017). Genetic variants of increased waist circumference in psychosis. *Psychiatr. Genet.* 0, 1. doi:10.1097/YPG.0000000000000181.

Inoue, S., Imamura, A., Okazaki, Y., Yokota, H., Arai, M., Hayashi, N., et al. (2007). Synaptotagmin XI as a candidate gene for susceptibility to schizophrenia. *Am. J. Med. Genet. Part B Neuropsychiatr. Genet.* 144, 332–340. doi:10.1002/ajmg.b.30465.

Iwata, K., Matsuzaki, H., Manabe, T., and Mori, N. (2011). Altering the expression balance of hnRNP C1 and C2 changes the expression of myelination-related genes. *Psychiatry Res.* 190, 364–366. doi:10.1016/j.psychres.2011.05.043.

J.Q., W., D.C., C., Y.L., T., S.P., T., Z.R., W., M.H., X., et al. (2014). Cognition impairment in schizophrenia patients with tardive dyskinesia: Association with plasma superoxide dismutase activity. *Schizophr. Res.* 152, 210–216. doi:10.1016/j.schres.2013.11.010.

Jana, M., and Pahan, K. (2013). Down-regulation of Myelin Gene Expression in Human Oligodendrocytes by Nitric Oxide: Implications for Demyelination in Multiple Sclerosis. *J. Clin. Cell. Immunol.* 4. doi:10.4172/2155-9899.1000157.

Ju, P., and Cui, D. (2015). The involvement of N-methyl-d-aspartate receptor (NMDAR) subunit NR1 in the pathophysiology of schizophrenia. *Acta Biochim. Biophys. Sin. (Shanghai).* 48, 209–219. doi:10.1093/abbs/gmv135.

Kalgutkar, A. S., Taylor, T. J., Venkatakrishnan, K., and Isin, E. M. (2003). Assessment of the contributions of CYP3A4 and CYP3A5 in the metabolism of the antipsychotic agent haloperidol to its potentially neurotoxic pyridinium metabolite and effect of antidepressants on the bioactivation pathway. *Drug Metab. Dispos.* 31, 243–249. doi:10.1124/dmd.31.3.243.

Kantoff, P. W., Higano, C. S., Shore, N. D., Berger, E. R., Small, E. J., Penson, D. F., et al. (2010). Effectiveness of Antipsychotic Drugs in Patients with Chronic Schizophrenia. *Clin. Trials* 363, 411–422. doi:10.1056/NEJMoa1402121.

Kim, S.-Y., Kaufman, M. J., Cohen, B. M., Jensen, J. E., Coyle, J. T., Du, F., et al. (2017). In Vivo Brain Glycine and Glutamate Concentrations in Patients with First-Episode Psychosis Measured by Echo-Time-Averaged Proton MR Spectroscopy at 4 Tesla. *Biol. Psychiatry*, 1–8. doi:10.1016/j.biopsych.2017.08.022.

Kinon, B. J., Gilmore, J. A., Liu, H., and Halbreich, U. M. (2003). Prevalence of hyperprolactinemia in schizophrenic patients treated with conventional antipsychotic medications or risperidone. *Psychoneuroendocrinology* 28, 55–68. doi:10.1016/S0306-4530(02)00127-0.

Kontkanen, O., and To, P. (2002). Antipsychotic drug treatment induces differential gene expression in the rat cortex. 1043–1053.

Law, A. J., Lipska, B. K., Weickert, C. S., Hyde, T. M., Straub, R. E., Hashimoto, R., et al. (2006). Neuregulin 1 transcripts are differentially expressed in schizophrenia and regulated by 5' SNPs associated with the disease. *Proc. Natl. Acad. Sci.* 103, 6747–6752. doi:10.1073/pnas.0602002103.

Leucht, S., Corves, C., Arbter, D., Engel, R. R., Li, C., and Davis, J. M. (2009). Second-generation versus first-generation antipsychotic drugs for schizophrenia: a meta-analysis. *Lancet* 373, 31–41. doi:10.1016/S0140-6736(08)61764-X.

Leucht, S., Pitschel-Walz, G., Abraham, D., and Kissling, W. (1999). Efficacy and extrapyramidal side-effects of the new antipsychotics olanzapine, quetiapine, risperidone, and sertindole compared to conventional antipsychotics and placebo. A meta-analysis of randomized controlled trials. *Schizophr. Res.* 35, 51–68. doi:10.1016/S0920-9964(98)00105-4.

Li, G.-Z., Vissers, J. P. C., Silva, J. C., Golick, D., Gorenstein, M. V., and Geromanos, S. J. (2009a). Database searching and accounting of multiplexed precursor and product ion spectra from the data independent analysis of simple and complex peptide mixtures. *Proteomics* 9, 1696–1719. doi:10.1002/pmic.200800564.

Li, J., Wang, H., and Rosenberg, P. A. (2009b). Vitamin K prevents oxidative cell death by inhibiting activation of 12-lipoxygenase in developing oligodendrocytes. *J. Neurosci. Res.* 87, 1997–2005. doi:10.1002/jnr.22029.

Lieberman, J. A., Stroup, T. S., Mcevoy, J. P., Swartz, M. S., Rosenheck, R. A., Perkins, D. O., et al. (2005). Effectiveness of Antipsychotic Drugs in Patients with Chronic Schizophrenia. *n engl j med* 35312353, 1209–23. Available at: http://www.nejm.org/doi/pdf/10.1056/NEJMoa051688 [Accessed January 9, 2018].

Linker, R. A., Mäurer, M., Gaupp, S., Martini, R., Holtmann, B., Giess, R., et al. (2002). CNTF is a major protective factor in demyelinating CNS disease: A neurotrophic cytokine as modulator in neuroinflammation. *Nat. Med.* 8, 620–624. doi:10.1038/nm0602-620.

Liu, Y. R., Hu, T. M., Lan, T. H., Chiu, H. J., Chang, Y. H., Chen, S. F., et al. (2014). Association of the PPAR-γ gene with altered glucose levels and psychosis profile in

schizophrenia patients exposed to antipsychotics. *Psychiatry Investig.* 11, 179–185. doi:10.4306/pi.2014.11.2.179.

Llerena, A., De La Rubia, A., Berecz, R., and Dorado, P. (2004). Relationship between haloperidol plasma concentration, debrisoquine metabolic ratio, CYP2D6 and CYP2C9 genotypes in psychiatric patients. *Pharmacopsychiatry* 37, 69–73. doi:10.1055/s-2004-815528.

Maas, D. A., Vallès, A., and Martens, G. J. M. (2017). Oxidative stress, prefrontal cortex hypomyelination and cognitive symptoms in schizophrenia. *Transl. Psychiatry* 7, e1171. doi:10.1038/tp.2017.138.

Magri, C., Gardella, R., Barlati, S. D., Podavini, D., Iatropoulos, P., Bonomi, S., et al. (2006). Glutamate AMPA receptor subunit 1 gene (GRIA1) and DSM-IV=TR schizophrenia: A pilot case-control association study in an Italian sample. *Am. J. Med. Genet. - Neuropsychiatr. Genet.* 141 B, 287–293. doi:10.1002/ajmg.b.30294.

Martins-de-Souza, D., Gattaz, W. F., Schmitt, A., Novello, J. C., Marangoni, S., Turck, C. W., et al. (2009). Proteome analysis of schizophrenia patients Wernicke's area reveals an energy metabolism dysregulation. *BMC Psychiatry* 9, 17. doi:10.1186/1471-244X-9-17.

Martins-de-Souza, D., Lebar, M., and Turck, C. W. (2011). Proteome analyses of cultured astrocytes treated with MK-801 and clozapine: similarities with schizophrenia. *Eur. Arch. Psychiatry Clin. Neurosci.* 261, 217–228. doi:10.1007/s00406-010-0166-2.

Matera, A. G., and Wang, Z. (2014). A day in the life of the spliceosome. *Nat. Rev. Mol. Cell Biol.* 15, 108–121. doi:10.1038/nrm3742.

Maynard, T. M., Sikich, L., Lieberman, J. a, and LaMantia, a S. (2001). Neural development, cell-cell signaling, and the "two-hit" hypothesis of schizophrenia. *Schizophr. Bull.* 27, 457–476. doi:10.1093/oxfordjournals.schbul.a006887.

Mead, A. N., and Stephens, D. N. (2003). Selective disruption of stimulus-reward learning in glutamate receptor gria1 knock-out mice. *J. Neurosci.* 23, 1041–8. Available at: http://www.ncbi.nlm.nih.gov/pubmed/12574434.

Melkersson, K. I., and Dahl, M. L. (2003). Relationship between levels of insulin or triglycerides and serum concentrations of the atypical antipsychotics clozapine and olanzapine in patients on treatment with therapeutic doses. *Psychopharmacology (Berl).* 170, 157–166. doi:10.1007/s00213-003-1529-4.

Mellick, R. S., and Bassett, R. L. (1956). The cerebrospinal-fluid glutamic oxaloacetic transaminase activity in neurological diseases. 1956–1958.

Middleton, F. A., Peng, L., Lewis, D. A., Levitt, P., and Mirnics, K. (2005). Altered Expression of 14-3-3 Genes in the Prefrontal Cortex of Subjects with Schizophrenia. *Neuropsychopharmacology* 30, 974–983. doi:10.1038/sj.npp.1300674.

Middleton, F. a, Mirnics, K., Pierri, J. N., Lewis, D. a, and Levitt, P. (2002). Gene expression profiling reveals alterations of specific metabolic pathways in schizophrenia. *J. Neurosci.* 22, 2718–2729. doi:20026209.

Mirnics, K., Middleton, F. A., Marquez, A., Lewis, D. A., and Levitt, P. (2000). Molecular Characterization of Schizophrenia Viewed by Microarray Analysis of Gene Expression in Prefrontal Cortex. *Neuron* 28, 53–67. doi:10.1016/S0896-6273(00)00085-4.

Ohnuma, T., Shibata, N., Maeshima, H., Baba, H., Hatano, T., Hanzawa, R., et al. (2009). Association analysis of glycine- and serine-related genes in a Japanese population of patients with schizophrenia. *Prog. Neuro-Psychopharmacology Biol. Psychiatry* 33, 511–518. doi:10.1016/j.pnpbp.2009.02.004.

Ozeki, Y., Sekine, M., Fujii, K., Watanabe, T., Okayasu, H., Takano, Y., et al. (2016). Phosphoserine phosphatase activity is elevated and correlates negatively with plasma d-serine concentration in patients with schizophrenia. *Psychiatry Res.* 237, 344–350. doi:10.1016/j.psychres.2016.01.010.

Perera, J., Tan, J. H., Jeevathayaparan, S., Chakravarthi, S., and Haleagrahara, N. (2011). Neuroprotective effects of alpha lipoic Acid on haloperidol-induced oxidative stress in the rat brain. *Cell Biosci* 1, 12. doi:2045-3701-1-12 [pii]\r10.1186/2045-3701-1-12.

Piomelli, D., and Greengard, P. (1990). Lipoxygenase metabolites of arachidonic acid in neuronal transmembrane signalling. *Trends Pharmacol. Sci.* 11, 367–373. doi:10.1016/0165-6147(90)90182-8.

Pugazhenthi, S., Wang, M., Pham, S., Sze, C.-I., and Eckman, C. B. (2011). Downregulation of CREB expression in Alzheimer's brain and in Aβ-treated rat hippocampal neurons. *Mol. Neurodegener.* 6, 60. doi:10.1186/1750-1326-6-60.

Qing, Y., Sun, L., Yang, C., Jiang, J., Yang, X., Hu, X., et al. (2016). Dysregulated 14-3-3 Family in Peripheral Blood Leukocytes of Patients with Schizophrenia. *Sci. Rep.* 6, 1–8. doi:10.1038/srep23791.

Ryan, M. M., Lockstone, H. E., Huffaker, S. J., Wayland, M. T., Webster, M. J., and Bahn, S. (2006). Gene expression analysis of bipolar disorder reveals downregulation of the ubiquitin cycle and alterations in synaptic genes. *Mol. Psychiatry* 11, 965–978. doi:10.1038/sj.mp.4001875.

Saia-cereda, V. M., and Santana, A. G. (2017). The Nuclear Proteome of White and Gray Matter from Schizophrenia Postmortem Brains. 37–52. doi:10.1159/000477299.

Saia, V. M., Juliana, C., Andrea, S. C., Falkai, P., Nascimento, J. M., and Souza, D. M. De (2015). Proteomics of the corpus callosum unravel pivotal players in the dysfunction of cell signaling , structure , and myelination in schizophrenia brains. *Eur. Arch. Psychiatry Clin. Neurosci.* 265, 601–612. doi:10.1007/s00406-015-0621-1.

Saini, H. S., Gorse, K. M., Boxer, L. M., and Sato-Bigbee, C. (2004). Neurotrophin-3 and a CREB-mediated signaling pathway regulate Bcl-2 expression in oligodendrocyte progenitor cells. *J. Neurochem.* 89, 951–961. doi:10.1111/j.1471-4159.2004.02365.x.

Samad, N., and Haleem, D. J. (2017). Antioxidant effects of rice bran oil mitigate repeated haloperidol-induced tardive dyskinesia in male rats. *Metab. Brain Dis.* 32, 1099–1107. doi:10.1007/s11011-017-0002-8.

Saura, C. A., and Valero, J. (2011). The role of CREB signaling in Alzheimer's disease and other cognitive disorders. *Rev. Neurosci.* 22, 153–169. doi:10.1515/RNS.2011.018.

Schmitt, A., Leonardi-Essmann, F., Durrenberger, P. F., Wichert, S. P., Spanagel, R., Arzberger, T., et al. (2012). Structural synaptic elements are differentially regulated in superior temporal cortex of schizophrenia patients. *Eur. Arch. Psychiatry Clin. Neurosci.* 262, 565–577. doi:10.1007/s00406-012-0306-y.

Schubert, K. O., Föcking, M., and Cotter, D. R. (2015). Proteomic pathway analysis of the hippocampus in schizophrenia and bipolar affective disorder implicates 14-3-3 signaling, aryl hydrocarbon receptor signaling, and glucose metabolism: Potential roles in GABAergic interneuron pathology. *Schizophr. Res.* 167, 64–72. doi:10.1016/j.schres.2015.02.002.

Shen, W. W. (1999). A history of antipsychotic drug development. *Compr. Psychiatry* 40, 407–414. doi:10.1016/S0010-440X(99)90082-2.

Steiner, J., Martins-de-Souza, D., Schiltz, K., Sarnyai, Z., Westphal, S., Isermann, B., et al. (2014). Clozapine promotes glycolysis and myelin lipid synthesis in cultured oligodendrocytes. *Front. Cell. Neurosci.* 8, 1–11. doi:10.3389/fncel.2014.00384.

Stephen, J., and Jonathan, A. (2010). Roles of the Akt / GSK-3 and Wnt Signaling Pathways in Schizophrenia and Antipsychotic Drug Ac. 388–396. doi:10.1176/appi.ajp.2009.08121873.

Tandon, R., and Halbreich, U. (2003). The second-generation "atypical" antipsychotics: Similar improved efficacy but different neuroendocrine side effects. *Psychoneuroendocrinology* 28, 1–7. doi:10.1016/S0306-4530(01)00100-7.

Tarazi, F., Baldessarini, R., Kula, N., and Zhang, K. (2003). Long-term effects of olanzapine, risperidone, and quetiapine on ionotropic glutamate receptor types: implications for antipsychotic drug treatment. *J. Pharmacol. …* 306, 1145–1151. doi:10.1124/jpet.103.052597.).

Thiselton, D. L., Vladimirov, V. I., Kuo, P. H., McClay, J., Wormley, B., Fanous, A., et al. (2008). AKT1 Is Associated with Schizophrenia Across Multiple Symptom Dimensions in the Irish Study of High Density Schizophrenia Families. *Biol. Psychiatry* 63, 449–457. doi:10.1016/j.biopsych.2007.06.005.

Thorburne, S. K., and Juurlink, B. H. (1996). Low glutathione and high iron govern the susceptibility of oligodendroglial precursors to oxidative stress. *J. Neurochem.* 67, 1014–22. doi:10.1046/j.1471-4159.1996.67031014.x.

Vichi, S., Sandström von Tobel, J., Gemma, S., Stanzel, S., Kopp-Schneider, A., Monnet-Tschudi, F., et al. (2015). Cell type-specific expression and localization of cytochrome P450 isoforms in tridimensional aggregating rat brain cell cultures. *Toxicol. Vitr.* 30, 176–184. doi:10.1016/j.tiv.2015.03.005.

Wang, H., Li, J., Follett, P. L., Zhang, Y., Cotanche, D. A., Jensen, F. E., et al. (2004). 12-Lipoxygenase plays a key role in cell death caused by glutathione depletion and arachidonic acid in rat oligodendrocytes. *Eur. J. Neurosci.* 20, 2049–2058. doi:10.1111/j.1460-9568.2004.03650.x.

Wang, S., Sdrulla, A. D., DiSibio, G., Bush, G., Nofziger, D., Hicks, C., et al. (1998). Notch receptor activation inhibits oligodendrocyte differentiation. *Neuron* 21, 63–75. doi:10.1016/S0896-6273(00)80515-2.

Wang, X., Zhong, P., Gu, Z., and Yan, Z. (2003). Regulation of NMDA Receptors by Dopamine D 4 Signaling in Prefrontal Cortex. *October* 23, 9852–9861. doi:10.1523/JNEUROSCI.1086-05.2005.

Waziri, R., Baruah, S., Hegwood, T. S., and Sherman, A. D. (1990). Abnormal serine hydroxymethyl transferase activity in the temporal lobes of schizophrenics. *Neurosci. Lett.* 120, 237–240. doi:10.1016/0304-3940(90)90048-E.

Wroblewski, F. (1958). The Clinical Significance of Alterations in Transaminase Activities of Serum and Other Body Fluids. *Adv. Clin. Chem.* 1, 313–351. doi:10.1016/S0065-2423(08)60362-5.

Yoon, S. C., Seo, M. S., Kim, S. H., Jeon, W. J., Ahn, Y. M., Kang, U. G., et al. (2008). The effect of MK-801 on mTOR/p70S6K and translation-related proteins in rat frontal cortex. *Neurosci. Lett.* 434, 23–28. doi:10.1016/j.neulet.2008.01.020.

Zheng, W., Wang, H., Zeng, Z., Lin, J., Little, P. J., Srivastava, L. K., et al. (2012). The possible role of the Akt signaling pathway in schizophrenia. *Brain Res.* 1470, 145–158. doi:10.1016/j.brainres.2012.06.032.

10. CONCLUSÃO FINAL

Como já descrito ao longo desta dissertação, a esquizofrenia consiste em um transtorno complexo e de caráter multifatorial. Desta forma, o estudo desta doença requer não apenas a compreensão de parâmetros clínicos e biológicos, mas é necessário também compreender as mudanças que ocorrem na biologia celular. Os estudos com tecidos *post mortem* e genéticos identificaram uma série de potenciais processos moleculares que precisam ser olhados no contexto celular. Desta forma, a primeira etapa deste trabalho foi realizada a otimização de um protocolo de cultivo da linhagem celular de oligodendrócitos humanos (MO3.13) e o tratamento de tais células com MK-801, que atua como antagonista do receptor de NMDA. Através deste, tentamos estabelecer um modelo *in vitro* da disfunção glutamatérgica frequentemente observada em pacientes com esquizofrenia. Isto posto, através deste protocolo pretendemos contribuir para estudos futuros que busquem identificar e compreender as modificações pontuais observadas na patofisiologia da esquizofrenia, especificamente na disfunção glutamatérgica em oligodendrócitos.

O tratamento da esquizofrenia consiste em uma combinação entre o uso de medicamentos e psicoterapia, que visam diminuir o quadro psicótico do paciente e assim melhorar a qualidade de vida do mesmo. Todavia, o abandono do tratamento pelo paciente devido aos efeitos colaterais que as drogas proporcionam e dificuldades no acerto do tratamento é frequente, resultando em inúmeros prejuízos, consistindo em uma das principais causas de morbidade psiquiátrica e reinternações. Visto a importância do tratamento medicamentoso na esquizofrenia, a segunda parte deste estudo consistiu no tratamento da linhagem celular de oligodendrócitos com quatro antipsicóticos (primeira e segunda geração) largamente utilizados na clínica. Embora os estudos *in vitro* sejam constituídos de uma grande quantidade de limitações, especialmente para o estudo de transtornos psiquiátricos, nossos resultados fornecem informações detalhadas sobre proteínas e vias de sinalização moduladas pelos quatro antipsicóticos aqui estudados. Através destes dados, pretendemos contribuir com a melhora na escolha de qual antipsicótico cada paciente deve receber em vista dos sintomas apresentados. Por exemplo, pacientes que apresentem maiores alterações na substância branca, implicando em uma disfunção nos oligodendrócitos, os resultados aqui apresentados poderiam auxiliar na escolha de qual o melhor medicamento a ser administrado. Para mais, a maioria dos estudos dos mecanismos de ação dos antipsicóticos *in vitro* é feito em neurônios. Dessa forma, os resultados aqui obtidos auxiliam no entendimento das alterações que os antipsicóticos promovem nos oligodendrócitos, que possuem papel chave no transtorno.

Portanto, as discussões e hipóteses propostas nesta dissertação podem ajudar na compreensão dos mecanismos de ação desses medicamentos em oligodendrócitos, fornecendo informações importantes para entender o funcionamento desses fármacos, auxiliando assim o médico psiquiatra na escolha da melhor droga baseado nas alterações específicas apresentadas por cada paciente.

11. PERSPECTIVAS

Este trabalho apresentou um protocolo de cultivo celular de uma linhagem de oligodendrócitos humanos (MO3.13) bem como o tratamento dessas células com quatro antipsicóticos largamente utilizados em pacientes com esquizofrenia. Destes tratamentos, foi possível identificar vias e proteínas moduladas por esses medicamentos, bem como os mecanismos em comum e específicos de cada droga. Desta forma, trabalhos futuros buscarão analisar proteínas e vias encontradas neste estudo, buscando compreender claramente o envolvimento destas no mecanismo de ação dos antipsicóticos e como as mesmas se relacionam com a patofisiologia da esquizofrenia.

12. REFERÊNCIAS BIBLIOGRÁFICAS (INTRODUÇÃO E CONCLUSÃO FINAL)

ABI-DARGHAM, A. et al. Increased baseline occupancy of D2 receptors by dopamine in schizophrenia. **Proceedings of the National Academy of Sciences of the United States of America**, v. 97, n. 14, p. 8104–8109, 2000.

ABI-DARGHAM, A.; MOORE, H. Prefrontal DA transmission at D1receptors and the pathology of schizophrenia. **Neuroscientist**, v. 9, n. 5, p. 404–416, 2003.

ADLER, C. M. et al. Comparison of ketamine-induced thought disorder in healthy volunteers and thought disorder in schizophrenia. **American Journal of Psychiatry**, v. 156, n. 10, p. 1646–1649, 1999.

AGONISTS, P. R. Therapeutic Potential of Peroxisome Proliferator-Activated Receptor Agonists for Neurological Disease. v. 5, n. 1, p. 1–3, 2003.

ALBRECHT, P. J. et al. CNTF-activated astrocytes release a soluble trophic activity for oligodendrocyte progenitors. **Neurochemical Research**, v. 32, n. 2, p. 263–271, 2007.

ALTAR, C. A. et al. Deficient hippocampal neuron expression of proteasome, ubiquitin, and mitochondrial genes in multiple schizophrenia cohorts. **Biological Psychiatry**, v. 58, n. 2, p. 85–96, 2005.

ALTAR, C. A. et al. Clinical validity of cytochrome P450 metabolism and serotonin gene variants in psychiatric pharmacotherapy. **International Review of Psychiatry**, v. 25, n. 5, p. 509–533, 2013.

AVRAMOPOULOS, D. Neuregulin 3 and its roles in schizophrenia risk and presentation. **American Journal of Medical Genetics, Part B: Neuropsychiatric Genetics**, n. April, p. 1–10, 2017.

BAE, J. W. et al. Association between polymorphisms of TAL1 gene and schizophrenia in a Korean population. **Psychiatric Genetics**, v. 22, n. 1, p. 50, 2012.

BALU, D. T.; COYLE, J. T. Neuroplasticity signaling pathways linked to the pathophysiology of schizophrenia. **Neuroscience and Biobehavioral Reviews**, v. 35, n. 3, p. 848–870, 2011.

BARTZOKIS, G. et al. Impact on intracortical myelination trajectory of long acting injection versus oral risperidone in first-episode schizophrenia. **Schizophrenia Research**, v. 140, n. 1–3, p. 122–128, 2012.

BEAULIEU, J.-M. et al. Regulation of Akt Signaling by D2 and D3 Dopamine Receptors In Vivo. **Journal of Neuroscience**, v. 27, n. 4, p. 881–885, 2007.

BLANKE, M. L.; VANDONGEN, A. M. J. **Activation Mechanisms of the NMDA Receptor**. [s.l.] CRC Press/Taylor & Francis, 2009.

BOUSMAN, C. A. et al. Positive symptoms of psychosis correlate with expression of ubiquitin proteasome genes in peripheral blood. **American Journal of Medical Genetics, Part B: Neuropsychiatric Genetics**, v. 153, n. 7, p. 1336–1341, 2010.

BOWLING, H. et al. Antipsychotics activate mTORC1-dependent translation to enhance neuronal morphological complexity. **Science signaling**, v. 7, n. 308, p. ra4, 14 jan. 2014.

BRANDÃO-TELES, C. et al. MK-801-Treated Oligodendrocytes as a Cellular Model to Study Schizophrenia. In: [s.l.] Springer, Cham, 2017. p. 269–277.

BRANDL, E. J. et al. Genetic variation in CYP3A43 is associated with response to antipsychotic medication. **Journal of Neural Transmission**, v. 122, n. 1, p. 29–34, 2015.

BREIER, A. F. et al. Clozapine and risperidone in chronic schizophrenia: Effects on symptoms, Parkinsonian side effects, and neuroendocrine response. **American Journal of Psychiatry**, v. 156, n. 2, p. 294–298, 1999.

BRUINS, A. P. Mechanistic aspects of electrospray ionization. **Journal of Chromatography A**, v. 794, n. 1–2, p. 345–357, 23 jan. 1998.

BUNTINX, M. et al. Characterization of three human oligodendroglial cell lines as a model to study oligodendrocyte injury: Morphology and oligodendrocyte-specific gene expression. **Journal of Neurocytology**, v. 32, n. 1, p. 25–38, 2003.

CARLSSON, A.; LINDQVIST, M. Effect of Chlorpromazine or Haloperidol on Formation of 3-Methoxytyramine and Normetanephrine in Mouse Brain. **Acta Pharmacologica et Toxicologica**, v. 20, n. 2, p. 140–144, 1963.

CARTER, C. J. EIF2B and oligodendrocyte survival: Where nature and nurture meet in bipolar disorder and schizophrenia? **Schizophrenia Bulletin**, v. 33, n. 6, p. 1343–1353, 2007.

CASSOLI, J. S. et al. Effect of MK-801 and Clozapine on the Proteome of Cultured Human Oligodendrocytes. v. 10, n. March, p. 1–14, 2016.

CASSOLI, J. S. et al. Ion Mobility-Enhanced Data-Independent Acquisitions Enable a Deep Proteomic Landscape of Oligodendrocytes. **PROTEOMICS**, v. 17, n. 21, p. 1700209, 1 nov. 2017.

CASSOLI, J. S.; MARTINS-DE-SOUZA, D. Comprehensive Shotgun Proteomic Analyses of Oligodendrocytes Using Ion Mobility and Data-Independent Acquisition. In: [s.l.] Humana Press, New York, NY, 2017. p. 65–74.

CHOI Y-K, GARDNER MP, T. F. Effects of risperidone on glutamate receptor subtypes in developing rat brain. **European Neuropsychopharmacology**, v. 19, n. 2, p. 77–84, 2009.

COYLE, J. T. The Glutamatergic Dysfunction Hypothesis for Schizophrenia. 1996.

CUMMINGS, K. A.; POPESCU, G. K. Glycine-dependent activation of NMDA receptors. **The Journal of General Physiology**, v. 145, n. 6, p. 513–527, 2015.

DEMJAHA, A. et al. Dopamine synthesis capacity in patients with treatment-resistant schizophrenia. **American Journal of Psychiatry**, v. 169, n. 11, p. 1203–1210, 2012.

DISTLER, U. et al. Drift time-specific collision energies enable deep-coverage data-independent acquisition proteomics. **Nature Methods**, v. 11, n. 2, p. 167–170, 2013.

EMAMIAN, E. S. et al. Convergent evidence for impaired AKT1-GSK3β signaling in schizophrenia. **Nature Genetics**, v. 36, n. 2, p. 131–137, 2004.

EMAMIAN, E. S. AKT/GSK3 signaling pathway and schizophrenia. **Frontiers in Molecular Neuroscience**, v. 5, n. March, p. 1–12, 2012.

ENGLISH, J. A. et al. Reduced protein synthesis in schizophrenia patient-derived olfactory cells. **Translational psychiatry**, v. 5, n. June, p. e663, 2015.

FLINT, D. J. et al. Effects of growth hormone and prolactin on adipose tissue development and function. **Pituitary**, v. 6, n. 2, p. 97–102, 2003.

FLYNN, S. W. et al. Abnormalities of myelination in schizophrenia detected in vivo with MRI, and post-mortem with analysis of oligodendrocyte proteins. **Molecular Psychiatry**, v. 8, n. 9, p. 811–820, 2003.

FU, H.; SUBRAMANIAN, R. R.; MASTERS, S. C. 14-3-3 P ROTEINS : Structure , Function , and Regulation. 2000.

FUJISAWA, H.; OKUNO, S. Regulation of the activity of tyrosine hydroxylase in the central nervous system. **Advances in enzyme regulation**, v. 28, p. 93–110, 1989.

GARCIA-BUENO, B.; PEREZ-NIEVAS, B. G.; LEZA, J. C. Is there a role for the nuclear receptor PPARgamma in neuropsychiatric diseases? **International Journal of Neuropsychopharmacology**, v. 13, n. 10, p. 1411–1429, 2010.

GROVER, S. et al. Possible beneficial effect of peroxisome proliferator-activated receptor (PPAR) - α and γ agonist against a rat model of oral dyskinesia. **Pharmacology Biochemistry and Behavior**, v. 111, p. 17–23, 2013.

GUEST, P. C. et al. MK-801 treatment affects glycolysis in oligodendrocytes more than in astrocytes and neuronal cells: insights for schizophrenia. **Frontiers in Cellular Neuroscience**, v. 9, n. May, p. 1–10, 2015.

HAHN, C.-G. et al. Altered neuregulin 1–erbB4 signaling contributes to NMDA> receptor hypofunction in schizophrenia. **Nature Medicine**, v. 12, n. 7, p. 824–828, 2006.

HAKAK, Y. et al. Genome-wide expression analysis reveals dysregulation of myelination-

related genes in chronic schizophrenia. **Proceedings of the National Academy of Sciences of the United States of America**, v. 98, n. 8, p. 4746–51, 10 abr. 2001.

HASHIMOTO, K. et al. Decreased Serum Levels of D-Serine in Patients With Schizophrenia. **Archives of General Psychiatry**, v. 60, n. 6, p. 572, 1 jun. 2003.

HASHIMOTO, K. et al. Reduced D-serine to total serine ratio in the cerebrospinal fluid of drug naive schizophrenic patients. **Progress in Neuro-Psychopharmacology and Biological Psychiatry**, v. 29, n. 5, p. 767–769, 2005.

HASHIMOTO, R. et al. Expression analysis of neuregulin-1 in the dorsolateral prefrontal cortex in schizophrenia. **Molecular psychiatry**, v. 9, n. 3, p. 299–307, 2004.

HAYASHI-TAKAGI, A. Synapse pathology and translational applications for schizophrenia. **Neuroscience Research**, v. 114, p. 3–8, 2016.

HE, W. et al. Adipose-specific peroxisome proliferator-activated receptor knockout causes insulin resistance in fat and liver but not in muscle. **Proceedings of the National Academy of Sciences**, v. 100, n. 26, p. 15712–15717, 2003.

HOFFMANN, EDMOND DE; STROOBANT, V. **Mass Spectrometry**. [s.l: s.n.].

HOWES, O. D. et al. Midbrain dopamine function in schizophrenia and depression: A post-mortem and positron emission tomographic imaging study. **Brain**, v. 136, n. 11, p. 3242–3251, 2013.

HUKIC, D. S. et al. Genetic variants of increased waist circumference in psychosis. **Psychiatric Genetics**, v. 0, p. 1, 2017.

INOUE, S. et al. Synaptotagmin XI as a candidate gene for susceptibility to schizophrenia. **American Journal of Medical Genetics, Part B: Neuropsychiatric Genetics**, v. 144, n. 3, p. 332–340, 2007.

IWATA, K. et al. Altering the expression balance of hnRNP C1 and C2 changes the expression of myelination-related genes. **Psychiatry Research**, v. 190, n. 2–3, p. 364–366, 2011.

J.Q., W. et al. Cognition impairment in schizophrenia patients with tardive dyskinesia: Association with plasma superoxide dismutase activity. **Schizophrenia Research**, v. 152, n. 1, p. 210–216, 2014.

JANA, M.; PAHAN, K. Down-regulation of Myelin Gene Expression in Human Oligodendrocytes by Nitric Oxide: Implications for Demyelination in Multiple Sclerosis. **Journal of clinical & cellular immunology**, v. 4, n. 312, 2013.

JARSKOG, L. F.; MIYAMOTO, S.; LIEBERMAN, J. A. Schizophrenia: New Pathological Insights and Therapies. **Annual Review of Medicine**, v. 58, n. 1, p. 49–61, 2007.

JAVITT, D. C.; ZUKIN, S. R. Recent advances in the phencyclidine model of schizophrenia. **American Journal of Psychiatry**, v. 148, n. 10, p. 1301–1308, out. 1991.

JENSEN, O. N. Interpreting the protein language using proteomics. **Nature Reviews Molecular Cell Biology**, v. 7, n. 6, p. 391–403, 2006.

JU, P.; CUI, D. The involvement of N-methyl-d-aspartate receptor (NMDAR) subunit NR1 in the pathophysiology of schizophrenia. **Acta Biochimica et Biophysica Sinica**, v. 48, n. 3, p. 209–219, 2015.

KAALUND, S. S. et al. Contrasting changes in DRD1 and DRD2 splice variant expression in schizophrenia and affective disorders, and associations with SNPs in postmortem brain. **Molecular Psychiatry**, v. 19, n. 12, p. 1258–1266, 2014.

KAISER, S. et al. Phencyclidine-induced changes in rat cortical gene expression identified by microarray analysis: implications for schizophrenia. **Neurobiology of disease**, v. 16, n. 1, p. 220–35, 2004.

KALGUTKAR, A. S. et al. Assessment of the contributions of CYP3A4 and CYP3A5 in the metabolism of the antipsychotic agent haloperidol to its potentially neurotoxic pyridinium metabolite and effect of antidepressants on the bioactivation pathway. **Drug Metabolism and Disposition**, v. 31, n. 3, p. 243–249, 2003.

KANTOFF, P. W. et al. Effectiveness of Antipsychotic Drugs in Patients with Chronic Schizophrenia. **Clinical Trials**, v. 363, p. 411–422, 2010.

KIM, J. S. et al. Low cerebrospinal fluid glutamate in schizophrenic patients and a new hypothesis on schizophrenia. **Neuroscience Letters**, v. 20, n. 3, p. 379–382, 1980.

KIM, S.-Y. et al. In Vivo Brain Glycine and Glutamate Concentrations in Patients with First-Episode Psychosis Measured by Echo-Time-Averaged Proton MR Spectroscopy at 4 Tesla. **Biological Psychiatry**, p. 1–8, 2017.

KINON, B. J. et al. Prevalence of hyperprolactinemia in schizophrenic patients treated with conventional antipsychotic medications or risperidone. **Psychoneuroendocrinology**, v. 28, n. SUPPL. 2, p. 55–68, 2003.

KONTKANEN, O.; TO, P. Antipsychotic drug treatment induces differential gene expression in the rat cortex. p. 1043–1053, 2002.

LARUELLE, M.; KEGELES, L. S.; ABI-DARGHAM, A. Glutamate, dopamine, and schizophrenia: from pathophysiology to treatment. **Annals of the New York Academy of Sciences**, v. 1003, p. 138–58, nov. 2003.

LAW, A. J. et al. Neuregulin 1 transcripts are differentially expressed in schizophrenia and regulated by 5' SNPs associated with the disease. **Proceedings of the National Academy of**

Sciences, v. 103, n. 17, p. 6747–6752, 2006.

LEUCHT, S. et al. Efficacy and extrapyramidal side-effects of the new antipsychotics olanzapine, quetiapine, risperidone, and sertindole compared to conventional antipsychotics and placebo. A meta-analysis of randomized controlled trials. **Schizophrenia Research**, v. 35, n. 1, p. 51–68, 1999.

LEUCHT, S. et al. Second-generation versus first-generation antipsychotic drugs for schizophrenia: a meta-analysis. **The Lancet**, v. 373, n. 9657, p. 31–41, 2009.

LEVIN, Y.; HRADETZKY, E.; BAHN, S. Quantification of proteins using data-independent analysis (MS E) in simple andcomplex samples: A systematic evaluation. **Proteomics**, v. 11, n. 16, p. 3273–3287, 2011.

LEWIS, D. A; LIEBERMAN, J. A. Catching up on schizophrenia: natural history and neurobiology. **Neuron**, v. 28, n. 2, p. 325–334, 2000.

LI, G.-Z. et al. Database searching and accounting of multiplexed precursor and product ion spectra from the data independent analysis of simple and complex peptide mixtures. **PROTEOMICS**, v. 9, n. 6, p. 1696–1719, 1 mar. 2009.

LI, J.; WANG, H.; ROSENBERG, P. A. Vitamin K prevents oxidative cell death by inhibiting activation of 12-lipoxygenase in developing oligodendrocytes. **Journal of Neuroscience Research**, v. 87, n. 9, p. 1997–2005, 2009.

LIEBERMAN, J. A. et al. Serotonergic basis of antipsychotic drug effects in schizophrenia. **Biological Psychiatry**, v. 44, n. 11, p. 1099–1117, 1998.

LIEBERMAN, J. A. et al. Effectiveness of Antipsychotic Drugs in Patients with Chronic Schizophrenia. **n engl j med**, v. 35312353, p. 1209–23, 2005.

LINDEN, D. E. J. The Challenges and Promise of Neuroimaging in Psychiatry. **Neuron**, v. 73, n. 1, p. 8–22, 2012.

LINK, A. J. et al. Direct analysis of protein complexes using mass spectrometry. **Nature Biotechnology**, v. 17, n. 7, p. 676–682, 1999.

LINKER, R. A. et al. CNTF is a major protective factor in demyelinating CNS disease: A neurotrophic cytokine as modulator in neuroinflammation. **Nature Medicine**, v. 8, n. 6, p. 620–624, 2002.

LIU, Y. R. et al. Association of the PPAR-γ gene with altered glucose levels and psychosis profile in schizophrenia patients exposed to antipsychotics. **Psychiatry Investigation**, v. 11, n. 2, p. 179–185, 2014.

LLERENA, A. et al. Relationship between haloperidol plasma concentration, debrisoquine metabolic ratio, CYP2D6 and CYP2C9 genotypes in psychiatric patients.

Pharmacopsychiatry, v. 37, n. 2, p. 69–73, 2004.

MAAS, D. A.; VALLÈS, A.; MARTENS, G. J. M. Oxidative stress, prefrontal cortex hypomyelination and cognitive symptoms in schizophrenia. **Translational Psychiatry**, v. 7, n. 7, p. e1171, 2017.

MACKAY, A. V et al. Increased brain dopamine and dopamine receptors in schizophrenia. **Archives of General Psychiatry**, v. 39, n. 9, p. 991–997, 1982.

MAGRI, C. et al. Glutamate AMPA receptor subunit 1 gene (GRIA1) and DSM-IV=TR schizophrenia: A pilot case-control association study in an Italian sample. **American Journal of Medical Genetics - Neuropsychiatric Genetics**, v. 141 B, n. 3, p. 287–293, 2006.

MAILMAN, R. B.; MURTHY, V. Third generation antipsychotic drugs: partial agonism or receptor functional selectivity? **Current pharmaceutical design**, v. 16, n. 5, p. 488–501, 2010.

MARTINS-DE-SOUZA, D. et al. Proteome analysis of schizophrenia patients Wernicke's area reveals an energy metabolism dysregulation. **BMC Psychiatry**, v. 9, n. 1, p. 17, 2009.

MARTINS-DE-SOUZA, D. et al. Proteome analysis of the thalamus and cerebrospinal fluid reveals glycolysis dysfunction and potential biomarkers candidates for schizophrenia. **Journal of Psychiatric Research**, v. 44, n. 16, p. 1176–1189, 2010.

MARTINS-DE-SOUZA, D.; LEBAR, M.; TURCK, C. W. Proteome analyses of cultured astrocytes treated with MK-801 and clozapine: similarities with schizophrenia. **European Archives of Psychiatry and Clinical Neuroscience**, v. 261, n. 3, p. 217–228, 2011.

MATERA, A. G.; WANG, Z. A day in the life of the spliceosome. **Nature Reviews Molecular Cell Biology**, v. 15, n. 2, p. 108–121, 2014.

MAYNARD, T. M. et al. Neural development, cell-cell signaling, and the "two-hit" hypothesis of schizophrenia. **Schizophrenia bulletin**, v. 27, n. 3, p. 457–476, 2001.

MCGRATH, J.; BROWN, A.; ST CLAIR, D. Prevention and schizophrenia - The role of dietary factors. **Schizophrenia Bulletin**, v. 37, n. 2, p. 272–283, 2011.

MEAD, A. N.; STEPHENS, D. N. Selective disruption of stimulus-reward learning in glutamate receptor gria1 knock-out mice. **The Journal of neuroscience : the official journal of the Society for Neuroscience**, v. 23, n. 3, p. 1041–8, 2003.

MELKERSSON, K. I.; DAHL, M. L. Relationship between levels of insulin or triglycerides and serum concentrations of the atypical antipsychotics clozapine and olanzapine in patients on treatment with therapeutic doses. **Psychopharmacology**, v. 170, n. 2, p. 157–166, 2003.

MELLICK, R. S.; BASSETT, R. L. The cerebrospinal-fluid glutamic oxaloacetic transaminase activity in neurological diseases. p. 1956–1958, 1956.

MEYER, J. M.; SIMPSON, G. M. From Chlorpromazine to Olanzapine: A Brief History of Antipsycholics. **#{149} September**, v. 48, n. 9, 1997.

MIDDLETON, F. A et al. Gene expression profiling reveals alterations of specific metabolic pathways in schizophrenia. **The Journal of neuroscience : the official journal of the Society for Neuroscience**, v. 22, n. 7, p. 2718–2729, 2002.

MIDDLETON, F. A. et al. Altered Expression of 14-3-3 Genes in the Prefrontal Cortex of Subjects with Schizophrenia. **Neuropsychopharmacology**, v. 30, n. 5, p. 974–983, 2005.

MIRNICS, K. et al. Molecular Characterization of Schizophrenia Viewed by Microarray Analysis of Gene Expression in Prefrontal Cortex. **Neuron**, v. 28, n. 1, p. 53–67, 2000.

MITA, T. et al. Decreased serotonin S2 and increased dopamine D2 receptors in chronic schizophrenics. **Biological Psychiatry**, v. 21, n. 14, p. 1407–1414, 1986.

MURRAY, R. M. Is schizophrenia a neurodevelopmental disorder? **British Medical Journal**, v. 295, p. 681, 1987.

NASCIMENTO, J. M.; MARTINS-DE-SOUZA, D. The proteome of schizophrenia. **npj Schizophrenia**, v. 1, n. October 2014, p. 14003, 2015.

NAVE, K.-A.; EHRENREICH, H. Myelination and Oligodendrocyte Functions in Psychiatric Diseases. **JAMA Psychiatry**, v. 71, n. 5, p. 582, 2014.

NEILL, J. C. et al. Animal models of cognitive dysfunction and negative symptoms of schizophrenia: Focus on NMDA receptor antagonism. **Pharmacology and Therapeutics**, v. 128, n. 3, p. 419–432, 2010.

OHNUMA, T. et al. Association analysis of glycine- and serine-related genes in a Japanese population of patients with schizophrenia. **Progress in Neuro-Psychopharmacology and Biological Psychiatry**, v. 33, n. 3, p. 511–518, 2009.

Oligodendroglial density in the prefrontal cortex in schizophrenia and mood disorders: a study from the Stanley Neuropathology Consortium. **Schizophrenia Research**, v. 67, n. 2–3, p. 269–275, 1 abr. 2004.

OLIVEIRA, B. M.; COORSSEN, J. R.; MARTINS-DE-SOUZA, D. 2DE: The Phoenix of Proteomics. **Journal of Proteomics**, v. 104, p. 140–150, 2014.

OWEN, M. J.; O'DONOVAN, M. C. Schizophrenia and the neurodevelopmental continuum:evidence from genomics. **World Psychiatry**, v. 16, n. 3, p. 227–235, 2017.

OWEN, M. J.; SAWA, A.; MORTENSEN, P. B. Schizophrenia. **The Lancet**, v. 388, n. 10039, p. 86–97, 2016.

OZEKI, Y. et al. Phosphoserine phosphatase activity is elevated and correlates negatively with plasma d-serine concentration in patients with schizophrenia. **Psychiatry Research**, v.

237, p. 344–350, 2016.

PAULSON, L. et al. Comparative genome- and proteome analysis of cerebral cortex from MK-801-treated rats. **Journal of Neuroscience Research**, v. 71, n. 4, p. 526–533, 15 fev. 2003.

PERERA, J. et al. Neuroprotective effects of alpha lipoic Acid on haloperidol-induced oxidative stress in the rat brain. **Cell Biosci**, v. 1, n. 1, p. 12, 2011.

PINBORG, L. H.; BAARE, W. Decreased Frontal Serotonin2A Receptor Binding in Antipsychotic-Naive Patients with First-Episode Schizophrenia. **Arch Gen Psychiatry**, v. 67, n. 1, p. 9–16, 2010.

PIOMELLI, D.; GREENGARD, P. Lipoxygenase metabolites of arachidonic acid in neuronal transmembrane signalling. **Trends in Pharmacological Sciences**, v. 11, n. 9, p. 367–373, 1990.

PRATA, D. P. et al. Risk variant of oligodendrocyte lineage transcription factor 2 is associated with reduced white matter integrity. **Human Brain Mapping**, v. 34, n. 9, p. 2025–2031, 2013.

PUGAZHENTHI, S. et al. Downregulation of CREB expression in Alzheimer's brain and in Aβ-treated rat hippocampal neurons. **Molecular neurodegeneration**, v. 6, n. 1, p. 60, 2011.

QING, Y. et al. Dysregulated 14-3-3 Family in Peripheral Blood Leukocytes of Patients with Schizophrenia. **Scientific Reports**, v. 6, p. 1–8, 2016.

RYAN, M. M. et al. Gene expression analysis of bipolar disorder reveals downregulation of the ubiquitin cycle and alterations in synaptic genes. **Molecular Psychiatry**, v. 11, n. 10, p. 965–978, 2006.

SAIA-CEREDA, V. M.; SANTANA, A. G. The Nuclear Proteome of White and Gray Matter from Schizophrenia Postmortem Brains. p. 37–52, 2017.

SAIA, V. M. et al. Proteomics of the corpus callosum unravel pivotal players in the dysfunction of cell signaling , structure , and myelination in schizophrenia brains. **European Archives of Psychiatry and Clinical Neuroscience**, v. 265, n. 7, p. 601–612, 2015.

SAINI, H. S. et al. Neurotrophin-3 and a CREB-mediated signaling pathway regulate Bcl-2 expression in oligodendrocyte progenitor cells. **Journal of Neurochemistry**, v. 89, n. 4, p. 951–961, 2004.

SAMAD, N.; HALEEM, D. J. Antioxidant effects of rice bran oil mitigate repeated haloperidol-induced tardive dyskinesia in male rats. **Metabolic Brain Disease**, v. 32, n. 4, p. 1099–1107, 2017.

SAURA, C. A.; VALERO, J. The role of CREB signaling in Alzheimer's disease and other

cognitive disorders. **Reviews in the Neurosciences**, v. 22, n. 2, p. 153–169, 2011.

SCHMITT, A. et al. Structural synaptic elements are differentially regulated in superior temporal cortex of schizophrenia patients. **European Archives of Psychiatry and Clinical Neuroscience**, v. 262, n. 7, p. 565–577, 2012.

SCHMITT, A. et al. The impact of environmental factors in severe psychiatric disorders. **Frontiers in Neuroscience**, v. 8, n. February, p. 1–10, 2014.

SCHUBERT, K. O.; FÖCKING, M.; COTTER, D. R. Proteomic pathway analysis of the hippocampus in schizophrenia and bipolar affective disorder implicates 14-3-3 signaling, aryl hydrocarbon receptor signaling, and glucose metabolism: Potential roles in GABAergic interneuron pathology. **Schizophrenia Research**, v. 167, n. 1–3, p. 64–72, 2015.

SHEN, W. W. A history of antipsychotic drug development. **Comprehensive Psychiatry**, v. 40, n. 6, p. 407–414, 1999.

SPOHN, H. E. Treatment of Schizophrenia. v. 30, n. 1, 1985.

STARK, A. K. et al. Glial Cell Loss in the Anterior Cingulate Cortex, a Subregion of the Prefrontal Cortex, in Subjects with Schizophrenia. **American Journal of Psychiatry**, v. 161, n. 5, p. 882–888, 2004.

STEINER, J. et al. Clozapine promotes glycolysis and myelin lipid synthesis in cultured oligodendrocytes. **Frontiers in Cellular Neuroscience**, v. 8, n. November, p. 1–11, 2014.

STEPHEN, J.; JONATHAN, A. Roles of the Akt / GSK-3 and Wnt Signaling Pathways in Schizophrenia and Antipsychotic Drug Ac. n. April, p. 388–396, 2010.

SULLIVAN, P. F.; DALY, M. J.; O'DONOVAN, M. Genetic architectures of psychiatric disorders: the emerging picture and its implications. **Nature Reviews Genetics**, v. 13, n. 8, p. 537–551, 2012.

TANDON, R.; HALBREICH, U. The second-generation "atypical" antipsychotics: Similar improved efficacy but different neuroendocrine side effects. **Psychoneuroendocrinology**, v. 28, n. SUPPL. 1, p. 1–7, 2003.

TARAZI, F. et al. Long-term effects of olanzapine, risperidone, and quetiapine on ionotropic glutamate receptor types: implications for antipsychotic drug treatment. **Journal of Pharmacology and …**, v. 306, n. 3, p. 1145–1151, 2003.

THISELTON, D. L. et al. AKT1 Is Associated with Schizophrenia Across Multiple Symptom Dimensions in the Irish Study of High Density Schizophrenia Families. **Biological Psychiatry**, v. 63, n. 5, p. 449–457, 2008.

THORBURNE, S. K.; JUURLINK, B. H. Low glutathione and high iron govern the susceptibility of oligodendroglial precursors to oxidative stress. **Journal of neurochemistry**,

v. 67, n. 3, p. 1014–22, 1996.

URANOVA, N. et al. Electron microscopy of oligodendroglia in severe mental illness. **Brain research bulletin**, v. 55, n. 5, p. 597–610, 15 jul. 2001.

VAN OS, J.; KAPUR, S. Schizophrenia. **The Lancet**, v. 374, n. 9690, p. 635–645, 2009.

VICHI, S. et al. Cell type-specific expression and localization of cytochrome P450 isoforms in tridimensional aggregating rat brain cell cultures. **Toxicology in Vitro**, v. 30, n. 1, p. 176–184, 2015.

VOINESKOS, A. N. et al. Oligodendrocyte genes, white matter tract integrity, and cognition in schizophrenia. **Cerebral Cortex**, v. 23, n. 9, p. 2044–2057, 2013.

WANG, H. et al. 12-Lipoxygenase plays a key role in cell death caused by glutathione depletion and arachidonic acid in rat oligodendrocytes. **European Journal of Neuroscience**, v. 20, n. 8, p. 2049–2058, 2004.

WANG, S. et al. Notch receptor activation inhibits oligodendrocyte differentiation. **Neuron**, v. 21, n. 1, p. 63–75, 1998.

WANG, X. et al. Regulation of NMDA Receptors by Dopamine D 4 Signaling in Prefrontal Cortex. **October**, v. 23, n. 30, p. 9852–9861, 2003.

WAZIRI, R. et al. Abnormal serine hydroxymethyl transferase activity in the temporal lobes of schizophrenics. **Neuroscience Letters**, v. 120, n. 2, p. 237–240, 1990.

WEINBERGER, D. R. Implications of normal Brain Development for the Pathogenesis of Schizphrenia. **Arch. Gen. Psychiatry**, v. 44, n. 7, p. 660–669, 1987.

WHO | Schizophrenia. **WHO**, 2016.

WILKINS, M. R. et al. Progress with proteome projects: Why all proteins expressed by a genome should be identified and how to do it. **Biotechnology and Genetic Engineering Reviews**, v. 13, n. 1, p. 19–50, 1996.

WROBLEWSKI, F. The Clinical Significance of Alterations in Transaminase Activities of Serum and Other Body Fluids. **Advances in Clinical Chemistry**, v. 1, n. C, p. 313–351, 1958.

XIU, Y. et al. White Matter Injuries Induced by MK-801 in a Mouse Model of Schizophrenia Based on NMDA Antagonism. **The Anatomical Record**, v. 297, n. 8, p. 1498–1507, 1 ago. 2014.

XU, M. Q. et al. Prenatal malnutrition and adult Schizophrenia: Further evidence from the 1959-1961 chinese famine. **Schizophrenia Bulletin**, v. 35, n. 3, p. 568–576, 2009.

YOON, S. C. et al. The effect of MK-801 on mTOR/p70S6K and translation-related proteins in rat frontal cortex. **Neuroscience Letters**, v. 434, n. 1, p. 23–28, 2008.

ZHENG, W. et al. The possible role of the Akt signaling pathway in schizophrenia. **Brain Research**, v. 1470, p. 145–158, 2012.

13. ANEXOS (CAPÍTULO 2)

Table 1: Proteins affected by chlorpromazine treatment

Table 1 - Proteins affected by chlorpromazine treatment

Accession	Gene	Anova (p)	log_2 Fold Change	Protein
Q9H3S1	SEMA4A	0,02038	-11,961	Semaphorin-4A
Q13797	ITGA9	0,03028	-7,910	Integrin alpha-9
O60308	CEP104	0,00360	-7,235	Centrosomal protein of 104 kDa
A0A0J9YYF7	DAAM2	0,01675	-6,539	Disheveled-associated activator of morphogenesis 2
Q14686	NCOA6	0,02527	-5,330	Nuclear receptor coactivator 6
Q8N3A8	PARP8	0,00180	-4,860	Poly [ADP-ribose] polymerase 8
Q70CQ4	USP31	0,00783	-4,397	Ubiquitin carboxyl-terminal hydrolase 31
C9JEH7	RPS4Y1	0,01591	-4,385	40S ribosomal protein S4_ Y isoform 1 (Fragment)
Q70EK8	USP53	0,02073	-4,184	Inactive ubiquitin carboxyl-terminal hydrolase 53
O00213	APBB1	0,04236	-4,135	Amyloid beta A4 precursor protein-binding family B member 1
P42771	CDKN2A	0,00711	-4,095	Cyclin-dependent kinase inhibitor 2A
P18754	RCC1	0,01131	-4,094	Regulator of chromosome condensation
Q92608	DOCK2	0,00540	-4,090	Dedicator of cytokinesis protein 2
P23193	TCEA1	0,04062	-4,000	Transcription elongation factor A protein 1
Q8N3Y3	LARGE2	0,04589	-3,962	LARGE xylosyl- and glucuronyltransferase 2
O95271	TNKS	0,00565	-3,916	Tankyrase-1
Q96MT3	PRICKLE1	0,03596	-3,697	Prickle-like protein 1
H0YLX2	RFX7	0,02495	-3,593	DNA-binding protein RFX7
H0YNH8	UACA	0,02982	-3,585	Uveal autoantigen with coiled-coil domains and ankyrin repeats
Q9UM07	PADI4	0,00818	-3,582	Protein-arginine deiminase type-4

Q92499	DDX1	0,00239	-3,533	ATP-dependent RNA helicase DDX1
P35503	UGT1A3	0,00051	-3,511	UDP-glucuronosyltransferase 1-3
Q96L34	MARK4	0,01581	-3,410	MAP/microtubule affinity-regulating kinase 4
Q8TF32	ZNF431	0,02135	-3,313	Zinc finger protein 431
Q96JW4	SLC41A2	0,00226	-3,266	Solute carrier family 41 member 2
P08922	ROS1	0,01591	-3,164	Proto-oncogene tyrosine-protein kinase ROS
Q96LT9	RNPC3	0,02813	-3,134	RNA-binding protein 40
K7ELH8	DPY19L3	0,01581	-3,068	Probable C-mannosyltransferase DPY19L3
A0A0C4DFN1	MFN1	0,01962	-3,066	Mitofusin-1
P42285	SKIV2L2	0,01189	-3,026	Superkiller viralicidic activity 2-like 2
O43861	ATP9B	0,00922	-2,964	Probable phospholipid-transporting ATPase IIB
Q92817	EVPL	0,00332	-2,962	Envoplakin
P48444	ARCN1	0,03330	-2,884	Coatomer subunit delta
Q9HAQ2	KIF9	0,01903	-2,828	Kinesin-like protein KIF9
Q9NRL2	BAZ1A	0,00706	-2,800	Bromodomain adjacent to zinc finger domain protein 1A
Q9H7X3	ZNF696	0,00416	-2,702	Zinc finger protein 696
Q5UIP0	RIF1	0,04600	-2,690	Telomere-associated protein RIF1
Q8TDD1	DDX54	0,00325	-2,662	ATP-dependent RNA helicase DDX54
A0A0C4DGS1	DDOST	0,00898	-2,616	Dolichyl-diphosphooligosaccharide--protein glycosyltransferase 48 kDa subunit
P07332	FES	0,01019	-2,616	Tyrosine-protein kinase Fes/Fps
Q14687	GSE1	0,01648	-2,609	Genetic suppressor element 1
P28749	RBL1	0,03717	-2,579	Retinoblastoma-like protein 1
C9J6P4	ZC3HAV1	0,04603	-2,577	Zinc finger CCCH-type antiviral protein 1
E7ESW6	WDR87	0,00049	-2,563	WD repeat-containing protein 87
J3KN29	PSMD9	0,02611	-2,542	26S proteasome non-ATPase regulatory subunit 9
P08581	MET	0,02251	-2,534	Hepatocyte growth factor receptor
Q9HBW1	LRRC4	0,00963	-2,528	Leucine-rich repeat-containing protein 4
Q14651	PLS1	0,03983	-2,430	Plastin-1

K7ELX4	FECH	0,00074	-2,422	Ferrochelatase_ mitochondrial (Fragment)
Q9UQ53	MGAT4B	0,01356	-2,420	Alpha-1_3-mannosyl-glycoprotein 4-beta-N-acetylglucosaminyltransferase B
Q86WI1	PKHD1L1	0,04303	-2,413	Fibrocystin-L
O76090	BEST1	0,04461	-2,406	Bestrophin-1
D6REX3	SEC31A	0,01971	-2,334	Protein transport protein Sec31A
O15066	KIF3B	0,00591	-2,268	Kinesin-like protein KIF3B
P25054	APC	0,00951	-2,260	Adenomatous polyposis coli protein
O60486	PLXNC1	0,04146	-2,245	Plexin-C1
Q8WWZ7	ABCA5	0,01165	-2,238	ATP-binding cassette sub-family A member 5
P55011	SLC12A2	0,00693	-2,189	Solute carrier family 12 member 2
Q5TAX3	ZCCHC11	0,01091	-2,174	Terminal uridylyltransferase 4
P05062	ALDOB	0,02315	-2,142	Fructose-bisphosphate aldolase B
P30876	POLR2B	0,01974	-2,131	DNA-directed RNA polymerase II subunit RPB2
Q9NY59	SMPD3	0,01337	-2,116	Sphingomyelin phosphodiesterase 3
Q8IYT4	KATNAL2	0,00197	-2,086	Katanin p60 ATPase-containing subunit A-like 2
Q8TF74	WIPF2	0,01392	-2,066	WAS/WASL-interacting protein family member 2
A0A087X295	WDR6	0,01996	-2,059	WD repeat-containing protein 6
Q86YV9	HPS6	0,02580	-2,041	Hermansky-Pudlak syndrome 6 protein
Q96GE4	CEP95	0,02233	-2,030	Centrosomal protein of 95 kDa
O95382	MAP3K6	0,01107	-2,014	Mitogen-activated protein kinase kinase kinase 6
Q8TE82	SH3TC1	0,04982	-2,003	SH3 domain and tetratricopeptide repeat-containing protein 1
Q8IYD8	FANCM	0,04317	-1,994	Fanconi anemia group M protein
P53675	CLTCL1	0,02094	-1,989	Clathrin heavy chain 2
Q9HCL0	PCDH18	0,00277	-1,985	Protocadherin-18
Q99541	PLIN2	0,03093	-1,930	Perilipin-2
O00567	NOP56	0,02166	-1,918	Nucleolar protein 56
O94769	ECM2	0,02776	-1,915	Extracellular matrix protein 2
Q13177	PAK2	0,01699	-1,911	Serine/threonine-protein kinase PAK 2
P11387	TOP1	0,00967	-1,906	DNA topoisomerase 1

O15381	NVL	0,04791	-1,906	Nuclear valosin-containing protein-like
A0A1B0GVY1	NEDD4L	0,00355	-1,887	E3 ubiquitin-protein ligase NEDD4-like
Q9Y5F2	PCDHB11	0,00528	-1,886	Protocadherin beta-11
Q9H1H9	KIF13A	0,00120	-1,857	Kinesin-like protein KIF13A
A1L170	C1orf226	0,01856	-1,836	Uncharacterized protein C1orf226
Q8WUY3	PRUNE2	0,00736	-1,800	Protein prune homolog 2
O00139	KIF2A	0,02831	-1,779	Kinesin-like protein KIF2A
B4DRP8	ZNF461	0,01644	-1,764	Zinc finger protein 461
A0A0A0MRP2	FPGT	0,02213	-1,764	Fucose-1-phosphate guanylyltransferase
Q8N944	AMER3	0,03422	-1,735	APC membrane recruitment protein 3
K7EMW4	NCLN	0,01418	-1,716	Nicalin
M0QYL3	HNRNPM	0,02844	-1,706	Heterogeneous nuclear ribonucleoprotein M (Fragment)
Q8WXE1	ATRIP	0,04406	-1,696	ATR-interacting protein
P55289	CDH12	0,00595	-1,681	Cadherin-12
Q6ZSZ6	TSHZ1	0,02532	-1,680	Teashirt homolog 1
Q13772	NCOA4	0,00634	-1,663	Nuclear receptor coactivator 4
P15822	HIVEP1	0,00883	-1,661	Zinc finger protein 40
Q9P2M7	CGN	0,04129	-1,639	Cingulin
A0A0A0MSY2	GTF2IRD2	0,00719	-1,635	General transcription factor II-I repeat domain-containing protein 2A
Q86XA9	HEATR5A	0,00372	-1,551	HEAT repeat-containing protein 5A
Q6W2J9	BCOR	0,00241	-1,522	BCL-6 corepressor
P14384	CPM	0,00841	-1,518	Carboxypeptidase M
P17980	PSMC3	0,00004	-1,516	26S protease regulatory subunit 6A
P54098	POLG	0,04503	-1,496	DNA polymerase subunit gamma-1
O43526	KCNQ2	0,02706	-1,494	Potassium voltage-gated channel subfamily KQT member 2
Q96N23	CFAP54	0,00439	-1,488	Cilia- and flagella-associated protein 54
P33993	MCM7	0,01365	-1,468	DNA replication licensing factor MCM7
P49321	NASP	0,00532	-1,464	Nuclear autoantigenic sperm protein

Q9NZU7	CABP1	0,03344	-1,457	Calcium-binding protein 1
E7ESP9	NEFM	0,04984	-1,457	Neurofilament medium polypeptide
Q9UKL3	CASP8AP2	0,03108	-1,443	CASP8-associated protein 2
P21359	NF1	0,02495	-1,441	Neurofibromin
E9PGT3	RPS6KA1	0,02143	-1,435	Ribosomal protein S6 kinase
Q86VV8	RTTN	0,01444	-1,431	Rotatin
Q5T4S7	UBR4	0,01716	-1,425	E3 ubiquitin-protein ligase UBR4
Q86W26	NLRP10	0,00523	-1,424	NACHT_ LRR and PYD domains-containing protein 10
P51795	CLCN5	0,00084	-1,421	H(+)/Cl(-) exchange transporter 5
F2Z3N3	OLFML2B	0,02163	-1,420	Olfactomedin-like protein 2B
A0AVT1	UBA6	0,02636	-1,420	Ubiquitin-like modifier-activating enzyme 6
Q9H2J7	SLC6A15	0,01817	-1,415	Sodium-dependent neutral amino acid transporter B(0)AT2
P11274	BCR	0,03392	-1,392	Breakpoint cluster region protein
Q5T3U5	ABCC10	0,03273	-1,374	Multidrug resistance-associated protein 7
Q15029	EFTUD2	0,02045	-1,373	116 kDa U5 small nuclear ribonucleoprotein component
Q6FI13	HIST2H2AA3	0,03962	-1,361	Histone H2A type 2-A
P08648	ITGA5	0,03604	-1,345	Integrin alpha-5
Q8NFM4	ADCY4	0,01595	-1,337	Adenylate cyclase type 4
O43909	EXTL3	0,00520	-1,330	Exostosin-like 3
Q8N1W1	ARHGEF28	0,04298	-1,329	Rho guanine nucleotide exchange factor 28
Q8NG48	LINS1	0,02032	-1,323	Protein Lines homolog 1
Q6ZNJ1	NBEAL2	0,00744	-1,307	Neurobeachin-like protein 2
Q86W92	PPFIBP1	0,01555	-1,306	Liprin-beta-1
Q6AI08	HEATR6	0,01611	-1,285	HEAT repeat-containing protein 6
O95402	MED26	0,02826	-1,282	Mediator of RNA polymerase II transcription subunit 26
Q4L235	AASDH	0,03275	-1,271	Acyl-CoA synthetase family member 4
A6H8M9	CDHR4	0,03470	-1,260	Cadherin-related family member 4
R4GN35	DENND4C	0,00003	-1,255	DENN domain-containing protein 4C

Q96QK1	VPS35	0,03241	-1,255	Vacuolar protein sorting-associated protein 35
Q5JYT7	KIAA1755	0,00396	-1,245	Uncharacterized protein KIAA1755
Q01105	SET	0,04248	-1,245	Protein SET
Q5TAT6	COL13A1	0,00367	-1,231	Collagen alpha-1(XIII) chain
Q15572	TAF1C	0,02000	-1,204	TATA box-binding protein-associated factor RNA polymerase I subunit C
Q01432	AMPD3	0,01277	-1,201	AMP deaminase 3
Q76M96	CCDC80	0,01559	-1,200	Coiled-coil domain-containing protein 80
Q6NUP7	PPP4R4	0,00329	-1,192	Serine/threonine-protein phosphatase 4 regulatory subunit 4
F8W031	#VALOR!	0,03713	-1,171	Uncharacterized protein (Fragment)
Q9UKE5	TNIK	0,00726	-1,150	TRAF2 and NCK-interacting protein kinase
Q9Y3R0	GRIP1	0,01579	-1,132	Glutamate receptor-interacting protein 1
A0A087WW76	ARHGAP21	0,01489	-1,125	Rho GTPase-activating protein 21
P31942	HNRNPH3	0,03784	-1,106	Heterogeneous nuclear ribonucleoprotein H3
Q96JG8	MAGED4	0,04695	-1,101	Melanoma-associated antigen D4
Q13393	PLD1	0,00038	-1,075	Phospholipase D1
D6W5U7	STAG3	0,00583	-1,062	Cohesin subunit SA-3
Q9BZX2	UCK2	0,00398	-1,047	Uridine-cytidine kinase 2
H0Y626	#VALOR!	0,01374	-1,035	Uncharacterized protein
Q0VG06	FAAP100	0,00309	-1,025	Fanconi anemia core complex-associated protein 100
O75592	MYCBP2	0,00357	-0,995	E3 ubiquitin-protein ligase MYCBP2
Q0VDD8	DNAH14	0,01004	-0,990	Dynein heavy chain 14_ axonemal
O75113	N4BP1	0,00129	-0,981	NEDD4-binding protein 1
H9KV53	AGBL2	0,03885	-0,979	Cytosolic carboxypeptidase 2
Q709C8	VPS13C	0,04018	-0,971	Vacuolar protein sorting-associated protein 13C
Q6TFL3	CCDC171	0,02623	-0,942	Coiled-coil domain-containing protein 171
O43933	PEX1	0,00399	-0,939	Peroxisome biogenesis factor 1
O75369	FLNB	0,00539	-0,937	Filamin-B
Q66K14	TBC1D9B	0,04279	-0,933	TBC1 domain family member 9B

A0A087WYZ7	SEMA4F	0,02666	-0,923	Semaphorin-4F
Q9UBN4	TRPC4	0,01847	-0,915	Short transient receptor potential channel 4
P54259	ATN1	0,01871	-0,912	Atrophin-1
B1AJZ9	FHAD1	0,03746	-0,900	Forkhead-associated domain-containing protein 1
P26373	RPL13	0,04142	-0,898	60S ribosomal protein L13
P46100	ATRX	0,00015	-0,893	Transcriptional regulator ATRX
P54284	CACNB3	0,03137	-0,881	Voltage-dependent L-type calcium channel subunit beta-3
J3KTL2	SRSF1	0,03892	-0,875	Serine/arginine-rich-splicing factor 1
Q9H0S4	DDX47	0,01212	-0,870	Probable ATP-dependent RNA helicase DDX47
Q96JM4	LRRIQ1	0,04431	-0,850	Leucine-rich repeat and IQ domain-containing protein 1
P32927	CSF2RB	0,01888	-0,815	Cytokine receptor common subunit beta
Q9UHL9	GTF2IRD1	0,01016	-0,797	General transcription factor II-I repeat domain-containing protein 1
Q969X6	UTP4	0,03200	-0,788	U3 small nucleolar RNA-associated protein 4 homolog
Q8N283	ANKRD35	0,01673	-0,750	Ankyrin repeat domain-containing protein 35
Q8WZ74	CTTNBP2	0,04055	-0,746	Cortactin-binding protein 2
H7BY35	RYR2	0,02364	-0,730	Ryanodine receptor 2
O75147	OBSL1	0,01322	-0,725	Obscurin-like protein 1
Q8NC51	SERBP1	0,04052	-0,711	Plasminogen activator inhibitor 1 RNA-binding protein
E7EWW0	C16orf62	0,00253	-0,685	UPF0505 protein C16orf62
Q6UB98	ANKRD12	0,00799	-0,672	Ankyrin repeat domain-containing protein 12
O75309	CDH16	0,04058	-0,663	Cadherin-16
E7ER45	MGAM	0,02801	-0,661	Maltase-glucoamylase_ intestinal
Q8TD31	CCHCR1	0,03121	-0,651	Coiled-coil alpha-helical rod protein 1
Q8WXU2	DYX1C1	0,04411	-0,644	Dyslexia susceptibility 1 candidate gene 1 protein
Q9Y228	TRAF3IP3	0,04435	-0,636	TRAF3-interacting JNK-activating modulator
Q9NSI6	BRWD1	0,00650	-0,632	Bromodomain and WD repeat-containing protein 1
P53779	MAPK10	0,04743	-0,629	Mitogen-activated protein kinase 10
P23921	RRM1	0,02347	-0,622	Ribonucleoside-diphosphate reductase large subunit

H0YJ75	PPP2R5C	0,01984	-0,604	Serine/threonine-protein phosphatase 2A 56 kDa regulatory subunit gamma isoform (Fragment)
Q9UKX3	MYH13	0,02805	-0,587	Myosin-13
Q8N8Z8	ZNF441	0,02080	-0,577	Zinc finger protein 441
Q6AHZ1	ZNF518A	0,00808	-0,576	Zinc finger protein 518A
Q96PE1	ADGRA2	0,03056	-0,573	Adhesion G protein-coupled receptor A2
Q12879	GRIN2A	0,01679	-0,571	Glutamate receptor ionotropic_ NMDA 2A
A0A0A0MS59	SRCAP	0,00249	-0,568	Helicase SRCAP
Q12929	EPS8	0,04139	-0,556	Epidermal growth factor receptor kinase substrate 8
J3QSU6	TNC	0,01108	-0,540	Tenascin
J3KQH6	PHC1	0,00884	-0,521	Polyhomeotic-like protein 1
Q5VT06	CEP350	0,02820	-0,510	Centrosome-associated protein 350
P49454	CENPF	0,02024	-0,507	Centromere protein F
O95755	RAB36	0,04722	-0,503	Ras-related protein Rab-36
Q01831	XPC	0,04741	-0,483	DNA repair protein complementing XP-C cells
E7EQR4	EZR	0,04999	-0,474	Ezrin
O14647	CHD2	0,00320	-0,468	Chromodomain-helicase-DNA-binding protein 2
Q9Y5S2	CDC42BPB	0,01548	-0,452	Serine/threonine-protein kinase MRCK beta
P07237	P4HB	0,01709	-0,436	Protein disulfide-isomerase
Q5T7B8	KIF24	0,01081	-0,427	Kinesin-like protein KIF24
Q9H2Y7	ZNF106	0,00458	-0,425	Zinc finger protein 106
O95757	HSPA4L	0,03368	-0,394	Heat shock 70 kDa protein 4L
Q3T8J9	GON4L	0,04839	-0,364	GON-4-like protein
Q92830	KAT2A	0,02396	-0,314	Histone acetyltransferase KAT2A
Q8NE28	STKLD1	0,01851	-0,314	Serine/threonine kinase-like domain-containing protein STKLD1
D3DQV9	EIF4G2	0,00622	-0,309	Eukaryotic translation initiation factor 4 gamma 2 (Fragment)
Q5VWN6	FAM208B	0,04698	-0,294	Protein FAM208B
Q96Q15	SMG1	0,03541	-0,279	Serine/threonine-protein kinase SMG1
Q8IWI9	MGA	0,01720	-0,246	MAX gene-associated protein

Q9Y2K3	MYH15	0,03358	-0,241	Myosin-15
Q16658	FSCN1	0,01669	0,239	Fascin
E9PF32	DENND3	0,04153	0,292	DENN domain-containing protein 3
P04075	ALDOA	0,01961	0,293	Fructose-bisphosphate aldolase A
Q8IZH2	XRN1	0,03714	0,308	5'-3' exoribonuclease 1
E7EUU4	EIF4G1	0,01693	0,365	Eukaryotic translation initiation factor 4 gamma 1
A0A0J9YXM6	WDR81	0,04086	0,377	WD repeat-containing protein 81
P14625	HSP90B1	0,04303	0,399	Endoplasmin
P62937	PPIA	0,02209	0,411	Peptidyl-prolyl cis-trans isomerase A
P08238	HSP90AB1	0,04725	0,421	Heat shock protein HSP 90-beta
P50990	CCT8	0,00562	0,421	T-complex protein 1 subunit theta
Q00839	HNRNPU	0,00793	0,421	Heterogeneous nuclear ribonucleoprotein U
Q9P1V8	SAMD15	0,01930	0,429	Sterile alpha motif domain-containing protein 15
Q5T5P2	KIAA1217	0,03593	0,436	Sickle tail protein homolog
Q7Z7M0	MEGF8	0,03696	0,440	Multiple epidermal growth factor-like domains protein 8
O75843	AP1G2	0,04503	0,446	AP-1 complex subunit gamma-like 2
Q9P1Z9	CCDC180	0,03602	0,461	Coiled-coil domain-containing protein 180
Q14571	ITPR2	0,04891	0,473	Inositol 1_4_5-trisphosphate receptor type 2
Q00872	MYBPC1	0,02179	0,480	Myosin-binding protein C_ slow-type
Q00610	CLTC	0,01460	0,495	Clathrin heavy chain 1
P62280	RPS11	0,01660	0,500	40S ribosomal protein S11
A6QL64	ANKRD36	0,00706	0,501	Ankyrin repeat domain-containing protein 36A
P06733	ENO1	0,00971	0,503	Alpha-enolase
O14802	POLR3A	0,02065	0,507	DNA-directed RNA polymerase III subunit RPC1
Q9BXW6	OSBPL1A	0,04158	0,509	Oxysterol-binding protein-related protein 1
O94875	SORBS2	0,02218	0,523	Sorbin and SH3 domain-containing protein 2
P54136	RARS	0,01858	0,524	Arginine--tRNA ligase_ cytoplasmic
Q15293	RCN1	0,02394	0,529	Reticulocalbin-1

A0A0U1RQF0	FASN	0,01061	0,531	Fatty acid synthase
Q9BXT5	TEX15	0,03028	0,534	Testis-expressed protein 15
Q96MT8	CEP63	0,03619	0,540	Centrosomal protein of 63 kDa
P05198	EIF2S1	0,04144	0,545	Eukaryotic translation initiation factor 2 subunit 1
Q07020	RPL18	0,03095	0,547	60S ribosomal protein L18
P62318	SNRPD3	0,03507	0,567	Small nuclear ribonucleoprotein Sm D3
O94851	MICAL2	0,02883	0,576	[F-actin]-methionine sulfoxide oxidase MICAL2
P34931	HSPA1L	0,02122	0,578	Heat shock 70 kDa protein 1-like
P29401	TKT	0,02840	0,586	Transketolase
P55060	CSE1L	0,02204	0,587	Exportin-2
Q13435	SF3B2	0,02601	0,605	Splicing factor 3B subunit 2
O15254	ACOX3	0,03808	0,606	Peroxisomal acyl-coenzyme A oxidase 3
Q5JPF3	ANKRD36C	0,04693	0,613	Ankyrin repeat domain-containing protein 36C
O60522	TDRD6	0,04397	0,615	Tudor domain-containing protein 6
Q9C0D0	PHACTR1	0,04443	0,617	Phosphatase and actin regulator 1
J3KTP0	LRRC37B	0,01809	0,617	Leucine-rich repeat-containing protein 37B
Q9UHJ3	SFMBT1	0,02506	0,624	Scm-like with four MBT domains protein 1
Q6ECI4	ZNF470	0,04190	0,625	Zinc finger protein 470
P07737	PFN1	0,02275	0,628	Profilin-1
Q96DY7	MTBP	0,03341	0,646	Mdm2-binding protein
Q9UKV3	ACIN1	0,02311	0,649	Apoptotic chromatin condensation inducer in the nucleus
Q15751	HERC1	0,02849	0,651	Probable E3 ubiquitin-protein ligase HERC1
P39019	RPS19	0,01007	0,653	40S ribosomal protein S19
Q9NZJ4	SACS	0,00306	0,653	Sacsin
Q8TD57	DNAH3	0,03359	0,660	Dynein heavy chain 3_ axonemal
F5GZ90	DTL	0,02898	0,665	Denticleless protein homolog
Q02224	CENPE	0,02749	0,670	Centromere-associated protein E
P18583	SON	0,02760	0,672	Protein SON

Q5M9N0	CCDC158	0,03557	0,678	Coiled-coil domain-containing protein 158
P60174	TPI1	0,04628	0,681	Triosephosphate isomerase
Q01518	CAP1	0,00350	0,685	Adenylyl cyclase-associated protein 1
Q15365	PCBP1	0,00872	0,690	Poly(rC)-binding protein 1
H3BMM9	RNPS1	0,01050	0,693	RNA-binding protein with serine-rich domain 1 (Fragment)
O14974	PPP1R12A	0,03974	0,700	Protein phosphatase 1 regulatory subunit 12A
P27708	CAD	0,01948	0,708	CAD protein
P62913	RPL11	0,00169	0,716	60S ribosomal protein L11
Q96EZ8	MCRS1	0,00741	0,718	Microspherule protein 1
A8MUS3	RPL23A	0,01273	0,720	60S ribosomal protein L23a
P62906	RPL10A	0,01269	0,720	60S ribosomal protein L10a
Q8NFF5	FLAD1	0,01098	0,726	FAD synthase
Q9H4B7	TUBB1	0,02230	0,730	Tubulin beta-1 chain
P27824	CANX	0,02752	0,733	Calnexin
Q02641	CACNB1	0,03109	0,737	Voltage-dependent L-type calcium channel subunit beta-1
O60706	ABCC9	0,02963	0,739	ATP-binding cassette sub-family C member 9
O43491	EPB41L2	0,03838	0,739	Band 4.1-like protein 2
Q9C005	DPY30	0,01634	0,740	Protein dpy-30 homolog
Q9NZI8	IGF2BP1	0,00048	0,744	Insulin-like growth factor 2 mRNA-binding protein 1
F5GZQ3	HADHB	0,01294	0,747	Trifunctional enzyme subunit beta_ mitochondrial
Q8TEX9	IPO4	0,04215	0,751	Importin-4
P27797	CALR	0,00041	0,751	Calreticulin
O75155	CAND2	0,03808	0,752	Cullin-associated NEDD8-dissociated protein 2
Q6SJ93	FAM111B	0,00704	0,760	Protein FAM111B
Q12955	ANK3	0,02914	0,773	Ankyrin-3
Q29RF7	PDS5A	0,01520	0,780	Sister chromatid cohesion protein PDS5 homolog A
Q5T5C0	STXBP5	0,00070	0,781	Syntaxin-binding protein 5
Q8IZQ8	MYOCD	0,04694	0,783	Myocardin
P11142	HSPA8	0,03881	0,783	Heat shock cognate 71 kDa protein

H0Y786	NEB	0,00660	0,784	Nebulin (Fragment)
P12268	IMPDH2	0,02215	0,787	Inosine-5'-monophosphate dehydrogenase 2
P19338	NCL	0,01222	0,798	Nucleolin
H0Y8Z7	DDX60	0,00973	0,803	Probable ATP-dependent RNA helicase DDX60 (Fragment)
Q9HAU0	PLEKHA5	0,00190	0,808	Pleckstrin homology domain-containing family A member 5
P23396	RPS3	0,00829	0,820	40S ribosomal protein S3
Q13009	TIAM1	0,02785	0,832	T-lymphoma invasion and metastasis-inducing protein 1
Q9BRZ2	TRIM56	0,01686	0,834	E3 ubiquitin-protein ligase TRIM56
P60953	CDC42	0,04939	0,838	Cell division control protein 42 homolog
G3V295	PSMA6	0,01987	0,843	Proteasome subunit alpha type
A0A0G2JNL3	MUC4	0,00265	0,848	Mucin-4
O00425	IGF2BP3	0,00338	0,848	Insulin-like growth factor 2 mRNA-binding protein 3
Q7Z333	SETX	0,04530	0,848	Probable helicase senataxin
Q7Z2Z1	TICRR	0,00980	0,849	Treslin
P32119	PRDX2	0,00587	0,851	Peroxiredoxin-2
Q96RU2	USP28	0,02240	0,854	Ubiquitin carboxyl-terminal hydrolase 28
Q9Y281	CFL2	0,01611	0,857	Cofilin-2
Q9UHD8	SEPT9	0,02344	0,863	Septin-9
Q9NZL3	ZNF224	0,02029	0,887	Zinc finger protein 224
Q15393	SF3B3	0,04654	0,894	Splicing factor 3B subunit 3
C9J0J7	PFN2	0,04268	0,895	Profilin
Q9UP95	SLC12A4	0,00769	0,901	Solute carrier family 12 member 4
Q9Y5H5	PCDHA9	0,04726	0,902	Protocadherin alpha-9
Q16851	UGP2	0,03624	0,904	UTP--glucose-1-phosphate uridylyltransferase
C9J5X1	IGF1R	0,00757	0,907	Tyrosine-protein kinase receptor
A6NKT7	RGPD3	0,02613	0,908	RanBP2-like and GRIP domain-containing protein 3
C9JE72	IQCE	0,01534	0,910	IQ domain-containing protein E (Fragment)
P60866	RPS20	0,00162	0,919	40S ribosomal protein S20

P08237	PFKM	0,00653	0,920	ATP-dependent 6-phosphofructokinase_ muscle type
O76021	RSL1D1	0,02342	0,920	Ribosomal L1 domain-containing protein 1
Q9HB71	CACYBP	0,02149	0,932	Calcyclin-binding protein
F5GXQ8	SYNE1	0,04815	0,938	Nesprin-1
Q12774	ARHGEF5	0,03187	0,938	Rho guanine nucleotide exchange factor 5
Q9Y2H6	FNDC3A	0,02120	0,943	Fibronectin type-III domain-containing protein 3A
Q68CZ2	TNS3	0,01034	0,944	Tensin-3
Q71DI3	HIST2H3A	0,04196	0,953	Histone H3.2
H7C3D3	ZYX	0,03972	0,967	Zyxin (Fragment)
Q9UG63	ABCF2	0,03158	0,969	ATP-binding cassette sub-family F member 2
Q15056	EIF4H	0,02939	0,975	Eukaryotic translation initiation factor 4H
Q9UBC5	MYO1A	0,02905	0,975	Unconventional myosin-Ia
P62805	HIST1H4A	0,01136	0,975	Histone H4
Q96T37	RBM15	0,00729	0,980	Putative RNA-binding protein 15
A0A0A0MQS9	LAMA4	0,03959	0,984	Laminin subunit alpha-4
P54687	BCAT1	0,01610	0,989	Branched-chain-amino-acid aminotransferase_ cytosolic
Q10472	GALNT1	0,02727	0,993	Polypeptide N-acetylgalactosaminyltransferase 1
Q5TAP6	UTP14C	0,00583	0,994	U3 small nucleolar RNA-associated protein 14 homolog C
Q9BZQ8	FAM129A	0,02190	0,998	Protein Niban
P23378	GLDC	0,01334	0,999	Glycine dehydrogenase (decarboxylating)_ mitochondrial
P46060	RANGAP1	0,01399	1,003	Ran GTPase-activating protein 1
Q9ULV0	MYO5B	0,03477	1,004	Unconventional myosin-Vb
P12111	COL6A3	0,03207	1,006	Collagen alpha-3(VI) chain
A6NE52	WDR97	0,04951	1,007	WD repeat-containing protein 97
Q9UI33	SCN11A	0,00538	1,009	Sodium channel protein type 11 subunit alpha
P17812	CTPS1	0,00345	1,016	CTP synthase 1
Q2M218	ZNF630	0,02942	1,018	Zinc finger protein 630
Q9UHC1	MLH3	0,01945	1,023	DNA mismatch repair protein Mlh3

Q9Y6K5	OAS3	0,01725	1,032	2'-5'-oligoadenylate synthase 3
Q99973	TEP1	0,02130	1,037	Telomerase protein component 1
A0A0C4DG89	DDX46	0,02257	1,038	Probable ATP-dependent RNA helicase DDX46
P30153	PPP2R1A	0,03622	1,046	Serine/threonine-protein phosphatase 2A 65 kDa regulatory subunit A alpha isoform
Q15746	MYLK	0,01852	1,050	Myosin light chain kinase_ smooth muscle
Q9NW13	RBM28	0,03005	1,052	RNA-binding protein 28
Q9NS87	KIF15	0,00091	1,056	Kinesin-like protein KIF15
Q07157	TJP1	0,00607	1,058	Tight junction protein ZO-1
Q66K74	MAP1S	0,00984	1,059	Microtubule-associated protein 1S
A0A0D9SFM0	SHPRH	0,00800	1,063	E3 ubiquitin-protein ligase SHPRH
Q9Y6M1	IGF2BP2	0,02410	1,071	Insulin-like growth factor 2 mRNA-binding protein 2
P13796	LCP1	0,01720	1,073	Plastin-2
P51991	HNRNPA3	0,01254	1,081	Heterogeneous nuclear ribonucleoprotein A3
A0A0A0MRL6	ABLIM1	0,02855	1,089	Actin-binding LIM protein 1
B1AQK6	CACNA1B	0,04320	1,095	Voltage-dependent N-type calcium channel subunit alpha
P32969	RPL9	0,00732	1,113	60S ribosomal protein L9
Q9UNU6	CYP8B1	0,04176	1,131	7-alpha-hydroxycholest-4-en-3-one 12-alpha-hydroxylase
P22234	PAICS	0,02931	1,131	Multifunctional protein ADE2
P23528	CFL1	0,01721	1,139	Cofilin-1
Q9Y678	COPG1	0,04714	1,153	Coatomer subunit gamma-1
Q5VZL5	ZMYM4	0,04605	1,164	Zinc finger MYM-type protein 4
P62244	RPS15A	0,04980	1,166	40S ribosomal protein S15a
O96013	PAK4	0,04477	1,172	Serine/threonine-protein kinase PAK 4
Q5JSZ5	PRRC2B	0,03443	1,173	Protein PRRC2B
Q6NSJ2	PHLDB3	0,00070	1,173	Pleckstrin homology-like domain family B member 3
P78352	DLG4	0,00310	1,174	Disks large homolog 4
M0R0P8	MYO9B	0,04557	1,174	Unconventional myosin-IXb
Q9BZ95	NSD3	0,00433	1,182	Histone-lysine N-methyltransferase NSD3

O15037	KHNYN	0,04178	1,182	Protein KHNYN
Q13796	SHROOM2	0,00133	1,203	Protein Shroom2
O75899	GABBR2	0,02634	1,223	Gamma-aminobutyric acid type B receptor subunit 2
E9PGC5	PTPRK	0,03202	1,227	Receptor-type tyrosine-protein phosphatase kappa
O00506	STK25	0,03548	1,233	Serine/threonine-protein kinase 25
O43390	HNRNPR	0,00312	1,236	Heterogeneous nuclear ribonucleoprotein R
Q8WUM4	PDCD6IP	0,00576	1,238	Programmed cell death 6-interacting protein
Q86UP0	CDH24	0,00280	1,240	Cadherin-24
Q92545	TMEM131	0,03431	1,244	Transmembrane protein 131
O15360	FANCA	0,00550	1,247	Fanconi anemia group A protein
Q5SNV9	C1orf167	0,01390	1,250	Uncharacterized protein C1orf167
Q7Z6E9	RBBP6	0,02354	1,252	E3 ubiquitin-protein ligase RBBP6
A0A087WZR9	PYCR2	0,01029	1,254	Pyrroline-5-carboxylate reductase
J3KNN5	DDX41	0,02297	1,256	Probable ATP-dependent RNA helicase DDX41 (Fragment)
G5E962	MAGEA11	0,00051	1,269	Melanoma antigen family A_ 11_ isoform CRA_a
O75153	CLUH	0,00245	1,270	Clustered mitochondria protein homolog
Q9BW19	KIFC1	0,01861	1,275	Kinesin-like protein KIFC1
F5GZS6	SLC3A2	0,04798	1,285	4F2 cell-surface antigen heavy chain
O15084	ANKRD28	0,02458	1,288	Serine/threonine-protein phosphatase 6 regulatory ankyrin repeat subunit A
K7EJL9	SEPT9	0,03898	1,291	Septin-9
P22079	LPO	0,04136	1,295	Lactoperoxidase
Q9UGL1	KDM5B	0,01082	1,316	Lysine-specific demethylase 5B
A0A0G2JHL1	GPANK1	0,00141	1,321	G patch domain and ankyrin repeat-containing protein 1
P45973	CBX5	0,01221	1,327	Chromobox protein homolog 5
P38159	RBMX	0,00602	1,333	RNA-binding motif protein_ X chromosome
Q8NCG7	DAGLB	0,02129	1,335	Sn1-specific diacylglycerol lipase beta
A0A0A0MSH9	CHD1L	0,00488	1,336	Chromodomain-helicase-DNA-binding protein 1-like
Q8IZ26	ZNF34	0,02281	1,346	Zinc finger protein 34

Q86TI0	TBC1D1	0,01690	1,350	TBC1 domain family member 1
A6NN73	GOLGA8CP	0,04715	1,350	Golgin subfamily A member 8C
Q8IZU2	WDR17	0,00326	1,357	WD repeat-containing protein 17
A0A087WTB9	POTEH	0,04628	1,359	POTE ankyrin domain family member H
P62269	RPS18	0,01035	1,366	40S ribosomal protein S18
P43304	GPD2	0,03291	1,366	Glycerol-3-phosphate dehydrogenase_ mitochondrial
E9PG32	DNAH12	0,04648	1,368	Dynein heavy chain 12_ axonemal
Q8NEU8	APPL2	0,02148	1,376	DCC-interacting protein 13-beta
P31949	S100A11	0,03682	1,380	Protein S100-A11
Q9NVM9	ASUN	0,00087	1,385	Protein asunder homolog
Q9P2J9	PDP2	0,00419	1,385	[Pyruvate dehydrogenase [acetyl-transferring]]-phosphatase 2_ mitochondrial
Q86VP6	CAND1	0,01697	1,386	Cullin-associated NEDD8-dissociated protein 1
F5H0F9	ANAPC5	0,00603	1,391	Anaphase-promoting complex subunit 5
Q9Y6W3	CAPN7	0,01958	1,395	Calpain-7
Q15643	TRIP11	0,00898	1,414	Thyroid receptor-interacting protein 11
A0A0G2JNU3	BDP1	0,01229	1,424	Transcription factor TFIIIB component B" homolog
A0A087WU64	POLA1	0,00234	1,427	DNA polymerase
O95831	AIFM1	0,00667	1,432	Apoptosis-inducing factor 1_ mitochondrial
Q96RV3	PCNX1	0,00057	1,449	Pecanex-like protein 1
Q13085	ACACA	0,00267	1,450	Acetyl-CoA carboxylase 1
Q9Y2H0	DLGAP4	0,00107	1,452	Disks large-associated protein 4
Q6PGP7	TTC37	0,00298	1,453	Tetratricopeptide repeat protein 37
Q0IIM8	TBC1D8B	0,02294	1,463	TBC1 domain family member 8B
Q9H4E7	DEF6	0,00895	1,469	Differentially expressed in FDCP 6 homolog
P30154	PPP2R1B	0,02056	1,480	Serine/threonine-protein phosphatase 2A 65 kDa regulatory subunit A beta isoform
P11217	PYGM	0,01272	1,502	Glycogen phosphorylase_ muscle form
Q9C0C2	TNKS1BP1	0,04353	1,529	182 kDa tankyrase-1-binding protein
H3BS19	ZNF469	0,01635	1,530	Zinc finger protein 469

Q9H6T0	ESRP2	0,02584	1,542	Epithelial splicing regulatory protein 2
Q6ZV73	FGD6	0,00895	1,544	FYVE_ RhoGEF and PH domain-containing protein 6
P54257	HAP1	0,04058	1,553	Huntingtin-associated protein 1
O14513	NCKAP5	0,01187	1,562	Nck-associated protein 5
P49792	RANBP2	0,01095	1,571	E3 SUMO-protein ligase RanBP2
P29597	TYK2	0,01321	1,576	Non-receptor tyrosine-protein kinase TYK2
A2VDJ0	KIAA0922	0,02029	1,604	Transmembrane protein 131-like
P40429	RPL13A	0,01307	1,610	60S ribosomal protein L13a
P31930	UQCRC1	0,00190	1,611	Cytochrome b-c1 complex subunit 1_ mitochondrial
Q2KHT3	CLEC16A	0,00757	1,631	Protein CLEC16A
Q9UBF2	COPG2	0,00446	1,634	Coatomer subunit gamma-2
Q9Y617	PSAT1	0,04078	1,634	Phosphoserine aminotransferase
Q8TBY0	RBM46	0,01695	1,639	Probable RNA-binding protein 46
P42126	ECI1	0,00173	1,642	Enoyl-CoA delta isomerase 1_ mitochondrial
Q9Y4E6	WDR7	0,00237	1,649	WD repeat-containing protein 7
Q9BVJ6	UTP14A	0,01955	1,656	U3 small nucleolar RNA-associated protein 14 homolog A
E9PKB1	CCDC15	0,04755	1,657	Coiled-coil domain-containing protein 15
Q00534	CDK6	0,02912	1,680	Cyclin-dependent kinase 6
Q92917	GPKOW	0,04981	1,680	G patch domain and KOW motifs-containing protein
P52907	CAPZA1	0,00347	1,703	F-actin-capping protein subunit alpha-1
Q5M775	SPECC1	0,01726	1,712	Cytospin-B
Q6UVM3	KCNT2	0,02004	1,721	Potassium channel subfamily T member 2
O00203	AP3B1	0,00288	1,724	AP-3 complex subunit beta-1
Q5T655	CFAP58	0,00826	1,733	Cilia- and flagella-associated protein 58
P14866	HNRNPL	0,01344	1,770	Heterogeneous nuclear ribonucleoprotein L
P30304	CDC25A	0,03495	1,775	M-phase inducer phosphatase 1
P35613	BSG	0,00042	1,783	Basigin
P32019	INPP5B	0,02046	1,805	Type II inositol 1_4_5-trisphosphate 5-phosphatase
O43361	ZNF749	0,01009	1,812	Zinc finger protein 749

Q86XK2	FBXO11	0,00008	1,818	F-box only protein 11
Q8WYA0	IFT81	0,00150	1,819	Intraflagellar transport protein 81 homolog
P63151	PPP2R2A	0,02836	1,821	Serine/threonine-protein phosphatase 2A 55 kDa regulatory subunit B alpha isoform
A0A087X1I8	ARMC9	0,00668	1,827	LisH domain-containing protein ARMC9
Q9ULT0	TTC7A	0,02643	1,830	Tetratricopeptide repeat protein 7A
P24043	LAMA2	0,04393	1,832	Laminin subunit alpha-2
Q9UBE0	SAE1	0,00129	1,833	SUMO-activating enzyme subunit 1
P15121	AKR1B1	0,03651	1,847	Aldose reductase
P55036	PSMD4	0,04522	1,854	26S proteasome non-ATPase regulatory subunit 4
P07996	THBS1	0,00141	1,858	Thrombospondin-1
Q5VWV2	PARD3	0,03675	1,869	Partitioning defective 3 homolog
Q13621	SLC12A1	0,00938	1,876	Solute carrier family 12 member 1
Q9UHP3	USP25	0,00024	1,878	Ubiquitin carboxyl-terminal hydrolase 25
Q6PJI9	WDR59	0,03224	1,880	WD repeat-containing protein 59
Q96JG6	VPS50	0,01015	1,881	Syndetin
Q96EP0	RNF31	0,00466	1,900	E3 ubiquitin-protein ligase RNF31
Q9HBI6	CYP4F11	0,03653	1,916	Phylloquinone omega-hydroxylase CYP4F11
J3QS41	HELZ	0,00144	1,931	Probable helicase with zinc finger domain
P31749	AKT1	0,02592	1,946	RAC-alpha serine/threonine-protein kinase
Q68DU8	KCTD16	0,04584	1,951	BTB/POZ domain-containing protein KCTD16
A2IDD5	CCDC78	0,00802	1,980	Coiled-coil domain-containing protein 78
P26641	EEF1G	0,03047	1,988	Elongation factor 1-gamma
Q15942	ZYX	0,00168	2,001	Zyxin
Q9Y613	FHOD1	0,03101	2,030	FH1/FH2 domain-containing protein 1
P19174	PLCG1	0,01240	2,037	1-phosphatidylinositol 4_5-bisphosphate phosphodiesterase gamma-1
Q8N9F8	ZNF454	0,03384	2,046	Zinc finger protein 454
P61026	RAB10	0,03741	2,050	Ras-related protein Rab-10
Q01581	HMGCS1	0,01691	2,078	Hydroxymethylglutaryl-CoA synthase_ cytoplasmic
Q86TB9	PATL1	0,01800	2,078	Protein PAT1 homolog 1

Q9Y2L8	ZKSCAN5	0,02883	2,083	Zinc finger protein with KRAB and SCAN domains 5
P51665	PSMD7	0,00016	2,086	26S proteasome non-ATPase regulatory subunit 7
P28072	PSMB6	0,01508	2,091	Proteasome subunit beta type-6
Q92835	INPP5D	0,01115	2,136	Phosphatidylinositol 3_4_5-trisphosphate 5-phosphatase 1
O14829	PPEF1	0,00285	2,140	Serine/threonine-protein phosphatase with EF-hands 1
P51617	IRAK1	0,01142	2,143	Interleukin-1 receptor-associated kinase 1
Q9BZF1	OSBPL8	0,02430	2,171	Oxysterol-binding protein-related protein 8
Q5SVJ8	KCNMA1	0,01040	2,181	Calcium-activated potassium channel subunit alpha-1
Q9NV72	ZNF701	0,00001	2,182	Zinc finger protein 701
P49006	MARCKSL1	0,00373	2,208	MARCKS-related protein
Q9H078	CLPB	0,01333	2,261	Caseinolytic peptidase B protein homolog
Q09161	NCBP1	0,00375	2,265	Nuclear cap-binding protein subunit 1
Q9H792	PEAK1	0,03530	2,267	Pseudopodium-enriched atypical kinase 1
O60506	SYNCRIP	0,01156	2,274	Heterogeneous nuclear ribonucleoprotein Q
O95782	AP2A1	0,00295	2,289	AP-2 complex subunit alpha-1
Q9UJZ1	STOML2	0,00122	2,298	Stomatin-like protein 2_ mitochondrial
P09958	FURIN	0,00092	2,324	Furin
Q569K6	CCDC157	0,04264	2,339	Coiled-coil domain-containing protein 157
O00534	VWA5A	0,00127	2,357	von Willebrand factor A domain-containing protein 5A
P52565	ARHGDIA	0,00199	2,367	Rho GDP-dissociation inhibitor 1
Q15637	SF1	0,01897	2,391	Splicing factor 1
Q13144	EIF2B5	0,02241	2,393	Translation initiation factor eIF-2B subunit epsilon
Q5HYC2	KIAA2026	0,00890	2,396	Uncharacterized protein KIAA2026
Q15436	SEC23A	0,01073	2,399	Protein transport protein Sec23A
Q7KZF4	SND1	0,00155	2,405	Staphylococcal nuclease domain-containing protein 1
Q68D06	SLFN13	0,02457	2,423	Schlafen family member 13
Q8IWZ3	ANKHD1	0,01416	2,425	Ankyrin repeat and KH domain-containing protein 1
Q13615	MTMR3	0,03333	2,443	Myotubularin-related protein 3
Q9NR09	BIRC6	0,03325	2,457	Baculoviral IAP repeat-containing protein 6

P35269	GTF2F1	0,03111	2,486	General transcription factor IIF subunit 1
A0A087X0T3	MYH7B	0,03425	2,490	Myosin-7B
Q07890	SOS2	0,00072	2,634	Son of sevenless homolog 2
Q06455	RUNX1T1	0,01695	2,679	Protein CBFA2T1
P07196	NEFL	0,02813	2,702	Neurofilament light polypeptide
Q9UKN7	MYO15A	0,03221	2,711	Unconventional myosin-XV
P30086	PEBP1	0,00474	2,717	Phosphatidylethanolamine-binding protein 1
E7ERK8	ARHGAP44	0,01739	2,723	Rho GTPase-activating protein 44
Q4ZG55	GREB1	0,02255	2,733	Protein GREB1
Q9UBG0	MRC2	0,01903	2,779	C-type mannose receptor 2
Q7Z6M4	MTERF4	0,01639	2,781	Transcription termination factor 4_ mitochondrial
P07355	ANXA2	0,00550	2,796	Annexin A2
Q8IWY9	CDAN1	0,01110	2,809	Codanin-1
Q6NV74	KIAA1211L	0,00365	2,904	Uncharacterized protein KIAA1211-like
Q13576	IQGAP2	0,00144	2,926	Ras GTPase-activating-like protein IQGAP2
Q9H2C0	GAN	0,00219	2,951	Gigaxonin
Q9H4B8	DPEP3	0,00101	2,991	Dipeptidase 3
A1KZ92	PXDNL	0,03737	3,007	Peroxidasin-like protein
Q8TAA3	PSMA8	0,03762	3,084	Proteasome subunit alpha type-7-like
Q7Z3E2	CCDC186	0,00434	3,105	Coiled-coil domain-containing protein 186
B1ALA9	PRPS1	0,00406	3,109	Ribose-phosphate pyrophosphokinase 1
Q58EX7	PLEKHG4	0,00477	3,133	Puratrophin-1
Q5JVL4	EFHC1	0,00633	3,141	EF-hand domain-containing protein 1
Q9BZA8	PCDH11Y	0,01517	3,143	Protocadherin-11 Y-linked
Q9HCE9	ANO8	0,00085	3,195	Anoctamin-8
Q9P2R3	ANKFY1	0,01008	3,206	Rabankyrin-5
A0A0U1RRB3	CMTR2	0,03421	3,213	Cap-specific mRNA (nucleoside-2'-O-)-methyltransferase 2
Q15021	NCAPD2	0,04293	3,257	Condensin complex subunit 1

Q9NQW8	CNGB3	0,00704	3,269	Cyclic nucleotide-gated cation channel beta-3
P61289	PSME3	0,01859	3,279	Proteasome activator complex subunit 3
Q6ZT07	TBC1D9	0,00289	3,315	TBC1 domain family member 9
Q9Y2G8	DNAJC16	0,02575	3,433	DnaJ homolog subfamily C member 16
A4FU69	EFCAB5	0,01074	3,496	EF-hand calcium-binding domain-containing protein 5
Q6P2C0	WDR93	0,00312	3,513	WD repeat-containing protein 93
Q13099	IFT88	0,01124	3,565	Intraflagellar transport protein 88 homolog
Q15238	PSG5	0,00395	3,713	Pregnancy-specific beta-1-glycoprotein 5
A0A087WUT6	EIF5B	0,00979	3,745	Eukaryotic translation initiation factor 5B
Q15459	SF3A1	0,00081	3,822	Splicing factor 3A subunit 1
Q6P2E9	EDC4	0,00049	3,823	Enhancer of mRNA-decapping protein 4
Q9UJU2	LEF1	0,00703	3,847	Lymphoid enhancer-binding factor 1
M0R2Z9	SUGP2	0,00026	3,885	SURP and G-patch domain-containing protein 2
O15014	ZNF609	0,00718	3,960	Zinc finger protein 609
P50552	VASP	0,00811	3,994	Vasodilator-stimulated phosphoprotein
A0A087WY96	SLC6A6	0,00169	4,013	Transporter
Q9Y487	ATP6V0A2	0,02093	4,014	V-type proton ATPase 116 kDa subunit a isoform 2
Q9H7F0	ATP13A3	0,02162	4,133	Probable cation-transporting ATPase 13A3
P17097	ZNF7	0,00559	4,300	Zinc finger protein 7
Q9HCS4	TCF7L1	0,00384	4,312	Transcription factor 7-like 1
F8W810	#VALOR!	0,02015	4,406	Uncharacterized protein
J3KNI1	COG4	0,00533	4,444	Conserved oligomeric Golgi complex subunit 4
Q86UV5	USP48	0,01307	4,673	Ubiquitin carboxyl-terminal hydrolase 48
P15313	ATP6V1B1	0,00030	4,698	V-type proton ATPase subunit B_ kidney isoform
A0A087WUK1	RYK	0,00013	4,832	Tyrosine-protein kinase RYK
Q9Y5G2	PCDHGB2	0,04291	4,901	Protocadherin gamma-B2
A2RUB1	MEIOC	0,00714	5,061	Meiosis-specific coiled-coil domain-containing protein MEIOC
A0A087WWP8	RSBN1	0,00221	5,227	Round spermatid basic protein 1

P08243	ASNS	0,04127	5,278	Asparagine synthetase [glutamine-hydrolyzing]
O60494	CUBN	0,03207	5,477	Cubilin
P0DJG4	THEGL	0,00002	5,510	Testicular haploid expressed gene protein-like
E2QRB3	PYCR1	0,00001	5,548	Pyrroline-5-carboxylate reductase 1_ isoform CRA_c
A0A0A6YYL4	CORO7-PAM16	0,00045	5,633	Coronin
Q9BXT8	RNF17	0,02227	5,808	RING finger protein 17
A8MTJ3	GNAT3	0,03181	6,344	Guanine nucleotide-binding protein G(t) subunit alpha-3
Q2TAY7	SMU1	0,00014	6,545	WD40 repeat-containing protein SMU1
O75821	EIF3G	0,00002	7,270	Eukaryotic translation initiation factor 3 subunit G
H3BTQ3	SLC19A1	0,00940	7,456	Folate transporter 1
Q8TF05	PPP4R1	0,00003	7,540	Serine/threonine-protein phosphatase 4 regulatory subunit 1

Table 2: Proteins affected by haloperidol treatment

Table 2 - Proteins affected by haloperidol treatment

Accession	Gene	Anova (p)	log2 Fold Change	Protein
Q12834	CDC20	0,00698	-10,28	Cell division cycle protein 20 homolog
P27694	RPA1	0,00112	-10,27	Replication protein A 70 kDa DNA-binding subunit
Q9BV20	MRI1	0,00045	-8,79	Methylthioribose-1-phosphate isomerase
Q2TAY7	SMU1	0,00326	-8,05	WD40 repeat-containing protein SMU1
Q13733	ATP1A4	0,00618	-7,53	Sodium/potassium-transporting ATPase subunit alpha-4
Q8ND30	PPFIBP2	0,04093	-7,18	Liprin-beta-2
Q8N8A2	ANKRD44	0,00381	-6,99	Serine/threonine-protein phosphatase 6 regulatory ankyrin repeat subunit B
J3KQ26	ARMC5	0,00074	-6,73	Armadillo repeat-containing protein 5
P36871	PGM1	0,01503	-6,69	Phosphoglucomutase-1
O14776	TCERG1	0,00001	-6,25	Transcription elongation regulator 1
P0C0L4	C4A	0,01022	-6,05	Complement C4-A
Q01850	CDR2	0,00136	-5,85	Cerebellar degeneration-related protein 2
P68431	HIST1H3A	0,03526	-5,21	Histone H3.1
P30084	ECHS1	0,01055	-5,12	Enoyl-CoA hydratase, mitochondrial
P00450	CP	0,00005	-4,99	Ceruloplasmin
Q6UB35	MTHFD1L	0,00002	-4,97	Monofunctional C1-tetrahydrofolate synthase, mitochondrial
Q14147	DHX34	0,00445	-4,44	Probable ATP-dependent RNA helicase DHX34
Q14693	LPIN1	0,03787	-4,35	Phosphatidate phosphatase LPIN1
Q9UPY3	DICER1	0,01409	-4,01	Endoribonuclease Dicer
Q13085	ACACA	0,00477	-3,90	Acetyl-CoA carboxylase 1
O75477	ERLIN1	0,00454	-3,89	Erlin-1
D6R9H6	CNOT6	0,00369	-3,82	CCR4-NOT transcription complex subunit 6 (Fragment)
Q5VIY5	ZNF468	0,00147	-3,77	Zinc finger protein 468
Q9UQ16	DNM3	0,03018	-3,67	Dynamin-3

Q9HB71	CACYBP	0,00195	-3,63	Calcyclin-binding protein
E9PFT6	HBD	0,00214	-3,62	Hemoglobin subunit delta
Q92794	KAT6A	0,03590	-3,61	Histone acetyltransferase KAT6A
Q9GZZ0	HOXD1	0,03083	-3,58	Homeobox protein Hox-D1
P11802	CDK4	0,00026	-3,46	Cyclin-dependent kinase 4
B4DZ84	MPP2	0,03059	-3,45	MAGUK p55 subfamily member 2
Q9UHJ3	SFMBT1	0,01020	-3,44	Scm-like with four MBT domains protein 1
B4DWR3	VBP1	0,03672	-3,37	Prefoldin subunit 3
Q9Y613	FHOD1	0,00064	-3,31	FH1/FH2 domain-containing protein 1
Q9Y6Y8	SEC23IP	0,00280	-3,29	SEC23-interacting protein
Q9ULI3	HEG1	0,00157	-3,29	Protein HEG homolog 1
Q99627	COPS8	0,01367	-3,22	COP9 signalosome complex subunit 8
Q5VT82	PCDH9	0,01328	-3,18	Protocadherin 9
Q9BZJ0	CRNKL1	0,01375	-3,13	Crooked neck-like protein 1
Q9UKY4	POMT2	0,00245	-3,11	Protein O-mannosyl-transferase 2
Q96RV3	PCNX	0,00502	-3,09	Pecanex-like protein 1
Q9UN37	VPS4A	0,01400	-3,07	Vacuolar protein sorting-associated protein 4A
Q96SL4	GPX7	0,00274	-3,05	Glutathione peroxidase 7
A6NKF2	ARID3C	0,01087	-3,00	AT-rich interactive domain-containing protein 3C
P09104	ENO2	0,00622	-2,96	Gamma-enolase
A0A087X176	QSOX2	0,01059	-2,94	Sulfhydryl oxidase
P62899	RPL31	0,00609	-2,94	60S ribosomal protein L31
P26006	ITGA3	0,01813	-2,88	Integrin alpha-3
P53814	SMTN	0,00749	-2,78	Smoothelin
Q8WUT4	LRRN4	0,00077	-2,78	Leucine-rich repeat neuronal protein 4
P42765	ACAA2	0,01768	-2,74	3-ketoacyl-CoA thiolase, mitochondrial
A6NE52	WDR97	0,01094	-2,74	WD repeat-containing protein 97
Q96HN2	AHCYL2	0,00465	-2,70	Adenosylhomocysteinase 3
Q9P243	ZFAT	0,00199	-2,56	Zinc finger protein ZFAT

O60333	KIF1B	0,01126	-2,54	Kinesin-like protein KIF1B
Q9H2K8	TAOK3	0,00352	-2,53	Serine/threonine-protein kinase TAO3
C9JX16	NAALADL1	0,00923	-2,47	N-acetylated-alpha-linked acidic dipeptidase-like protein
Q96AY4	TTC28	0,00705	-2,46	Tetratricopeptide repeat protein 28
B8ZZ55	C2orf70	0,01041	-2,45	UPF0573 protein C2orf70
F5H6I7	ATL3	0,00063	-2,42	Atlastin-3
O14917	PCDH17	0,00049	-2,36	Protocadherin-17
A0A087WUL9	PSMD13	0,04146	-2,34	26S proteasome non-ATPase regulatory subunit 13
P07384	CAPN1	0,04837	-2,34	Calpain-1 catalytic subunit
P55145	MANF	0,00001	-2,33	Mesencephalic astrocyte-derived neurotrophic factor
P10244	MYBL2	0,01537	-2,31	Myb-related protein B
O95785	WIZ	0,00000	-2,30	Protein Wiz
Q9NWH9	SLTM	0,02374	-2,27	SAFB-like transcription modulator
Q8N465	D2HGDH	0,04871	-2,27	D-2-hydroxyglutarate dehydrogenase, mitochondrial
O60266	ADCY3	0,00420	-2,25	Adenylate cyclase type 3
P04818	TYMS	0,00216	-2,19	Thymidylate synthase
Q15056	EIF4H	0,00782	-2,15	Eukaryotic translation initiation factor 4H
Q58FG1	HSP90AA4P	0,01514	-2,11	Putative heat shock protein HSP 90-alpha A4
P42677	RPS27	0,00005	-2,10	40S ribosomal protein S27
Q2PPJ7	RALGAPA2	0,00225	-2,07	Ral GTPase-activating protein subunit alpha-2
Q9BUF5	TUBB6	0,00740	-2,06	Tubulin beta-6 chain
Q9C0D5	TANC1	0,01295	-2,06	Protein TANC1
Q9UPN4	CEP131	0,00659	-2,04	Centrosomal protein of 131 kDa
P62942	FKBP1A	0,02875	-2,03	Peptidyl-prolyl cis-trans isomerase FKBP1A
O60303	KIAA0556	0,04926	-2,03	Uncharacterized protein KIAA0556
Q99714	HSD17B10	0,00420	-2,01	3-hydroxyacyl-CoA dehydrogenase type-2
A0A0A0MR03	CTDP1	0,01008	-2,00	RNA polymerase II subunit A C-terminal domain phosphatase
Q9P2D7	DNAH1	0,00400	-1,99	Dynein heavy chain 1, axonemal

P24539	ATP5F1	0,04913	-1,99	ATP synthase F(0) complex subunit B1, mitochondrial
P28702	RXRB	0,04146	-1,98	Retinoic acid receptor RXR-beta
Q6P0N0	MIS18BP1	0,00428	-1,96	Mis18-binding protein 1
Q9Y6E2	BZW2	0,00799	-1,95	Basic leucine zipper and W2 domain-containing protein 2
Q9UDT6	CLIP2	0,03800	-1,94	CAP-Gly domain-containing linker protein 2
P51665	PSMD7	0,00220	-1,94	26S proteasome non-ATPase regulatory subunit 7
Q86YJ6	THNSL2	0,01706	-1,93	Threonine synthase-like 2
P13056	NR2C1	0,01513	-1,91	Nuclear receptor subfamily 2 group C member 1
Q9UKD1	GMEB2	0,00607	-1,91	Glucocorticoid modulatory element-binding protein 2
Q9BQ70	TCF25	0,01617	-1,91	Transcription factor 25
Q9BX63	BRIP1	0,01617	-1,91	Fanconi anemia group J protein
Q969G9	NKD1	0,01773	-1,89	Protein naked cuticle homolog 1
Q5T9B7	AK1	0,00318	-1,89	Adenylate kinase isoenzyme 1
Q9HBR0	SLC38A10	0,00601	-1,89	Putative sodium-coupled neutral amino acid transporter 10
Q6UWP8	SBSN	0,03521	-1,89	Suprabasin
P00441	SOD1	0,00069	-1,88	Superoxide dismutase [Cu-Zn]
Q149N8	SHPRH	0,03918	-1,88	E3 ubiquitin-protein ligase SHPRH
C9JJ19	MRPS34	0,04082	-1,86	28S ribosomal protein S34, mitochondrial
Q5T1J5	CHCHD2P9	0,00000	-1,84	Putative coiled-coil-helix-coiled-coil-helix domain-containing protein CHCHD2P9, mitochondrial
K7EQA1	PDCD5	0,00290	-1,83	Programmed cell death protein 5
P98171	ARHGAP4	0,01924	-1,82	Rho GTPase-activating protein 4
Q2UY09	COL28A1	0,00215	-1,82	Collagen alpha-1(XXVIII) chain
P84085	ARF5	0,03392	-1,82	ADP-ribosylation factor 5
P31930	UQCRC1	0,00539	-1,80	Cytochrome b-c1 complex subunit 1, mitochondrial
Q8WVS4	WDR60	0,01511	-1,78	WD repeat-containing protein 60
P04899	GNAI2	0,04149	-1,77	Guanine nucleotide-binding protein G(i) subunit alpha-2
P42126	ECI1	0,00018	-1,76	Enoyl-CoA delta isomerase 1, mitochondrial
Q9UHI8	ADAMTS1	0,00255	-1,76	A disintegrin and metalloproteinase with thrombospondin motifs 1
D3TTY5	TNFAIP3	0,02071	-1,75	Truncated tumor necrosis factor alpha-induced protein 3

Q0VDF9	HSPA14	0,01616	-1,75	Heat shock 70 kDa protein 14
P02461	COL3A1	0,00001	-1,75	Collagen alpha-1(III) chain
Q01780	EXOSC10	0,02082	-1,74	Exosome component 10
Q8NHW5	RPLP0P6	0,03204	-1,73	60S acidic ribosomal protein P0-like
Q6B0I6	KDM4D	0,03645	-1,72	Lysine-specific demethylase 4D
P15531	NME1	0,03627	-1,71	Nucleoside diphosphate kinase A
Q5BJF6	ODF2	0,02141	-1,70	Outer dense fiber protein 2
O15440	ABCC5	0,00013	-1,67	Multidrug resistance-associated protein 5
P12821	ACE	0,00435	-1,67	Angiotensin-converting enzyme
Q6P3S1	DENND1B	0,02346	-1,66	DENN domain-containing protein 1B
Q5VWN6	FAM208B	0,01877	-1,66	Protein FAM208B
Q9C0F0	ASXL3	0,00045	-1,66	Putative Polycomb group protein ASXL3
P11182	DBT	0,00924	-1,65	Lipoamide acyltransferase component of branched-chain alpha-keto acid dehydrogenase complex, mitochondrial
Q9H792	PEAK1	0,00274	-1,64	Pseudopodium-enriched atypical kinase 1
Q15262	PTPRK	0,03510	-1,63	Receptor-type tyrosine-protein phosphatase kappa
Q13547	HDAC1	0,04909	-1,62	Histone deacetylase 1
P09467	FBP1	0,01850	-1,61	Fructose-1,6-bisphosphatase 1
Q9Y4D7	PLXND1	0,00331	-1,60	Plexin-D1
Q9BVA1	TUBB2B	0,00011	-1,60	Tubulin beta-2B chain
E9PF10	NUP155	0,04352	-1,59	Nuclear pore complex protein Nup155
P53618	COPB1	0,03798	-1,58	Coatomer subunit beta
Q96CT7	CCDC124	0,00245	-1,58	Coiled-coil domain-containing protein 124
Q9P218	COL20A1	0,00028	-1,58	Collagen alpha-1(XX) chain
O14559	ARHGAP33	0,00000	-1,57	Rho GTPase-activating protein 33
Q9Y5F6	PCDHGC5	0,03038	-1,55	Protocadherin gamma-C5
Q9H6S0	YTHDC2	0,00000	-1,55	Probable ATP-dependent RNA helicase YTHDC2
P57721	PCBP3	0,00695	-1,55	Poly(rC)-binding protein 3
Q7Z4H7	HAUS6	0,01478	-1,54	HAUS augmin-like complex subunit 6
Q9NZJ4	SACS	0,00022	-1,54	Sacsin

P05198	EIF2S1	0,04594	-1,53	Eukaryotic translation initiation factor 2 subunit 1
Q8TDY2	RB1CC1	0,00239	-1,52	RB1-inducible coiled-coil protein 1
Q5GLZ8	HERC4	0,03350	-1,52	Probable E3 ubiquitin-protein ligase HERC4
Q9BWF3	RBM4	0,00283	-1,52	RNA-binding protein 4
O95071	UBR5	0,04997	-1,52	E3 ubiquitin-protein ligase UBR5
Q96N46	TTC14	0,00010	-1,50	Tetratricopeptide repeat protein 14
Q9Y2M5	KLHL20	0,00045	-1,50	Kelch-like protein 20
Q99447	PCYT2	0,00051	-1,49	Ethanolamine-phosphate cytidylyltransferase
Q9NR48	ASH1L	0,00653	-1,49	Histone-lysine N-methyltransferase ASH1L
Q9Y5G9	PCDHGA4	0,01122	-1,48	Protocadherin gamma-A4
P51003	PAPOLA	0,03232	-1,47	Poly(A) polymerase alpha
P62258	YWHAE	0,00216	-1,47	14-3-3 protein epsilon
F8VVT9	AGAP2	0,00130	-1,46	Arf-GAP with GTPase, ANK repeat and PH domain-containing protein 2
Q9NPQ8	RIC8A	0,03052	-1,46	Synembryn-A
Q9P278	FNIP2	0,00000	-1,46	Folliculin-interacting protein 2
Q9BYX4	IFIH1	0,01365	-1,43	Interferon-induced helicase C domain-containing protein 1
Q5TZA2	CROCC	0,01010	-1,43	Rootletin
P07858	CTSB	0,00192	-1,42	Cathepsin B
Q15008	PSMD6	0,02498	-1,41	26S proteasome non-ATPase regulatory subunit 6
O60486	PLXNC1	0,00379	-1,41	Plexin-C1
E5RJU9	MTDH	0,04552	-1,41	Protein LYRIC
Q8IVF5	TIAM2	0,00003	-1,40	T-lymphoma invasion and metastasis-inducing protein 2
H0YAK3	CDH18	0,00296	-1,40	Cadherin-18 (Fragment)
O00541	PES1	0,01197	-1,40	Pescadillo homolog
Q8N3D4	EHBP1L1	0,00177	-1,40	EH domain-binding protein 1-like protein 1
Q8IW19	APLF	0,02405	-1,40	Aprataxin and PNK-like factor
P12004	PCNA	0,00563	-1,39	Proliferating cell nuclear antigen
P51617	IRAK1	0,00531	-1,38	Interleukin-1 receptor-associated kinase 1
P28370	SMARCA1	0,02681	-1,37	Probable global transcription activator SNF2L1

H3BTX9	ACSM2B	0,01447	-1,36	Acyl-coenzyme A synthetase ACSM2B, mitochondrial
O43615	TIMM44	0,04002	-1,36	Mitochondrial import inner membrane translocase subunit TIM44
P47756	CAPZB	0,00955	-1,35	F-actin-capping protein subunit beta
Q68DK2	ZFYVE26	0,00013	-1,35	Zinc finger FYVE domain-containing protein 26
P08758	ANXA5	0,04364	-1,34	Annexin A5
E7ETY7	GPX8	0,01018	-1,33	Glutathione peroxidase
Q9C0A1	ZFHX2	0,00682	-1,33	Zinc finger homeobox protein 2
Q9NYU2	UGGT1	0,00084	-1,32	UDP-glucose:glycoprotein glucosyltransferase 1
P67870	CSNK2B	0,01688	-1,32	Casein kinase II subunit beta
Q9C0A6	SETD5	0,02260	-1,32	SET domain-containing protein 5
O75083	WDR1	0,04975	-1,32	WD repeat-containing protein 1
Q9BTE1	DCTN5	0,00152	-1,32	Dynactin subunit 5
P51858	HDGF	0,00051	-1,31	Hepatoma-derived growth factor
Q96C23	GALM	0,03122	-1,31	Aldose 1-epimerase
Q9BYU1	PBX4	0,00583	-1,31	Pre-B-cell leukemia transcription factor 4
P51114	FXR1	0,01322	-1,31	Fragile X mental retardation syndrome-related protein 1
Q5VSY0	GKAP1	0,00170	-1,30	G kinase-anchoring protein 1
Q9Y4G8	RAPGEF2	0,00219	-1,29	Rap guanine nucleotide exchange factor 2
Q01432	AMPD3	0,03301	-1,28	AMP deaminase 3
Q99962	SH3GL2	0,00482	-1,28	Endophilin-A1
Q92598	HSPH1	0,00046	-1,28	Heat shock protein 105 kDa
F8VWT9	HECTD4	0,03564	-1,28	Probable E3 ubiquitin-protein ligase HECTD4
Q9NVE5	USP40	0,00047	-1,27	Ubiquitin carboxyl-terminal hydrolase 40
Q9BXK5	BCL2L13	0,00840	-1,27	Bcl-2-like protein 13
A6QL64	ANKRD36	0,00277	-1,26	Ankyrin repeat domain-containing protein 36A
P16157	ANK1	0,03671	-1,25	Ankyrin-1
Q13330	MTA1	0,00706	-1,23	Metastasis-associated protein MTA1
Q9HBG6	IFT122	0,02811	-1,23	Intraflagellar transport protein 122 homolog
B5MCK8	GGT2	0,00057	-1,23	Inactive gamma-glutamyltranspeptidase 2

G3V325	ATP5J2-PTCD1	0,00004	-1,22	Protein ATP5J2-PTCD1
O94989	ARHGEF15	0,03998	-1,21	Rho guanine nucleotide exchange factor 15
Q9Y6N6	LAMC3	0,00052	-1,21	Laminin subunit gamma-3
Q9NVH1	DNAJC11	0,01197	-1,19	DnaJ homolog subfamily C member 11
G3V0I5	NDUFV1	0,01830	-1,19	NADH dehydrogenase (Ubiquinone) flavoprotein 1, 51kDa, isoform CRA_c
P24534	EEF1B2	0,00016	-1,18	Elongation factor 1-beta
Q9Y3Y2	CHTOP	0,04695	-1,18	Chromatin target of PRMT1 protein
P31689	DNAJA1	0,00001	-1,18	DnaJ homolog subfamily A member 1
Q02809	PLOD1	0,03081	-1,17	Procollagen-lysine,2-oxoglutarate 5-dioxygenase 1
Q5T4U5	ACADM	0,02818	-1,17	Acyl-Coenzyme A dehydrogenase, C-4 to C-12 straight chain, isoform CRA_a
A0A0A0MTP3	MPHOSPH9	0,04607	-1,17	M-phase phosphoprotein 9
P49790	NUP153	0,00675	-1,17	Nuclear pore complex protein Nup153
P31150	GDI1	0,00245	-1,17	Rab GDP dissociation inhibitor alpha
Q5QNZ2	ATP5F1	0,02896	-1,16	ATP synthase F(0) complex subunit B1, mitochondrial
P19823	ITIH2	0,00268	-1,16	Inter-alpha-trypsin inhibitor heavy chain H2
Q13233	MAP3K1	0,00079	-1,16	Mitogen-activated protein kinase kinase kinase 1
P46100	ATRX	0,01006	-1,15	Transcriptional regulator ATRX
P28066	PSMA5	0,01963	-1,14	Proteasome subunit alpha type-5
Q9Y2G5	POFUT2	0,02864	-1,13	GDP-fucose protein O-fucosyltransferase 2
Q14240	EIF4A2	0,00678	-1,12	Eukaryotic initiation factor 4A-II
P16260	SLC25A16	0,01131	-1,12	Graves disease carrier protein
O75128	COBL	0,04859	-1,12	Protein cordon-bleu
P11388	TOP2A	0,00347	-1,12	DNA topoisomerase 2-alpha
P52815	MRPL12	0,00055	-1,11	39S ribosomal protein L12, mitochondrial
B4DLN1	#VALOR!	0,00055	-1,11	Uncharacterized protein
Q15389	ANGPT1	0,00068	-1,11	Angiopoietin-1
Q14674	ESPL1	0,03833	-1,11	Separin
O14782	KIF3C	0,03293	-1,11	Kinesin-like protein KIF3C

Q8IZY2	ABCA7	0,00119	-1,10	ATP-binding cassette sub-family A member 7
Q02750	MAP2K1	0,00675	-1,10	Dual specificity mitogen-activated protein kinase kinase 1
P63220	RPS21	0,00007	-1,10	40S ribosomal protein S21
A0A087WV65	ZBTB44	0,03969	-1,09	Zinc finger and BTB domain-containing protein 44
Q2M1P5	KIF7	0,00416	-1,09	Kinesin-like protein KIF7
A0A0A0MTS2	GPI	0,00001	-1,09	Glucose-6-phosphate isomerase (Fragment)
O95171	SCEL	0,02154	-1,09	Sciellin
O14686	KMT2D	0,00563	-1,08	Histone-lysine N-methyltransferase 2D
Q8IX07	ZFPM1	0,03628	-1,08	Zinc finger protein ZFPM1
A3KMH1	VWA8	0,00841	-1,08	von Willebrand factor A domain-containing protein 8
Q9NQX4	MYO5C	0,00019	-1,08	Unconventional myosin-Vc
Q9ULV0	MYO5B	0,04863	-1,07	Unconventional myosin-Vb
H3BP57	MPI	0,03327	-1,05	Mannose-6-phosphate isomerase (Fragment)
Q12873	CHD3	0,00058	-1,04	Chromodomain-helicase-DNA-binding protein 3
Q96Q15	SMG1	0,00298	-1,04	Serine/threonine-protein kinase SMG1
P55283	CDH4	0,00102	-1,04	Cadherin-4
Q9NTK5	OLA1	0,00139	-1,03	Obg-like ATPase 1
O43765	SGTA	0,00000	-1,02	Small glutamine-rich tetratricopeptide repeat-containing protein alpha
Q96AA8	JAKMIP2	0,00003	-1,02	Janus kinase and microtubule-interacting protein 2
P62081	RPS7	0,00052	-1,02	40S ribosomal protein S7
Q969X6	UTP4	0,02000	-1,02	U3 small nucleolar RNA-associated protein 4 homolog
Q86V81	ALYREF	0,00015	-1,02	THO complex subunit 4
P11908	PRPS2	0,02049	-1,01	Ribose-phosphate pyrophosphokinase 2
Q00534	CDK6	0,00029	-1,01	Cyclin-dependent kinase 6
Q9P275	USP36	0,04887	-1,01	Ubiquitin carboxyl-terminal hydrolase 36
P98179	RBM3	0,00000	-1,01	RNA-binding protein 3
P50993	ATP1A2	0,00001	-1,00	Sodium/potassium-transporting ATPase subunit alpha-2
Q15459	SF3A1	0,00622	-1,00	Splicing factor 3A subunit 1

E7EPU2	DIP2C	0,03678	-1,00	Disco-interacting protein 2 homolog C
P20839	IMPDH1	0,01310	-0,99	Inosine-5'-monophosphate dehydrogenase 1
D6RGG3	COL12A1	0,03235	-0,99	Collagen alpha-1(XII) chain
A0A087WVN1	METTL10	0,00931	-0,99	Protein-lysine N-methyltransferase METTL10
P22102	GART	0,00148	-0,99	Trifunctional purine biosynthetic protein adenosine-3
P02751	FN1	0,02334	-0,98	Fibronectin
Q9UI15	TAGLN3	0,00036	-0,98	Transgelin-3
O00468	AGRN	0,00607	-0,98	Agrin
A0A087WZE4	SPTA1	0,00721	-0,97	Spectrin alpha chain, erythrocytic 1
O95834	EML2	0,00662	-0,97	Echinoderm microtubule-associated protein-like 2
Q9HAV7	GRPEL1	0,00007	-0,97	GrpE protein homolog 1, mitochondrial
Q04637	EIF4G1	0,04591	-0,97	Eukaryotic translation initiation factor 4 gamma 1
Q15102	PAFAH1B3	0,00038	-0,97	Platelet-activating factor acetylhydrolase IB subunit gamma
C9JI87	VDAC1	0,01849	-0,96	Voltage-dependent anion-selective channel protein 1 (Fragment)
P48741	HSPA7	0,02137	-0,96	Putative heat shock 70 kDa protein 7
Q9Y5M8	SRPRB	0,04803	-0,95	Signal recognition particle receptor subunit beta
P62851	RPS25	0,00616	-0,95	40S ribosomal protein S25
Q0VDD8	DNAH14	0,03128	-0,95	Dynein heavy chain 14, axonemal
Q8N7B9	EFCAB3	0,00055	-0,95	EF-hand calcium-binding domain-containing protein 3
P15822	HIVEP1	0,00043	-0,95	Zinc finger protein 40
P46778	RPL21	0,00077	-0,95	60S ribosomal protein L21
P49721	PSMB2	0,01830	-0,94	Proteasome subunit beta type-2
Q5VT25	CDC42BPA	0,00018	-0,94	Serine/threonine-protein kinase MRCK alpha
P57737	CORO7	0,01663	-0,93	Coronin-7
Q14699	RFTN1	0,01702	-0,93	Raftlin
P62266	RPS23	0,00055	-0,92	40S ribosomal protein S23
Q9BYT8	NLN	0,02428	-0,92	Neurolysin, mitochondrial
B0QZ18	CPNE1	0,01008	-0,91	Copine-1

P17022	ZNF18	0,01207	-0,91	Zinc finger protein 18
Q149M9	NWD1	0,00260	-0,91	NACHT domain- and WD repeat-containing protein 1
Q03164	KMT2A	0,00130	-0,90	Histone-lysine N-methyltransferase 2A
Q14BN4	SLMAP	0,00052	-0,89	Sarcolemmal membrane-associated protein
Q14444	CAPRIN1	0,00007	-0,89	Caprin-1
Q15029	EFTUD2	0,00470	-0,89	116 kDa U5 small nuclear ribonucleoprotein component
Q96CX2	KCTD12	0,00051	-0,88	BTB/POZ domain-containing protein KCTD12
P18206	VCL	0,01523	-0,88	Vinculin
O43166	SIPA1L1	0,00529	-0,88	Signal-induced proliferation-associated 1-like protein 1
Q8NC51	SERBP1	0,00004	-0,87	Plasminogen activator inhibitor 1 RNA-binding protein
A0A0A0MRE9	AKAP9	0,03997	-0,87	A-kinase anchor protein 9
Q7Z2Y5	NRK	0,00189	-0,87	Nik-related protein kinase
B8ZZU8	TCEB2	0,00320	-0,87	Transcription elongation factor B (SIII), polypeptide 2 (18kDa, elongin B), isoform CRA_b
Q969P6	TOP1MT	0,00003	-0,87	DNA topoisomerase I, mitochondrial
E9PKF8	EIF4G2	0,00263	-0,86	Eukaryotic translation initiation factor 4 gamma 2 (Fragment)
P10809	HSPD1	0,00000	-0,86	60 kDa heat shock protein, mitochondrial
Q9NRR5	UBQLN4	0,01821	-0,86	Ubiquilin-4
Q9NVE7	PANK4	0,04522	-0,86	Pantothenate kinase 4
Q9Y3I0	RTCB	0,00226	-0,85	tRNA-splicing ligase RtcB homolog
O95613	PCNT	0,00412	-0,85	Pericentrin
P62249	RPS16	0,00010	-0,85	40S ribosomal protein S16
E9PAV3	NACA	0,00110	-0,85	Nascent polypeptide-associated complex subunit alpha, muscle-specific form
Q92900	UPF1	0,00346	-0,85	Regulator of nonsense transcripts 1
W4VSQ9	TRIP10	0,00355	-0,85	Cdc42-interacting protein 4
P18077	RPL35A	0,00342	-0,84	60S ribosomal protein L35a
Q07021	C1QBP	0,01256	-0,84	Complement component 1 Q subcomponent-binding protein, mitochondrial
Q9NXZ1	SAGE1	0,01703	-0,83	Sarcoma antigen 1
O60341	KDM1A	0,00647	-0,83	Lysine-specific histone demethylase 1A

B1AK53	ESPN	0,00196	-0,83	Espin
P50213	IDH3A	0,03926	-0,83	Isocitrate dehydrogenase [NAD] subunit alpha, mitochondrial
P26641	EEF1G	0,04747	-0,82	Elongation factor 1-gamma
P0C0S5	H2AFZ	0,00034	-0,82	Histone H2A.Z
P05976	MYL1	0,00515	-0,81	Myosin light chain 1/3, skeletal muscle isoform
P17987	TCP1	0,00050	-0,81	T-complex protein 1 subunit alpha
Q8TCU4	ALMS1	0,00122	-0,81	Alstrom syndrome protein 1
P05141	SLC25A5	0,01011	-0,81	ADP/ATP translocase 2
O00299	CLIC1	0,00028	-0,81	Chloride intracellular channel protein 1
O76094	SRP72	0,00022	-0,80	Signal recognition particle subunit SRP72
Q92870	APBB2	0,02556	-0,80	Amyloid beta A4 precursor protein-binding family B member 2
Q9HCK4	ROBO2	0,00270	-0,80	Roundabout homolog 2
Q6P0Q8	MAST2	0,01098	-0,79	Microtubule-associated serine/threonine-protein kinase 2
P00338	LDHA	0,00510	-0,79	L-lactate dehydrogenase A chain
C9JEH7	RPS4Y1	0,02701	-0,79	40S ribosomal protein S4, Y isoform 1 (Fragment)
Q9Y285	FARSA	0,00029	-0,78	Phenylalanine--tRNA ligase alpha subunit
Q5TCS8	AK9	0,02180	-0,78	Adenylate kinase 9
V9GYD9	CELF2	0,01657	-0,78	CUGBP Elav-like family member 2
B1AJZ9	FHAD1	0,00634	-0,77	Forkhead-associated domain-containing protein 1
P21817	RYR1	0,01704	-0,77	Ryanodine receptor 1
Q9P2R7	SUCLA2	0,00258	-0,77	Succinyl-CoA ligase [ADP-forming] subunit beta, mitochondrial
P78371	CCT2	0,00075	-0,76	T-complex protein 1 subunit beta
F5GWF6	CCT2	0,00075	-0,76	T-complex protein 1 subunit beta
E7EMC7	SQSTM1	0,03595	-0,76	Sequestosome-1
O95711	LY86	0,04395	-0,76	Lymphocyte antigen 86
Q8TDM6	DLG5	0,00001	-0,76	Disks large homolog 5
A8MYA2	CXorf49	0,01191	-0,75	Uncharacterized protein CXorf49
P62263	RPS14	0,00758	-0,75	40S ribosomal protein S14
Q6ZS30	NBEAL1	0,00090	-0,75	Neurobeachin-like protein 1

Q5T3Q7	HEATR1	0,00522	-0,75	HEAT repeat-containing protein 1
O15417	TNRC18	0,00609	-0,75	Trinucleotide repeat-containing gene 18 protein
P23526	AHCY	0,00017	-0,74	Adenosylhomocysteinase
Q92499	DDX1	0,00466	-0,74	ATP-dependent RNA helicase DDX1
P49207	RPL34	0,00000	-0,74	60S ribosomal protein L34
P50395	GDI2	0,00569	-0,74	Rab GDP dissociation inhibitor beta
Q8NBJ5	COLGALT1	0,00275	-0,73	Procollagen galactosyltransferase 1
O60888	CUTA	0,00012	-0,73	Protein CutA
Q9UL12	SARDH	0,01587	-0,72	Sarcosine dehydrogenase, mitochondrial
P15880	RPS2	0,00199	-0,72	40S ribosomal protein S2
Q14974	KPNB1	0,00011	-0,72	Importin subunit beta-1
P62241	RPS8	0,00084	-0,72	40S ribosomal protein S8
O15090	ZNF536	0,02138	-0,72	Zinc finger protein 536
Q9UKY7	CDV3	0,00076	-0,72	Protein CDV3 homolog
J3KQ96	TCOF1	0,00622	-0,71	Treacle protein (Fragment)
P60842	EIF4A1	0,00005	-0,71	Eukaryotic initiation factor 4A-I
P39019	RPS19	0,00002	-0,71	40S ribosomal protein S19
P32119	PRDX2	0,00599	-0,71	Peroxiredoxin-2
Q8IWD5	MFSD6L	0,00050	-0,71	Major facilitator superfamily domain-containing protein 6-like
Q13635	PTCH1	0,02785	-0,70	Protein patched homolog 1
P46783	RPS10	0,01647	-0,70	40S ribosomal protein S10
A0A024R4E5	HDLBP	0,00174	-0,70	High density lipoprotein binding protein (Vigilin), isoform CRA_a
Q9C0G6	DNAH6	0,04467	-0,69	Dynein heavy chain 6, axonemal
P62906	RPL10A	0,00960	-0,69	60S ribosomal protein L10a
H7BXE0	ARHGAP40	0,00925	-0,69	Rho GTPase-activating protein 40 (Fragment)
P26373	RPL13	0,00729	-0,69	60S ribosomal protein L13
P07195	LDHB	0,00048	-0,69	L-lactate dehydrogenase B chain
Q8WWI1	LMO7	0,01551	-0,69	LIM domain only protein 7
Q9Y6M1	IGF2BP2	0,01098	-0,68	Insulin-like growth factor 2 mRNA-binding protein 2

Q86UT6	NLRX1	0,03581	-0,68	NLR family member X1
Q9Y265	RUVBL1	0,01302	-0,68	RuvB-like 1
P27635	RPL10	0,00004	-0,67	60S ribosomal protein L10
P62937	PPIA	0,00003	-0,67	Peptidyl-prolyl cis-trans isomerase A
C9J9K3	RPSA	0,00007	-0,67	40S ribosomal protein SA (Fragment)
P49458	SRP9	0,00013	-0,67	Signal recognition particle 9 kDa protein
J3QTJ5	LRRC37A3	0,00624	-0,67	Leucine-rich repeat-containing protein 37A3
Q05639	EEF1A2	0,00990	-0,67	Elongation factor 1-alpha 2
Q5T890	ERCC6L2	0,00015	-0,67	DNA excision repair protein ERCC-6-like 2
P62277	RPS13	0,00688	-0,67	40S ribosomal protein S13
O95336	PGLS	0,00283	-0,66	6-phosphogluconolactonase
P60866	RPS20	0,00003	-0,66	40S ribosomal protein S20
P30044	PRDX5	0,01118	-0,66	Peroxiredoxin-5, mitochondrial
Q9Y262	EIF3L	0,00086	-0,65	Eukaryotic translation initiation factor 3 subunit L
Q6TFL3	CCDC171	0,03696	-0,65	Coiled-coil domain-containing protein 171
P14649	MYL6B	0,01459	-0,65	Myosin light chain 6B
Q07020	RPL18	0,00155	-0,65	60S ribosomal protein L18
P12236	SLC25A6	0,03299	-0,65	ADP/ATP translocase 3
P62280	RPS11	0,01605	-0,64	40S ribosomal protein S11
Q16363	LAMA4	0,01606	-0,64	Laminin subunit alpha-4
P35241	RDX	0,01751	-0,64	Radixin
P26038	MSN	0,01751	-0,64	Moesin
P15311	EZR	0,01751	-0,64	Ezrin
Q6W3E5	GDPD4	0,02994	-0,64	Glycerophosphodiester phosphodiesterase domain-containing protein 4
Q9P0L9	PKD2L1	0,02160	-0,64	Polycystic kidney disease 2-like 1 protein
E9PM69	PSMC3	0,00296	-0,64	26S protease regulatory subunit 6A
Q562R1	ACTBL2	0,01694	-0,64	Beta-actin-like protein 2
Q9H501	ESF1	0,03083	-0,64	ESF1 homolog
P18669	PGAM1	0,01054	-0,63	Phosphoglycerate mutase 1

Q02878	RPL6	0,00051	-0,63	60S ribosomal protein L6
Q9UG01	IFT172	0,04154	-0,63	Intraflagellar transport protein 172 homolog
P49454	CENPF	0,01657	-0,63	Centromere protein F
H3BN98	#VALOR!	0,00018	-0,63	Uncharacterized protein (Fragment)
P28072	PSMB6	0,00029	-0,63	Proteasome subunit beta type-6
P38919	EIF4A3	0,00089	-0,62	Eukaryotic initiation factor 4A-III
Q13418	ILK	0,00120	-0,62	Integrin-linked protein kinase
P08708	RPS17	0,00072	-0,62	40S ribosomal protein S17
O14522	PTPRT	0,03788	-0,62	Receptor-type tyrosine-protein phosphatase T
P14174	MIF	0,00210	-0,62	Macrophage migration inhibitory factor
Q92901	RPL3L	0,01556	-0,61	60S ribosomal protein L3-like
O94812	BAIAP3	0,04077	-0,61	BAI1-associated protein 3
Q13185	CBX3	0,00009	-0,60	Chromobox protein homolog 3
P83731	RPL24	0,00001	-0,60	60S ribosomal protein L24
P50914	RPL14	0,00002	-0,60	60S ribosomal protein L14
Q6IPX4	RPS16	0,00096	-0,60	40S ribosomal protein S16
O14617	AP3D1	0,00008	-0,60	AP-3 complex subunit delta-1
Q9Y2W1	THRAP3	0,01294	-0,60	Thyroid hormone receptor-associated protein 3
Q9UI30	TRMT112	0,00003	-0,60	Multifunctional methyltransferase subunit TRM112-like protein
P52948	NUP98	0,01090	-0,60	Nuclear pore complex protein Nup98-Nup96
P17661	DES	0,00016	-0,59	Desmin
Q9NQ66	PLCB1	0,00553	-0,59	1-phosphatidylinositol 4,5-bisphosphate phosphodiesterase beta-1
Q7L014	DDX46	0,00556	-0,59	Probable ATP-dependent RNA helicase DDX46
P31946	YWHAB	0,00172	-0,59	14-3-3 protein beta/alpha
P07954	FH	0,00111	-0,59	Fumarate hydratase, mitochondrial
P17066	HSPA6	0,00018	-0,59	Heat shock 70 kDa protein 6
J3KPS3	ALDOA	0,01104	-0,59	Fructose-bisphosphate aldolase
P31040	SDHA	0,00996	-0,59	Succinate dehydrogenase [ubiquinone] flavoprotein subunit, mitochondrial
P49368	CCT3	0,00246	-0,59	T-complex protein 1 subunit gamma

P09211	GSTP1	0,00595	-0,58	Glutathione S-transferase P
Q92973	TNPO1	0,00067	-0,58	Transportin-1
E7ETK0	RPS24	0,00230	-0,57	40S ribosomal protein S24
P49773	HINT1	0,00046	-0,57	Histidine triad nucleotide-binding protein 1
O94776	MTA2	0,00003	-0,57	Metastasis-associated protein MTA2
P51610	HCFC1	0,02168	-0,57	Host cell factor 1
P61978	HNRNPK	0,00209	-0,57	Heterogeneous nuclear ribonucleoprotein K
Q9BZE4	GTPBP4	0,00646	-0,57	Nucleolar GTP-binding protein 1
O00425	IGF2BP3	0,02731	-0,57	Insulin-like growth factor 2 mRNA-binding protein 3
P30041	PRDX6	0,00014	-0,56	Peroxiredoxin-6
P62244	RPS15A	0,00029	-0,55	40S ribosomal protein S15a
P62857	RPS28	0,01273	-0,55	40S ribosomal protein S28
P62753	RPS6	0,01022	-0,55	40S ribosomal protein S6
Q9Y266	NUDC	0,00018	-0,55	Nuclear migration protein nudC
P62829	RPL23	0,00129	-0,55	60S ribosomal protein L23
O43175	PHGDH	0,00021	-0,54	D-3-phosphoglycerate dehydrogenase
P00558	PGK1	0,00012	-0,54	Phosphoglycerate kinase 1
P61981	YWHAG	0,00056	-0,54	14-3-3 protein gamma
Q15084	PDIA6	0,00472	-0,53	Protein disulfide-isomerase A6
P49407	ARRB1	0,00098	-0,53	Beta-arrestin-1
P28340	POLD1	0,02857	-0,53	DNA polymerase delta catalytic subunit
Q14697	GANAB	0,00142	-0,52	Neutral alpha-glucosidase AB
O43242	PSMD3	0,01552	-0,52	26S proteasome non-ATPase regulatory subunit 3
P40227	CCT6A	0,00257	-0,52	T-complex protein 1 subunit zeta
O75533	SF3B1	0,00329	-0,52	Splicing factor 3B subunit 1
Q06830	PRDX1	0,00302	-0,52	Peroxiredoxin-1
P61586	RHOA	0,00527	-0,52	Transforming protein RhoA
Q12774	ARHGEF5	0,00817	-0,52	Rho guanine nucleotide exchange factor 5
P63000	RAC1	0,00131	-0,51	Ras-related C3 botulinum toxin substrate 1

O15031	PLXNB2	0,02755	-0,51	Plexin-B2
P62191	PSMC1	0,00851	-0,51	26S protease regulatory subunit 4
Q9Y6V0	PCLO	0,02296	-0,51	Protein piccolo
Q15031	LARS2	0,03826	-0,50	Probable leucine--tRNA ligase, mitochondrial
P25705	ATP5A1	0,04246	-0,50	ATP synthase subunit alpha, mitochondrial
Q9UHP3	USP25	0,01334	-0,49	Ubiquitin carboxyl-terminal hydrolase 25
P18124	RPL7	0,03265	-0,49	60S ribosomal protein L7
P43304	GPD2	0,00982	-0,49	Glycerol-3-phosphate dehydrogenase, mitochondrial
P00451	F8	0,02233	-0,49	Coagulation factor VIII
P06733	ENO1	0,01266	-0,48	Alpha-enolase
Q13243	SRSF5	0,00385	-0,48	Serine/arginine-rich splicing factor 5
P53621	COPA	0,00187	-0,48	Coatomer subunit alpha
F8W0P7	ATP5B	0,02610	-0,48	ATP synthase subunit beta, mitochondrial (Fragment)
Q13838	DDX39B	0,00104	-0,48	Spliceosome RNA helicase DDX39B
O00148	DDX39A	0,00104	-0,48	ATP-dependent RNA helicase DDX39A
H0Y400	DDX39B	0,00104	-0,48	Spliceosome RNA helicase DDX39B (Fragment)
P46777	RPL5	0,03643	-0,48	60S ribosomal protein L5
A0A0A6YYF3	GPR75-ASB3	0,00240	-0,47	Protein GPR75-ASB3
Q9Y490	TLN1	0,01327	-0,47	Talin-1
P35579	MYH9	0,00125	-0,47	Myosin-9
P62917	RPL8	0,00928	-0,47	60S ribosomal protein L8
P22087	FBL	0,00693	-0,47	rRNA 2'-O-methyltransferase fibrillarin
P48681	NES	0,00004	-0,46	Nestin
P16401	HIST1H1B	0,00996	-0,46	Histone H1.5
Q9Y2X3	NOP58	0,00714	-0,46	Nucleolar protein 58
P07205	PGK2	0,02191	-0,46	Phosphoglycerate kinase 2
Q8NAV2	C8orf58	0,00023	-0,46	Uncharacterized protein C8orf58
A0A087WTP3	KHSRP	0,00529	-0,46	Far upstream element-binding protein 2

Q9Y3B7	MRPL11	0,02118	-0,46	39S ribosomal protein L11, mitochondrial
P42766	RPL35	0,00711	-0,46	60S ribosomal protein L35
Q13435	SF3B2	0,01387	-0,46	Splicing factor 3B subunit 2
P08238	HSP90AB1	0,00006	-0,46	Heat shock protein HSP 90-beta
A8MUS3	RPL23A	0,04506	-0,45	60S ribosomal protein L23a
P62701	RPS4X	0,00475	-0,45	40S ribosomal protein S4, X isoform
P54886	ALDH18A1	0,00458	-0,45	Delta-1-pyrroline-5-carboxylate synthase
Q12830	BPTF	0,01480	-0,45	Nucleosome-remodeling factor subunit BPTF
P04843	RPN1	0,03239	-0,45	Dolichyl-diphosphooligosaccharide--protein glycosyltransferase subunit 1
P62269	RPS18	0,02057	-0,44	40S ribosomal protein S18
P61160	ACTR2	0,04175	-0,44	Actin-related protein 2
P46776	RPL27A	0,00037	-0,44	60S ribosomal protein L27a
P04792	HSPB1	0,00808	-0,44	Heat shock protein beta-1
O43390	HNRNPR	0,01842	-0,44	Heterogeneous nuclear ribonucleoprotein R
P18754	RCC1	0,04087	-0,44	Regulator of chromosome condensation
P33992	MCM5	0,02101	-0,43	DNA replication licensing factor MCM5
Q9H307	PNN	0,01152	-0,43	Pinin
P35232	PHB	0,00836	-0,42	Prohibitin
P06748	NPM1	0,00043	-0,42	Nucleophosmin
Q99623	PHB2	0,00123	-0,42	Prohibitin-2
P25398	RPS12	0,01184	-0,42	40S ribosomal protein S12
P61026	RAB10	0,00627	-0,41	Ras-related protein Rab-10
O15217	GSTA4	0,02655	-0,41	Glutathione S-transferase A4
P31948	STIP1	0,03216	-0,41	Stress-induced-phosphoprotein 1
H3BLZ8	DDX17	0,00202	-0,40	Probable ATP-dependent RNA helicase DDX17
Q9HCK8	CHD8	0,03232	-0,39	Chromodomain-helicase-DNA-binding protein 8
P20700	LMNB1	0,00268	-0,39	Lamin-B1
P30101	PDIA3	0,00423	-0,39	Protein disulfide-isomerase A3
Q5TCY1	TTBK1	0,01113	-0,39	Tau-tubulin kinase 1

P04406	GAPDH	0,02057	-0,38	Glyceraldehyde-3-phosphate dehydrogenase
P49915	GMPS	0,02733	-0,38	GMP synthase [glutamine-hydrolyzing]
P07339	CTSD	0,00513	-0,38	Cathepsin D
P0DMV9	HSPA1B	0,03212	-0,38	Heat shock 70 kDa protein 1B
P31153	MAT2A	0,02699	-0,38	S-adenosylmethionine synthase isoform type-2
P52272	HNRNPM	0,00047	-0,37	Heterogeneous nuclear ribonucleoprotein M
Q13283	G3BP1	0,00491	-0,36	Ras GTPase-activating protein-binding protein 1
P29323	EPHB2	0,02439	-0,36	Ephrin type-B receptor 2
P13674	P4HA1	0,02145	-0,36	Prolyl 4-hydroxylase subunit alpha-1
Q15417	CNN3	0,01088	-0,36	Calponin-3
Q96AG4	LRRC59	0,00947	-0,35	Leucine-rich repeat-containing protein 59
Q13275	SEMA3F	0,00024	-0,35	Semaphorin-3F
P19338	NCL	0,02174	-0,35	Nucleolin
Q8NBS9	TXNDC5	0,02854	-0,35	Thioredoxin domain-containing protein 5
P34931	HSPA1L	0,02053	-0,35	Heat shock 70 kDa protein 1-like
P07237	P4HB	0,04018	-0,35	Protein disulfide-isomerase
P06576	ATP5B	0,00125	-0,34	ATP synthase subunit beta, mitochondrial
Q16658	FSCN1	0,00106	-0,34	Fascin
P08670	VIM	0,00027	-0,34	Vimentin
Q9BS26	ERP44	0,03290	-0,33	Endoplasmic reticulum resident protein 44
P54136	RARS	0,02546	-0,32	Arginine--tRNA ligase, cytoplasmic
A0A087WTI1	RAB1B	0,02047	-0,31	Ras-related protein Rab-1B
Q5U651	RASIP1	0,01012	-0,30	Ras-interacting protein 1
P38570	ITGAE	0,00992	-0,30	Integrin alpha-E
P40926	MDH2	0,00982	-0,29	Malate dehydrogenase, mitochondrial
Q14669	TRIP12	0,01695	-0,28	E3 ubiquitin-protein ligase TRIP12
A0A087X2D0	SRSF3	0,03391	-0,28	Serine/arginine-rich-splicing factor 3
P18084	ITGB5	0,04718	-0,27	Integrin beta-5

P22626	HNRNPA2B1	0,01891	-0,26	Heterogeneous nuclear ribonucleoproteins A2/B1
P62805	HIST1H4A	0,01683	-0,25	Histone H4
Q99832	CCT7	0,04078	-0,23	T-complex protein 1 subunit eta
P13010	XRCC5	0,02362	-0,16	X-ray repair cross-complementing protein 5
Q14696	MESDC2	0,00818	0,32	LDLR chaperone MESD
P20742	PZP	0,00448	0,33	Pregnancy zone protein
P38159	RBMX	0,04192	0,35	RNA-binding motif protein, X chromosome
Q70CQ4	USP31	0,02721	0,36	Ubiquitin carboxyl-terminal hydrolase 31
Q14764	MVP	0,01733	0,40	Major vault protein
Q13315	ATM	0,00741	0,47	Serine-protein kinase ATM
Q14344	GNA13	0,04316	0,49	Guanine nucleotide-binding protein subunit alpha-13
P69905	HBA1	0,03632	0,50	Hemoglobin subunit alpha
P49257	LMAN1	0,04790	0,51	Protein ERGIC-53
P35637	FUS	0,01962	0,52	RNA-binding protein FUS
Q9Y485	DMXL1	0,03324	0,54	DmX-like protein 1
P61221	ABCE1	0,01823	0,55	ATP-binding cassette sub-family E member 1
A0A087WXI0	RAB44	0,02844	0,56	Ras-related protein Rab-44
P56282	POLE2	0,02514	0,57	DNA polymerase epsilon subunit 2
O00160	MYO1F	0,01551	0,57	Unconventional myosin-If
Q9UKX3	MYH13	0,03397	0,60	Myosin-13
Q86TW2	ADCK1	0,04257	0,60	Uncharacterized aarF domain-containing protein kinase 1
Q15717	ELAVL1	0,01753	0,61	ELAV-like protein 1
E9PLU0	PDHX	0,03803	0,62	Pyruvate dehydrogenase protein X component, mitochondrial (Fragment)
Q14684	RRP1B	0,03771	0,62	Ribosomal RNA processing protein 1 homolog B
Q9UMZ3	PTPRQ	0,00419	0,62	Phosphatidylinositol phosphatase PTPRQ
P49748	ACADVL	0,00363	0,63	Very long-chain specific acyl-CoA dehydrogenase, mitochondrial
P16403	HIST1H1C	0,01198	0,63	Histone H1.2
P31939	ATIC	0,02321	0,64	Bifunctional purine biosynthesis protein PURH

O95573	ACSL3	0,03768	0,64	Long-chain-fatty-acid--CoA ligase 3
Q9Y5J7	TIMM9	0,03212	0,66	Mitochondrial import inner membrane translocase subunit Tim9
O75179	ANKRD17	0,04049	0,66	Ankyrin repeat domain-containing protein 17
Q9Y5J1	UTP18	0,01567	0,72	U3 small nucleolar RNA-associated protein 18 homolog
Q8NFU7	TET1	0,01441	0,72	Methylcytosine dioxygenase TET1
Q9H6R4	NOL6	0,00211	0,73	Nucleolar protein 6
Q02818	NUCB1	0,04584	0,73	Nucleobindin-1
P62195	PSMC5	0,00107	0,74	26S protease regulatory subunit 8
Q8NDH6	ICA1L	0,04964	0,75	Islet cell autoantigen 1-like protein
A0A075B739	CCDC187	0,02729	0,76	Coiled-coil domain-containing protein 187
Q9NZ71	RTEL1	0,01975	0,77	Regulator of telomere elongation helicase 1
O75347	TBCA	0,02107	0,77	Tubulin-specific chaperone A
Q8NCX0	CCDC150	0,01079	0,79	Coiled-coil domain-containing protein 150
Q9H6U6	BCAS3	0,04307	0,79	Breast carcinoma-amplified sequence 3
Q70EL1	USP54	0,00960	0,79	Inactive ubiquitin carboxyl-terminal hydrolase 54
P46821	MAP1B	0,04809	0,79	Microtubule-associated protein 1B
F8W1G6	PCBP2	0,00010	0,80	Poly(rC)-binding protein 2 (Fragment)
Q9Y2K3	MYH15	0,02598	0,80	Myosin-15
Q8N4C8	MINK1	0,02914	0,80	Misshapen-like kinase 1
Q8NI35	INADL	0,03769	0,82	InaD-like protein
M0R2J8	DCDC1	0,00420	0,82	Doublecortin domain-containing protein 1
Q9Y4L1	HYOU1	0,02256	0,83	Hypoxia up-regulated protein 1
P53675	CLTCL1	0,00134	0,83	Clathrin heavy chain 2
O15523	DDX3Y	0,01227	0,83	ATP-dependent RNA helicase DDX3Y
Q52LR7	EPC2	0,00361	0,84	Enhancer of polycomb homolog 2
Q96PK6	RBM14	0,00018	0,85	RNA-binding protein 14
Q9C0C6	CIPC	0,04590	0,85	CLOCK-interacting pacemaker
Q14204	DYNC1H1	0,00166	0,85	Cytoplasmic dynein 1 heavy chain 1
Q9H361	PABPC3	0,02295	0,86	Polyadenylate-binding protein 3

P24752	ACAT1	0,00519	0,87	Acetyl-CoA acetyltransferase, mitochondrial
Q96C45	ULK4	0,02469	0,88	Serine/threonine-protein kinase ULK4
P49006	MARCKSL1	0,02705	0,88	MARCKS-related protein
Q5TAA0	TTC22	0,02331	0,89	Tetratricopeptide repeat protein 22
E9PAL5	COL6A5	0,00322	0,89	Collagen alpha-5(VI) chain
P43356	MAGEA2	0,00225	0,90	Melanoma-associated antigen 2
Q13618	CUL3	0,00004	0,90	Cullin-3
J3KMX3	AFP	0,01988	0,90	Alpha-fetoprotein
Q7Z6E9	RBBP6	0,01610	0,91	E3 ubiquitin-protein ligase RBBP6
E7EQB2	LTF	0,00081	0,91	Lactotransferrin (Fragment)
Q9UKE5	TNIK	0,00036	0,91	TRAF2 and NCK-interacting protein kinase
Q86UL8	MAGI2	0,03632	0,91	Membrane-associated guanylate kinase, WW and PDZ domain-containing protein 2
Q9BQG0	MYBBP1A	0,02073	0,91	Myb-binding protein 1A
F6WH68	RTEL1-TNFRSF6B	0,00048	0,92	Regulator of telomere elongation helicase 1
Q9ULJ3	ZBTB21	0,03545	0,92	Zinc finger and BTB domain-containing protein 21
A0A0C4DGG9	CHD4	0,01714	0,93	Chromodomain-helicase-DNA-binding protein 4
Q9HCD6	TANC2	0,01860	0,93	Protein TANC2
O75335	PPFIA4	0,02148	0,94	Liprin-alpha-4
Q5VT06	CEP350	0,03195	0,94	Centrosome-associated protein 350
Q96Q27	ASB2	0,01084	0,95	Ankyrin repeat and SOCS box protein 2
A0A0A0MQW0	MYEF2	0,00009	0,95	Myelin expression factor 2
P50579	METAP2	0,02640	0,95	Methionine aminopeptidase 2
P02768	ALB	0,00041	0,96	Serum albumin
Q12996	CSTF3	0,02639	0,97	Cleavage stimulation factor subunit 3
O15056	SYNJ2	0,01578	0,98	Synaptojanin-2
F8W7A7	CCDC178	0,00100	0,98	Coiled-coil domain-containing protein 178
Q9Y4G6	TLN2	0,01171	0,98	Talin-2
Q53H82	LACTB2	0,00059	1,00	Beta-lactamase-like protein 2

Q6W4X9	MUC6	0,01601	1,01	Mucin-6
O60488	ACSL4	0,00214	1,01	Long-chain-fatty-acid--CoA ligase 4
P01266	TG	0,01084	1,02	Thyroglobulin
O75717	WDHD1	0,04368	1,03	WD repeat and HMG-box DNA-binding protein 1
P18583	SON	0,00425	1,03	Protein SON
P33993	MCM7	0,00696	1,04	DNA replication licensing factor MCM7
Q9Y6D9	MAD1L1	0,00052	1,04	Mitotic spindle assembly checkpoint protein MAD1
Q96T37	RBM15	0,00372	1,04	Putative RNA-binding protein 15
P35749	MYH11	0,01500	1,05	Myosin-11
Q86XL3	ANKLE2	0,04325	1,05	Ankyrin repeat and LEM domain-containing protein 2
Q02388	COL7A1	0,00081	1,05	Collagen alpha-1(VII) chain
Q9NWB7	IFT57	0,00311	1,06	Intraflagellar transport protein 57 homolog
Q9NXF1	TEX10	0,04251	1,07	Testis-expressed sequence 10 protein
Q9H3R0	KDM4C	0,00614	1,09	Lysine-specific demethylase 4C
Q9H8V3	ECT2	0,00058	1,09	Protein ECT2
O75494	SRSF10	0,04721	1,10	Serine/arginine-rich splicing factor 10
Q8TDZ2	MICAL1	0,02137	1,10	Protein-methionine sulfoxide oxidase MICAL1
Q16352	INA	0,02639	1,10	Alpha-internexin
P13639	EEF2	0,01659	1,10	Elongation factor 2
Q8N8E3	CEP112	0,00002	1,11	Centrosomal protein of 112 kDa
Q15311	RALBP1	0,04591	1,12	RalA-binding protein 1
Q99490	AGAP2	0,00017	1,13	Arf-GAP with GTPase, ANK repeat and PH domain-containing protein 2
Q9UBB9	TFIP11	0,00380	1,13	Tuftelin-interacting protein 11
Q8TEK3	DOT1L	0,00320	1,14	Histone-lysine N-methyltransferase, H3 lysine-79 specific
Q5JVL4	EFHC1	0,00293	1,14	EF-hand domain-containing protein 1
H7C103	ECT2	0,00066	1,14	Protein ECT2 (Fragment)
Q92947	GCDH	0,02853	1,14	Glutaryl-CoA dehydrogenase, mitochondrial
Q9NXB0	MKS1	0,02162	1,15	Meckel syndrome type 1 protein
Q9BY84	DUSP16	0,04091	1,15	Dual specificity protein phosphatase 16

Q9P2L0	WDR35	0,01019	1,16	WD repeat-containing protein 35
Q05469	LIPE	0,01129	1,16	Hormone-sensitive lipase
Q9UN79	SOX13	0,00674	1,16	Transcription factor SOX-13
O14980	XPO1	0,00494	1,16	Exportin-1
P46939	UTRN	0,01122	1,18	Utrophin
O75962	TRIO	0,00152	1,18	Triple functional domain protein
P33151	CDH5	0,00252	1,20	Cadherin-5
Q5JWF2	GNAS	0,00084	1,20	Guanine nucleotide-binding protein G(s) subunit alpha isoforms XLas
P11940	PABPC1	0,00379	1,20	Polyadenylate-binding protein 1
Q9P1Z9	CCDC180	0,00025	1,21	Coiled-coil domain-containing protein 180
A7KAX9	ARHGAP32	0,04859	1,21	Rho GTPase-activating protein 32
P02765	AHSG	0,03289	1,21	Alpha-2-HS-glycoprotein
Q6PHR2	ULK3	0,00401	1,21	Serine/threonine-protein kinase ULK3
Q9BW19	KIFC1	0,00497	1,21	Kinesin-like protein KIFC1
O15117	FYB	0,00071	1,22	FYN-binding protein
A0A096LPG1	HMCN2	0,04045	1,22	Hemicentin-2 (Fragment)
H7C1M2	SON	0,04221	1,22	Protein SON (Fragment)
Q460N5	PARP14	0,00053	1,22	Poly [ADP-ribose] polymerase 14
P0CG39	POTEJ	0,00895	1,23	POTE ankyrin domain family member J
P46940	IQGAP1	0,02241	1,24	Ras GTPase-activating-like protein IQGAP1
C9JMQ6	HDLBP	0,03303	1,24	Vigilin (Fragment)
P61970	NUTF2	0,01140	1,25	Nuclear transport factor 2
Q8IX01	SUGP2	0,02625	1,26	SURP and G-patch domain-containing protein 2
Q07092	COL16A1	0,02235	1,26	Collagen alpha-1(XVI) chain
Q8TE57	ADAMTS16	0,00075	1,26	A disintegrin and metalloproteinase with thrombospondin motifs 16
P21359	NF1	0,01371	1,27	Neurofibromin
H0YLN8	TRPM7	0,01994	1,27	Transient receptor potential cation channel subfamily M member 7
A2PYH4	HFM1	0,01755	1,27	Probable ATP-dependent DNA helicase HFM1

X6RFL8	RAB14	0,00327	1,29	Ras-related protein Rab-14 (Fragment)
P35626	ADRBK2	0,00215	1,29	Beta-adrenergic receptor kinase 2
Q9Y450	HBS1L	0,00232	1,29	HBS1-like protein
Q9HC10	OTOF	0,00286	1,32	Otoferlin
P49326	FMO5	0,03752	1,32	Dimethylaniline monooxygenase [N-oxide-forming] 5
Q70J99	UNC13D	0,00004	1,33	Protein unc-13 homolog D
P09669	COX6C	0,01755	1,34	Cytochrome c oxidase subunit 6C
Q9Y4F4	FAM179B	0,01498	1,34	Protein FAM179B
O43776	NARS	0,00267	1,35	Asparagine--tRNA ligase, cytoplasmic
Q9UHC1	MLH3	0,00895	1,35	DNA mismatch repair protein Mlh3
O94988	FAM13A	0,00168	1,36	Protein FAM13A
E7ESC9	WDR17	0,00002	1,36	WD repeat-containing protein 17
O75197	LRP5	0,00003	1,38	Low-density lipoprotein receptor-related protein 5
Q86WI3	NLRC5	0,02984	1,39	Protein NLRC5
A0A0C4DGK3	SYNE2	0,00077	1,40	Nesprin-2
Q08945	SSRP1	0,01730	1,41	FACT complex subunit SSRP1
P20618	PSMB1	0,04121	1,42	Proteasome subunit beta type-1
O60391	GRIN3B	0,00156	1,42	Glutamate receptor ionotropic, NMDA 3B
Q9UHD1	CHORDC1	0,04944	1,43	Cysteine and histidine-rich domain-containing protein 1
P10515	DLAT	0,04389	1,43	Dihydrolipoyllysine-residue acetyltransferase component of pyruvate dehydrogenase complex, mitochondrial
E7EW31	PROB1	0,00429	1,43	Proline-rich basic protein 1
F8VUX9	WDR90	0,00025	1,43	WD repeat-containing protein 90
P53396	ACLY	0,00001	1,45	ATP-citrate synthase
Q96C92	SDCCAG3	0,00491	1,45	Serologically defined colon cancer antigen 3
Q9H0J4	QRICH2	0,01031	1,46	Glutamine-rich protein 2
Q9Y6D6	ARFGEF1	0,00066	1,46	Brefeldin A-inhibited guanine nucleotide-exchange protein 1
Q8NF50	DOCK8	0,00451	1,47	Dedicator of cytokinesis protein 8
P42695	NCAPD3	0,01157	1,47	Condensin-2 complex subunit D3

Q9H0X9	OSBPL5	0,00596	1,47	Oxysterol-binding protein-related protein 5
Q9NQX1	PRDM5	0,00214	1,47	PR domain zinc finger protein 5
Q9H6D7	HAUS4	0,04075	1,48	HAUS augmin-like complex subunit 4
O60522	TDRD6	0,00273	1,48	Tudor domain-containing protein 6
Q5JTV8	TOR1AIP1	0,01026	1,49	Torsin-1A-interacting protein 1
O60437	PPL	0,02795	1,49	Periplakin
Q86UP3	ZFHX4	0,00010	1,49	Zinc finger homeobox protein 4
Q5JQF8	PABPC1L2A	0,00517	1,50	Polyadenylate-binding protein 1-like 2
Q9HCC0	MCCC2	0,00294	1,50	Methylcrotonoyl-CoA carboxylase beta chain, mitochondrial
C9J9W2	LASP1	0,03484	1,51	LIM and SH3 domain protein 1 (Fragment)
P48764	SLC9A3	0,04720	1,51	Sodium/hydrogen exchanger 3
Q09161	NCBP1	0,00775	1,52	Nuclear cap-binding protein subunit 1
Q8IZT6	ASPM	0,00080	1,52	Abnormal spindle-like microcephaly-associated protein
Q9P227	ARHGAP23	0,01950	1,55	Rho GTPase-activating protein 23
Q9P0V9	SEPT10	0,00007	1,55	Septin-10
P14678	SNRPB	0,01014	1,55	Small nuclear ribonucleoprotein-associated proteins B and B'
P38405	GNAL	0,00571	1,56	Guanine nucleotide-binding protein G(olf) subunit alpha
O14524	NEMP1	0,04960	1,58	Nuclear envelope integral membrane protein 1
Q86UK7	ZNF598	0,01645	1,58	Zinc finger protein 598
Q8IVU3	HERC6	0,00033	1,60	Probable E3 ubiquitin-protein ligase HERC6
E9PJZ7	PPFIA1	0,00225	1,60	Liprin-alpha-1
P63010	AP2B1	0,00004	1,60	AP-2 complex subunit beta
A0A0A0MTT5	CTAG1B	0,04776	1,61	Cancer/testis antigen 1
P13611	VCAN	0,01980	1,63	Versican core protein
Q58FF3	HSP90B2P	0,03657	1,64	Putative endoplasmin-like protein
Q9P2N2	ARHGAP28	0,04480	1,65	Rho GTPase-activating protein 28
Q8IYW2	CFAP46	0,03833	1,65	Cilia- and flagella-associated protein 46
Q8NBJ9	SIDT2	0,03367	1,66	SID1 transmembrane family member 2

Q0D2I5	IFFO1	0,00396	1,66	Intermediate filament family orphan 1
Q7RTV0	PHF5A	0,00542	1,67	PHD finger-like domain-containing protein 5A
Q02224	CENPE	0,00129	1,68	Centromere-associated protein E
O75140	DEPDC5	0,03011	1,68	DEP domain-containing protein 5
Q9NSI6	BRWD1	0,00080	1,69	Bromodomain and WD repeat-containing protein 1
B1ANS9	WDR64	0,00622	1,70	WD repeat-containing protein 64
Q6DRA6	HIST2H2BD	0,01287	1,73	Putative histone H2B type 2-D
B4DUT8	CNN2	0,00006	1,73	Calponin
Q12767	TMEM94	0,00801	1,73	Transmembrane protein 94
Q7Z6Z7	HUWE1	0,01858	1,73	E3 ubiquitin-protein ligase HUWE1
Q99999	GAL3ST1	0,00722	1,73	Galactosylceramide sulfotransferase
Q9Y5H5	PCDHA9	0,00682	1,73	Protocadherin alpha-9
O75116	ROCK2	0,01145	1,73	Rho-associated protein kinase 2
Q2KHT3	CLEC16A	0,00001	1,74	Protein CLEC16A
P30613	PKLR	0,00001	1,74	Pyruvate kinase PKLR
O14787	TNPO2	0,00001	1,75	Transportin-2
O75334	PPFIA2	0,00412	1,77	Liprin-alpha-2
P39023	RPL3	0,00553	1,77	60S ribosomal protein L3
O75886	STAM2	0,04502	1,78	Signal transducing adapter molecule 2
P35221	CTNNA1	0,00021	1,79	Catenin alpha-1
P13797	PLS3	0,00010	1,79	Plastin-3
Q96LI5	CNOT6L	0,00117	1,80	CCR4-NOT transcription complex subunit 6-like
O15042	U2SURP	0,00426	1,80	U2 snRNP-associated SURP motif-containing protein
Q99965	ADAM2	0,00130	1,81	Disintegrin and metalloproteinase domain-containing protein 2
Q96TA1	FAM129B	0,00003	1,81	Niban-like protein 1
A0A087X0T3	MYH7B	0,00005	1,81	Myosin-7B
Q12852	MAP3K12	0,00047	1,85	Mitogen-activated protein kinase kinase kinase 12
Q5T5P2	KIAA1217	0,00089	1,85	Sickle tail protein homolog

J3KRR7	CYLD	0,00066	1,85	Ubiquitin carboxyl-terminal hydrolase CYLD
Q96SK2	TMEM209	0,00722	1,86	Transmembrane protein 209
Q92793	CREBBP	0,00268	1,87	CREB-binding protein
Q14964	RAB39A	0,04122	1,88	Ras-related protein Rab-39A
Q9HB55	CYP3A43	0,00039	1,88	Cytochrome P450 3A43
Q8N4C6	NIN	0,00627	1,88	Ninein
Q5SRE7	PHYHD1	0,02027	1,89	Phytanoyl-CoA dioxygenase domain-containing protein 1
S4R417	RPS15	0,02983	1,89	40S ribosomal protein S15
Q7Z5M8	ABHD12B	0,00022	1,90	Protein ABHD12B
Q96MR6	CFAP57	0,00000	1,90	Cilia- and flagella-associated protein 57
Q9H7P9	PLEKHG2	0,00015	1,91	Pleckstrin homology domain-containing family G member 2
Q9HAU0	PLEKHA5	0,04060	1,91	Pleckstrin homology domain-containing family A member 5
A0A087WUB1	CCDC129	0,03776	1,93	Coiled-coil domain-containing protein 129
Q9NZL3	ZNF224	0,02361	1,94	Zinc finger protein 224
O96028	WHSC1	0,00151	1,94	Histone-lysine N-methyltransferase NSD2
E9PEZ1	CUL9	0,02280	1,99	Cullin-9
Q9H040	SPRTN	0,02100	2,00	SprT-like domain-containing protein Spartan
Q6P1R3	MSANTD2	0,02204	2,00	Myb/SANT-like DNA-binding domain-containing protein 2
Q8IYM0	FAM186B	0,00008	2,00	Protein FAM186B
Q6ZVH7	ESPNL	0,00000	2,00	Espin-like protein
Q8N806	UBR7	0,01125	2,00	Putative E3 ubiquitin-protein ligase UBR7
A2A3F7	TRPM3	0,00053	2,01	Transient receptor potential cation channel subfamily M member 3
Q13247	SRSF6	0,01172	2,02	Serine/arginine-rich splicing factor 6
Q969Z0	TBRG4	0,01850	2,03	Protein TBRG4
O14976	GAK	0,00311	2,03	Cyclin-G-associated kinase
H3BNV2	NQO1	0,00073	2,04	NAD(P)H dehydrogenase [quinone] 1
A0A0U1RRI6	CENPVP3	0,00000	2,04	Protein CENPVP3
G3V599	#VALOR!	0,01771	2,05	Uncharacterized protein

O95428	PAPLN	0,01594	2,05	Papilin
Q9UNH7	SNX6	0,01373	2,05	Sorting nexin-6
O75427	LRCH4	0,00575	2,06	Leucine-rich repeat and calponin homology domain-containing protein 4
Q5TA12	DOPEY1	0,00075	2,06	Protein dopey-1
Q9NQA5	TRPV5	0,02536	2,06	Transient receptor potential cation channel subfamily V member 5
H0Y390	MACF1	0,00002	2,07	Microtubule-actin cross-linking factor 1, isoforms 1/2/3/5 (Fragment)
O14556	GAPDHS	0,00107	2,08	Glyceraldehyde-3-phosphate dehydrogenase, testis-specific
I3L2J0	CIC	0,02988	2,08	Protein capicua homolog
A0A087WWF5	CSNK1G2	0,03426	2,09	Casein kinase I isoform gamma-2 (Fragment)
Q3KP44	ANKRD55	0,01597	2,09	Ankyrin repeat domain-containing protein 55
Q8N9W4	GOLGA6L2	0,00358	2,10	Golgin subfamily A member 6-like protein 2
Q13363	CTBP1	0,00075	2,10	C-terminal-binding protein 1
Q86X40	LRRC28	0,01988	2,10	Leucine-rich repeat-containing protein 28
P20338	RAB4A	0,00013	2,11	Ras-related protein Rab-4A
Q38SD2	LRRK1	0,00000	2,11	Leucine-rich repeat serine/threonine-protein kinase 1
Q8N6G6	ADAMTSL1	0,00399	2,13	ADAMTS-like protein 1
O95754	SEMA4F	0,00000	2,13	Semaphorin-4F
P18054	ALOX12	0,01275	2,14	Arachidonate 12-lipoxygenase, 12S-type
P04181	OAT	0,02699	2,15	Ornithine aminotransferase, mitochondrial
Q7Z2Z2	EFTUD1	0,00070	2,15	Elongation factor Tu GTP-binding domain-containing protein 1
A0A087WUA8	PCDH15	0,04425	2,15	Protocadherin-15
P53804	TTC3	0,00062	2,16	E3 ubiquitin-protein ligase TTC3
Q9UKN8	GTF3C4	0,00014	2,16	General transcription factor 3C polypeptide 4
Q71F56	MED13L	0,00222	2,16	Mediator of RNA polymerase II transcription subunit 13-like
Q2M3T9	HYAL4	0,00012	2,17	Hyaluronidase-4
E9PEF1	PDE2A	0,00001	2,18	cGMP-dependent 3',5'-cyclic phosphodiesterase
P61011	SRP54	0,00001	2,18	Signal recognition particle 54 kDa protein
O75145	PPFIA3	0,00082	2,19	Liprin-alpha-3

P01891	HLA-A	0,00041	2,19	HLA class I histocompatibility antigen, A-68 alpha chain
Q92783	STAM	0,00422	2,20	Signal transducing adapter molecule 1
Q9Y5E5	PCDHB4	0,00427	2,21	Protocadherin beta-4
Q9UI46	DNAI1	0,00253	2,22	Dynein intermediate chain 1, axonemal
Q7Z3Z4	PIWIL4	0,02312	2,22	Piwi-like protein 4
E7ESZ3	PLEKHG2	0,00000	2,23	Pleckstrin homology domain-containing family G member 2
Q8IYB7	DIS3L2	0,00342	2,23	DIS3-like exonuclease 2
Q9BVP2	GNL3	0,04925	2,24	Guanine nucleotide-binding protein-like 3
A0A087WZH7	MARCKS	0,02419	2,26	Myristoylated alanine-rich C-kinase substrate
Q2NL82	TSR1	0,00764	2,27	Pre-rRNA-processing protein TSR1 homolog
Q15181	PPA1	0,00339	2,28	Inorganic pyrophosphatase
A0A087WVS8	MOB2	0,02063	2,29	MOB kinase activator 2
Q96KC9	CABS1	0,00011	2,31	Calcium-binding and spermatid-specific protein 1
Q04912	MST1R	0,00002	2,32	Macrophage-stimulating protein receptor
P40692	MLH1	0,03573	2,33	DNA mismatch repair protein Mlh1
G3XAG5	CLCN4	0,01210	2,36	Chloride channel protein
Q16787	LAMA3	0,03037	2,39	Laminin subunit alpha-3
O14795	UNC13B	0,00012	2,40	Protein unc-13 homolog B
Q92993	KAT5	0,00176	2,41	Histone acetyltransferase KAT5
F5H5D3	TUBA1C	0,00931	2,42	Tubulin alpha-1C chain
Q15007	WTAP	0,00280	2,42	Pre-mRNA-splicing regulator WTAP
A0A087WZA1	FAM228B	0,00162	2,42	HCG1820835, isoform CRA_a
Q15021	NCAPD2	0,03683	2,43	Condensin complex subunit 1
Q8WX93	PALLD	0,00053	2,47	Palladin
Q14005	IL16	0,00014	2,49	Pro-interleukin-16
E9PEJ6	ATP11A	0,00028	2,50	Phospholipid-transporting ATPase
P52746	ZNF142	0,01877	2,50	Zinc finger protein 142
G5E9C0	SP110	0,02384	2,50	SP110 nuclear body protein, isoform CRA_b

O94915	FRYL	0,03405	2,52	Protein furry homolog-like
O15085	ARHGEF11	0,00034	2,52	Rho guanine nucleotide exchange factor 11
Q92526	CCT6B	0,00674	2,55	T-complex protein 1 subunit zeta-2
O60346	PHLPP1	0,02346	2,57	PH domain leucine-rich repeat-containing protein phosphatase 1
Q8IYT4	KATNAL2	0,02008	2,59	Katanin p60 ATPase-containing subunit A-like 2
Q96RK4	BBS4	0,00149	2,60	Bardet-Biedl syndrome 4 protein
A0A0U1RR20	PRG4	0,01837	2,61	Proteoglycan 4
O94856	NFASC	0,01239	2,62	Neurofascin
Q8NFM4	ADCY4	0,00118	2,63	Adenylate cyclase type 4
Q68EN5	KIAA0895L	0,00004	2,65	Uncharacterized protein KIAA0895-like
Q8WVM8	SCFD1	0,01237	2,65	Sec1 family domain-containing protein 1
Q99435	NELL2	0,01493	2,70	Protein kinase C-binding protein NELL2
Q9H0H5	RACGAP1	0,01290	2,71	Rac GTPase-activating protein 1
H3BQG7	FBXO31	0,00093	2,73	F-box only protein 31
Q9ULK0	GRID1	0,01526	2,73	Glutamate receptor ionotropic, delta-1
Q5JNZ5	RPS26P11	0,00317	2,74	Putative 40S ribosomal protein S26-like 1
A6NES4	MROH2A	0,01239	2,75	Maestro heat-like repeat-containing protein family member 2A
Q7RTU9	STRC	0,00002	2,75	Stereocilin
O60711	LPXN	0,00182	2,75	Leupaxin
Q9NRL2	BAZ1A	0,00129	2,77	Bromodomain adjacent to zinc finger domain protein 1A
A0A087WYA1	MYO15A	0,00833	2,80	Unconventional myosin-XV
Q9Y4F1	FARP1	0,00004	2,82	FERM, RhoGEF and pleckstrin domain-containing protein 1
P07864	LDHC	0,00026	2,85	L-lactate dehydrogenase C chain
Q14687	GSE1	0,00001	2,85	Genetic suppressor element 1
Q5JZY3	EPHA10	0,00420	2,85	Ephrin type-A receptor 10
Q96M42	LINC00479	0,00055	2,85	Putative uncharacterized protein encoded by LINC00479
O60282	KIF5C	0,00075	2,86	Kinesin heavy chain isoform 5C
Q7Z388	DPY19L4	0,01020	2,86	Probable C-mannosyltransferase DPY19L4

Q9UMX0	UBQLN1	0,00042	2,88	Ubiquilin-1
Q8NB66	UNC13C	0,00007	2,88	Protein unc-13 homolog C
P42229	STAT5A	0,00297	2,88	Signal transducer and activator of transcription 5A
Q16836	HADH	0,00007	2,92	Hydroxyacyl-coenzyme A dehydrogenase, mitochondrial
Q9NVR2	INTS10	0,00055	2,95	Integrator complex subunit 10
Q5SRH9	TTC39A	0,01005	2,96	Tetratricopeptide repeat protein 39A
Q9P2D0	IBTK	0,01228	2,98	Inhibitor of Bruton tyrosine kinase
B5MCJ9	TRIM66	0,00733	2,98	Tripartite motif-containing protein 66
Q9Y2H0	DLGAP4	0,00513	3,00	Disks large-associated protein 4
Q9Y228	TRAF3IP3	0,01199	3,01	TRAF3-interacting JNK-activating modulator
O00499	BIN1	0,00014	3,02	Myc box-dependent-interacting protein 1
A0A0C4DGQ1	ZSCAN5A	0,00034	3,03	Zinc finger and SCAN domain-containing protein 5A
Q9HCX4	TRPC7	0,00857	3,05	Short transient receptor potential channel 7
J3KQN4	RPL36A	0,01672	3,05	60S ribosomal protein L36a
A0A0U1RR27	DENND4A	0,01751	3,06	C-myc promoter-binding protein
Q06265	EXOSC9	0,00198	3,08	Exosome complex component RRP45
Q15257	PPP2R4	0,02857	3,09	Serine/threonine-protein phosphatase 2A activator
A0A0G2JLW6	DLGAP2	0,00002	3,12	Disks large-associated protein 2
O43307	ARHGEF9	0,00531	3,13	Rho guanine nucleotide exchange factor 9
Q6ZMI3	GLDN	0,02694	3,21	Gliomedin
Q9UPQ7	PDZRN3	0,00020	3,23	E3 ubiquitin-protein ligase PDZRN3
Q8IYB8	SUPV3L1	0,00240	3,29	ATP-dependent RNA helicase SUPV3L1, mitochondrial
Q13023	AKAP6	0,00242	3,31	A-kinase anchor protein 6
Q0PNE2	ELP6	0,03094	3,34	Elongator complex protein 6
O75147	OBSL1	0,00001	3,42	Obscurin-like protein 1
Q92696	RABGGTA	0,00126	3,46	Geranylgeranyl transferase type-2 subunit alpha
Q9Y2L1	DIS3	0,00492	3,49	Exosome complex exonuclease RRP44
Q8TER5	ARHGEF40	0,00159	3,52	Rho guanine nucleotide exchange factor 40

F2Z393	TALDO1	0,00069	3,57	Transaldolase
O60763	USO1	0,00071	3,61	General vesicular transport factor p115
Q92896	GLG1	0,00122	3,67	Golgi apparatus protein 1
Q9HAR2	ADGRL3	0,00031	3,68	Adhesion G protein-coupled receptor L3
Q8TF74	WIPF2	0,00578	3,69	WAS/WASL-interacting protein family member 2
Q00987	MDM2	0,00010	3,74	E3 ubiquitin-protein ligase Mdm2
A0A087WSV6	LILRB1	0,00476	3,92	Leukocyte immunoglobulin-like receptor subfamily B member 1
Q8NBJ4	GOLM1	0,02480	3,93	Golgi membrane protein 1
Q5T5X7	BEND3	0,00236	4,09	BEN domain-containing protein 3
Q07075	ENPEP	0,00241	4,11	Glutamyl aminopeptidase
Q9P0J0	NDUFA13	0,00336	4,17	NADH dehydrogenase [ubiquinone] 1 alpha subcomplex subunit 13
A0A0G2JPP5	SCRIB	0,00128	4,37	Protein scribble homolog
Q16798	ME3	0,00020	4,41	NADP-dependent malic enzyme, mitochondrial
Q86VS3	IQCH	0,00024	4,47	IQ domain-containing protein H
Q9NZU7	CABP1	0,01479	4,51	Calcium-binding protein 1
Q96BY6	DOCK10	0,00015	4,54	Dedicator of cytokinesis protein 10
Q9UHX1	PUF60	0,00003	4,56	Poly(U)-binding-splicing factor PUF60
Q9UBW8	COPS7A	0,00035	4,64	COP9 signalosome complex subunit 7a
F5H094	#VALOR!	0,00073	4,78	Solute carrier organic anion transporter family member
Q8WXX0	DNAH7	0,00087	4,81	Dynein heavy chain 7, axonemal
O96019	ACTL6A	0,00011	4,89	Actin-like protein 6A
Q96SZ6	CDK5RAP1	0,00004	5,05	CDK5 regulatory subunit-associated protein 1
H0Y4I5	CHADL	0,00014	5,45	Chondroadherin-like protein (Fragment)
Q14746	COG2	0,01997	5,93	Conserved oligomeric Golgi complex subunit 2
P62714	PPP2CB	0,00002	9,74	Serine/threonine-protein phosphatase 2A catalytic subunit beta isoform

Table 3: Ingenuity canonical pathway analysis for oligodendrocyte treated with first generation antipsychotics

Table 3 - Ingenuity canonical pathway analysis for oligodendrocyte treated with first generation antipsychotics

Treatment	Ingenuity Canonical Pathways	p-value	Ratio
Chlorpromazine	Actin Cytoskeleton Signaling	3,55E-04	17/221 (0,0769)
Chlorpromazine	Aldosterone Signaling in Epithelial Cells	4,37E-03	12/167 (0,0719)
Chlorpromazine	Breast Cancer Regulation by Stathmin1	3,98E-02	11/202 (0,0545)
Chlorpromazine	Cdc42 Signaling	4,79E-04	12/129 (0,093)
Chlorpromazine	CTLA4 Signaling in Cytotoxic T Lymphocytes	6,76E-04	10/98 (0,102)
Chlorpromazine	Epithelial Adherens Junction Signaling	3,72E-03	11/143 (0,0769)
Chlorpromazine	ERK/MAPK Signaling	3,55E-02	11/198 (0,0556)
Chlorpromazine	Germ Cell-Sertoli Cell Junction Signaling	4,79E-03	12/169 (0,071)
Chlorpromazine	Glioblastoma Multiforme Signaling	8,13E-03	11/159 (0,0692)
Chlorpromazine	Huntington's Disease Signaling	1,32E-02	14/240 (0,0583)
Chlorpromazine	ILK Signaling	1,91E-03	14/192 (0,0729)
Chlorpromazine	Integrin Signaling	1,78E-03	15/212 (0,0708)
Chlorpromazine	mTOR Signaling	8,91E-05	17/197 (0,0863)
Chlorpromazine	PI3K/AKT Signaling	3,09E-04	12/123 (0,0976)
Chlorpromazine	Rac Signaling	2,45E-03	10/116 (0,0862)
Chlorpromazine	Regulation of Actin-based Motility by Rho	2,34E-04	10/86 (0,116)
Chlorpromazine	Regulation of eIF4 and p70S6K Signaling	1,70E-07	19/154 (0,123)
Chlorpromazine	RhoA Signaling	3,55E-03	10/122 (0,082)
Chlorpromazine	RhoGDI Signaling	1,95E-03	10/122 (0,0756)
Chlorpromazine	Signaling by Rho Family GTPases	3,09E-03	16/247 (0,0648)
Chlorpromazine	Tight Junction Signaling	1,45E-03	13/166 (0,0783)
Chlorpromazine	Wnt/β-catenin Signaling	1,26E-02	11/169 (0,0651)

Specific to Chlorpromazine
Shared between Chlorpromazine and
Specific to Haloperidol

Treatment	Ingenuity Canonical Pathways	p-value	Ratio
Haloperidol	14-3-3-mediated Signaling	0,0354813	11/130 (0,0846)
Haloperidol	Actin Cytoskeleton Signaling	7,76E-05	24/221 (0,109)
Haloperidol	Agranulocyte Adhesion and Diapedesis	0,030903	14/176 (0,0795)
Haloperidol	Aldosterone Signaling in Epithelial Cells	0,0041687	16/167 (0,0958)
Haloperidol	Aryl Hydrocarbon Receptor Signaling	0,0089125	13/135 (0,0963)
Haloperidol	Axonal Guidance Signaling	0,0012883	35/445 (0,0787)
Haloperidol	Breast Cancer Regulation by Stathmin1	0,0003802	21/201 (0,104)
Haloperidol	Cardiac Hypertrophy Signaling	0,020893	18/233 (0,0773)
Haloperidol	Cellular Effects of Sildenafil (Viagra)	0,0125893	12/126 (0,0952)
Haloperidol	Clathrin-mediated Endocytosis Signaling	0,0194984	16/198 (0,0808)
Haloperidol	CXCR4 Signaling	0,0081283	15/164 (0,0915)
Haloperidol	EIF2 Signaling	1,58E-27	56/212 (0,264)
Haloperidol	Ephrin Receptor Signaling	0,0054954	16/172 (0,093)
Haloperidol	Epithelial Adherens Junction Signaling	0,0002884	17/143 (0,119)
Haloperidol	Germ Cell-Sertoli Cell Junction Signaling	0,0107152	15/169 (0,0888)
Haloperidol	Gluconeogenesis I	2,29E-10	12/25 (0,48)
Haloperidol	Glycolysis I	2,45E-09	11/24 (0,458)
Haloperidol	GNRH Signaling	0,030903	11/127 (0,0866)
Haloperidol	Gα12/13 Signaling	0,0371535	11/131 (0,084)
Haloperidol	Hepatic Fibrosis / Hepatic Stellate Cell Activation	0,0380189	14/181 (0,0773)
Haloperidol	ILK Signaling	0,0070795	17/192 (0,0885)
Haloperidol	Mitochondrial Dysfunction	0,0389045	13/165 (0,0788)
Haloperidol	Molecular Mechanisms of Cancer	0,0331131	23/370 (0,0676)
Haloperidol	mTOR Signaling	1,58E-13	37/197 (0,188)
Haloperidol	NRF2-mediated Oxidative Stress Response	0,0275423	15/190 (0,0789)
Haloperidol	p70S6K Signaling	0,0165959	12/131 (0,0916)
Haloperidol	Phagosome Maturation	0,0239883	12/138 (0,087)
Haloperidol	Phospholipase C Signaling	0,0398107	17/234 (0,0726)
Haloperidol	PI3K/AKT Signaling	0,0251189	11/123 (0,0894)
Haloperidol	Protein Kinase A Signaling	0,0048978	29/380 (0,0763)
Haloperidol	Protein Ubiquitination Pathway	4,90E-07	32/264 (0,121)

Haloperidol	Regulation of eIF4 and p70S6K Signaling	6,31E-18	38/154 (0,247)
Haloperidol	RhoA Signaling	0,001349	14/122 (0,115)
Haloperidol	RhoGDI Signaling	2,88E-07	25/172 (0,145)
Haloperidol	Role of Tissue Factor in Cancer	0,047863	10/120 (0,0833)
Haloperidol	Signaling by Rho Family GTPases	9,12E-06	28/247 (0,113)
Haloperidol	Sumoylation Pathway	0,0013804	12/96 (0,125)
Haloperidol	Synaptic Long Term Depression	0,0281838	12/141 (0,0851)
Haloperidol	Thrombin Signaling	0,0050119	18/201 (0,0896)
Haloperidol	Tight Junction Signaling	0,0038905	16/166 (0,0964)

Table 4: Proteins affected by quetiapine treatment

Table 4: Proteins affected by quetiapine treatment

Accession	Gene	Anova (p)	log_2 Fold change	Protein
A0A0G2JNK3	NLRP7	0,01389	-13,82	NACHT_ LRR and PYD domains-containing protein 7
P28074	PSMB5	0,03780	-11,76	Proteasome subunit beta type-5
Q14247	CTTN	0,01279	-6,19	Src substrate cortactin
Q9ULL4	PLXNB3	0,04564	-6,10	Plexin-B3
Q9H239	MMP28	0,02439	-5,48	Matrix metalloproteinase-28
E9PFV2	PPARG	0,01725	-3,49	Peroxisome proliferator-activated receptor gamma
P62917	RPL8	0,03636	-2,89	60S ribosomal protein L8
Q8IZ26	ZNF34	0,02125	-2,86	Zinc finger protein 34
Q08752	PPID	0,01453	-2,86	Peptidyl-prolyl cis-trans isomerase D
Q9Y6V7	DDX49	0,04443	-2,83	Probable ATP-dependent RNA helicase DDX49
Q9UBJ2	ABCD2	0,04697	-2,82	ATP-binding cassette sub-family D member 2
Q93074	MED12	0,02646	-1,75	Mediator of RNA polymerase II transcription subunit 12
Q96JI7	SPG11	0,02877	-1,60	Spatacsin
Q5T9S5	CCDC18	0,03835	-1,09	Coiled-coil domain-containing protein 18
P27635	RPL10	0,01242	-0,96	60S ribosomal protein L10
Q6ZS17	FAM65A	0,03188	-0,49	Protein FAM65A
P08758	ANXA5	0,04080	0,62	Annexin A5
P52209	PGD	0,03739	0,76	6-phosphogluconate dehydrogenase_ decarboxylating
Q96AY3	FKBP10	0,02844	0,77	Peptidyl-prolyl cis-trans isomerase FKBP10
A0A096LNH2	EFCAB8	0,04933	0,80	EF-hand calcium-binding domain-containing protein 8
O75037	KIF21B	0,02142	1,00	Kinesin-like protein KIF21B
Q9NSB2	KRT84	0,00263	1,00	Keratin_ type II cuticular Hb4
Q8N2E2	VWDE	0,01517	1,02	von Willebrand factor D and EGF domain-containing protein
Q8IZT6	ASPM	0,00344	1,09	Abnormal spindle-like microcephaly-associated protein
Q8WWZ7	ABCA5	0,04577	1,16	ATP-binding cassette sub-family A member 5
Q8WX93	PALLD	0,03069	1,23	Palladin

A0A087WX35	KCTD17	0,03722	1,49	BTB/POZ domain-containing protein KCTD17
O94829	IPO13	0,01661	1,51	Importin-13
P61758	VBP1	0,02749	1,57	Prefoldin subunit 3
Q9UQ84	EXO1	0,04444	1,63	Exonuclease 1
Q7Z5K2	WAPL	0,03611	1,74	Wings apart-like protein homolog
P00505	GOT2	0,02052	1,77	Aspartate aminotransferase_ mitochondrial
Q5UE93	PIK3R6	0,02627	1,77	Phosphoinositide 3-kinase regulatory subunit 6
O43304	SEC14L5	0,02934	1,81	SEC14-like protein 5
Q15056	EIF4H	0,02141	1,81	Eukaryotic translation initiation factor 4H
A0A087WW83	GPR179	0,04608	1,85	Probable G-protein-coupled receptor 179
O95049	TJP3	0,03661	1,87	Tight junction protein ZO-3
Q96B18	DACT3	0,04851	1,93	Dapper homolog 3
Q9HCC9	ZFYVE28	0,04330	1,94	Lateral signaling target protein 2 homolog
Q14586	ZNF267	0,03859	1,95	Zinc finger protein 267
P54098	POLG	0,04287	1,97	DNA polymerase subunit gamma-1
Q9P219	CCDC88C	0,02935	2,00	Protein Daple
Q8ND30	PPFIBP2	0,02737	2,15	Liprin-beta-2
Q8IUG5	MYO18B	0,03612	2,18	Unconventional myosin-XVIIIb
P28838	LAP3	0,02974	2,18	Cytosol aminopeptidase
D6RJ07	ZNF346	0,03113	2,21	Zinc finger protein 346
G5EA30	CELF1	0,04004	2,24	CUG triplet repeat_ RNA binding protein 1_ isoform CRA_c
A4FU69	EFCAB5	0,03151	2,25	EF-hand calcium-binding domain-containing protein 5
Q8TF46	DIS3L	0,00931	2,25	DIS3-like exonuclease 1
F5H0U2	C2CD3	0,02844	2,28	C2 domain-containing protein 3
Q8IYE1	CCDC13	0,04694	2,31	Coiled-coil domain-containing protein 13
Q04721	NOTCH2	0,04134	2,33	Neurogenic locus notch homolog protein 2
Q9BZJ4	SLC25A39	0,01842	2,34	Solute carrier family 25 member 39
P29320	EPHA3	0,00230	2,35	Ephrin type-A receptor 3
P10721	KIT	0,01668	2,39	Mast/stem cell growth factor receptor Kit
F8W8Y7	ARMCX4	0,00262	2,39	Armadillo repeat-containing X-linked protein 4
Q9P107	GMIP	0,01039	2,50	GEM-interacting protein
A0A0B4J1V8	PPAN-	0,02556	2,53	HCG2039996

	P2RY11			
O95741	CPNE6	0,00752	2,58	Copine-6
A0A087WSV6	LILRB1	0,00839	2,60	Leukocyte immunoglobulin-like receptor subfamily B member 1
Q9ULV0	MYO5B	0,02013	2,62	Unconventional myosin-Vb
Q9Y613	FHOD1	0,01717	2,68	FH1/FH2 domain-containing protein 1
P0CG41	CTAGE8	0,04395	2,70	cTAGE family member 8
P48380	RFX3	0,01441	2,72	Transcription factor RFX3
Q9P1Z2	CALCOCO1	0,03795	2,74	Calcium-binding and coiled-coil domain-containing protein 1
O14578	CIT	0,02328	2,78	Citron Rho-interacting kinase
Q96E52	OMA1	0,02671	2,80	Metalloendopeptidase OMA1_ mitochondrial
Q8TAB3	PCDH19	0,01237	2,80	Protocadherin-19
Q76N32	CEP68	0,00731	3,00	Centrosomal protein of 68 kDa
Q9NZM5	GLTSCR2	0,04394	3,02	Glioma tumor suppressor candidate region gene 2 protein
H0YBT7	HSF4	0,00132	3,06	Heat shock factor protein 4 (Fragment)
Q86UT6	NLRX1	0,00871	3,08	NLR family member X1
Q08174	PCDH1	0,02342	3,20	Protocadherin-1
P51617	IRAK1	0,01264	3,22	Interleukin-1 receptor-associated kinase 1
A0A087WTA8	COL1A2	0,00363	3,28	Collagen alpha-2(I) chain
Q13972	RASGRF1	0,03250	3,30	Ras-specific guanine nucleotide-releasing factor 1
Q502W7	CCDC38	0,03615	3,56	Coiled-coil domain-containing protein 38
Q9BXL5	HEMGN	0,04102	3,63	Hemogen
Q2M1K9	ZNF423	0,04968	3,64	Zinc finger protein 423
A0A087WX34	RPGRIP1L	0,01514	3,65	Protein fantom
P17023	ZNF19	0,00179	3,68	Zinc finger protein 19
A6NHC0	CAPN8	0,00744	3,71	Calpain-8
Q9C0A6	SETD5	0,04484	3,77	SET domain-containing protein 5
Q96N22	ZNF681	0,00117	4,37	Zinc finger protein 681
Q9HCC0	MCCC2	0,02612	4,51	Methylcrotonoyl-CoA carboxylase beta chain_ mitochondrial
Q6ZUB1	SPATA31E1	0,00016	4,73	Spermatogenesis-associated protein 31E1
A6NI28	ARHGAP42	0,02396	4,78	Rho GTPase-activating protein 42
Q9C091	GREB1L	0,03997	4,78	GREB1-like protein

A0A0D9SG04	COBLL1	0,00343	4,81	Cordon-bleu protein-like 1
P50750	CDK9	0,03387	4,98	Cyclin-dependent kinase 9
O95071	UBR5	0,00793	5,00	E3 ubiquitin-protein ligase UBR5
Q9NVR5	DNAAF2	0,01727	5,69	Protein kintoun
P31946	YWHAB	0,03126	5,93	14-3-3 protein beta/alpha
Q9P1Z9	CCDC180	0,02174	6,12	Coiled-coil domain-containing protein 180

Table 5: Proteins affected by risperidone treatment

Table 5: Proteins affected by risperidone treatment

Accession	Gene	Anova (p)	log_2 Fold change	Protein
A5D8V7	CCDC151	0,00778	-21,19	Coiled-coil domain-containing protein 151
P52306	RAP1GDS1	0,00325	-18,43	Rap1 GTPase-GDP dissociation stimulator 1
Q13332	PTPRS	0,03155	-15,53	Receptor-type tyrosine-protein phosphatase S
O00505	KPNA3	0,01215	-14,72	Importin subunit alpha-4
B3KTM8	MORF4L1	0,02775	-13,60	Mortality factor 4-like protein 1
H0Y8A4	RYK	0,00452	-13,35	Tyrosine-protein kinase RYK (Fragment)
A0A0S2Z4Q7	ST3GAL5	0,00417	-11,83	Lactosylceramide alpha-2_3-sialyltransferase (Fragment)
F8VRH0	PCBP2	0,00444	-11,51	Poly(rC)-binding protein 2 (Fragment)
Q96PJ5	FCRL4	0,04893	-11,49	Fc receptor-like protein 4
O95453	PARN	0,04976	-11,12	Poly(A)-specific ribonuclease PARN
Q96JP0	FEM1C	0,00304	-10,80	Protein fem-1 homolog C
Q99523	SORT1	0,00934	-10,51	Sortilin
B7ZC32	KIF28P	0,00014	-10,49	Kinesin-like protein KIF28P
Q9HCL0	PCDH18	0,02047	-10,24	Protocadherin-18
V9GZ56	LSM4	0,03658	-9,92	U6 snRNA-associated Sm-like protein LSm4 (Fragment)
Q9NYV6	RRN3	0,00119	-9,85	RNA polymerase I-specific transcription initiation factor RRN3
O15440	ABCC5	0,00014	-9,79	Multidrug resistance-associated protein 5
Q5W0A0	ERICH6B	0,00001	-9,68	Glutamate-rich protein 6B
P07910	HNRNPC	0,00225	-9,63	Heterogeneous nuclear ribonucleoproteins C1/C2
O94972	TRIM37	0,00056	-9,47	E3 ubiquitin-protein ligase TRIM37
P20815	CYP3A5	0,00097	-9,38	Cytochrome P450 3A5
G3V4R5	ZC3H14	0,01221	-9,27	Zinc finger CCCH domain-containing protein 14 (Fragment)
A0A087WXF6	NDUFS7	0,00001	-9,22	NADH dehydrogenase [ubiquinone] iron-sulfur protein 7_ mitochondrial
Q9Y2R4	DDX52	0,00113	-9,05	Probable ATP-dependent RNA helicase DDX52
Q9Y5W7	SNX14	0,02174	-9,05	Sorting nexin-14

E9PIR9	CRYBG2	0,02075	-8,99	Crystallin beta-gamma domain-containing 2
Q8NCE0	TSEN2	0,03561	-8,95	tRNA-splicing endonuclease subunit Sen2
O43148	RNMT	0,01181	-8,91	mRNA cap guanine-N7 methyltransferase
Q8N684	CPSF7	0,04570	-8,72	Cleavage and polyadenylation specificity factor subunit 7
P39748	FEN1	0,00278	-8,54	Flap endonuclease 1
Q13214	SEMA3B	0,03539	-8,09	Semaphorin-3B
Q6NZY4	ZCCHC8	0,03888	-7,96	Zinc finger CCHC domain-containing protein 8
P08240	SRPRA	0,00004	-7,93	Signal recognition particle receptor subunit alpha
A8CG34	POM121C	0,00298	-7,91	Nuclear envelope pore membrane protein POM 121C
P11233	RALA	0,00162	-7,90	Ras-related protein Ral-A
Q99570	PIK3R4	0,00004	-7,84	Phosphoinositide 3-kinase regulatory subunit 4
Q96G03	PGM2	0,00063	-7,81	Phosphoglucomutase-2
Q96GE4	CEP95	0,02451	-7,77	Centrosomal protein of 95 kDa
Q86XP3	DDX42	0,00452	-7,68	ATP-dependent RNA helicase DDX42
O75525	KHDRBS3	0,02439	-7,41	KH domain-containing_ RNA-binding_ signal transduction-associated protein 3
Q8N139	ABCA6	0,00201	-7,36	ATP-binding cassette sub-family A member 6
P09001	MRPL3	0,01709	-7,17	39S ribosomal protein L3_ mitochondrial
Q14573	ITPR3	0,00000	-7,04	Inositol 1_4_5-trisphosphate receptor type 3
Q96GE5	ZNF799	0,00259	-7,03	Zinc finger protein 799
Q8TAD4	SLC30A5	0,02812	-7,02	Zinc transporter 5
O15173	PGRMC2	0,00080	-7,00	Membrane-associated progesterone receptor component 2
O60312	ATP10A	0,01632	-6,94	Probable phospholipid-transporting ATPase VA
B3KNS5	C7orf43	0,03705	-6,93	Uncharacterized protein C7orf43
Q5VUB5	FAM171A1	0,00039	-6,92	Protein FAM171A1
B4DKB2	ECE1	0,01535	-6,87	Endothelin-converting enzyme 1
Q9Y3P9	RABGAP1	0,00174	-6,85	Rab GTPase-activating protein 1
P08582	MELTF	0,02737	-6,78	Melanotransferrin
Q96JK9	MAML3	0,00010	-6,76	Mastermind-like protein 3
P06753	TPM3	0,01642	-6,74	Tropomyosin alpha-3 chain
P19388	POLR2E	0,00434	-6,69	DNA-directed RNA polymerases I_ II_ and III subunit RPABC1
Q502W7	CCDC38	0,03551	-6,66	Coiled-coil domain-containing protein 38

Q8N158	GPC2	0,00467	-6,64	Glypican-2
O75821	EIF3G	0,01256	-6,59	Eukaryotic translation initiation factor 3 subunit G
Q9ULI3	HEG1	0,00516	-6,58	Protein HEG homolog 1
Q96KN2	CNDP1	0,00009	-6,55	Beta-Ala-His dipeptidase
Q5JZY3	EPHA10	0,00003	-6,48	Ephrin type-A receptor 10
Q6ZSI9	CAPN12	0,02704	-6,47	Calpain-12
J3QQQ0	LIPG	0,03407	-6,31	Endothelial lipase
Q7Z449	CYP2U1	0,00021	-6,26	Cytochrome P450 2U1
D6REC4	CFAP99	0,00522	-6,18	Cilia- and flagella-associated protein 99
Q9Y5H2	PCDHGA11	0,00361	-6,17	Protocadherin gamma-A11
Q14914	PTGR1	0,00072	-6,16	Prostaglandin reductase 1
Q9BTY7	HGH1	0,00143	-6,12	Protein HGH1 homolog
J3QSU1	LRRC37B	0,00356	-6,11	Leucine-rich repeat-containing protein 37B
Q5T4T6	SYCP2L	0,00757	-6,07	Synaptonemal complex protein 2-like
A6NJL1	ZSCAN5B	0,01446	-6,05	Zinc finger and SCAN domain-containing protein 5B
G5E9C8	SOS1	0,01872	-6,02	Son of sevenless homolog 1
O15047	SETD1A	0,00046	-5,95	Histone-lysine N-methyltransferase SETD1A
O15427	SLC16A3	0,00543	-5,95	Monocarboxylate transporter 4
P19105	MYL12A	0,04722	-5,94	Myosin regulatory light chain 12A
P13646	KRT13	0,00034	-5,93	Keratin_ type I cytoskeletal 13
M0R3C7	SYMPK	0,00724	-5,90	Symplekin
Q9H5Z1	DHX35	0,00192	-5,88	Probable ATP-dependent RNA helicase DHX35
Q9Y5F0	PCDHB13	0,00708	-5,85	Protocadherin beta-13
E9PLL4	NR1H3	0,00915	-5,85	Oxysterols receptor LXR-alpha
O75330	HMMR	0,01071	-5,84	Hyaluronan mediated motility receptor
Q12972	PPP1R8	0,02010	-5,83	Nuclear inhibitor of protein phosphatase 1
Q3ZCM7	TUBB8	0,00515	-5,79	Tubulin beta-8 chain
Q14832	GRM3	0,04440	-5,78	Metabotropic glutamate receptor 3
A1L4H1	SSC5D	0,01398	-5,78	Soluble scavenger receptor cysteine-rich domain-containing protein SSC5D
P09661	SNRPA1	0,03163	-5,76	U2 small nuclear ribonucleoprotein A'
O60231	DHX16	0,00037	-5,76	Putative pre-mRNA-splicing factor ATP-dependent RNA helicase DHX16

A0A0A0MRT8	SPAG6	0,00000	-5,72	Sperm-associated antigen 6
Q8N3D4	EHBP1L1	0,02080	-5,72	EH domain-binding protein 1-like protein 1
Q9BXR0	QTRT1	0,04960	-5,71	Queuine tRNA-ribosyltransferase catalytic subunit 1
Q8TDW7	FAT3	0,00515	-5,70	Protocadherin Fat 3
Q5W5X9	TTC23	0,00020	-5,64	Tetratricopeptide repeat protein 23
Q7Z5J4	RAI1	0,01307	-5,64	Retinoic acid-induced protein 1
P26447	S100A4	0,01448	-5,64	Protein S100-A4
O95747	OXSR1	0,00422	-5,62	Serine/threonine-protein kinase OSR1
P48643	CCT5	0,00452	-5,60	T-complex protein 1 subunit epsilon
Q6NWY9	PRPF40B	0,01950	-5,58	Pre-mRNA-processing factor 40 homolog B
P00403	MT-CO2	0,00782	-5,56	Cytochrome c oxidase subunit 2
Q9BX69	CARD6	0,01063	-5,55	Caspase recruitment domain-containing protein 6
O94804	STK10	0,02790	-5,54	Serine/threonine-protein kinase 10
P09601	HMOX1	0,01639	-5,52	Heme oxygenase 1
Q9NY15	STAB1	0,02701	-5,52	Stabilin-1
Q96MS0	ROBO3	0,03249	-5,51	Roundabout homolog 3
P61163	ACTR1A	0,02621	-5,46	Alpha-centractin
E5RJM0	CPEB4	0,00127	-5,39	Cytoplasmic polyadenylation element-binding protein 4
P62304	SNRPE	0,00468	-5,34	Small nuclear ribonucleoprotein E
Q9Y2L8	ZKSCAN5	0,01829	-5,34	Zinc finger protein with KRAB and SCAN domains 5
Q9BZE2	PUS3	0,00033	-5,31	tRNA pseudouridine(38/39) synthase
Q9Y5I3	PCDHA1	0,00685	-5,30	Protocadherin alpha-1
Q10570	CPSF1	0,01249	-5,27	Cleavage and polyadenylation specificity factor subunit 1
Q9BVS5	TRMT61B	0,00113	-5,26	tRNA (adenine(58)-N(1))-methyltransferase_ mitochondrial
Q14831	GRM7	0,00523	-5,23	Metabotropic glutamate receptor 7
E7EQI7	WASHC5	0,00282	-5,23	WASH complex subunit 5
Q9UJ41	RABGEF1	0,00194	-5,21	Rab5 GDP/GTP exchange factor
Q9BYH1	SEZ6L	0,04464	-5,21	Seizure 6-like protein
G5EA42	TMOD2	0,01366	-5,20	Tropomodulin 2 (Neuronal)_ isoform CRA_a
Q9Y6B7	AP4B1	0,00215	-5,17	AP-4 complex subunit beta-1
Q5JPH6	EARS2	0,02490	-5,16	Probable glutamate--tRNA ligase_ mitochondrial

Q7L2E3	DHX30	0,03047	-5,15	Putative ATP-dependent RNA helicase DHX30
Q9P2S2	NRXN2	0,02254	-5,15	Neurexin-2
Q8IYE0	CCDC146	0,01531	-5,12	Coiled-coil domain-containing protein 146
Q13416	ORC2	0,03416	-5,12	Origin recognition complex subunit 2
J3QR12	ASPSCR1	0,00111	-5,10	Tether-containing UBX domain for GLUT4
O43795	MYO1B	0,01372	-5,09	Unconventional myosin-Ib
F5GX99	CLPB	0,00029	-5,07	Caseinolytic peptidase B protein homolog
Q5SXH7	PLEKHS1	0,01598	-5,05	Pleckstrin homology domain-containing family S member 1
P49790	NUP153	0,00124	-4,99	Nuclear pore complex protein Nup153
Q9UKA1	FBXL5	0,00963	-4,99	F-box/LRR-repeat protein 5
Q92529	SHC3	0,00166	-4,99	SHC-transforming protein 3
P54687	BCAT1	0,03568	-4,98	Branched-chain-amino-acid aminotransferase_ cytosolic
Q6P4F7	ARHGAP11A	0,00723	-4,97	Rho GTPase-activating protein 11A
A8K968	EPB41L3	0,02615	-4,95	Band 4.1-like protein 3
Q13829	TNFAIP1	0,04185	-4,91	BTB/POZ domain-containing adapter for CUL3-mediated RhoA degradation protein 2
Q16630	CPSF6	0,01231	-4,87	Cleavage and polyadenylation specificity factor subunit 6
Q9Y383	LUC7L2	0,00018	-4,84	Putative RNA-binding protein Luc7-like 2
Q92879	CELF1	0,00010	-4,84	CUGBP Elav-like family member 1
Q9Y4W6	AFG3L2	0,04390	-4,83	AFG3-like protein 2
O14830	PPEF2	0,00467	-4,82	Serine/threonine-protein phosphatase with EF-hands 2
O95382	MAP3K6	0,03154	-4,79	Mitogen-activated protein kinase kinase kinase 6
O75038	PLCH2	0,03118	-4,75	1-phosphatidylinositol 4_5-bisphosphate phosphodiesterase eta-2
O00330	PDHX	0,01767	-4,75	Pyruvate dehydrogenase protein X component_ mitochondrial
O00482	NR5A2	0,00194	-4,73	Nuclear receptor subfamily 5 group A member 2
P19793	RXRA	0,03024	-4,71	Retinoic acid receptor RXR-alpha
Q03701	CEBPZ	0,00493	-4,68	CCAAT/enhancer-binding protein zeta
Q9H0K6	PUS7L	0,00299	-4,65	Pseudouridylate synthase 7 homolog-like protein
Q96AB3	ISOC2	0,00352	-4,64	Isochorismatase domain-containing protein 2
Q9BTV7	CABLES2	0,00158	-4,63	CDK5 and ABL1 enzyme substrate 2
P17038	ZNF43	0,00027	-4,62	Zinc finger protein 43
Q9NQC3	RTN4	0,02400	-4,62	Reticulon-4

P00747	PLG	0,01992	-4,61	Plasminogen
B5MCU0	R3HDM2	0,00588	-4,60	R3H domain-containing protein 2
O75170	PPP6R2	0,00144	-4,60	Serine/threonine-protein phosphatase 6 regulatory subunit 2
Q15723	ELF2	0,03698	-4,58	ETS-related transcription factor Elf-2
Q9C040	TRIM2	0,00920	-4,57	Tripartite motif-containing protein 2
F8W9E7	ELMO3	0,04773	-4,56	Engulfment and cell motility protein 3
Q9UQ74	PSG8	0,00133	-4,54	Pregnancy-specific beta-1-glycoprotein 8
Q6IBW4	NCAPH2	0,00821	-4,53	Condensin-2 complex subunit H2
E9PS17	SCYL1	0,00116	-4,45	N-terminal kinase-like protein
Q96SJ8	TSPAN18	0,01128	-4,45	Tetraspanin-18
Q9Y2X0	MED16	0,04342	-4,45	Mediator of RNA polymerase II transcription subunit 16
Q9BSJ8	ESYT1	0,00208	-4,44	Extended synaptotagmin-1
Q13045	FLII	0,01674	-4,43	Protein flightless-1 homolog
Q15459	SF3A1	0,00777	-4,41	Splicing factor 3A subunit 1
V9GXZ4	FPGT-TNNI3K	0,00300	-4,40	FPGT-TNNI3K readthrough
Q14651	PLS1	0,02333	-4,37	Plastin-1
Q8TE49	OTUD7A	0,02901	-4,37	OTU domain-containing protein 7A
Q8TE82	SH3TC1	0,00952	-4,36	SH3 domain and tetratricopeptide repeat-containing protein 1
Q96RN1	SLC26A8	0,00643	-4,36	Testis anion transporter 1
Q562R1	ACTBL2	0,00457	-4,36	Beta-actin-like protein 2
Q9HBR0	SLC38A10	0,00162	-4,34	Putative sodium-coupled neutral amino acid transporter 10
Q5T6P1	SLAIN1	0,01701	-4,33	SLAIN motif-containing protein 1 (Fragment)
Q8NG66	NEK11	0,02880	-4,33	Serine/threonine-protein kinase Nek11
O96028	NSD2	0,00752	-4,33	Histone-lysine N-methyltransferase NSD2
Q8TDZ2	MICAL1	0,00551	-4,33	[F-actin]-methionine sulfoxide oxidase MICAL1
Q6ZWB6	KCTD8	0,00134	-4,32	BTB/POZ domain-containing protein KCTD8
Q69YN4	KIAA1429	0,02532	-4,30	Protein virilizer homolog
E9PNM1	FDFT1	0,00300	-4,30	Squalene synthase
A0A0A0MQV3	KIRREL2	0,03095	-4,30	Kin of IRRE-like protein 2
Q9H3P2	NELFA	0,01788	-4,26	Negative elongation factor A

Q15573	TAF1A	0,00203	-4,26	TATA box-binding protein-associated factor RNA polymerase I subunit A
P80192	MAP3K9	0,02340	-4,23	Mitogen-activated protein kinase kinase kinase 9
A0A0A6YYG7	NCAPH2	0,01615	-4,22	Condensin-2 complex subunit H2
Q9NW64	RBM22	0,03971	-4,21	Pre-mRNA-splicing factor RBM22
P61960	UFM1	0,00360	-4,20	Ubiquitin-fold modifier 1
Q2TAY7	SMU1	0,00507	-4,20	WD40 repeat-containing protein SMU1
P01833	PIGR	0,00056	-4,17	Polymeric immunoglobulin receptor
Q9NYA1	SPHK1	0,00063	-4,15	Sphingosine kinase 1
K7ERQ8	#VALOR!	0,01009	-4,14	Uncharacterized protein (Fragment)
A0A1W2PR94	DTHD1	0,00229	-4,13	Death domain-containing protein 1
P26368	U2AF2	0,00131	-4,13	Splicing factor U2AF 65 kDa subunit
O60218	AKR1B10	0,03879	-4,13	Aldo-keto reductase family 1 member B10
E9PAN7	RPS6KA1	0,00817	-4,13	Ribosomal protein S6 kinase alpha-1
A8MT37	GSK3A	0,01762	-4,09	Glycogen synthase kinase-3 alpha
O14593	RFXANK	0,03183	-4,08	DNA-binding protein RFXANK
Q8NER1	TRPV1	0,01140	-4,07	Transient receptor potential cation channel subfamily V member 1
Q8WWQ0	PHIP	0,00606	-4,05	PH-interacting protein
O43264	ZW10	0,02503	-4,04	Centromere/kinetochore protein zw10 homolog
Q68CQ4	DIEXF	0,00304	-4,03	Digestive organ expansion factor homolog
A0A0A0MSB8	EXOC7	0,04082	-4,01	Exocyst complex component 7
Q7Z3E1	TIPARP	0,02133	-3,97	TCDD-inducible poly [ADP-ribose] polymerase
Q96KQ4	PPP1R13B	0,02118	-3,94	Apoptosis-stimulating of p53 protein 1
Q7Z591	AKNA	0,00254	-3,91	AT-hook-containing transcription factor
E9PG37	ARHGEF3	0,04711	-3,91	Rho guanine nucleotide exchange factor 3
P38405	GNAL	0,00008	-3,91	Guanine nucleotide-binding protein G(olf) subunit alpha
O43405	COCH	0,00695	-3,90	Cochlin
A0A087WVN3	TNFAIP3	0,00461	-3,90	Tumor necrosis factor alpha-induced protein 3
P47972	NPTX2	0,00345	-3,88	Neuronal pentraxin-2
Q9NZM4	BICRA	0,03860	-3,87	BRD4-interacting chromatin-remodeling complex-associated protein
Q9HAV0	GNB4	0,03117	-3,82	Guanine nucleotide-binding protein subunit beta-4

P05976	MYL1	0,02323	-3,81	Myosin light chain 1/3_ skeletal muscle isoform
Q8N0Y2	ZNF444	0,00131	-3,81	Zinc finger protein 444
P19113	HDC	0,03730	-3,80	Histidine decarboxylase
Q9UNA1	ARHGAP26	0,00054	-3,80	Rho GTPase-activating protein 26
P46977	STT3A	0,03814	-3,79	Dolichyl-diphosphooligosaccharide--protein glycosyltransferase subunit STT3A
Q12849	GRSF1	0,02333	-3,77	G-rich sequence factor 1
J3KPP4	LUC7L3	0,02052	-3,76	Cisplatin resistance-associated overexpressed protein_ isoform CRA_b
Q8IY17	PNPLA6	0,00952	-3,75	Neuropathy target esterase
D6RCA9	C4orf47	0,00161	-3,75	UPF0602 protein C4orf47 (Fragment)
Q86SQ9	DHDDS	0,02112	-3,75	Dehydrodolichyl diphosphate synthase complex subunit DHDDS
Q9UK32	RPS6KA6	0,01465	-3,74	Ribosomal protein S6 kinase alpha-6
P27658	COL8A1	0,01143	-3,74	Collagen alpha-1(VIII) chain
Q9Y561	LRP12	0,00660	-3,72	Low-density lipoprotein receptor-related protein 12
Q8NAB2	KBTBD3	0,01239	-3,72	Kelch repeat and BTB domain-containing protein 3
C9JHN6	HDLBP	0,04846	-3,69	Vigilin (Fragment)
Q9Y4L1	HYOU1	0,00087	-3,68	Hypoxia up-regulated protein 1
Q99714	HSD17B10	0,02381	-3,68	3-hydroxyacyl-CoA dehydrogenase type-2
Q68DK2	ZFYVE26	0,02281	-3,68	Zinc finger FYVE domain-containing protein 26
Q00987	MDM2	0,02237	-3,68	E3 ubiquitin-protein ligase Mdm2
D6RDG3	BTF3	0,02170	-3,68	Transcription factor BTF3 (Fragment)
O94818	NOL4	0,01021	-3,64	Nucleolar protein 4
P49221	TGM4	0,00968	-3,63	Protein-glutamine gamma-glutamyltransferase 4
Q86XI2	NCAPG2	0,00630	-3,62	Condensin-2 complex subunit G2
P43304	GPD2	0,00027	-3,62	Glycerol-3-phosphate dehydrogenase_ mitochondrial
Q49A92	C8orf34	0,00440	-3,60	Uncharacterized protein C8orf34
Q8WXF1	PSPC1	0,00184	-3,57	Paraspeckle component 1
M0QY37	TUBB4A	0,00455	-3,57	Tubulin beta-4A chain
O00463	TRAF5	0,00622	-3,57	TNF receptor-associated factor 5
Q9Y6R6	ZNF780B	0,04447	-3,57	Zinc finger protein 780B
Q13033	STRN3	0,00005	-3,55	Striatin-3
Q8TDY2	RB1CC1	0,01947	-3,55	RB1-inducible coiled-coil protein 1

P20339	RAB5A	0,00296	-3,55	Ras-related protein Rab-5A
O43182	ARHGAP6	0,01139	-3,53	Rho GTPase-activating protein 6
P22307	SCP2	0,03118	-3,53	Non-specific lipid-transfer protein
Q9UPQ3	AGAP1	0,00432	-3,51	Arf-GAP with GTPase_ ANK repeat and PH domain-containing protein 1
Q00266	MAT1A	0,03260	-3,49	S-adenosylmethionine synthase isoform type-1
E9PDJ4	DOCK8	0,01268	-3,48	Dedicator of cytokinesis protein 8
J3KSB5	NF1	0,00060	-3,48	Neurofibromin (Fragment)
Q12879	GRIN2A	0,00620	-3,48	Glutamate receptor ionotropic_ NMDA 2A
P22455	FGFR4	0,04749	-3,48	Fibroblast growth factor receptor 4
Q96JH8	RADIL	0,00659	-3,44	Ras-associating and dilute domain-containing protein
A0A0C4DFM1	TM9SF4	0,00086	-3,44	Transmembrane 9 superfamily member
Q9HBX9	RXFP1	0,02632	-3,41	Relaxin receptor 1
Q86VV4	RANBP3L	0,02181	-3,40	Ran-binding protein 3-like
Q6P2C0	WDR93	0,00842	-3,39	WD repeat-containing protein 93
Q9P202	WHRN	0,00536	-3,37	Whirlin
Q6SZW1	SARM1	0,02791	-3,36	Sterile alpha and TIR motif-containing protein 1
J3QRU1	YES1	0,03300	-3,34	Tyrosine-protein kinase
P24941	CDK2	0,00117	-3,34	Cyclin-dependent kinase 2
O95758	PTBP3	0,02305	-3,33	Polypyrimidine tract-binding protein 3
Q92804	TAF15	0,01551	-3,33	TATA-binding protein-associated factor 2N
Q9H0C5	BTBD1	0,00396	-3,31	BTB/POZ domain-containing protein 1
Q2M1Z3	ARHGAP31	0,01047	-3,31	Rho GTPase-activating protein 31
Q05D60	DEUP1	0,00138	-3,31	Deuterosome assembly protein 1
P51571	SSR4	0,01062	-3,31	Translocon-associated protein subunit delta
Q96BD6	SPSB1	0,02762	-3,29	SPRY domain-containing SOCS box protein 1
O60828	PQBP1	0,00029	-3,27	Polyglutamine-binding protein 1
Q96C45	ULK4	0,00600	-3,27	Serine/threonine-protein kinase ULK4
O75530	EED	0,02456	-3,26	Polycomb protein EED
Q8IXK2	GALNT12	0,02423	-3,26	Polypeptide N-acetylgalactosaminyltransferase 12
Q9H4L4	SENP3	0,02751	-3,26	Sentrin-specific protease 3
Q8NET4	RTL9	0,00584	-3,24	Retrotransposon Gag-like protein 9

Q7Z7F4	PRES	0,00815	-3,23	Prestin
P38570	ITGAE	0,01096	-3,22	Integrin alpha-E
H3BM14	NUB1	0,00302	-3,22	NEDD8 ultimate buster 1
Q6PCB7	SLC27A1	0,00334	-3,22	Long-chain fatty acid transport protein 1
Q96AQ6	PBXIP1	0,00077	-3,22	Pre-B-cell leukemia transcription factor-interacting protein 1
Q6UVM3	KCNT2	0,04158	-3,22	Potassium channel subfamily T member 2
Q13576	IQGAP2	0,03133	-3,21	Ras GTPase-activating-like protein IQGAP2
P40938	RFC3	0,01073	-3,20	Replication factor C subunit 3
Q9Y5H1	PCDHGA2	0,02201	-3,18	Protocadherin gamma-A2
Q70EL4	USP43	0,01723	-3,17	Ubiquitin carboxyl-terminal hydrolase 43
H0Y4L1	BAG6	0,01909	-3,17	Large proline-rich protein BAG6 (Fragment)
A8MTM1	CBR1	0,03803	-3,17	Carbonyl reductase [NADPH] 1
Q6EMB2	TTLL5	0,04068	-3,16	Tubulin polyglutamylase TTLL5
P51687	SUOX	0,00459	-3,15	Sulfite oxidase_ mitochondrial
Q7Z6G8	ANKS1B	0,01614	-3,14	Ankyrin repeat and sterile alpha motif domain-containing protein 1B
Q9P2I0	CPSF2	0,00740	-3,14	Cleavage and polyadenylation specificity factor subunit 2
P35711	SOX5	0,00424	-3,14	Transcription factor SOX-5
P26232	CTNNA2	0,00162	-3,14	Catenin alpha-2
Q16798	ME3	0,03681	-3,13	NADP-dependent malic enzyme_ mitochondrial
D6RFZ9	RACK1	0,02532	-3,13	Receptor of-activated protein C kinase 1 (Fragment)
O14530	TXNDC9	0,00684	-3,13	Thioredoxin domain-containing protein 9
Q9UKA9	PTBP2	0,03194	-3,12	Polypyrimidine tract-binding protein 2
P41279	MAP3K8	0,02507	-3,12	Mitogen-activated protein kinase kinase kinase 8
Q8ND23	CARMIL3	0,03014	-3,12	Capping protein_ Arp2/3 and myosin-I linker protein 3
P20702	ITGAX	0,00942	-3,12	Integrin alpha-X
Q8NE86	MCU	0,02255	-3,12	Calcium uniporter protein_ mitochondrial
Q8TEA7	TBCK	0,01409	-3,12	TBC domain-containing protein kinase-like protein
Q96BR5	COA7	0,01078	-3,10	Cytochrome c oxidase assembly factor 7
C9IZN3	ACTR3C	0,00387	-3,09	Actin-related protein 3C (Fragment)
Q9UFN0	NIPSNAP3A	0,04258	-3,09	Protein NipSnap homolog 3A
Q58FF8	HSP90AB2P	0,02110	-3,09	Putative heat shock protein HSP 90-beta 2

Q8WUH6	TMEM263	0,01525	-3,09	Transmembrane protein 263
Q07021	C1QBP	0,03593	-3,09	Complement component 1 Q subcomponent-binding protein_ mitochondrial
P21359	NF1	0,00346	-3,09	Neurofibromin
O94823	ATP10B	0,04540	-3,08	Probable phospholipid-transporting ATPase VB
P01031	C5	0,00752	-3,08	Complement C5
Q5VUJ6	LRCH2	0,04764	-3,08	Leucine-rich repeat and calponin homology domain-containing protein 2
Q9BVA0	KATNB1	0,00350	-3,08	Katanin p80 WD40 repeat-containing subunit B1
P32969	RPL9	0,00303	-3,06	60S ribosomal protein L9
P30566	ADSL	0,02154	-3,06	Adenylosuccinate lyase
Q2VIQ3	KIF4B	0,00445	-3,06	Chromosome-associated kinesin KIF4B
A2PYH4	HFM1	0,00542	-3,06	Probable ATP-dependent DNA helicase HFM1
Q96RU2	USP28	0,01415	-3,06	Ubiquitin carboxyl-terminal hydrolase 28
P63252	KCNJ2	0,00181	-3,04	Inward rectifier potassium channel 2
Q7Z4L5	TTC21B	0,00373	-3,04	Tetratricopeptide repeat protein 21B
Q9P2J9	PDP2	0,00521	-3,02	[Pyruvate dehydrogenase [acetyl-transferring]]-phosphatase 2_ mitochondrial
Q6ZNL6	FGD5	0,00812	-3,01	FYVE_ RhoGEF and PH domain-containing protein 5
Q15303	ERBB4	0,00669	-3,01	Receptor tyrosine-protein kinase erbB-4
Q60I27	ALS2CL	0,00478	-2,99	ALS2 C-terminal-like protein
A0A0A0MQU4	SCLY	0,04515	-2,98	Selenocysteine lyase
Q5PR19	#VALOR!	0,04399	-2,98	Putative UPF0607 protein LOC392364
Q8TEB1	DCAF11	0,00691	-2,97	DDB1- and CUL4-associated factor 11
Q9NP73	ALG13	0,03022	-2,96	Putative bifunctional UDP-N-acetylglucosamine transferase and deubiquitinase ALG13
O00459	PIK3R2	0,01520	-2,95	Phosphatidylinositol 3-kinase regulatory subunit beta
Q9P0J1	PDP1	0,04970	-2,95	[Pyruvate dehydrogenase [acetyl-transferring]]-phosphatase 1_ mitochondrial
P08572	COL4A2	0,02632	-2,95	Collagen alpha-2(IV) chain
Q9NTI5	PDS5B	0,00178	-2,95	Sister chromatid cohesion protein PDS5 homolog B
Q8TD19	NEK9	0,03629	-2,92	Serine/threonine-protein kinase Nek9
Q9BZM6	ULBP1	0,00936	-2,91	NKG2D ligand 1
H0YJL9	AJUBA	0,04011	-2,90	LIM domain-containing protein ajuba (Fragment)
A0A087WVS7	INPP5J	0,01050	-2,89	Phosphatidylinositol 4_5-bisphosphate 5-phosphatase A

O94906	PRPF6	0,03446	-2,88	Pre-mRNA-processing factor 6
Q5SX86	GDI2	0,00867	-2,87	Rab GDP dissociation inhibitor (Fragment)
O15455	TLR3	0,02062	-2,87	Toll-like receptor 3
H7BZ52	ZSWIM8	0,02181	-2,86	Zinc finger SWIM domain-containing protein 8
Q5T795	MDN1	0,02210	-2,85	Midasin (Fragment)
Q96FE5	LINGO1	0,01559	-2,85	Leucine-rich repeat and immunoglobulin-like domain-containing nogo receptor-interacting protein 1
Q86UE4	MTDH	0,00683	-2,85	Protein LYRIC
Q9NXF1	TEX10	0,00097	-2,85	Testis-expressed protein 10
O60303	KIAA0556	0,00068	-2,84	Protein KIAA0556
Q68CR1	SEL1L3	0,00882	-2,82	Protein sel-1 homolog 3
I3L1Y5	P4HB	0,00745	-2,82	Protein disulfide-isomerase
Q02818	NUCB1	0,01667	-2,82	Nucleobindin-1
P17980	PSMC3	0,00977	-2,81	26S proteasome regulatory subunit 6A
P20290	BTF3	0,04619	-2,80	Transcription factor BTF3
Q96A23	CPNE4	0,04769	-2,80	Copine-4
Q6IPX4	RPS16	0,01771	-2,79	40S ribosomal protein S16
M0R210	RPS16	0,02396	-2,79	40S ribosomal protein S16
Q9BY77	POLDIP3	0,00564	-2,79	Polymerase delta-interacting protein 3
P46092	CCR10	0,01829	-2,79	C-C chemokine receptor type 10
P42331	ARHGAP25	0,03878	-2,78	Rho GTPase-activating protein 25
P22460	KCNA5	0,01325	-2,77	Potassium voltage-gated channel subfamily A member 5
Q13428	TCOF1	0,00679	-2,77	Treacle protein
Q05209	PTPN12	0,04482	-2,76	Tyrosine-protein phosphatase non-receptor type 12
Q9Y597	KCTD3	0,02091	-2,75	BTB/POZ domain-containing protein KCTD3
Q9NYZ3	GTSE1	0,01735	-2,73	G2 and S phase-expressed protein 1
P35670	ATP7B	0,00207	-2,71	Copper-transporting ATPase 2
Q8NEV4	MYO3A	0,04711	-2,71	Myosin-IIIa
Q8N3T6	TMEM132C	0,00461	-2,70	Transmembrane protein 132C
Q8NEV8	EXPH5	0,00098	-2,70	Exophilin-5
O95466	FMNL1	0,01648	-2,68	Formin-like protein 1
H0YNW5	DUT	0,00229	-2,67	Deoxyuridine 5'-triphosphate nucleotidohydrolase_ mitochondrial

Q14CN2	CLCA4	0,01732	-2,67	Calcium-activated chloride channel regulator 4
Q9Y2U8	LEMD3	0,01963	-2,64	Inner nuclear membrane protein Man1
Q9BXS5	AP1M1	0,02760	-2,63	AP-1 complex subunit mu-1
A6NML8	DIAPH2	0,01324	-2,62	Diaphanous homolog 2 (Drosophila)_ isoform CRA_c
P36575	ARR3	0,03482	-2,61	Arrestin-C
C9JQ00	TUBA4A	0,01193	-2,61	Tubulin alpha chain (Fragment)
Q86TW2	ADCK1	0,04211	-2,60	Uncharacterized aarF domain-containing protein kinase 1
P49721	PSMB2	0,03426	-2,59	Proteasome subunit beta type-2
Q2VWP7	PRTG	0,00934	-2,59	Protogenin
Q9C005	DPY30	0,01162	-2,58	Protein dpy-30 homolog
Q8N9W8	FAM71D	0,00013	-2,57	Protein FAM71D
O15360	FANCA	0,00344	-2,57	Fanconi anemia group A protein
Q9H3H1	TRIT1	0,01547	-2,57	tRNA dimethylallyltransferase_ mitochondrial
Q9BZH6	WDR11	0,03727	-2,56	WD repeat-containing protein 11
Q96G01	BICD1	0,03770	-2,54	Protein bicaudal D homolog 1
Q6UWU2	GLB1L	0,00953	-2,54	Beta-galactosidase-1-like protein
P00558	PGK1	0,01896	-2,54	Phosphoglycerate kinase 1
Q9BYC5	FUT8	0,00179	-2,53	Alpha-(1_6)-fucosyltransferase
Q8TAT5	NEIL3	0,02606	-2,53	Endonuclease 8-like 3
P32780	GTF2H1	0,04052	-2,52	General transcription factor IIH subunit 1
P20823	HNF1A	0,03569	-2,52	Hepatocyte nuclear factor 1-alpha
P54257	HAP1	0,03619	-2,52	Huntingtin-associated protein 1
F8W6W8	RIMS2	0,03328	-2,51	Regulating synaptic membrane exocytosis protein 2 (Fragment)
Q9Y3R5	DOPEY2	0,01889	-2,51	Protein dopey-2
Q96HE9	PRR11	0,03507	-2,51	Proline-rich protein 11
P32929	CTH	0,00274	-2,49	Cystathionine gamma-lyase
P55259	GP2	0,01766	-2,49	Pancreatic secretory granule membrane major glycoprotein GP2
Q53TQ3	INO80D	0,01833	-2,49	INO80 complex subunit D
Q9P0W8	SPATA7	0,03396	-2,49	Spermatogenesis-associated protein 7
P16499	PDE6A	0,02870	-2,49	Rod cGMP-specific 3'_5'-cyclic phosphodiesterase subunit alpha
P11234	RALB	0,01419	-2,48	Ras-related protein Ral-B

P84095	RHOG	0,02641	-2,48	Rho-related GTP-binding protein RhoG
Q14511	NEDD9	0,02376	-2,48	Enhancer of filamentation 1
A0A1B0GUB3	ASAH1	0,04713	-2,47	Acid ceramidase (Fragment)
P62995	TRA2B	0,00225	-2,47	Transformer-2 protein homolog beta
Q9NUZ1	ACOXL	0,03531	-2,46	Acyl-coenzyme A oxidase-like protein
P84077	ARF1	0,00567	-2,46	ADP-ribosylation factor 1
J3QKD2	ZMYND11	0,03619	-2,46	Zinc finger MYND domain-containing protein 11
Q9Y487	ATP6V0A2	0,00901	-2,46	V-type proton ATPase 116 kDa subunit a isoform 2
Q13618	CUL3	0,02483	-2,45	Cullin-3
P51957	NEK4	0,01062	-2,45	Serine/threonine-protein kinase Nek4
P08621	SNRNP70	0,00864	-2,44	U1 small nuclear ribonucleoprotein 70 kDa
Q9NQ29	LUC7L	0,03518	-2,44	Putative RNA-binding protein Luc7-like 1
E7EVL1	ADCY8	0,03395	-2,43	Adenylate cyclase type 8
J3KNL6	SEC16A	0,02675	-2,43	Protein transport protein Sec16A
F1T0I1	SEC16A	0,03494	-2,43	Protein transport protein Sec16A
Q9NWH9	SLTM	0,01403	-2,42	SAFB-like transcription modulator
O95835	LATS1	0,04004	-2,42	Serine/threonine-protein kinase LATS1
P52907	CAPZA1	0,03838	-2,42	F-actin-capping protein subunit alpha-1
Q96H22	CENPN	0,00070	-2,42	Centromere protein N
O43502	RAD51C	0,03360	-2,41	DNA repair protein RAD51 homolog 3
O60341	KDM1A	0,03338	-2,41	Lysine-specific histone demethylase 1A
H7C3D2	LMCD1	0,02442	-2,40	LIM and cysteine-rich domains protein 1
Q5XPI4	RNF123	0,04014	-2,39	E3 ubiquitin-protein ligase RNF123
O75445	USH2A	0,00348	-2,39	Usherin
Q9H361	PABPC3	0,00116	-2,38	Polyadenylate-binding protein 3
Q53HC5	KLHL26	0,00151	-2,38	Kelch-like protein 26
P25705	ATP5A1	0,01325	-2,36	ATP synthase subunit alpha_ mitochondrial
E9PKC0	PLEKHA7	0,03666	-2,36	Pleckstrin homology domain-containing family A member 7
Q9H3S7	PTPN23	0,03235	-2,36	Tyrosine-protein phosphatase non-receptor type 23
P46821	MAP1B	0,00090	-2,35	Microtubule-associated protein 1B
Q14181	POLA2	0,02015	-2,33	DNA polymerase alpha subunit B

Q96SR6	ZNF382	0,00099	-2,33	Zinc finger protein 382
Q93100	PHKB	0,04887	-2,32	Phosphorylase b kinase regulatory subunit beta
E7EV09	DYNC1I2	0,00350	-2,31	Cytoplasmic dynein 1 intermediate chain 2 (Fragment)
P36507	MAP2K2	0,03903	-2,31	Dual specificity mitogen-activated protein kinase kinase 2
H0YCK9	SPO11	0,02930	-2,30	Meiotic recombination protein SPO11 (Fragment)
Q8N8E3	CEP112	0,00974	-2,29	Centrosomal protein of 112 kDa
Q8IX12	CCAR1	0,04223	-2,28	Cell division cycle and apoptosis regulator protein 1
P35626	GRK3	0,04091	-2,28	Beta-adrenergic receptor kinase 2
Q7Z4H8	KDELC2	0,00501	-2,28	KDEL motif-containing protein 2
O75367	H2AFY	0,02494	-2,27	Core histone macro-H2A.1
A0A087WWV6	TYW1B	0,04133	-2,27	S-adenosyl-L-methionine-dependent tRNA 4-demethylwyosine synthase
P13645	KRT10	0,03047	-2,27	Keratin_ type I cytoskeletal 10
P35052	GPC1	0,04395	-2,27	Glypican-1
Q6IA69	NADSYN1	0,00080	-2,26	Glutamine-dependent NAD(+) synthetase
Q9NRP0	OSTC	0,01839	-2,26	Oligosaccharyltransferase complex subunit OSTC
Q15223	NECTIN1	0,02164	-2,26	Nectin-1
Q9BQT9	CLSTN3	0,00030	-2,25	Calsyntenin-3
H3BLV9	SRPK1	0,03058	-2,24	SRSF protein kinase 1 (Fragment)
Q01814	ATP2B2	0,00551	-2,24	Plasma membrane calcium-transporting ATPase 2
Q53GL0	PLEKHO1	0,00154	-2,24	Pleckstrin homology domain-containing family O member 1
Q8TE60	ADAMTS18	0,00640	-2,23	A disintegrin and metalloproteinase with thrombospondin motifs 18
Q9H7C4	SYNC	0,04100	-2,23	Syncoilin
Q13409	DYNC1I2	0,01094	-2,21	Cytoplasmic dynein 1 intermediate chain 2
P28838	LAP3	0,00309	-2,21	Cytosol aminopeptidase
O76094	SRP72	0,04609	-2,21	Signal recognition particle subunit SRP72
Q9Y4C8	RBM19	0,02998	-2,21	Probable RNA-binding protein 19
O94830	DDHD2	0,03584	-2,20	Phospholipase DDHD2
Q9Y471	CMAHP	0,03512	-2,20	Inactive cytidine monophosphate-N-acetylneuraminic acid hydroxylase
Q9H7M6	ZSWIM4	0,04639	-2,20	Zinc finger SWIM domain-containing protein 4
Q13164	MAPK7	0,01207	-2,20	Mitogen-activated protein kinase 7
Q14164	IKBKE	0,02998	-2,19	Inhibitor of nuclear factor kappa-B kinase subunit epsilon

Q49A88	CCDC14	0,00647	-2,17	Coiled-coil domain-containing protein 14
H0YEX5	SF3B2	0,02179	-2,17	Splicing factor 3B subunit 2 (Fragment)
A0A1B0GW36	QRICH2	0,02597	-2,16	Glutamine-rich protein 2
Q86T82	USP37	0,03540	-2,14	Ubiquitin carboxyl-terminal hydrolase 37
P45973	CBX5	0,04061	-2,14	Chromobox protein homolog 5
Q9Y5X3	SNX5	0,03028	-2,13	Sorting nexin-5
A0A0A0MSA4	EPB41L3	0,00669	-2,12	Band 4.1-like protein 3
Q92797	SYMPK	0,00698	-2,12	Symplekin
P04844	RPN2	0,03844	-2,12	Dolichyl-diphosphooligosaccharide--protein glycosyltransferase subunit 2
F8WDV0	IPO11	0,01119	-2,11	Importin-11
Q92643	PIGK	0,00220	-2,11	GPI-anchor transamidase
Q8IYT4	KATNAL2	0,01703	-2,11	Katanin p60 ATPase-containing subunit A-like 2
G5E9W2	CHPF2	0,01819	-2,10	Hexosyltransferase
P21580	TNFAIP3	0,03328	-2,10	Tumor necrosis factor alpha-induced protein 3
P50851	LRBA	0,02946	-2,09	Lipopolysaccharide-responsive and beige-like anchor protein
Q6ZV29	PNPLA7	0,02967	-2,09	Patatin-like phospholipase domain-containing protein 7
Q15046	KARS	0,02704	-2,08	Lysine--tRNA ligase
E5RHQ9	LRRC69	0,01874	-2,08	Leucine-rich repeat-containing protein 69
Q07283	TCHH	0,03867	-2,08	Trichohyalin
Q68DC2	ANKS6	0,01859	-2,08	Ankyrin repeat and SAM domain-containing protein 6
Q9NQ11	ATP13A2	0,03495	-2,07	Cation-transporting ATPase 13A2
A6NN90	C2orf81	0,00241	-2,04	Uncharacterized protein C2orf81
A9UJQ1	MFNG	0,00752	-2,04	Beta-1_3-N-acetylglucosaminyltransferase manic fringe (Fragment)
Q6S8J3	POTEE	0,00119	-2,04	POTE ankyrin domain family member E
Q9H4I3	TRABD	0,03493	-2,03	TraB domain-containing protein
P62851	RPS25	0,00621	-2,03	40S ribosomal protein S25
A5A3E0	POTEF	0,00111	-2,03	POTE ankyrin domain family member F
F8VW96	CSRP2	0,04615	-2,03	Cysteine and glycine-rich protein 2
Q92896	GLG1	0,03266	-2,03	Golgi apparatus protein 1
Q9UNS2	COPS3	0,02633	-2,02	COP9 signalosome complex subunit 3

O14979	HNRNPDL	0,03819	-2,01	Heterogeneous nuclear ribonucleoprotein D-like
Q9NV79	PCMTD2	0,03041	-1,99	Protein-L-isoaspartate O-methyltransferase domain-containing protein 2
Q04323	UBXN1	0,00411	-1,99	UBX domain-containing protein 1
Q9Y613	FHOD1	0,04499	-1,98	FH1/FH2 domain-containing protein 1
Q8IWE2	FAM114A1	0,04955	-1,98	Protein NOXP20
P49257	LMAN1	0,00382	-1,98	Protein ERGIC-53
P28330	ACADL	0,01341	-1,97	Long-chain specific acyl-CoA dehydrogenase_ mitochondrial
P04843	RPN1	0,01044	-1,97	Dolichyl-diphosphooligosaccharide--protein glycosyltransferase subunit 1
B4DXU5	NR1H3	0,01261	-1,96	Oxysterols receptor LXR-alpha
O75179	ANKRD17	0,04473	-1,96	Ankyrin repeat domain-containing protein 17
P42166	TMPO	0,02753	-1,96	Lamina-associated polypeptide 2_ isoform alpha
Q5BKZ1	ZNF326	0,01249	-1,95	DBIRD complex subunit ZNF326
Q9Y2V7	COG6	0,03367	-1,94	Conserved oligomeric Golgi complex subunit 6
O43490	PROM1	0,04271	-1,93	Prominin-1
Q9Y6D9	MAD1L1	0,03216	-1,93	Mitotic spindle assembly checkpoint protein MAD1
Q8WUD1	RAB2B	0,00723	-1,92	Ras-related protein Rab-2B
Q502W6	VWA3B	0,00454	-1,92	von Willebrand factor A domain-containing protein 3B
Q86UW6	N4BP2	0,00425	-1,91	NEDD4-binding protein 2
O15061	SYNM	0,00929	-1,91	Synemin
Q96NW4	ANKRD27	0,03488	-1,91	Ankyrin repeat domain-containing protein 27
Q96Q27	ASB2	0,02624	-1,90	Ankyrin repeat and SOCS box protein 2
Q9NZN3	EHD3	0,04415	-1,89	EH domain-containing protein 3
P45452	MMP13	0,03929	-1,89	Collagenase 3
O15078	CEP290	0,04945	-1,89	Centrosomal protein of 290 kDa
Q86UW7	CADPS2	0,04675	-1,88	Calcium-dependent secretion activator 2
O94916	NFAT5	0,00237	-1,88	Nuclear factor of activated T-cells 5
Q9H6D7	HAUS4	0,01823	-1,87	HAUS augmin-like complex subunit 4
P20594	NPR2	0,02947	-1,86	Atrial natriuretic peptide receptor 2
P26641	EEF1G	0,03226	-1,86	Elongation factor 1-gamma
P41252	IARS	0,03388	-1,85	Isoleucine--tRNA ligase_ cytoplasmic
K7EK91	DNAH17	0,02613	-1,84	Dynein heavy chain 17_ axonemal

A0A087X2I1	PSMC6	0,03596	-1,84	26S protease regulatory subunit 10B
Q9UID3	VPS51	0,01729	-1,81	Vacuolar protein sorting-associated protein 51 homolog
Q16822	PCK2	0,00578	-1,79	Phosphoenolpyruvate carboxykinase [GTP]_ mitochondrial
O75317	USP12	0,03487	-1,79	Ubiquitin carboxyl-terminal hydrolase 12
Q15003	NCAPH	0,02045	-1,79	Condensin complex subunit 2
Q15399	TLR1	0,04259	-1,79	Toll-like receptor 1
Q9UJW8	ZNF180	0,04568	-1,79	Zinc finger protein 180
A0A087WZT0	SAMD4B	0,02637	-1,79	Protein Smaug homolog 2
P10515	DLAT	0,04121	-1,78	Dihydrolipoyllysine-residue acetyltransferase component of pyruvate dehydrogenase complex_ mitochondrial
Q96MW5	COG8	0,03320	-1,78	Conserved oligomeric Golgi complex subunit 8
Q9Y2I6	NINL	0,02783	-1,77	Ninein-like protein
Q13402	MYO7A	0,00667	-1,76	Unconventional myosin-VIIa
Q9NVE7	PANK4	0,00760	-1,76	Pantothenate kinase 4
O14967	CLGN	0,03456	-1,75	Calmegin
P32121	ARRB2	0,03391	-1,75	Beta-arrestin-2
Q15437	SEC23B	0,01955	-1,75	Protein transport protein Sec23B
Q9NRR5	UBQLN4	0,03047	-1,74	Ubiquilin-4
Q13310	PABPC4	0,02007	-1,73	Polyadenylate-binding protein 4
Q8IX29	FBXO16	0,03126	-1,73	F-box only protein 16
Q13619	CUL4A	0,00907	-1,72	Cullin-4A
P57764	GSDMD	0,02273	-1,72	Gasdermin-D
Q92560	BAP1	0,02490	-1,71	Ubiquitin carboxyl-terminal hydrolase BAP1
G3V325	ATP5J2-PTCD1	0,02419	-1,70	ATP5J2-PTCD1 readthrough
Q9BZ71	PITPNM3	0,03393	-1,70	Membrane-associated phosphatidylinositol transfer protein 3
E7ENV7	CPNE8	0,03955	-1,70	Copine-8
A8K2U0	A2ML1	0,02827	-1,70	Alpha-2-macroglobulin-like protein 1
H3BTA3	STUB1	0,00930	-1,67	E3 ubiquitin-protein ligase CHIP (Fragment)
O94776	MTA2	0,04339	-1,66	Metastasis-associated protein MTA2
P39656	DDOST	0,03534	-1,66	Dolichyl-diphosphooligosaccharide--protein glycosyltransferase 48 kDa subunit
Q9UPV9	TRAK1	0,02028	-1,66	Trafficking kinesin-binding protein 1

O15195	VILL	0,01203	-1,66	Villin-like protein
P51991	HNRNPA3	0,00085	-1,64	Heterogeneous nuclear ribonucleoprotein A3
Q9Y2L9	LRCH1	0,00085	-1,63	Leucine-rich repeat and calponin homology domain-containing protein 1
P42261	GRIA1	0,04594	-1,63	Glutamate receptor 1
Q86U38	NOP9	0,01581	-1,61	Nucleolar protein 9
Q9Y2G4	ANKRD6	0,01465	-1,61	Ankyrin repeat domain-containing protein 6
A4UGR9	XIRP2	0,01908	-1,61	Xin actin-binding repeat-containing protein 2
H0Y8G5	HNRNPD	0,02903	-1,60	Heterogeneous nuclear ribonucleoprotein D0 (Fragment)
Q96A83	COL26A1	0,04480	-1,60	Collagen alpha-1(XXVI) chain
P11717	IGF2R	0,04501	-1,59	Cation-independent mannose-6-phosphate receptor
E9PN67	NIN	0,02024	-1,58	Ninein
P62913	RPL11	0,03493	-1,58	60S ribosomal protein L11
Q9UM21	MGAT4A	0,02347	-1,57	Alpha-1_3-mannosyl-glycoprotein 4-beta-N-acetylglucosaminyltransferase A
P62888	RPL30	0,04326	-1,57	60S ribosomal protein L30
K7EQA1	PDCD5	0,03132	-1,57	Programmed cell death protein 5
Q96SI9	STRBP	0,04480	-1,55	Spermatid perinuclear RNA-binding protein
Q9BYC2	OXCT2	0,02964	-1,54	Succinyl-CoA:3-ketoacid coenzyme A transferase 2_ mitochondrial
Q7Z2T5	TRMT1L	0,03317	-1,53	TRMT1-like protein
O75529	TAF5L	0,01040	-1,53	TAF5-like RNA polymerase II p300/CBP-associated factor-associated factor 65 kDa subunit 5L
P11047	LAMC1	0,04192	-1,52	Laminin subunit gamma-1
Q9UG01	IFT172	0,00824	-1,52	Intraflagellar transport protein 172 homolog
Q15008	PSMD6	0,00874	-1,51	26S proteasome non-ATPase regulatory subunit 6
Q9Y5S9	RBM8A	0,02301	-1,51	RNA-binding protein 8A
Q96AG4	LRRC59	0,01794	-1,50	Leucine-rich repeat-containing protein 59
Q96GQ7	DDX27	0,04588	-1,50	Probable ATP-dependent RNA helicase DDX27
Q15365	PCBP1	0,03007	-1,49	Poly(rC)-binding protein 1
Q70CQ4	USP31	0,02564	-1,48	Ubiquitin carboxyl-terminal hydrolase 31
Q96PV4	PNMA5	0,02862	-1,48	Paraneoplastic antigen-like protein 5
Q14683	SMC1A	0,01908	-1,48	Structural maintenance of chromosomes protein 1A
P78527	PRKDC	0,00705	-1,47	DNA-dependent protein kinase catalytic subunit
O00423	EML1	0,01070	-1,47	Echinoderm microtubule-associated protein-like 1

P30041	PRDX6	0,00021	-1,47	Peroxiredoxin-6
Q9UKX2	MYH2	0,02452	-1,43	Myosin-2
O95905	ECD	0,03402	-1,42	Protein ecdysoneless homolog
Q9UI33	SCN11A	0,00323	-1,40	Sodium channel protein type 11 subunit alpha
Q9BXP5	SRRT	0,02819	-1,40	Serrate RNA effector molecule homolog
A0A087WVW4	TGM5	0,02623	-1,40	Protein-glutamine gamma-glutamyltransferase 5
P43121	MCAM	0,03414	-1,39	Cell surface glycoprotein MUC18
Q9NQW8	CNGB3	0,03469	-1,39	Cyclic nucleotide-gated cation channel beta-3
Q92925	SMARCD2	0,04954	-1,39	SWI/SNF-related matrix-associated actin-dependent regulator of chromatin subfamily D member 2
Q06787	FMR1	0,03619	-1,38	Synaptic functional regulator FMR1
Q07666	KHDRBS1	0,03917	-1,36	KH domain-containing_ RNA-binding_ signal transduction-associated protein 1
O94813	SLIT2	0,02450	-1,34	Slit homolog 2 protein
Q9Y2V3	RAX	0,01806	-1,34	Retinal homeobox protein Rx
Q9H497	TOR3A	0,04646	-1,33	Torsin-3A
P38919	EIF4A3	0,00436	-1,32	Eukaryotic initiation factor 4A-III
Q8TC12	RDH11	0,04418	-1,31	Retinol dehydrogenase 11
Q9NUX5	POT1	0,00956	-1,29	Protection of telomeres protein 1
Q8IVF4	DNAH10	0,00506	-1,28	Dynein heavy chain 10_ axonemal
B0I1T2	MYO1G	0,02552	-1,28	Unconventional myosin-Ig
Q8IYD1	GSPT2	0,04313	-1,25	Eukaryotic peptide chain release factor GTP-binding subunit ERF3B
Q5VU57	AGBL4	0,04758	-1,25	Cytosolic carboxypeptidase 6
Q9UQ80	PA2G4	0,01229	-1,25	Proliferation-associated protein 2G4
H0YBN4	PABPC1	0,03145	-1,22	Polyadenylate-binding protein 1 (Fragment)
H0Y2W2	ATAD3A	0,03581	-1,22	ATPase family AAA domain-containing protein 3A (Fragment)
Q8ND90	PNMA1	0,04206	-1,22	Paraneoplastic antigen Ma1
Q68E01	INTS3	0,04627	-1,22	Integrator complex subunit 3
H3BVC7	RPS15A	0,03748	-1,21	40S ribosomal protein S15a (Fragment)
P14174	MIF	0,01030	-1,20	Macrophage migration inhibitory factor
Q8IZS8	CACNA2D3	0,00062	-1,20	Voltage-dependent calcium channel subunit alpha-2/delta-3
Q9NVI7	ATAD3A	0,04012	-1,19	ATPase family AAA domain-containing protein 3A
F5GXQ8	SYNE1	0,04479	-1,18	Nesprin-1

B4E0Y9	STK26	0,04080	-1,17	Serine/threonine-protein kinase 26
P07339	CTSD	0,03848	-1,16	Cathepsin D
C9JD91	PTPN23	0,01523	-1,15	Tyrosine-protein phosphatase non-receptor type 23 (Fragment)
Q02108	GUCY1A3	0,04889	-1,14	Guanylate cyclase soluble subunit alpha-3
P08183	ABCB1	0,04460	-1,14	Multidrug resistance protein 1
P55060	CSE1L	0,02595	-1,14	Exportin-2
E7EV10	MTA3	0,04429	-1,12	Metastasis-associated protein MTA3
Q9NR99	MXRA5	0,02648	-1,11	Matrix-remodeling-associated protein 5
C9JKR8	MSL3	0,03147	-1,11	Male-specific lethal 3 homolog (Fragment)
Q9ULW0	TPX2	0,03564	-1,09	Targeting protein for Xklp2
P50748	KNTC1	0,04656	-1,07	Kinetochore-associated protein 1
O15050	TRANK1	0,02561	-1,06	TPR and ankyrin repeat-containing protein 1
O60240	PLIN1	0,04865	-1,05	Perilipin-1
X6RLX0	ERC1	0,03653	-1,05	ELKS/Rab6-interacting/CAST family member 1
Q63HQ2	EGFLAM	0,01011	-1,04	Pikachurin
Q92917	GPKOW	0,03659	-1,04	G patch domain and KOW motifs-containing protein
Q03252	LMNB2	0,03748	-1,03	Lamin-B2
A0A1W2PPJ3	SCN1A	0,03789	-1,00	Sodium channel protein
Q9Y2X3	NOP58	0,01587	-1,00	Nucleolar protein 58
Q13151	HNRNPA0	0,00905	-0,99	Heterogeneous nuclear ribonucleoprotein A0
A6NES4	MROH2A	0,02964	-0,99	Maestro heat-like repeat-containing protein family member 2A
Q96F86	EDC3	0,01018	-0,98	Enhancer of mRNA-decapping protein 3
P02786	TFRC	0,00218	-0,94	Transferrin receptor protein 1
Q01844	EWSR1	0,04000	-0,94	RNA-binding protein EWS
P61353	RPL27	0,00440	-0,92	60S ribosomal protein L27
Q15477	SKIV2L	0,03666	-0,90	Helicase SKI2W
P09630	HOXC6	0,00100	-0,90	Homeobox protein Hox-C6
P43034	PAFAH1B1	0,04788	-0,81	Platelet-activating factor acetylhydrolase IB subunit alpha
P07196	NEFL	0,04401	-0,80	Neurofilament light polypeptide
P46013	MKI67	0,02944	-0,75	Proliferation marker protein Ki-67
P23378	GLDC	0,01652	-0,67	Glycine dehydrogenase (decarboxylating)_ mitochondrial

D6RF62	PAICS	0,02603	-0,43	Multifunctional protein ADE2
Q7Z406	MYH14	0,03224	-0,41	Myosin-14
Q9UK12	ZNF222	0,03118	-0,14	Zinc finger protein 222
P15056	BRAF	0,02775	-0,10	Serine/threonine-protein kinase B-raf
Q9P2U7	SLC17A7	0,04443	0,01	Vesicular glutamate transporter 1
P52209	PGD	0,01659	0,49	6-phosphogluconate dehydrogenase_ decarboxylating
Q9UER7	DAXX	0,02308	0,64	Death domain-associated protein 6
Q02539	HIST1H1A	0,04053	0,72	Histone H1.1
Q6QNK2	ADGRD1	0,04139	0,75	Adhesion G-protein coupled receptor D1
P14373	TRIM27	0,03292	0,80	Zinc finger protein RFP
P51531	SMARCA2	0,04266	0,83	Probable global transcription activator SNF2L2
Q8WZ74	CTTNBP2	0,01530	0,90	Cortactin-binding protein 2
Q86VS3	IQCH	0,04243	0,93	IQ domain-containing protein H
P24534	EEF1B2	0,01367	0,95	Elongation factor 1-beta
P26196	DDX6	0,03318	1,05	Probable ATP-dependent RNA helicase DDX6
P25205	MCM3	0,04578	1,06	DNA replication licensing factor MCM3
O94887	FARP2	0,03809	1,08	FERM_ RhoGEF and pleckstrin domain-containing protein 2
F5H1Z6	STARD10	0,04211	1,10	START domain-containing protein 10 (Fragment)
Q96PC5	MIA2	0,01674	1,11	Melanoma inhibitory activity protein 2
P68371	TUBB4B	0,04439	1,12	Tubulin beta-4B chain
P23467	PTPRB	0,02905	1,14	Receptor-type tyrosine-protein phosphatase beta
P07355	ANXA2	0,03592	1,18	Annexin A2
Q2M1P5	KIF7	0,04612	1,23	Kinesin-like protein KIF7
Q29RF7	PDS5A	0,00731	1,27	Sister chromatid cohesion protein PDS5 homolog A
P29401	TKT	0,03976	1,30	Transketolase
Q92835	INPP5D	0,04606	1,32	Phosphatidylinositol 3_4_5-trisphosphate 5-phosphatase 1
Q8N8Z6	DCBLD1	0,04652	1,33	Discoidin_ CUB and LCCL domain-containing protein 1
P28066	PSMA5	0,02265	1,33	Proteasome subunit alpha type-5
P82932	MRPS6	0,03901	1,34	28S ribosomal protein S6_ mitochondrial
Q9ULT0	TTC7A	0,00027	1,37	Tetratricopeptide repeat protein 7A
P54762	EPHB1	0,04497	1,38	Ephrin type-B receptor 1

Q8IYM2	SLFN12	0,03000	1,39	Schlafen family member 12
O75154	RAB11FIP3	0,03530	1,41	Rab11 family-interacting protein 3
Q6ZU80	CEP128	0,03575	1,45	Centrosomal protein of 128 kDa
Q9UI47	CTNNA3	0,03796	1,47	Catenin alpha-3
Q6PCT2	FBXL19	0,01745	1,50	F-box/LRR-repeat protein 19
P53597	SUCLG1	0,04197	1,50	Succinate--CoA ligase [ADP/GDP-forming] subunit alpha_ mitochondrial
Q14566	MCM6	0,01821	1,51	DNA replication licensing factor MCM6
E7EMW7	UBR5	0,03937	1,51	E3 ubiquitin-protein ligase UBR5
F8W9U4	MAP4	0,04076	1,51	Microtubule-associated protein
Q8NG31	KNL1	0,00415	1,52	Kinetochore scaffold 1
P26006	ITGA3	0,02576	1,53	Integrin alpha-3
Q92786	PROX1	0,02389	1,58	Prospero homeobox protein 1
Q15811	ITSN1	0,04849	1,63	Intersectin-1
Q02809	PLOD1	0,03348	1,63	Procollagen-lysine_2-oxoglutarate 5-dioxygenase 1
Q96PK6	RBM14	0,03650	1,64	RNA-binding protein 14
Q9BWT3	PAPOLG	0,04176	1,64	Poly(A) polymerase gamma
Q5T6W2	HNRNPK	0,03206	1,65	Heterogeneous nuclear ribonucleoprotein K (Fragment)
P61978	HNRNPK	0,03206	1,65	Heterogeneous nuclear ribonucleoprotein K
P46063	RECQL	0,02742	1,66	ATP-dependent DNA helicase Q1
P08603	CFH	0,04789	1,69	Complement factor H
Q96IR2	ZNF845	0,02305	1,70	Zinc finger protein 845
O15067	PFAS	0,03936	1,72	Phosphoribosylformylglycinamidine synthase
P15144	ANPEP	0,01613	1,73	Aminopeptidase N
Q9BQI3	EIF2AK1	0,01567	1,73	Eukaryotic translation initiation factor 2-alpha kinase 1
O43660	PLRG1	0,03519	1,73	Pleiotropic regulator 1
P78371	CCT2	0,02638	1,75	T-complex protein 1 subunit beta
P39060	COL18A1	0,02935	1,75	Collagen alpha-1(XVIII) chain
Q6ZMV9	KIF6	0,01638	1,77	Kinesin-like protein KIF6
P01266	TG	0,03474	1,77	Thyroglobulin
P10070	GLI2	0,01018	1,77	Zinc finger protein GLI2
Q9UL54	TAOK2	0,03507	1,79	Serine/threonine-protein kinase TAO2

O75541	ZNF821	0,03003	1,79	Zinc finger protein 821
B1AJZ9	FHAD1	0,02269	1,82	Forkhead-associated domain-containing protein 1
Q8N7X0	ADGB	0,00069	1,87	Androglobin
H7BZ55	CROCC2	0,04931	1,89	Putative ciliary rootlet coiled-coil protein 2
Q8WWN8	ARAP3	0,02322	1,91	Arf-GAP with Rho-GAP domain_ ANK repeat and PH domain-containing protein 3
Q08289	CACNB2	0,02109	1,92	Voltage-dependent L-type calcium channel subunit beta-2
Q9Y6L7	TLL2	0,02453	1,93	Tolloid-like protein 2
Q9Y6M1	IGF2BP2	0,04232	1,94	Insulin-like growth factor 2 mRNA-binding protein 2
A8TX70	COL6A5	0,00928	1,94	Collagen alpha-5(VI) chain
Q8IX18	DHX40	0,04930	1,94	Probable ATP-dependent RNA helicase DHX40
P26583	HMGB2	0,02901	1,95	High mobility group protein B2
Q9UHC6	CNTNAP2	0,03474	1,96	Contactin-associated protein-like 2
Q01105	SET	0,02992	1,98	Protein SET
Q14980	NUMA1	0,00167	2,00	Nuclear mitotic apparatus protein 1
Q92630	DYRK2	0,00744	2,02	Dual specificity tyrosine-phosphorylation-regulated kinase 2
Q8IYM0	FAM186B	0,02041	2,04	Protein FAM186B
Q9H2K8	TAOK3	0,02374	2,06	Serine/threonine-protein kinase TAO3
Q10471	GALNT2	0,04217	2,07	Polypeptide N-acetylgalactosaminyltransferase 2
O00267	SUPT5H	0,01348	2,09	Transcription elongation factor SPT5
Q6P2Q9	PRPF8	0,03865	2,09	Pre-mRNA-processing-splicing factor 8
Q9ULL1	PLEKHG1	0,03869	2,09	Pleckstrin homology domain-containing family G member 1
P25685	DNAJB1	0,04897	2,09	DnaJ homolog subfamily B member 1
Q12756	KIF1A	0,02570	2,11	Kinesin-like protein KIF1A
E5RI46	G3BP1	0,03119	2,12	Ras GTPase-activating protein-binding protein 1 (Fragment)
Q9NW13	RBM28	0,01121	2,14	RNA-binding protein 28
Q9BZ29	DOCK9	0,01181	2,15	Dedicator of cytokinesis protein 9
P78362	SRPK2	0,04080	2,16	SRSF protein kinase 2
Q52LW3	ARHGAP29	0,01994	2,17	Rho GTPase-activating protein 29
Q0VAK6	LMOD3	0,04999	2,19	Leiomodin-3
A0A0A0MSY4	DOCK9	0,02069	2,20	Dedicator of cytokinesis protein 9
P46778	RPL21	0,01507	2,21	60S ribosomal protein L21

Q9Y2L5	TRAPPC8	0,00949	2,21	Trafficking protein particle complex subunit 8
A0A0B4J2H4	LOC102724023	0,01406	2,23	Uncharacterized protein
P12814	ACTN1	0,00855	2,24	Alpha-actinin-1
Q92576	PHF3	0,00124	2,25	PHD finger protein 3
Q9H0B3	KIAA1683	0,03523	2,28	Uncharacterized protein KIAA1683
Q9UHB9	SRP68	0,04648	2,28	Signal recognition particle subunit SRP68
Q9UPU9	SAMD4A	0,01371	2,28	Protein Smaug homolog 1
Q58FF3	HSP90B2P	0,01478	2,29	Putative endoplasmin-like protein
A6NK02	TRIM75P	0,04902	2,29	Putative tripartite motif-containing protein 75
P34931	HSPA1L	0,00402	2,29	Heat shock 70 kDa protein 1-like
Q86Y79	PTRH1	0,03001	2,29	Probable peptidyl-tRNA hydrolase
Q9Y2E4	DIP2C	0,03616	2,31	Disco-interacting protein 2 homolog C
Q16543	CDC37	0,03401	2,31	Hsp90 co-chaperone Cdc37
Q9P2N2	ARHGAP28	0,01169	2,31	Rho GTPase-activating protein 28
Q6P179	ERAP2	0,00302	2,32	Endoplasmic reticulum aminopeptidase 2
O43175	PHGDH	0,02033	2,35	D-3-phosphoglycerate dehydrogenase
Q8IZX4	TAF1L	0,00075	2,36	Transcription initiation factor TFIID subunit 1-like
Q86YS7	C2CD5	0,01416	2,36	C2 domain-containing protein 5
P08729	KRT7	0,01169	2,37	Keratin_ type II cytoskeletal 7
Q8IWR0	ZC3H7A	0,01430	2,39	Zinc finger CCCH domain-containing protein 7A
O00445	SYT5	0,02833	2,40	Synaptotagmin-5
Q6P4R8	NFRKB	0,01012	2,41	Nuclear factor related to kappa-B-binding protein
P49748	ACADVL	0,01737	2,42	Very long-chain specific acyl-CoA dehydrogenase_ mitochondrial
P35442	THBS2	0,03246	2,44	Thrombospondin-2
P62753	RPS6	0,01290	2,44	40S ribosomal protein S6
C9JRZ6	CHCHD3	0,02218	2,46	MICOS complex subunit
O00522	KRIT1	0,03664	2,46	Krev interaction trapped protein 1
P38606	ATP6V1A	0,00780	2,46	V-type proton ATPase catalytic subunit A
O60437	PPL	0,04675	2,51	Periplakin
O00219	HAS3	0,01013	2,52	Hyaluronan synthase 3
Q9Y4E6	WDR7	0,00071	2,55	WD repeat-containing protein 7

Q9NYT6	ZNF226	0,04124	2,55	Zinc finger protein 226
G5E9A7	DMWD	0,00528	2,57	Dystrophia myotonica WD repeat-containing protein
O96000	NDUFB10	0,04714	2,59	NADH dehydrogenase [ubiquinone] 1 beta subcomplex subunit 10
C9JFV4	PELP1	0,00338	2,60	Proline-_ glutamic acid- and leucine-rich protein 1
P54868	HMGCS2	0,03621	2,60	Hydroxymethylglutaryl-CoA synthase_ mitochondrial
Q9UPW0	FOXJ3	0,01871	2,60	Forkhead box protein J3
Q9NSU2	TREX1	0,03536	2,60	Three-prime repair exonuclease 1
P28074	PSMB5	0,02659	2,61	Proteasome subunit beta type-5
E9PC69	MARK2	0,01704	2,63	Non-specific serine/threonine protein kinase
P25054	APC	0,01858	2,64	Adenomatous polyposis coli protein
O00443	PIK3C2A	0,02134	2,65	Phosphatidylinositol 4-phosphate 3-kinase C2 domain-containing subunit alpha
Q9P273	TENM3	0,03886	2,65	Teneurin-3
I3L0M9	ELOB	0,04225	2,70	Elongin-B (Fragment)
Q9H4L7	SMARCAD1	0,03550	2,71	SWI/SNF-related matrix-associated actin-dependent regulator of chromatin subfamily A containing DEAD/H box 1
Q12789	GTF3C1	0,00067	2,71	General transcription factor 3C polypeptide 1
K7ENM7	#VALOR!	0,01553	2,72	Uncharacterized protein
Q9UKU0	ACSL6	0,02462	2,72	Long-chain-fatty-acid--CoA ligase 6
P31946	YWHAB	0,02461	2,73	14-3-3 protein beta/alpha
Q99536	VAT1	0,02585	2,73	Synaptic vesicle membrane protein VAT-1 homolog
Q9Y5T5	USP16	0,01866	2,74	Ubiquitin carboxyl-terminal hydrolase 16
O95613	PCNT	0,01320	2,74	Pericentrin
Q9NZN9	AIPL1	0,01374	2,77	Aryl-hydrocarbon-interacting protein-like 1
Q9H3N1	TMX1	0,03187	2,78	Thioredoxin-related transmembrane protein 1
P67870	CSNK2B	0,00903	2,79	Casein kinase II subunit beta
P07237	P4HB	0,03032	2,79	Protein disulfide-isomerase
Q14146	URB2	0,02954	2,79	Unhealthy ribosome biogenesis protein 2 homolog
Q14126	DSG2	0,02216	2,83	Desmoglein-2
Q9UKE5	TNIK	0,01818	2,84	TRAF2 and NCK-interacting protein kinase
Q0JRZ9	FCHO2	0,04015	2,86	F-BAR domain only protein 2
P42679	MATK	0,04637	2,88	Megakaryocyte-associated tyrosine-protein kinase
P46100	ATRX	0,01345	2,89	Transcriptional regulator ATRX

Q5T200	ZC3H13	0,00509	2,91	Zinc finger CCCH domain-containing protein 13
Q9P2F5	STOX2	0,00268	2,93	Storkhead-box protein 2
A0A0D9SEP4	NRXN1	0,01589	2,94	Neurexin-1-beta
Q9UKV8	AGO2	0,00673	2,94	Protein argonaute-2
P53618	COPB1	0,00663	2,94	Coatomer subunit beta
Q86UL8	MAGI2	0,04386	3,00	Membrane-associated guanylate kinase_ WW and PDZ domain-containing protein 2
Q6TFL4	KLHL24	0,01613	3,01	Kelch-like protein 24
C9J069	C9orf172	0,00684	3,02	Uncharacterized protein C9orf172
Q9NRD9	DUOX1	0,03229	3,03	Dual oxidase 1
Q9UHF7	TRPS1	0,04792	3,04	Zinc finger transcription factor Trps1
B8ZZD4	TAX1BP1	0,00848	3,05	Tax1-binding protein 1
O00308	WWP2	0,01225	3,06	NEDD4-like E3 ubiquitin-protein ligase WWP2
Q63HN8	RNF213	0,00930	3,07	E3 ubiquitin-protein ligase RNF213
Q9NWH7	SPATA6	0,03336	3,09	Spermatogenesis-associated protein 6
Q86UP2	KTN1	0,04034	3,09	Kinectin
P50914	RPL14	0,04167	3,09	60S ribosomal protein L14
Q96M86	DNHD1	0,04395	3,11	Dynein heavy chain domain-containing protein 1
Q13867	BLMH	0,02384	3,12	Bleomycin hydrolase
Q8NH19	OR10AG1	0,03554	3,13	Olfactory receptor 10AG1
P49454	CENPF	0,01989	3,14	Centromere protein F
P35612	ADD2	0,02482	3,14	Beta-adducin
A0A1B0GUS7	UNC13B	0,01493	3,17	Protein unc-13 homolog B
Q9Y3A5	SBDS	0,01293	3,19	Ribosome maturation protein SBDS
Q3L8U1	CHD9	0,04873	3,20	Chromodomain-helicase-DNA-binding protein 9
H0Y5E3	TTLL3	0,02801	3,21	Tubulin monoglycylase TTLL3 (Fragment)
P11182	DBT	0,03547	3,21	Lipoamide acyltransferase component of branched-chain alpha-keto acid dehydrogenase complex_ mitochondrial
Q07343	PDE4B	0,01249	3,22	cAMP-specific 3'_5'-cyclic phosphodiesterase 4B
Q13137	CALCOCO2	0,03695	3,22	Calcium-binding and coiled-coil domain-containing protein 2
Q2TBA0	KLHL40	0,01113	3,23	Kelch-like protein 40
Q9UGR2	ZC3H7B	0,02580	3,26	Zinc finger CCCH domain-containing protein 7B

Q92887	ABCC2	0,04452	3,27	Canalicular multispecific organic anion transporter 1
Q6ZU15	SEPT14	0,00986	3,28	Septin-14
C9JEB6	HDAC7	0,01143	3,31	Histone deacetylase 7 (Fragment)
A7E2V4	ZSWIM8	0,01232	3,34	Zinc finger SWIM domain-containing protein 8
O60884	DNAJA2	0,04992	3,36	DnaJ homolog subfamily A member 2
P58397	ADAMTS12	0,02735	3,36	A disintegrin and metalloproteinase with thrombospondin motifs 12
Q9ULU4	ZMYND8	0,03937	3,39	Protein kinase C-binding protein 1
P14866	HNRNPL	0,03728	3,42	Heterogeneous nuclear ribonucleoprotein L
P00451	F8	0,01276	3,43	Coagulation factor VIII
P15086	CPB1	0,01607	3,44	Carboxypeptidase B
Q9P2D6	FAM135A	0,04535	3,46	Protein FAM135A
Q8TCX5	RHPN1	0,00509	3,47	Rhophilin-1
O94983	CAMTA2	0,02440	3,50	Calmodulin-binding transcription activator 2
Q3V6T2	CCDC88A	0,03426	3,50	Girdin
P08708	RPS17	0,00374	3,52	40S ribosomal protein S17
Q4R9M9	KIF1Bbeta	0,01657	3,53	Kinesin family member 1Bbeta isoform II
Q9Y3F4	STRAP	0,00359	3,58	Serine-threonine kinase receptor-associated protein
A0A087WVC1	DDX50	0,02465	3,60	ATP-dependent RNA helicase DDX50
Q96Q05	TRAPPC9	0,02431	3,60	Trafficking protein particle complex subunit 9
Q2KHM9	KIAA0753	0,04197	3,61	Protein moonraker
V9GYM8	ARHGEF2	0,02265	3,65	Rho guanine nucleotide exchange factor 2
Q07002	CDK18	0,00965	3,65	Cyclin-dependent kinase 18
O95876	WDPCP	0,00847	3,65	WD repeat-containing and planar cell polarity effector protein fritz homolog
A0A088AWP5	PRUNE2	0,00535	3,68	Protein prune homolog 2
Q14315	FLNC	0,04108	3,70	Filamin-C
F8W703	ROBO2	0,00167	3,70	Roundabout homolog 2
P14649	MYL6B	0,03670	3,74	Myosin light chain 6B
O60336	MAPKBP1	0,00869	3,76	Mitogen-activated protein kinase-binding protein 1
Q5T7N3	KANK4	0,02981	3,78	KN motif and ankyrin repeat domain-containing protein 4
P16615	ATP2A2	0,00678	3,80	Sarcoplasmic/endoplasmic reticulum calcium ATPase 2

P10253	GAA	0,00264	3,80	Lysosomal alpha-glucosidase
E9PF82	CAMK2D	0,01621	3,82	Calcium/calmodulin-dependent protein kinase type II subunit delta
P37275	ZEB1	0,01797	3,83	Zinc finger E-box-binding homeobox 1
Q9NR12	PDLIM7	0,01010	3,87	PDZ and LIM domain protein 7
Q96J02	ITCH	0,00794	3,88	E3 ubiquitin-protein ligase Itchy homolog
P19320	VCAM1	0,01827	3,89	Vascular cell adhesion protein 1
Q96RT1	ERBIN	0,01833	3,96	Erbin
A2A3N6	PIPSL	0,00358	3,97	Putative PIP5K1A and PSMD4-like protein
Q9H0E9	BRD8	0,00314	3,97	Bromodomain-containing protein 8
Q8TER5	ARHGEF40	0,04748	3,99	Rho guanine nucleotide exchange factor 40
P20340	RAB6A	0,00949	4,03	Ras-related protein Rab-6A
Q9HCM1	KIAA1551	0,01024	4,04	Uncharacterized protein KIAA1551
O43707	ACTN4	0,00586	4,14	Alpha-actinin-4
O76031	CLPX	0,01016	4,16	ATP-dependent Clp protease ATP-binding subunit clpX-like_ mitochondrial
Q9H2U2	PPA2	0,04730	4,20	Inorganic pyrophosphatase 2_ mitochondrial
Q8NFZ5	TNIP2	0,01790	4,22	TNFAIP3-interacting protein 2
Q9Y4F1	FARP1	0,00747	4,24	FERM_ RhoGEF and pleckstrin domain-containing protein 1
Q9UQP3	TNN	0,00042	4,27	Tenascin-N
P61313	RPL15	0,00976	4,29	60S ribosomal protein L15
Q9H6E5	TUT1	0,00926	4,31	Speckle targeted PIP5K1A-regulated poly(A) polymerase
P16591	FER	0,00214	4,31	Tyrosine-protein kinase Fer
Q92901	RPL3L	0,00645	4,32	60S ribosomal protein L3-like
Q5M775	SPECC1	0,04102	4,33	Cytospin-B
Q13009	TIAM1	0,00586	4,36	T-lymphoma invasion and metastasis-inducing protein 1
Q9P2B4	CTTNBP2NL	0,00799	4,42	CTTNBP2 N-terminal-like protein
Q6W4X9	MUC6	0,00213	4,46	Mucin-6
Q14318	FKBP8	0,02209	4,47	Peptidyl-prolyl cis-trans isomerase FKBP8
Q16186	ADRM1	0,04358	4,47	Proteasomal ubiquitin receptor ADRM1
A0A087WX20	MLH1	0,04280	4,50	DNA mismatch repair protein Mlh1 (Fragment)
P20701	ITGAL	0,00512	4,51	Integrin alpha-L
Q6Q788	APOA5	0,02457	4,53	Apolipoprotein A-V

P42336	PIK3CA	0,00640	4,55	Phosphatidylinositol 4_5-bisphosphate 3-kinase catalytic subunit alpha isoform
Q3KQU3	MAP7D1	0,03044	4,59	MAP7 domain-containing protein 1
Q96S59	RANBP9	0,01393	4,62	Ran-binding protein 9
Q9BZF1	OSBPL8	0,01502	4,62	Oxysterol-binding protein-related protein 8
Q9C0H9	SRCIN1	0,00948	4,67	SRC kinase signaling inhibitor 1
P04150	NR3C1	0,04665	4,67	Glucocorticoid receptor
Q68DQ2	CRYBG3	0,00455	4,76	Very large A-kinase anchor protein
Q58FG1	HSP90AA4P	0,04168	4,78	Putative heat shock protein HSP 90-alpha A4
Q9UIB8	CD84	0,01048	4,78	SLAM family member 5
E7ES33	SEPT7	0,03814	4,81	Septin-7
Q8IWJ2	GCC2	0,02365	4,83	GRIP and coiled-coil domain-containing protein 2
A6NHC0	CAPN8	0,03912	4,84	Calpain-8
O14617	AP3D1	0,00439	4,89	AP-3 complex subunit delta-1
O15240	VGF	0,02904	4,90	Neurosecretory protein VGF
O14513	NCKAP5	0,00667	4,91	Nck-associated protein 5
Q5XX13	FBXW10	0,03475	4,93	F-box/WD repeat-containing protein 10
A0A088AWN8	NARF	0,00722	4,93	Nuclear prelamin A recognition factor
B5MC15	CBLB	0,00007	4,94	Cas-Br-M (Murine) ecotropic retroviral transforming sequence b_ isoform CRA_a
Q16670	ZSCAN26	0,00030	4,99	Zinc finger and SCAN domain-containing protein 26
P16260	SLC25A16	0,02018	5,02	Graves disease carrier protein
Q96RT7	TUBGCP6	0,01677	5,04	Gamma-tubulin complex component 6
Q12959	DLG1	0,00273	5,06	Disks large homolog 1
Q5XUX1	FBXW9	0,00302	5,11	F-box/WD repeat-containing protein 9
Q9Y5F8	PCDHGB7	0,00891	5,11	Protocadherin gamma-B7
A0A0A0MRG9	CDK5RAP2	0,00687	5,13	CDK5 regulatory subunit-associated protein 2
Q9Y6Y1	CAMTA1	0,02595	5,16	Calmodulin-binding transcription activator 1
A0A087WZR0	PCSK6	0,00006	5,17	Proprotein convertase subtilisin/kexin type 6
H3BTR4	CENPT	0,00703	5,27	Centromere protein T
P05165	PCCA	0,00648	5,33	Propionyl-CoA carboxylase alpha chain_ mitochondrial
Q5VZM2	RRAGB	0,01592	5,33	Ras-related GTP-binding protein B

P35222	CTNNB1	0,04267	5,37	Catenin beta-1
Q9NQ36	SCUBE2	0,00074	5,45	Signal peptide_ CUB and EGF-like domain-containing protein 2
Q2NL98	VMAC	0,02304	5,48	Vimentin-type intermediate filament-associated coiled-coil protein
P42702	LIFR	0,00364	5,50	Leukemia inhibitory factor receptor
Q8NDA2	HMCN2	0,00103	5,54	Hemicentin-2
B2RPK0	HMGB1P1	0,01532	5,57	Putative high mobility group protein B1-like 1
Q9P0T4	ZNF581	0,00776	5,58	Zinc finger protein 581
Q32MQ0	ZNF750	0,04102	5,69	Zinc finger protein 750
K7EMP1	CC2D1A	0,00576	5,76	Coiled-coil and C2 domain-containing protein 1A (Fragment)
P30626	SRI	0,00554	5,78	Sorcin
P00367	GLUD1	0,03127	5,88	Glutamate dehydrogenase 1_ mitochondrial
Q96H55	MYO19	0,01965	5,92	Unconventional myosin-XIX
O14639	ABLIM1	0,04060	5,93	Actin-binding LIM protein 1
O95373	IPO7	0,00887	5,95	Importin-7
O43157	PLXNB1	0,00803	5,96	Plexin-B1
A6NI28	ARHGAP42	0,04140	5,99	Rho GTPase-activating protein 42
P21796	VDAC1	0,03407	5,99	Voltage-dependent anion-selective channel protein 1
Q8IUH5	ZDHHC17	0,02982	6,03	Palmitoyltransferase ZDHHC17
Q99551	MTERF1	0,04411	6,19	Transcription termination factor 1_ mitochondrial
P51858	HDGF	0,04223	6,19	Hepatoma-derived growth factor
Q9BVA1	TUBB2B	0,00982	6,20	Tubulin beta-2B chain
Q9BUR4	WRAP53	0,01647	6,28	Telomerase Cajal body protein 1
E9PGC0	RASA1	0,01013	6,36	Ras GTPase-activating protein 1
P56524	HDAC4	0,00742	6,38	Histone deacetylase 4
Q12767	TMEM94	0,02204	6,56	Transmembrane protein 94
D6RIA3	LOC285556	0,00525	6,61	Uncharacterized protein
F8W7U8	MRE11	0,00917	6,64	Double-strand break repair protein MRE11
Q9H422	HIPK3	0,00496	6,68	Homeodomain-interacting protein kinase 3
Q8N8Q3	ENDOV	0,00436	6,78	Endonuclease V
Q8IYL2	TRMT44	0,03410	7,05	Probable tRNA (uracil-O(2)-)-methyltransferase
O00409	FOXN3	0,01085	7,16	Forkhead box protein N3

P82094	TMF1	0,00532	7,16	TATA element modulatory factor
Q8N2N9	ANKRD36B	0,00198	7,27	Ankyrin repeat domain-containing protein 36B
Q9HC35	EML4	0,02746	7,29	Echinoderm microtubule-associated protein-like 4
Q9NTJ3	SMC4	0,03491	7,34	Structural maintenance of chromosomes protein 4
P09429	HMGB1	0,02041	7,37	High mobility group protein B1
Q9NVM9	INTS13	0,00557	7,51	Integrator complex subunit 13
P13688	CEACAM1	0,00398	7,59	Carcinoembryonic antigen-related cell adhesion molecule 1
Q9Y228	TRAF3IP3	0,01971	7,59	TRAF3-interacting JNK-activating modulator
O15056	SYNJ2	0,02922	7,60	Synaptojanin-2
P49354	FNTA	0,02413	7,61	Protein farnesyltransferase/geranylgeranyltransferase type-1 subunit alpha
Q659C4	LARP1B	0,02102	7,91	La-related protein 1B
Q96M96	FGD4	0,00986	7,92	FYVE_ RhoGEF and PH domain-containing protein 4
P23415	GLRA1	0,00714	8,11	Glycine receptor subunit alpha-1
Q5I0G2	PRL	0,01579	8,38	Growth hormone A1
F6S1J4	C16orf62	0,04287	8,56	UPF0505 protein C16orf62
Q9H5I5	PIEZO2	0,00025	8,81	Piezo-type mechanosensitive ion channel component 2
B2WTI4	JMJD6	0,02983	9,22	Bifunctional arginine demethylase and lysyl-hydroxylase JMJD6
E7ERS3	ZC3H18	0,00017	9,31	Zinc finger CCCH domain-containing protein 18
A2RTX5	TARSL2	0,03806	9,34	Probable threonine--tRNA ligase 2_ cytoplasmic
Q9UI17	DMGDH	0,01573	9,37	Dimethylglycine dehydrogenase_ mitochondrial
Q9Y4C2	TCAF1	0,02492	9,55	TRPM8 channel-associated factor 1
F8W079	ATP5B	0,03573	10,05	ATP synthase subunit beta_ mitochondrial (Fragment)
Q8NHH9	ATL2	0,04236	10,16	Atlastin-2
D6RJB7	ANKRD31	0,00170	10,17	Putative ankyrin repeat domain-containing protein 31
P01236	PRL	0,02337	10,58	Prolactin
B4DY26	TGFBR1	0,02334	11,00	Receptor protein serine/threonine kinase
Q01484	ANK2	0,02588	11,73	Ankyrin-2
P08069	IGF1R	0,00013	11,87	Insulin-like growth factor 1 receptor
Q9BXU1	STK31	0,03167	12,01	Serine/threonine-protein kinase 31
Q5VV43	KIAA0319	0,02274	12,75	Dyslexia-associated protein KIAA0319

Table 6: Ingenuity canonical pathway analysis for oligodendrocyte treated with second generation antipsychotics

Table 6 - Ingenuity canonical pathway analysis for oligodendrocyte treated with second generation antipsychotics

Treatment	Ingenuity Canonical Pathways	p-value	Ratio	Treatment	Ingenuity Canonical Pathways	p-value	Ratio
Risperidone	Epithelial Adherens Junction Signaling	1,23E-06	22/143 (0,154)	Quetiapine	Glutamate Degradation II	1,45E-02	1/3 (0,333)
Risperidone	Germ Cell-Sertoli Cell Junction Signaling	1,78E-06	24/169 (0,142)	Quetiapine	Aspartate Biosynthesis	1,45E-02	1/3 (0,333)
Risperidone	EIF2 Signaling	1,07E-05	26/212 (0,123)	Quetiapine	Pentose Phosphate Pathway (Oxidative Branch)	1,91E-02	1/4 (0,25)
Risperidone	Sertoli Cell-Sertoli Cell Junction Signaling	2,82E-05	22/173 (0,127)	Quetiapine	L-cysteine Degradation I	1,91E-02	1/4 (0,25)
Risperidone	Remodeling of Epithelial Adherens Junctions	6,17E-05	12/66 (0,182)	Quetiapine	Aspartate Degradation II	3,31E-02	1/7 (0,143)
Risperidone	Axonal Guidance Signaling	0,000105	40/445 (0,0899)	Quetiapine	Ephrin A Signaling	3,39E-02	2/60 (0,0333)
Risperidone	14-3-3-mediated Signaling	0,000158	17/130 (0,131)	Quetiapine	Leucine Degradation I	4,27E-02	1/9 (0,111)
Risperidone	PTEN Signaling	0,000178	16/119 (0,134)	Quetiapine	Myc Mediated Apoptosis Signaling	4,47E-02	2/70 (0,0286)
Risperidone	PDGF Signaling	0,000347	13/90 (0,144)	Quetiapine	Calcium Transport I	4,68E-02	1/10 (0,1)
Risperidone	Gap Junction Signaling	0,000417	19/167 (0,114)	Quetiapine	Pentose Phosphate Pathway	4,68E-02	1/10 (0,1)
Risperidone	CREB Signaling in Neurons	0,000501	20/183 (0,109)				
Risperidone	CNTF Signaling	0,000513	10/60 (0,167)				
Risperidone	Integrin Signaling	0,000562	22/212 (0,104)				
Risperidone	NGF Signaling	0,000562	15/119 (0,126)				
Risperidone	Antiproliferative Role of Somatostatin Receptor 2	0,000589	11/72 (0,153)				
Risperidone	Breast Cancer Regulation by Stathmin1	0,000724	21/202 (0,104)				
Risperidone	Role of p14/p19ARF in Tumor Suppression	0,000741	8/42 (0,19)				
Risperidone	Paxillin Signaling	0,000776	14/110 (0,127)				
Risperidone	PI3K/AKT Signaling	0,000794	15/123 (0,122)				
Risperidone	Endometrial Cancer Signaling	0,000871	10/64 (0,156)				
Risperidone	Regulation of eIF4 and p70S6K Signaling	0,001148	17/154 (0,11)				

Risperidone	Chronic Myeloid Leukemia Signaling	0,001259	13/103 (0,126)
Risperidone	Reelin Signaling in Neurons	0,001445	12/92 (0,13)
Risperidone	Thrombin Signaling	0,001622	20/201 (0,0995)
Risperidone	Cardiac Hypertrophy Signaling	0,001905	22/233 (0,0944)
Risperidone	IL-4 Signaling	0,00263	11/86 (0,128)
Risperidone	HGF Signaling	0,003162	13/114 (0,114)
Risperidone	GDNF Family Ligand-Receptor Interactions	0,003311	10/76 (0,132)
Risperidone	Non-Small Cell Lung Cancer Signaling	0,003631	10/77 (0,13)
Risperidone	Glioblastoma Multiforme Signaling	0,004074	16/159 (0,101)
Risperidone	Melanoma Signaling	0,004467	8/55 (0,145)
Risperidone	Actin Cytoskeleton Signaling	0,004898	20/221 (0,0905)
Risperidone	EGF Signaling	0,005012	9/68 (0,132)
Risperidone	Prostate Cancer Signaling	0,005248	11/94 (0,117)
Risperidone	CXCR4 Signaling	0,005495	16/164 (0,0976)
Risperidone	FLT3 Signaling in Hematopoietic Progenitor Cells	0,005754	10/82 (0,122)
Risperidone	Huntington's Disease Signaling	0,005888	21/240 (0,0875)
Risperidone	Relaxin Signaling	0,006026	15/151 (0,0993)
Risperidone	Molecular Mechanisms of Cancer	0,006607	29/370 (0,0784)
Risperidone	Inosine-5'-phosphate Biosynthesis II	0,006607	2/3 (0,667)
Risperidone	Colorectal Cancer Metastasis Signaling	0,006761	21/243 (0,0864)
Risperidone	Glioma Signaling	0,006918	12/111 (0,108)
Risperidone	Antiproliferative Role of TOB in T Cell Signaling	0,007079	5/26 (0,192)
Risperidone	FAK Signaling	0,007244	11/98 (0,112)
Risperidone	Small Cell Lung Cancer Signaling	0,007244	10/85 (0,118)
Risperidone	Hereditary Breast Cancer Signaling	0,007762	14/141 (0,0993)
Risperidone	GM-CSF Signaling	0,007943	9/73 (0,123)
Risperidone	Endothelin-1 Signaling	0,008128	17/186 (0,0914)
Risperidone	PAK Signaling	0,008318	11/100 (0,11)

Risperidone	RANK Signaling in Osteoclasts	0,008318	11/100 (0,11)
Risperidone	Cancer Drug Resistance By Drug Efflux	0,008318	7/49 (0,143)
Risperidone	Estrogen Receptor Signaling	0,008511	13/128 (0,102)
Risperidone	Neuropathic Pain Signaling In Dorsal Horn Neurons	0,008511	12/114 (0,105)
Risperidone	B Cell Receptor Signaling	0,008511	17/187 (0,0909)
Risperidone	Protein Kinase A Signaling	0,009333	29/380 (0,0763)
Risperidone	D-myo-inositol (1,4,5)-trisphosphate Degradation	0,009333	4/18 (0,222)
Risperidone	Role of NFAT in Cardiac Hypertrophy	0,01	17/190 (0,0895)
Risperidone	Gα12/13 Signaling	0,010233	13/131 (0,0992)
Risperidone	Glucocorticoid Receptor Signaling	0,010471	23/285 (0,0807)
Risperidone	Pancreatic Adenocarcinoma Signaling	0,010965	12/118 (0,102)
Risperidone	Pyridoxal 5'-phosphate Salvage Pathway	0,010965	8/64 (0,125)
Risperidone	IL-2 Signaling	0,010965	8/64 (0,125)
Risperidone	1D-myo-inositol Hexakisphosphate Biosynthesis II (Mammalian)	0,011482	4/19 (0,211)
Risperidone	D-myo-inositol (1,3,4)-trisphosphate Biosynthesis	0,011482	4/19 (0,211)
Risperidone	Mouse Embryonic Stem Cell Pluripotency	0,011749	11/105 (0,105)
Risperidone	CD40 Signaling	0,012023	9/78 (0,115)
Risperidone	Role of Tissue Factor in Cancer	0,012589	12/120 (0,1)
Risperidone	IGF-1 Signaling	0,012589	11/106 (0,104)
Risperidone	FcγRIIB Signaling in B Lymphocytes	0,012882	7/53 (0,132)
Risperidone	Purine Nucleotides De Novo Biosynthesis II	0,01349	3/11 (0,273)
Risperidone	Tight Junction Signaling	0,013804	15/166 (0,0904)
Risperidone	Lymphotoxin β Receptor Signaling	0,014454	8/67 (0,119)
Risperidone	Telomerase Signaling	0,014454	11/108 (0,102)
Risperidone	ErbB2-ErbB3 Signaling	0,015488	8/86 (0,118)
Risperidone	Amyotrophic Lateral Sclerosis Signaling	0,016218	11/110 (0,1)
Risperidone	Sumoylation Pathway	0,016596	10/96 (0,104)
Risperidone	Role of IL-17A in Arthritis	0,016982	8/69 (0,116)

Risperidone	Cleavage and Polyadenylation of Pre-mRNA	0,017378	3/12 (0,25)
Risperidone	Calcium Signaling	0,017378	15/171 (0,0877)
Risperidone	Prolactin Signaling	0,017783	9/83 (0,108)
Risperidone	Phospholipase C Signaling	0,017783	19/234 (0,0812)
Risperidone	Melanocyte Development and Pigmentation Signaling	0,017783	10/97 (0,103)
Risperidone	Myc Mediated Apoptosis Signaling	0,018197	8/70 (0,114)
Risperidone	Glioma Invasiveness Signaling	0,018197	8/70 (0,114)
Risperidone	ErbB4 Signaling	0,018197	8/70 (0,114)
Risperidone	TR/RXR Activation	0,019055	10/98 (0,102)
Risperidone	Caveolar-mediated Endocytosis Signaling	0,019953	8/71 (0,113)
Risperidone	PKCθ Signaling in T Lymphocytes	0,019953	12/128 (0,0938)
Risperidone	Leukocyte Extravasation Signaling	0,020893	17/206 (0,0825)
Risperidone	Phagosome Formation	0,023442	11/116 (0,0948)
Risperidone	Virus Entry via Endocytic Pathways	0,024547	10/102 (0,098)
Risperidone	NF-κB Signaling	0,024547	15/178 (0,0843)
Risperidone	Superpathway of D-myo-inositol (1,4,5)-trisphosphate Metabolism	0,025704	4/24 (0,167)
Risperidone	mTOR Signaling	0,027542	16/197 (0,0812)
Risperidone	Role of PI3K/AKT Signaling in the Pathogenesis of Influenza	0,02884	8/76 (0,105)
Risperidone	Neurotrophin/TRK Signaling	0,02884	8/76 (0,105)
Risperidone	Signaling by Rho Family GTPases	0,02884	19/247 (0,0769)
Risperidone	Acetyl-CoA Biosynthesis I (Pyruvate Dehydrogenase Complex)	0,0302	2/6 (0,333)
Risperidone	PXR/RXR Activation	0,0302	7/63 (0,111)
Risperidone	Angiopoietin Signaling	0,030903	8/77 (0,104)
Risperidone	Acute Myeloid Leukemia Signaling	0,032359	9/92 (0,0978)
Risperidone	Systemic Lupus Erythematosus Signaling	0,032359	17/217 (0,0783)
Risperidone	T Cell Receptor Signaling	0,034674	10/108 (0,0926)
Risperidone	Thrombopoietin Signaling	0,035481	7/65 (0,108)
Risperidone	CD27 Signaling in Lymphocytes	0,037154	6/52 (0,115)

Risperidone	Docosahexaenoic Acid (DHA) Signaling	0,037154	6/52 (0,115)
Risperidone	Thyroid Cancer Signaling	0,037154	5/39 (0,128)
Risperidone	Granzyme B Signaling	0,038019	3/16 (0,188)
Risperidone	Mismatch Repair in Eukaryotes	0,038019	3/16 (0,188)
Risperidone	Cellular Effects of Sildenafil (Viagra)	0,039811	11/126 (0,0873)
Risperidone	Renal Cell Carcinoma Signaling	0,039811	8/81 (0,0988)
Risperidone	p53 Signaling	0,039811	10/111 (0,0901)
Risperidone	Cell Cycle Control of Chromosomal Replication	0,040738	5/40 (0,125)
Risperidone	Ovarian Cancer Signaling	0,041687	12/143 (0,0839)
Risperidone	ILK Signaling	0,043652	15/192 (0,0781)
Risperidone	IL-3 Signaling	0,044668	8/83 (0,0964)
Risperidone	Growth Hormone Signaling	0,044668	8/83 (0,0964)
Risperidone	Granzyme A Signaling	0,044668	3/17 (0,176)
Risperidone	Superpathway of Inositol Phosphate Compounds	0,045709	17/227 (0,0749)
Risperidone	Regulation of Cellular Mechanics by Calpain Protease	0,046774	6/55 (0,109)
Risperidone	Histamine Biosynthesis	0,047863	1/1 (1)
Risperidone	L-cysteine Degradation II	0,047863	1/1 (1)
Risperidone	Sulfite Oxidation IV	0,047863	1/1 (1)

UNICAMP
COORDENADORIA DE PÓS-GRADUAÇÃO
INSTITUTO DE BIOLOGIA
Universidade Estadual de Campinas
Caixa Postal 6109. 13083-970, Campinas, SP, Brasil
Fone (19) 3521-6378. email: cpgib@unicamp.br
IB

DECLARAÇÃO

Em observância ao **§5º do Artigo 1º da Informação CCPG-UNICAMP/001/15**, referente a Bioética e Biossegurança, declaro que o conteúdo de minha Dissertação de Mestrado, intitulada "***Empregando a proteômica para compreender os mecanismos de ação dos antipsicóticos em oligodendrócitos***", desenvolvida no Programa de Pós-Graduação em Biologia Funcional e Molecular do Instituto de Biologia da Unicamp, não versa sobre pesquisa envolvendo seres humanos, animais ou temas afetos a Biossegurança.

Assinatura: _____
Nome do(a) aluno(a): Caroline Brandão Teles

Assinatura: _____
Nome do(a) orientador(a): Daniel Martins de Souza

Data: 13/06/2018

Declaração

As cópias de artigos de minha autoria ou de minha co-autoria, já publicados ou submetidos para publicação em revistas científicas ou anais de congressos sujeitos a arbitragem, que constam da minha Dissertação/Tese de Mestrado/Doutorado, intitulada **Empregando a proteômica para compreender os mecanismos de ação dos antipsicóticos em oligodendrócitos**, não infringem os dispositivos da Lei n.° 9.610/98, nem o direito autoral de qualquer editora.

Campinas, 13 de Junho de 2018

Assinatura : _____
Nome do(a) autor(a): **Caroline Brandão Teles**
RG n.° 32.537.033-3

Assinatura : _____
Nome do(a) orientador(a): **Daniel Martins de Souza**
RG n.° 32.431.379-2